Integrated Vehicle Dynamics Control Using Active Steering, Driveline and Braking

by

Junjie He, BEng, MEng

Submitted in accordance with the requirements for the degree of

Doctor of Philosophy

The University of Leeds

School of Mechanical Engineering

May 2005

The candidate confirms that the work submitted is his own and that appropriate credit has been given where reference has been made to the work of others

Acknowledgements

I wish to thank my supervisors, Prof. David Crolla, Dr Martin Levesley and Dr Warren Manning, for their patient instructions, valuable guidance and insightful discussions throughout this research. I am particularly grateful to Prof. Crolla and Dr Manning for their detailed comments and corrections on an earlier version of the manuscript.

I would like to extend my gratitude to Mr Mick Martin and Mr D Readman of Vehicle Dynamics and Control Lab for their technical support and assistance. An acknowledge must also go to the ORS Awards and Tetley and Lupton Scholarships from Leeds University for the financial support during the course of this research.

I want to thank my lovely wife, Xuelian, for the endless love, tremendous support and encouragement she has provided throughout my PhD study.

Last but not least, special thanks go to my parents, brother and sister for their moral support and love.

Abstract

This thesis investigates the principle of integrated vehicle dynamics control through proposing a new control configuration to coordinate active steering subsystems and dynamic stability control (DSC) subsystems. The active steering subsystems include Active Front Steering (AFS) and Active Rear Steering (ARS); the dynamic stability control subsystems include driveline based, brake based and driveline plus brake based DSC subsystems.

A nonlinear vehicle handling model is developed for this study, incorporating the load transfer effects and nonlinear tyre characteristics. This model consists of 8 degrees of freedom that include longitudinal, lateral and yaw motions of the vehicle and body roll motion relative to the chassis about the roll axis as well as the rotational dynamics of four wheels. The lateral vehicle dynamics are analysed for the entire handling region and two distinct control objectives are defined, i.e. steerability and stability which correspond to yaw rate tracking and sideslip motion bounding, respectively.

Active steering subsystem controllers and dynamic stability subsystem controller are designed by using the Sliding Mode Control (SMC) technique and phase-plane method, respectively. The former is used as the steerability controller to track the reference yaw rate and the latter serves as the stability controller to bound the sideslip motion of the vehicle. Both stand-alone controllers are evaluated over a range of different handling regimes. The stand-alone steerability controllers are found to be very effective in improving vehicle steering response up to the handling limit and the stand-alone stability controller is found to be capable of performing the task of maintaining vehicle stability at the operating points where the active steering subsystems cannot.

Based on the two independently developed stand-alone controllers, a novel rule based integration scheme for AFS and driveline plus brake based DSC is proposed to optimise the overall vehicle performance by minimising interactions between the two subsystems and extending functionalities of individual subsystems. The proposed

integrated control system is assessed by comparing it to corresponding combined control. Through the simulation work conducted under critical driving conditions, the proposed integrated control system is found to lead to a trade-off between stability and limit steerability, improved vehicle stability and reduced influence on the longitudinal vehicle dynamics.

Publications

1. **He, J.**, Crolla, D.A., Levesley, M.C. and Manning, W.J., "Integrated chassis control through coordination of active front steering and intelligent torque distribution," *Proc. of the 7th International Symposium on Advanced Vehicle Control, AVEC'04*, Arnhem, the Netherlands, pp. 333-339, 23-27 August, 2004.

2. **He, J.**, Crolla, D.A., Levesley, M.C. and Manning, W.J., "Integrated active steering and variable torque distribution control for improving vehicle handling and stability," *SAE 2004 World Congress*, Detroit, USA, 2004-01-1071, 8-11 March, 2004.

3. **He, J.**, Crolla, D.A., Levesley, M.C. and Manning, W.J., "Coordinated active rear steering and variable torque distribution control for improving vehicle directional stability," *Systems Science,* Vol. 29, No. 1, pp. 119-133, 2003.

4. **He, J.**, Crolla, D.A., Levesley, M.C. and Manning, W.J., "Coordinated active rear steering and variable torque distribution control for vehicle stability enhancement," *Proc. of the 16th Int. Conf. on Systems Engineering, ICSE'2003*, Coventry, UK, Vol. 1, pp. 243-248, 9-11 September, 2003.

Contents

List of Figures

List of Tables

Notations

a_x	vehicle longitudinal acceleration (m/s^2)
a_y	vehicle lateral acceleration (m/s^2)
a_{yss}	steady-state vehicle lateral acceleration (m/s^2)
b	y-intercept of the original reference region boundaries
b'	y-intercept of the control boundaries for stability controller
C_f	front axle cornering stiffness (N/rad)
C_r	rear axle cornering stiffness (N/rad)
$C_{\phi f}$	front suspension roll damping (Nm/rad/s)
$C_{\phi r}$	rear suspension roll damping (Nm/rad/s)
e	error between system output and reference signal
$e_{\beta\dot{\beta}}$	stability error (-)
e_λ	error between desired and actual wheel slip ratios (-)
f_r	rolling resistance coefficient (-)
F_r	rolling resistance (N)
F_x	resultant longitudinal force in the vehicle fixed axes (N)
ΔF_x	longitudinal force difference between left and right wheels (N)
F_{xw}	longitudinal tyre force (N)
F_{xwss}	steady-state longitudinal tyre force (N)
F_y	resultant lateral force in the vehicle fixed axes (N)
F_{yw}	lateral tyre force (N)
F_{ywss}	steady-state lateral tyre force (N)
F_z	vertical tyre load (N)
F_{z0}	static vertical tyre load (N)
F_{zf0}	static vertical tyre load on the front axle (N)
F_{zr0}	static vertical tyre load on the rear axle (N)

F_{zax}	load transfer due to longitudinal acceleration (N)
F_{zay}	load transfer due to lateral acceleration (N)
$F_{zayf(1)}$	lateral load transfer associated with front unsprung mass (N)
$F_{zayr(1)}$	lateral load transfer associated with rear unsprung mass (N)
$F_{zayf(2)}$	front lateral load transfer associated with sprung mass (N)
$F_{zayr(2)}$	rear lateral load transfer associated with sprung mass (N)
$F_{z\phi}$	load transfer due to body roll motion (N)
h	distance from sprung mass CG to roll axis (m)
h_{cg}	height of vehicle CG (m)
h_{cgs}	height of sprung mass CG (m)
h_f	height of front roll centre (m)
h_r	height of rear roll centre (m)
h_{uf}	height of front unsprung mass CG (m)
h_{ur}	height of rear unsprung mass CG (m)
I_w	wheel moment of inertia about spin axis (kgm^2)
I_{xx}	sprung mass moment of inertia about roll axis (kgm^2)
I_{xxs}	sprung mass moment of inertia about x-axis (kgm^2)
I_{xz}	sprung mass product of inertia about roll and yaw axes (kgm^2)
I_{zz}	vehicle moment of inertia about z-axis (kgm^2)
I_{zzf}	front unsprung mass moment of inertia about its CG (kgm^2)
I_{zzr}	rear unsprung mass moment of inertia about its CG (kgm^2)
I_{zzs}	sprung mass moment of inertia about z-axis (kgm^2)
$k_{\beta\dot{\beta}}$	slope of reference regions
$K_{\phi f}$	front suspension roll stiffness (Nm/rad)
$K_{\phi r}$	rear suspension roll stiffness (Nm/rad)
K_u	understeer gradient (deg/g)
l_{cg}	longitudinal distance from sprung mass CG to vehicle CG (m)

l_f	distance from vehicle CG to front axle (m)
l_{fs}	distance from sprung mass CG to front axle (m)
l_r	distance from vehicle CG to rear axle (m)
l_{rs}	distance from sprung mass CG to rear axle (m)
l	wheelbase (m)
m	total mass of the vehicle (kg)
m_s	sprung mass (kg)
m_{uf}	front unsprung mass (kg)
m_{ur}	rear unsprung mass (kg)
M_x	resultant roll moment (Nm)
M_z	resultant yaw moment (Nm)
M_{zc}	corrective yaw moment generated by active control (Nm)
M_{zw}	tyre self-aligning moment (Nm)
n	system order (-)
n_s	steering ratio (-)
p	roll rate (rad/s)
r	yaw rate (rad/s)
r_d	reference yaw rate (rad/s)
r_{ss}	steady-state yaw rate (rad/s)
R	radius of the turn (m)
R_w	tyre rolling radius (m)
RL_x	longitudinal tyre relaxation length (m)
RL_y	lateral tyre relaxation length (m)
t_f	front wheel track (m)
t_r	rear wheel track (m)
T	wheel torque (Nm)
T_b	wheel brake torque (Nm)
T_{cl}	torque transferred by left-hand clutch of the torque transfer differential (Nm)

T_{cr}	torque transferred by right-hand clutch of the torque transfer differential (Nm)
T_d	wheel driving torque (Nm)
T_{in}	input torque of the torque transfer differential (Nm)
T_l	left wheel torque (Nm)
T_r	right wheel torque (Nm)
T_x	torque transferred from the differential case to the three-gang gearing in the torque transfer differential (Nm)
ΔT	torque difference between left and right wheels (Nm)
V_x	vehicle forward speed (m/s)
V_{xw}	wheel centre longitudinal speed in the wheel axis system (m/s)
V_y	vehicle lateral speed (m/s)
V_{yw}	wheel centre lateral speed in the wheel axis system (m/s)
W	vehicle weight (N)
$\mathbf{x}$	state vector

Greek Symbols

α	tyre slip angle (rad)
β	vehicle sideslip angle (rad)
δ_f	front wheel steer angle (rad)
$\Delta\delta_f$	total corrective steer angle (rad)
$\Delta\delta'_f$	corrective steer angle for stability control (rad)
δ_{fc}	corrective steer angle demanded by AFS controller (rad)
δ_{fd}	steer angle applied at front wheels by the driver (rad)
δ_r	rear wheel steer angle (rad)
δ_{sw}	steering wheel angle (rad)
ε	small positive scalar (-)
E	small positive scalar (-)
κ	positive constant (-)

λ	longitudinal slip ratio of tyres (-)
λ_d	desired longitudinal slip ratio of tyres (-)
μ	road surface coefficient of friction (-)
τ_{xl}	time constant for longitudinal tyre force (s)
τ_{yl}	time constant for lateral tyre force (s)
ϕ	roll angle (rad)
ψ	yaw (heading) angle (rad)
ω	wheel angular speed (rad/s)
ω_c	differential case speed (rad/s)
ω_{cl}	left-hand inner clutch plate speed (torque transfer differential) (rad/s)
ω_{cr}	right-hand inner clutch plate speed (torque transfer differential) (rad/s)
ω_l	left-hand wheel speed (rad/s)
ω_r	right-hand wheel speed (rad/s)

Subscripts

1	front left wheel
2	front right wheel
3	rear left wheel
4	rear right wheel

Abbreviations

2WS	2 Wheel Steering
2NVM	2DOF Nonlinear Vehicle Model
4WS	4 Wheel Steering
4WD	4 Wheel Drive
ABS	Anti-lock Braking System
AFS	Active Front Steering
A4S	Active Four Wheel Steering
ARS	Active Rear Steering
ASC	Active Stability Control
ATDS	Active Torque Distribution System
AYC	Active Yaw Control
CG	Centre of Gravity
CVT	Continuously Variable Transmission
DOF	Degree of Freedom
DSC	Dynamic Stability Control
DYC	Direct Yaw Moment Control
FWD	Front Wheel Drive
IC	Internal Combustion
IWD	Inner Wheel Drive
IWTC	Individual Wheel Torque Control
LQR	Linear Quadratic Regulator
LSD	Limited Slip Differential
NLVM	Nonlinear Vehicle Model
OWD	Outer Wheel Drive
PID	Proportional Integral Derivative
RMD	Roll Moment Distribution
RWD	Rear Wheel Drive
SBW	Steer By Wire
SMC	Sliding Mode Control
TCS	Traction Control System

VDM	Vehicle Dynamics Management
VTD	Variable Torque Distribution

Chapter 1

Introduction

Abstract: *This chapter presents a background description of the research undertaken. An introduction briefly describes the current development of active vehicle dynamics control. Subsequently, the need for control system integration and potential benefits of such integration are explained. The chapter concludes with the outline of the thesis contents.*

1.1 Introduction to Active Vehicle Dynamics Control

With the rapid development of electronics, sensor and actuator technologies, microprocessor-based digital controls have been extensively applied to various automobile subsystems for years. In particular, in the field of vehicle dynamics, a large number of active control systems have been developed to improve vehicle performance and active safety by using either various actuation concepts or advanced control methodologies. Considerable improvements have been achieved through active control of individual aspects of the vehicle dynamics and the resultant vehicles are safer, more comfortable from the occupants point of view and more controllable with respect to vehicle handling.

Various vehicle dynamics control systems can be categorised into three areas: longitudinal control, lateral control and vertical control in terms of the three

translational vehicle motions that control systems directly aim to affect. These systems were usually developed independently to improve vehicle traction performance, handling performance and ride comfort, respectively. For example, Anti-lock Braking Systems (ABS) or Traction Control Systems (TCS) can automatically modulate the braking or tractive force to improve the braking or traction performance of the vehicle. During cornering, Active Front/Rear Steering (AFS/ARS) systems or Dynamic Stability Control (DSC) systems may become active to keep the vehicle on the desired path and maintain vehicle stability. Active suspension systems can influence the vertical force between wheels and vehicle body in order to improve both ride quality and handling performance. In the case of vertical control, the driver has no direct control authority over the vertical motion of the vehicle which can be regulated by the active controllers. It should be noted that the above categorisation is based on functionalities or control tasks rather than actuation concepts which imply how the control actions are physically implemented.

In this thesis, the focus is devoted to active control of vehicle handling. Herein, handling specifically refers to the lateral vehicle dynamics. It does not include active systems such as TCS as they are directly related to the longitudinal behaviour. It does however include systems such as single-wheel braking and variable torque distribution controls which are used to affect the lateral handling by taking advantage of the interactions between the longitudinal and lateral tyre forces.

1.1.1 Driver-vehicle system

The vehicle handling characteristics cannot be viewed in isolation without any consideration of humans as controllers. Basically, drivers can control vehicle dynamic behaviour through three control inputs: the throttle and brake pedals for controlling the longitudinal motion (forward speed and longitudinal acceleration) and the steering wheel for influencing the lateral motion (directional control), respectively. As the control of the lateral vehicle dynamics is of primary interest in this thesis, only the driver steer input will be examined in more detail here.

The steering tasks of the driver can be separated into two categories: the primary *path following* task and the secondary *stabilisation* (or *disturbance attenuation*) task

(Ackermann, 1997). For *path following* the driver applies appropriate control action to guide the vehicle travelling along the planned path. In the case of *stabilisation*, the driver must compensate for any deviations from the desired path by applying counteracting inputs at the steering wheel. The driver mainly performs the above tasks by monitoring feedback information from the vehicle motion, e.g. position on the road and steering feel. The driver and vehicle interaction thus forms a closed-loop system of Figure 1.1. During everyday driving, human drivers however prefer to invest the minimum effort and like to be relieved of the need for persistent control action (Crolla, 1992). An important demand for the vehicle handling performance is therefore to avoid any unpredictable variations or changes in the vehicle dynamic response to driver steer inputs.

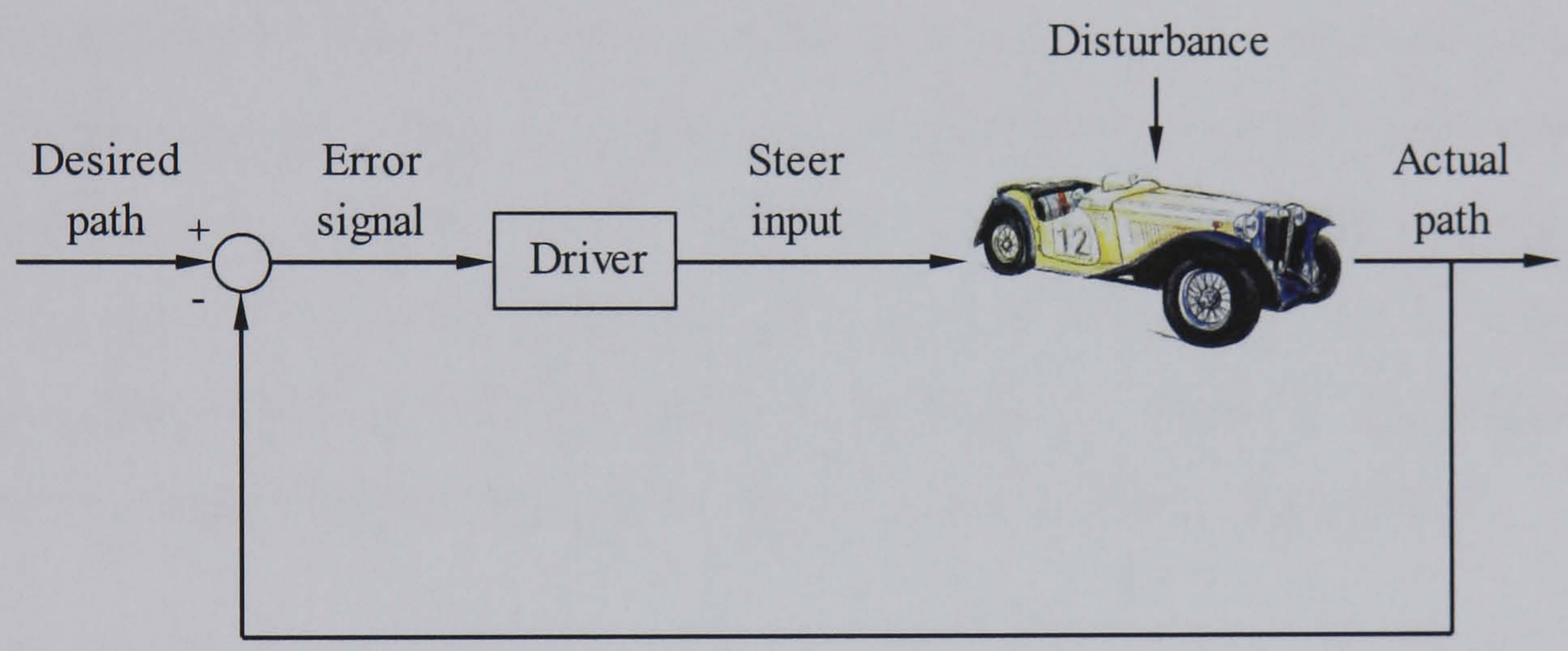

Figure 1.1 Block diagram of the driver-vehicle closed-loop system

1.1.2 Motivation and framework for active vehicle dynamics control

Generally, in nearly all driving situations, the handling response of a vehicle is primarily determined by the forces generated at the contact patch between tyre and road surface. Tyre forces, however, are limited by the road surface coefficient of friction and the instantaneous vertical load of the tyre. Modern vehicles perform very well when operated under typical conditions such as clean, dry and smooth road surfaces at moderate speeds. Under these conditions, the tyres may remain within the linear range of operation and normal drivers can handle the vehicle without any difficulty. In such situations, the dynamic response of the vehicle is predictable to the driver and the driver can experience the driving pleasure. However, as operating conditions become less typical, for example driving the vehicle on slippery or rough roads at too high speeds, vehicle handling behaviour may change dramatically and

become unpredictable, increasing driver stress and reducing safety. Under these conditions, the tyres normally approach or reach the limit of adhesion and the level of control mainly depends on the skills of the driver. Another case is that when the vehicle is subject to external disturbances arising from crosswind or split-μ braking, the driver requires some reaction time to make a decision and to take actions, and then the driver may overreact to the disturbances and make situations worse.

Therefore, the primary motivation for active vehicle dynamics control is to increase the range of conditions under which the vehicle behaves predictably so that the driver is not caught by surprise and can use his driving skills acquired during normal driving to control the vehicle in emergency manoeuvres. Consequently the driver workload can be significantly relieved and vehicle stability can be improved. In addition, active controls can also be used to enhance vehicle comfort and response in normal/typical driving situations with which normal drivers are familiar. The third goal is to maintain consistent vehicle behaviour in the presence of system parameter variations (e.g. change in the vehicle forward speed) and external disturbances. As an overall aim, vehicle motions should be minimised in response to external disturbances and optimised in some sense in response to driver control inputs (Crolla, 1992).

Figure 1.2 shows the generalised framework for active vehicle dynamics control. Herein, driver inputs are applied to both the vehicle and a reference model which is utilised to represent the ideal vehicle response with respect to driver inputs. The actual response of the vehicle is then compared with that of the reference model and the difference between them is used by the controller to determine the control effort. Finally the actuator takes actions to cause the vehicle to follow the desired response produced by the reference model. Hereinafter, the active control systems are designed to assist the driver by applying additional control actions or by modifying driver steer inputs. That is, in the whole vehicle system, the driver still serves as the primary controller and the active controllers are utilised as the secondary ones.

One should note that due to the lack of well-understood driver models, handling analysis in this thesis is mainly based on open-loop study where tests are intended to show the vehicle characteristics in response to driver steer inputs. In other words, it is assumed that the driver does not make any corrections to the steering wheel angle

after applying an initial steer input for negotiating a specific manoeuvre. The functions of these control systems are therefore to change and improve the open-loop vehicle handling behaviour. These compensations take place before the variations in the open-loop vehicle behaviour are recognised by the driver and thus the driver can concentrate more on the task of *path following*. The generic structure of Figure 1.2 can be applied to integrated as well as stand-alone vehicle dynamics control systems.

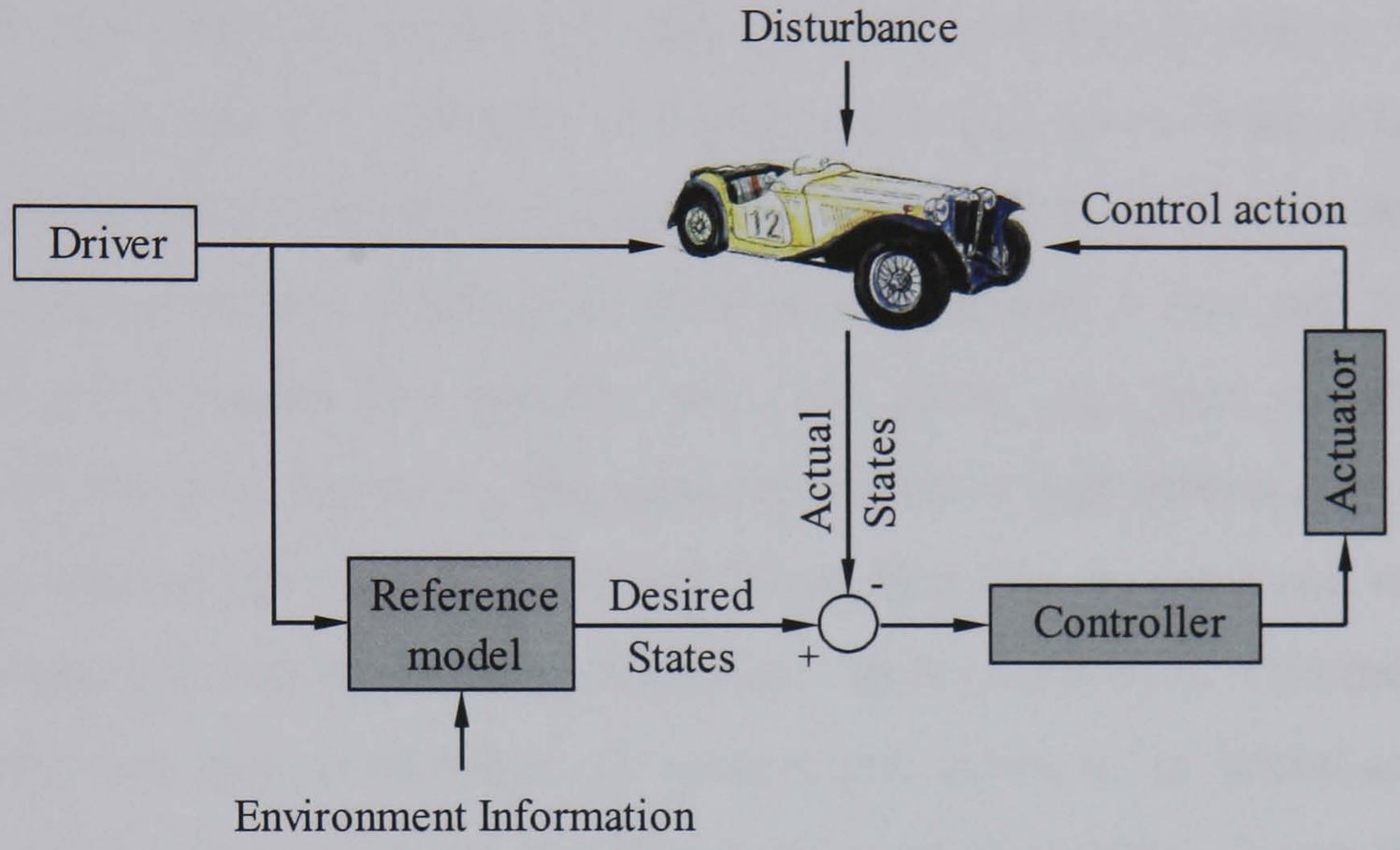

Figure 1.2 Generalised framework for active vehicle dynamics control

1.1.3 Active control of vehicle handling

Various stand-alone control systems have been developed for the purpose of active control of vehicle handling. These stand-alone control systems have effective regions and basic functions of their own and may fall into one of the following three categories in terms of the tyre forces which they directly aim to affect.

- Active steering systems: Active Front Steering (AFS), Active Rear Steering (ARS) and Active Four Wheel Steering (A4S);
- Active roll moment distribution control systems: Active Roll Bar, Active Suspension and Controllable Dampers;
- Dynamic stability control (DSC) systems: driveline based DSC and brake based DSC.

By modifying the steer angles of front or/and rear wheels, active steering systems directly affect lateral tyre forces of the corresponding axle, and consequently vehicle

handling. However, due to the inherent saturation property of lateral tyre forces with respect to tyre slip angles, these active control systems are most effective in the linear regime, where the lateral tyre force is proportional to the corresponding slip angle. The effect of active steering systems diminishes sharply when the lateral acceleration becomes large or the limit of tyre adhesion is approached.

In the case of active roll moment distribution control, the front/rear split ratio of the total lateral load transfer can be affected by changing the roll moment distribution between the front and rear suspension. During cornering, lateral load transfer across both axles takes place and leads to a reduction in lateral force of the corresponding axle due to the nonlinear relationship between lateral tyre forces and tyre vertical loads. The more lateral load transfer per axle occurs, the less the lateral force capability for that axle. Hence, by changing the front/rear distribution ratio of the total lateral load transfer, the balance of lateral forces between the front and rear ends of the vehicle and thus vehicle handling behaviour can be modulated. This mechanism is quite a subtle one because its effect increases in proportion to the lateral acceleration, which is indeed a measure of the handling severity (Selby, 2003). It can therefore be used to effectively influence vehicle handling in mid to high-range lateral accelerations.

In contrast, both driveline based and brake based dynamic stability control systems utilise differential longitudinal tyre forces between two sides of the vehicle to directly generate a corrective yaw moment and to maintain vehicle stability. Such systems are particularly powerful when the vehicle approaches the performance limit where the lateral tyre force is close to or even reaches saturation. Dynamic stability control systems, especially the brake based ones are however only desirable for limit handling rather than normal driving situations. This is due to the braking effect which interferes with the longitudinal vehicle dynamics and may be objectionable to the driver.

Different stand-alone vehicle dynamics control systems are therefore optimised individually in specific regions of the lateral vehicle dynamics and there is no single system which can be effective throughout the vehicle handling regime or in all driving situations. In other words, simultaneous presence of various stand-alone vehicle dynamics control systems on a single vehicle is inevitable in order to keep the vehicle

stable at all times. This actually raises the question how to organise these stand-alone systems in order to achieve an improved overall vehicle performance.

1.2 Integrated Vehicle Dynamics Control

Active vehicle dynamics control systems do not control vehicle motions directly but by modulating the tyre forces. All tyre forces are however generally coupled and the vehicle motions are interconnected. The control of vehicle dynamics in one direction may also indirectly influence other vehicle motions. For example, the use of single-wheel braking to control vehicle stability will certainly interfere with the longitudinal vehicle dynamics. In addition, control objectives of different stand-alone control systems may also be in conflict. Furthermore, the increase in separate sensors, actuators and power supplies resulting from new functions with respect to vehicle dynamics control will result in an increase in system complexity, cost and weight which are apparently commercially undesirable. Figure 1.3 schematically shows a control configuration similar to that presented by Coelingh *et al.* (2002) with stand-alone control systems operating in a combined or parallel manner. As can be seen, overall system complexity increases dramatically as the number of actuators, sensors and functions increases.

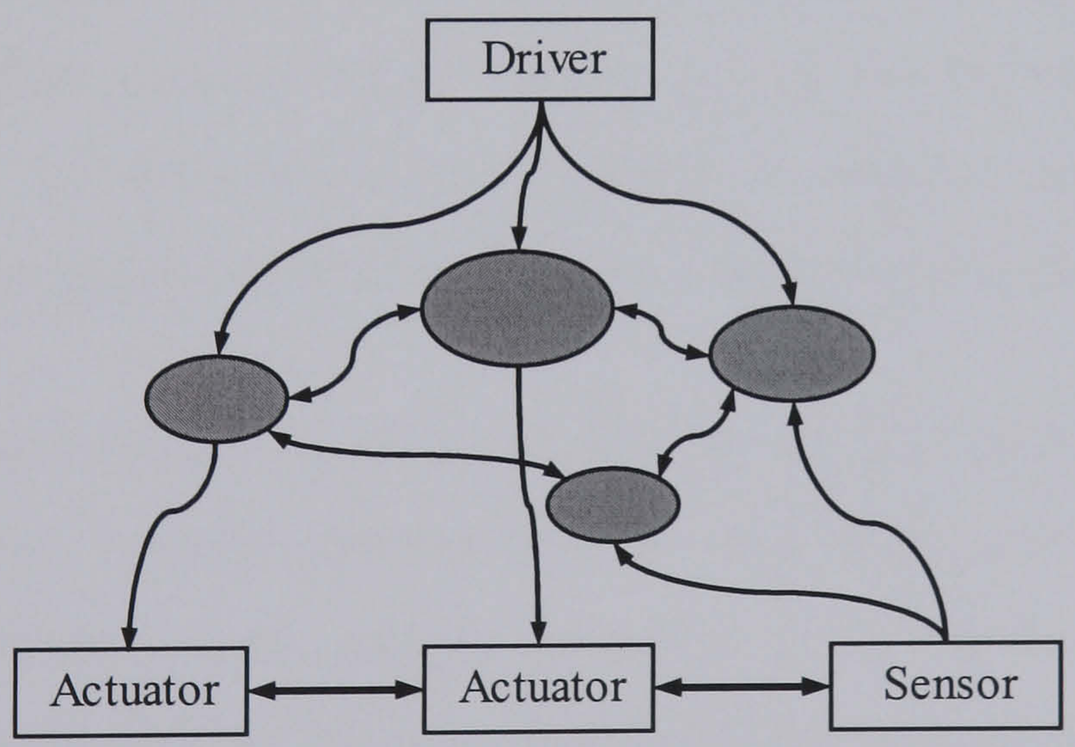

Figure 1.3 Schematics of the combined control configuration

Therefore, in order to achieve an improved overall vehicle performance, vehicle dynamics control should be performed in an integrated rather than combined manner. The difference between combined and integrated control will be explained in Section 2.5. In this thesis, the term "integrated" is limited to the functional integration of

vehicle dynamics control systems rather than the hardware integration. But integrated vehicle dynamic control does benefit from sharing sensor information and actuator operation. Finally all of the existing stand-alone control systems will work together and achieve synergies, anticipating driver and vehicle actions and reacting in the coordinated way. As a result, the overall effect is the optimal vehicle dynamics control. Eventually, drivers will benefit from enhanced vehicle dynamic response and safety, ranging from normal driving conditions to extreme manoeuvres, especially in bad weather or on unpredictable road surfaces. Consequently the design of integrated control systems is the next important step of the development of active vehicle dynamics control.

Potential benefits of system integration

In addition to the advantage of improving vehicle dynamic response as discussed above, the integration of vehicle dynamics control systems also has the following potential benefits:

- Cost and system complexity reduction - this can be achieved by avoiding unnecessary duplication of components and by sharing sensor information. Stand-alone vehicle dynamics control systems have sets of sensors and actuators of their own. The integration of these systems would remove the implicit limit of a one-to-one relationship between control objectives and corresponding sets of sensors and actuators. In addition, it is possible to achieve redundancy through information sharing and communication between different control systems.

- Flexibility improvement - with a specific design approach, the integration of vehicle dynamics control systems permits a modular and distributed design process. The whole control and development work can be broken down into several sub-tasks and each sub-task may then be designed separately. This may form a standard or generic system configuration and permit the plug-and-play operation for all stand-alone control systems (Gordon *et al.*, 2003).

The potential for these advantages is obviously limited by the level of integration and the number of stand-alone control systems available. There are two different approaches which can be used to design integrated vehicle dynamics control systems.

One is referred to as the *bottom-up* approach which uses two or more previously developed stand-alone control systems to design the integrated control system; the other is called the *top-down* approach which employs multivariable control techniques to design a model based global controller with the subsystem interactions considered in the control design process. These two approaches and their applications will be described further in the following Chapter. In this thesis only two of the three stand-alone vehicle dynamics control systems described in Section 1.1.3, active steering system which includes AFS and ARS and dynamic stability control system (both driveline based and brake based) will be examined to form the final integration.

1.3 Thesis Outline

In order to address the problems raised above, the remainder of the thesis is organised as follows:

In Chapter 2, a detailed review of published papers relating to the control of vehicle handling is presented. The review examines a large number of stand-alone and integrated vehicle dynamics control systems that have been studied for improving vehicle handling performance. The relative merits of two different concepts of system integration are also analysed and associated conclusions are included. In the context of this broad review, the aims and objectives for this research are defined.

In Chapter 3, the necessary level of vehicle modelling required for simulation studies is described. Both the 2DOF linear bicycle model for controller design and an 8DOF nonlinear vehicle model for control performance evaluation are developed.

In Chapter 4, a thorough analysis of the uncontrolled lateral vehicle dynamics is performed as a first step towards handling control system design. Different aspects of the lateral vehicle dynamics and three distinct regions with respect to the level of lateral acceleration are identified. Two distinct control objectives, steerability and stability which cover the entire range of vehicle handling are defined. The corresponding control tasks range from improving vehicle steering response for normal driving situations to maintaining vehicle stability during emergency

manoeuvres. In particular, the relationship between the two control objectives established in this thesis over the entire range of vehicle handling enables a new control configuration to be proposed. Different functions of individual controllers are then formulated and each stand-alone control system is assigned a suitable control task.

In Chapter 5, the design of the active steering subsystem (AFS and ARS) controllers is presented. In accordance with the steerability objective, the 2DOF linear bicycle model is used as the reference model to represent the ideal behaviour of the vehicle in response to driver steer inputs. The sliding mode control (SMC) technique is then employed for controller design in order to achieve robustness with respect to vehicle system parameter variations and external disturbances. In order to fully evaluate the performance of the stand-alone steerability controllers, the ability of these systems to affect vehicle handling over a wide range of handling regimes is analysed. New results clarifying the relative performance properties of AFS and ARS are presented. In addition, the functional difference between AFS and ARS is also compared in terms of the ability to generate the required corrective yaw moment.

In Chapter 6, the dynamic stability subsystem controller is designed using the phase-plane method. A reference stable region is defined through vehicle stability analysis in the phase plane of the vehicle sideslip angle and its angular velocity. Both driveline based and brake based DSC subsystems are developed and new results comparing the relative merits of these two systems are presented. In order to reduce the negative effects of individual actuation concepts, a new DSC subsystem which combines torque transfer and single-wheel braking is proposed. In addition, for the driveline based subsystem, a non-conventional torque transfer differential model is also introduced to allow both the amount and direction of torque transfer on the driving axle to be controlled.

In Chapter 7, the design of a novel integrated vehicle dynamics control system is presented. Combined control of the two subsystems, AFS and driveline plus brake based DSC is first examined to form the benchmark for further integration analysis. A rule based integration scheme is then proposed to coordinate the control actions of the two corresponding stand-alone controllers. The proposed integrated control system is

compared with the combined control system for various manoeuvres. Simulation results for this approach are presented and the improvements in overall vehicle handling performance are analysed.

Chapter 8 highlights some key conclusions of the thesis and recommendations for further research based on the outcomes of the thesis.

Chapter 2

Literature Review

Abstract: *A detailed review of published work relating to both stand-alone and integrated vehicle dynamics control systems for vehicle handling is given in this chapter. The current state of stand-alone vehicle dynamics control systems is first examined and then followed by a survey of integrated vehicle dynamics control systems and a discussion of the reviewed studies. Finally, the aims and objectives of the research are specified.*

2.1 Introduction

The development of active systems for the control of vehicle handling has been ongoing since the beginning of 1980's, with Active Rear Steering (ARS) being the first to receive considerable attention (Sharp and Crolla, 1988; Furukawa *et al.*, 1989), which was then followed by the introduction of Active Four Wheel Steering (A4S) (Nagai, 1989). From the start of 1990's, Direct Yaw Moment Control (DYC) or functionally similar, Variable Torque Distribution (VTD) control began to attract more interest largely by making use of the existing ABS/TCS hardware (Naito *et al.*,

1990; Motoyama *et al.*, 1993; Inagaki *et al.*, 1994). In addition to this, Roll Moment Distribution (RMD) control also began to be introduced around this time (Abe, 1992; Williams and Haddad, 1995; Everett *et al.*, 2000; Konik *et al.*, 2000). More recently, much interest has been concentrated on the research of Active Front Steering (AFS) or Steer-By-Wire (SBW) technique (Ono *et al.*, 1998; Mammar and Koenig, 2002). In particular, AFS has begun to attract new commercial interest since its first introduction by BMW on their 5 Series in 2004.

Due to the functional overlaps or interactions between different stand-alone vehicle dynamics control systems, the concept of integrated vehicle dynamics control has been proposed in order to achieve optimum overall vehicle performance. The following sections will be devoted to presenting an extensive review of literature relating to active vehicle dynamics control systems for vehicle handling. In line with the scope of this thesis, the review of stand-alone vehicle dynamics control systems will be restricted to the two chosen categories of active steering and dynamic stability control systems. However, in order to examine the general concepts of integration, active suspension systems will be taken into account in the review of integrated vehicle dynamics control systems.

2.2 Stand-alone Vehicle Dynamics Control Systems

2.2.1 Active steering systems

Active steering systems affect vehicle handling behaviour through directly modulating the generation of lateral tyre forces. In this section three active steering schemes, Active Rear Steering (ARS), Active Front Steering (AFS) and Active Four Wheel Steering (A4S) will be examined, respectively.

Active Rear Steering (ARS)

Active rear steering has received extensive attention from both automakers and academia and has been regarded as a promising tool to improve vehicle handling since the beginning of 1980's. In practice, several Japanese manufacturers tried ARS systems commercially around this time, but few now remain. Recently, ARS has received more interest in the USA for large pick-up trucks, e.g. GM Chevrolet

Silverado. The control objectives of active rear steering systems vary widely: some aim to minimise vehicle sideslip angle (off-tracking) and others attempt to create a neutral handling characteristic or follow the desired dynamic model.

The most common control task for ARS is to minimise the sideslip angle of the vehicle so that the centre of gravity (CG) follows the given path. In the early 1980's, front wheel steer angle feedforward ARS systems were developed and some were commercially used. Among them, Shibahata *et al.* (1986) and Takiguchi *et al.* (1986) for Mazda proposed the so-called speed sensing ARS. In this system, at low speeds the rear wheels are steered in the opposite direction to the front ones for better manoeuvrability, and at high speeds the converse will be the case to offer stability augmentation.

Sano *et al.* (1986, 1988) for Honda contend that similar improvements to those mentioned above can be achieved by varying the rear/front steer angle ratio according to the steering wheel angle such that for small steering wheel angles the front and rear wheels steer in the same direction, but when the steering wheel is turned in a large angle, the rear wheels steer in the opposite direction to the front ones. The contention is based on the fact that large steering wheel angle inputs are normally not used at high speeds while they are usual for low speed manoeuvring.

A similar idea can be found in Fukui *et al.* (1988) where for quick turning of the steering wheel the rear wheels should be steered in the opposite sense to the front wheels, but for slow turning of the steering wheel the rear wheels would be steered in the same sense as the front ones. Control laws of these systems are derived so that the vehicle sideslip angle becomes zero in both steady and transient states. In such ARS systems, the yaw rate response to steer inputs becomes that of a first order system. Whilst the feedforward ARS can to some extent improve vehicle handling, it cannot compensate for external disturbances such as crosswinds or split-μ braking.

To overcome the above problem, yaw rate feedback ARS is developed (Sato, 1983, 1991; Whitehead, 1988; Yamamoto *et al.*, 1989; Xia and Law, 1992; Tanizaki and Yamanaka, 1998). The control law of such ARS is derived from an inverse model of the 2DOF linear single track model and is a combination of front wheel steer angle

feedforward and yaw rate feedback to make the vehicle sideslip angle to be zero at all times. Computer simulations confirm the effectiveness of the proposed control strategy, especially when the vehicle is subject to external disturbances. However, robustness of the developed ARS with respect to vehicle forward speed and road friction coefficient variations is questionable.

Wakamatsu *et al.* (1996) propose an adaptive sideslip angle minimisation ARS which consists of feedforward compensation, yaw rate feedback and a simple road friction coefficient estimator to minimise the vehicle sideslip angle even on slippery road surfaces. In principle, the proposed adaptive ARS is similar to the above yaw rate feedback ARS in terms of control objective and strategy. The overall control system is formulated as an Internal Model Control structure with two degrees of freedom in which the feedforward compensator is dependent on the estimated friction coefficient, compared with the fixed gain in the above yaw rate feedback ARS and the linear feedback compensator is designed by μ-synthesis to provide robustness against model and estimation errors. Performance improvements induced by the proposed ARS, especially in robustness to road friction coefficient variations over feedforward only and fixed-gain yaw rate feedback ARS can be seen through both simulation and experimental results.

In addition to conventional control techniques mentioned above, intelligent control techniques such as fuzzy logic control have been applied to ARS as well. Szosland (2000) proposes a feedforward fuzzy logic ARS controller to minimise vehicle sideslip angle. The control law is formulated by taking the front wheel steer angle and vehicle speed into account, i.e. the rear wheel steer angle is determined by the fuzzy logic controller with front wheel steer angle and speed dependent nonlinear front-to-rear steer ratio being inputs. This method is shown to be effective in a specific nonlinear vehicle model at high speeds but no consideration is taken on how to actively steer the rear wheels at low speeds. In addition, though the descriptions of related inputs and outputs of the fuzzy controller in terms of fuzzy sets and linguistic variables are given which is the unique value of such a technique, there is no discussion of how the rule base is derived. Furthermore, once again, lack of feedback in the whole control structure cannot guarantee vehicle stability when the vehicle is subject to changing environmental conditions.

The sideslip angle minimisation ARS does provide improvements in terms of quicker steering response and better stability compared with the conventional 2WS, however it is at the expense of excessive understeer (Senger and Schwartz, 1987). Whitehead (1988) and Nalecz *et al.* (1989) argue that improvements in vehicle handing induced by such ARS systems are slight and only correspond to high frequency excitation at high speeds. In other words, benefits of reduction in vehicle sideslip angle are only tangible in rarely occurring situations such as an extreme manoeuvre likely leading to instability. Shibahata *et al.* (1986) also report that steering the rear wheels in the opposite direction to the front ones at a large angle is not very effective in improving low speed manoeuvrability because it makes the rear end of the vehicle 'stick out' further toward the outside of the curve.

As an alternative to the zero sideslip angle control strategy, a control logic which is based on model following control techniques is proposed to make the vehicle to follow the desired dynamic model through the state feedback of both yaw rate and sideslip angle (Hirano and Fukatani, 1996, 1998). An observer whose parameters vary with vehicle forward speed is used to estimate both yaw rate and sideslip angle by applying a frequency filter. The total rear wheel steer angle is the sum of a feedforward part which is derived by an inverse model of the desired dynamics and used to compensate for the steady state response and a feedback part which is calculated based on μ-synthesis to guarantee the robust control performance in spite of changes in vehicle parameters and to compensate for the transient dynamics. In addition, the feedback controller gain is designed to be frequency dependent so that the control performance varies according to frequency, i.e. high gain in low frequency ranges for good performance and low gain in high frequency ranges for robustness. Whilst both simulations and actual tests demonstrate the effectiveness of the proposed controller, using only one input to control two states is a questionable technique.

Active Front Steering (AFS)

In recent years, being an effective tool to affect vehicle handling, active front steering has attracted more and more attention. Such active handling control usually serves as a steering support system by applying an additional steer angle to the driver's steer command. Due to the extra steering action, AFS should be constructed with the steer-

by-wire concept, but at the present time, it could be implemented by superimposing a controller on the conventional steering system, as shown in Figure 2.1.

Wang and Nagai (1992) develop an AFS system to track the reference yaw rate and lateral acceleration by using a pole-assignment self-tuning adaptive control algorithm and a least-square parameter identification method. In this paper the characteristic polynomial of the closed-loop system is assigned to be equal to the denominator of the transfer function of the reference model. The proposed controller is designed in discrete time to respond adaptively to the changes in the vehicle-environment system. Whilst it is found through simulations that the adaptive controller can improve vehicle handling response and reduce driver steering burden in the presence of sudden changes of road friction during turning along a circular curve, the effect of vehicle forward speed variation on the proposed controller is not investigated.

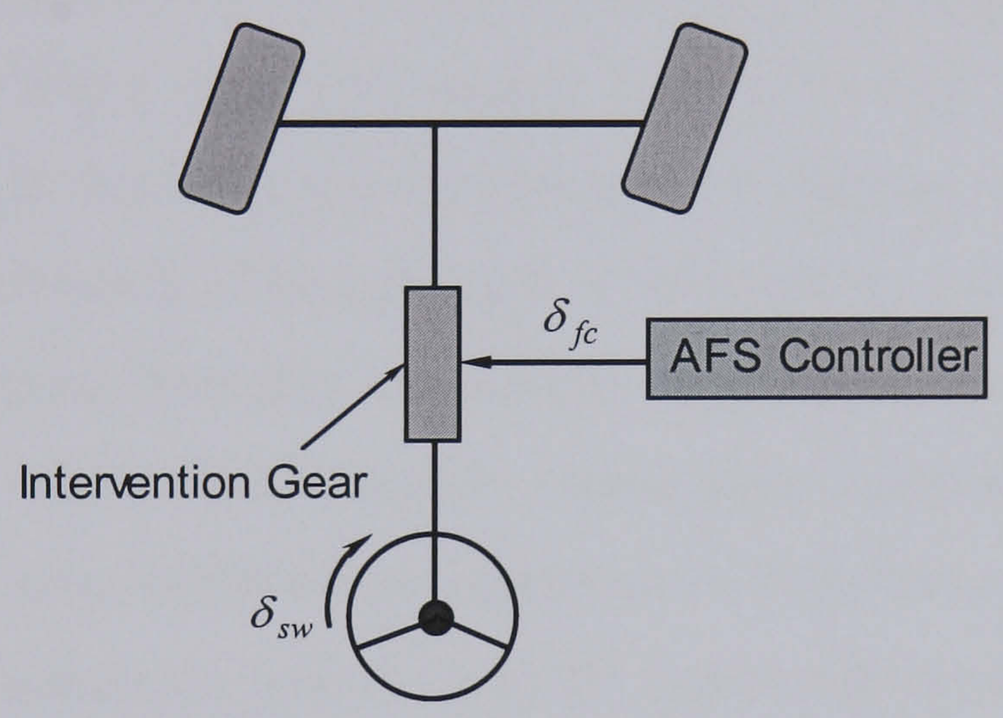

Figure 2.1 Schematics of AFS system actuation

Tagawa *et al.* (1996) propose an AFS controller based on a robust model matching algorithm to achieve robustness with respect to parameter variations and disturbances such as varying speed and road surface friction. The proposed controller is used to realise the desired closed-loop frequency characteristics between the driver steer input and vehicle yaw rate rather than follow a reference signal. An interesting aspect of the study is that the ratio of yaw rate and vehicle forward speed is chosen as the feedback variable in the controller design so that a constant circular radius may be maintained for a constant steer input even in the presence of speed change. Computer simulations in both frequency and time domains are carried out to show the effectiveness of developed controller. However, the fact that there is no description of the model used for simulations is the main weakness of this paper.

Ono *et al.* (1996, 1998) provide a new way to analyse vehicle stability using bifurcation theory. The stability analysis is performed through a study of the vehicle state trajectories in the yaw rate - sideslip angle plane. This work gives explanations to a number of well-known features of vehicle dynamics such as the effect of rear lateral tyre force saturation on vehicle stability and the so-called "counter steering" which is often used by skilled drivers to get through sharp cornering. An adaptive H_∞ controller based on the model following structure is then proposed and shown to effectively stabilise a vehicle through identifying the peak cornering force of a tyre and limiting the steering wheel angle so that all tyres work in the unsaturated regions on the slip-force curve. Whilst the work is clear and well argued, the use of a simplified linear vehicle model for demonstrating the effectiveness of the proposed control strategy weakens its persuasion.

A body of work, (Ackermann *et al.*, 1996; Ackermann, 1997; Ackermann and Bünte, 1997; Sienel, 1997; Wang and Ackermann, 1998), develop a concept of robust unilateral decoupling to attenuate yaw disturbance by making yaw rate unobservable from the lateral acceleration. Through such a decoupling, the proposed controller attempts to take over the disturbance attenuation task and only leave the primary path-following duty to the driver. Both computer simulations and road tests are carried out and clearly show the effect of the robust controller on disturbance rejection. However, the inspected driving situations largely lie in the linear region of the vehicle handling dynamics and do not result in large sideslip angle so that lateral tyre force nonlinearities are not accounted for in these tests. In addition, the robust decoupling may increase the degree of instability when tyres reach their performance limits and lateral tyre forces are saturated. Accordingly, whilst the work is theoretically thorough, the controller effectiveness is not verified over a wide enough handling regime to reach useful conclusions.

Two papers (Mammar and Baghdassarian, 2000; Mammar and Koenig, 2002), the latter in particular, present a complete discussion of coprime factors based two-degree-of-freedom H_∞ AFS controller synthesis for both good yaw rate tracking and disturbance rejection. The former formulates a highly idealised robust controller while the latter introduces several refinements over the previous work. Both papers report that increasing speed and road adhesion reduction have the same effect on vehicle

stability and easily lead to damping reduction through the study of vehicle stability in the yaw rate - sideslip angle plane. Several simulations at different speeds and on various road surfaces are carried out to verify the work using a nonlinear vehicle model with a Pacejka pure lateral slip tyre model, however the load transfer and roll mode which play a crucial role in the lateral vehicle dynamics, especially in high lateral acceleration region are not considered.

Huh and Kim (2001) propose an AFS system to maintain the optimal lateral tyre forces during steering. An Extended Kalman Filter is used to estimate the individual lateral tyre forces and a fuzzy logic controller is then designed to compensate for the lack of lateral tyre forces experienced on low-μ surfaces. The work is verified by using a steering Hardware-In-the-Loop system under different road friction conditions. Though the proposed control and estimation techniques are found to be effective, some undesirable high frequency dynamics introduced in the controller output is not explained and may limit its application.

Güvenc *et al.* (2001) provide an AFS controller design using a two degrees of freedom control structure to improve yaw dynamics in terms of steering command tracking and disturbance rejection. The robust controller is designed to intervene only when necessary with a low frequency fading feature which is achieved through the disturbance observer and a velocity gain scheduled implementation is employed. Whilst computer simulations demonstrate the effectiveness of the proposed controller, the specific six operating conditions for controller design and linear simulations used in the paper do not represent the real driving tasks and situations.

Active Four Wheel Steering (A4S)

This section will consider the Active Four Wheel Steering (A4S) systems in which both front and rear wheels can be actively steered in order to control the balance of lateral tyre forces on front and rear axles. Such systems are actually designed on the basis of multi-input-multi-output control techniques.

Nagai (1989) proposes a LQR A4S controller using model following control strategy. The controller is designed to track the reference yaw rate and sideslip angle. Two

control laws: feedforward compensation only and both feedforward and feedback compensations are formulated to actively steer front and rear wheels cooperatively. Computer simulations and experiment demonstrate that the transient steering response of the vehicle with A4S can be improved regardless of the existence of feedback compensation, but much higher stability under side wind gust can be achieved only by the A4S controller with both feedforward and feedback compensations. As the proposed LQR controllers are derived completely from the virtual vehicle model, the problem of robustness against varying velocity and road friction condition remains. In addition, there is no detailed description of both the reference model and the vehicle model used for simulations.

A simple 2DOF controller for A4S which consists of both feedforward and feedback compensations using a model following control strategy is presented in (Aga *et al.*, 1990). A linear control law derived in the frequency domain is used for both yaw rate and sideslip angle tracking. The control performance is verified in simulation on a linear vehicle model and subjective evaluation of this system by test drivers suggests the controlled vehicle is more responsive to steer inputs and more stable against external disturbances but experiences increased roll rate which is undesirable from the driver point of view. To cope with this problem, the control law in which both feedforward and feedback gains can be calculated on line by least squares method is redesigned to track the desired yaw rate and roll angle. Simulation and experimental results at a specific speed show both better yaw rate tracking and smoother roll response compared to both feedforward only and feedback only ARS. However, the difference between the simulated and tested response characteristics especially at high frequencies suggests that the linear nominal model based simple frequency controller lacks robustness with respect to external disturbances. This may be the key concern in real implementations.

An ARS based A4S system can be found in (Lin, 1992). This work refines the yaw rate feedback ARS by adding an extra yaw rate feedback control to the front wheels so as to overcome the oversteer tendency at low speeds and extreme understeer at high speeds of the zero sideslip angle ARS. The proposed closed-loop controller still attempts to minimise the vehicle sideslip angle and at the same time maintain a constant steering characteristic similar to the passive vehicle. The extra linear

feedback controller is formulated using the 2DOF linear bicycle model and makes the steering characteristics of the vehicle equipped with A4S independent of vehicle speed. From the simulation results in both frequency and time domains it is found that the proposed control system is effective in improving vehicle transient response and appears to achieve a similar handling feeling to the passive vehicle. Nevertheless, it is not clear whether this analysis remains valid on a nonlinear vehicle model.

Ackermann (1990, 1993, 1994) provides a theoretical and comparative study of the design of robust active steering controllers. The initial study (1990) proposes an AFS control law to decouple the yaw mode from the lateral mode of the front axle and help the driver track a given path by yaw rate feedback to the front wheels. To overcome the drawback of degraded yaw damping induced by the AFS control law, a second control loop is introduced to make yaw dynamics independent of vehicle velocity through yaw rate feedback to rear wheel steering. Although simulations of disturbance rejection are carried out and some results are presented, no description of an appropriate vehicle model is provided and it fails to demonstrate improvements in vehicle handling in the nonlinear regime. In addition, although the work states that the proposed controllers are robust, there is however no related study given in the papers.

The design of a robust A4S controller can be found in (Gianone *et al.*, 1995). The work compares the conventional LQR controller with the combined robust LQR/ H_∞ controller for ARS and A4S with respect to yaw rate and sideslip angle tracking. In this study, a structured description of parameter variations and disturbance rejection for A4S vehicles is given first and then followed by the optimal robust controller design. Only the variation in rear tyre cornering stiffness is treated as uncertainty and the worst case simulation for both state tracking and disturbance rejection is performed on a linear vehicle model. Though the simulations verify the effectiveness of the proposed robust controller in this specific design case, the inclusion of other uncertainties such as vehicle forward speed and road friction condition and the use of a nonlinear vehicle model would provide more insight to the features of this controller.

Horiuchi *et al.* (1996) investigate another robust A4S controller using a two-degree-of-freedom control structure in which a feedforward controller is designed based on

an inverse linear model to track the reference yaw rate and lateral acceleration and a feedback H_∞ controller is formulated to provide robustness to model uncertainty and external disturbances. Whilst both step steer simulations of a nonlinear vehicle model with load transfer and nonlinear tyre characteristics included and proving ground tests show robustness of the proposed controller with respect to vehicle speed and road friction, a broader range of simulations would be more insightful and useful to demonstrate the control performance.

A similar study to (Lin, 1992) is presented in (Kleine and Van Niekerk, 1998) based on the well-known Whitehead (1989) control law which leads to zero sideslip angle. The proposed A4S controller attempts to eliminate the extreme understeer tendency induced by the Whitehead control law and to provide steering response similar to that of the passive vehicles through additional yaw rate feedback to the front wheels. This paper reports that the feedback of yaw rate to both front and rear wheels can provide decoupling of sideslip mode and yaw rate even though it is not complete and meanwhile reduce both sideslip and yaw rate to be stable first order systems. The theoretical analysis is performed on a linear bicycle model and the resultant feedback gain is velocity dependent. Simulations using an appropriate nonlinear vehicle model demonstrate that the extended controller improves yaw response in terms of rise time and increased damping without losing the ability to minimise sideslip angle. In addition, the strong understeer characteristic found in Whitehead's algorithm is removed as well. Frequency analysis also shows that the yaw rate gain can be kept constant up to a higher frequency and phase lag is smaller compared to the passive and ARS controlled vehicles. Though vehicle handling response is shown to be improved in terms of rapid transient behaviour, there is no description of what is the ideal or driver preferred steering characteristics. Furthermore, robustness with respect to vehicle forward speed variations needs to be analysed to draw useful conclusions.

Summary

The preceding section has reviewed a large amount of work relating to active steering systems for vehicle handling control. ARS, AFS and A4S all have received a great deal of attention due to the demand for developing active safety systems and intelligent highway systems.

The most common objective of ARS seems to minimise vehicle sideslip angle for off-tracking reduction and steering response improvement. This however usually leads to excessive understeer which in turn deteriorates vehicle steering response. Few papers have addressed this problem and most of the studies reviewed above concentrate only on this specific control objective, though the selection of appropriate control tasks is the key to an effective control system. Unfortunately, this has not been given consideration with respect to ARS and therefore it is difficult to fully evaluate ARS and compare ARS with other active steering systems.

In the case of AFS, dominant studies have focused on developing complex control laws rather than presenting a realistic and general discussion of the vehicle dynamics problem. Although various advanced control techniques have been applied to the controller design, no paper has presented any investigation about the functional limitations of the proposed controller, especially in the nonlinear region of tyre dynamics. The work reviewed largely aims to improve yaw dynamics in terms of steering command following and disturbance rejection. However, these studies mostly emphasize linear handling models and the lack of severe manoeuvres for control performance evaluation is the main drawback of such systems.

The A4S approach allows two vehicle states, yaw rate and sideslip angle to be controlled simultaneously by two control inputs, front and rear wheel steer angles. Both ARS based A4S for reducing the strong understeer tendency caused by ARS and model following A4S for vehicle state tracking are proposed using various robust and optimal control techniques. A4S studies reviewed above however have the same problem of lacking analysis of the vehicle dynamics problem.

In summary, all the active steering systems presented in the literature have the following common shortcomings: i) the use of excessively simple models, especially tyre models for evaluating complex or even nonlinear controllers; ii) the lack of realistic handling manoeuvres used to fully investigate the performance and limitations of the proposed control systems; iii) the lack of thorough analysis of the vehicle dynamics problem. Therefore, the design of active steering systems needs to be refined in the light of clear and well-defined control objectives for improving vehicle handling over the entire range of vehicle handling. In addition, the utilisation

of advanced control techniques for active steering systems cannot be said to be advantageous unless the studies consider a vehicle model with appropriate degree of complexity and an appropriately broad range of handling manoeuvres for control performance evaluation.

2.2.2 Dynamic stability control systems

Dynamic Stability Control (DSC) is another active safety technology introduced since ABS and TCS. This technology uses differential longitudinal tyre forces, either driving or braking forces, to generate a corrective yaw moment and then to control vehicle lateral and yaw motions under emergency conditions. Figure 2.2 shows the operation principle of DSC systems through the tyre friction circle when the vehicle approaches the handling limit. In such a situation, little additional lateral tyre force is available due to the tyre force saturation properties. However the potential for generating enough differential longitudinal force between left and right sides of the vehicle and then a corrective yaw moment can be expected. In this section, both driveline based and brake based DSC systems will be reviewed.

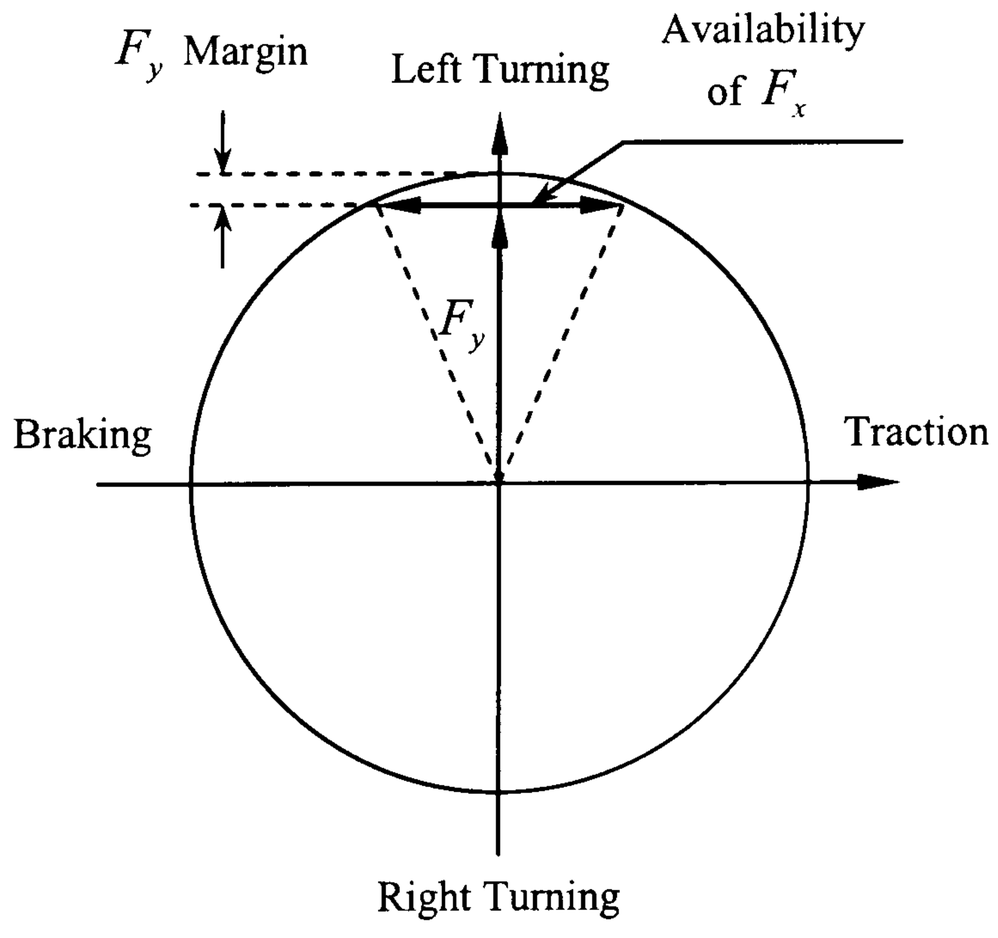

Figure 2.2 Schematic operation principle of dynamic stability control systems

Brake based dynamic stability control systems

The brake based dynamic stability control systems, or referred to as Direct Yaw Moment Control (DYC) can stabilise vehicles by braking one or more wheels to produce the required corrective yaw moment. These systems are well developed and investigated in the literature and are the most common in practice by far. Such

systems can share hardware such as sensors and actuators with ABS so that the cost of implementation can be significantly reduced. Due to the introduction of braking forces, brake based DSC is only desirable to influence vehicle handling at or close to the performance limit. The braking actions are performed automatically and regardless of whether or not the driver applies the brakes. More detailed description and analysis of DSC will be presented in Chapter 6. The literature in this area can be categorised in terms of different controlled variables, i.e. yaw rate, sideslip angle, sideslip angle/sideslip angular velocity and the combination of yaw rate and sideslip angle.

Control of vehicle yaw rate

Abe *et al.* (1996) compare the various control laws for both 4WS and DYC. This work first analyses the drawback of 4WS systems in extreme driving situations and then proposes DYC to overcome this drawback. In order to choose the suitable control strategy for DYC, a comprehensive comparison of both zero sideslip angle and yaw rate tracking strategies by either feedforward only or combined feedforward and feedback control is presented through computer simulations on a nonlinear vehicle model. In addition, a simple scheme for the cooperative control of 4WS and DYC is presented in this study as well. All the control laws are derived using a 2DOF linear bicycle model and it is concluded by the authors that the yaw rate tracking control strategy is more suitable for DYC.

Buckholtz (2002a) proposes a knowledge/rule based intelligent controller for vehicle stability enhancement. The fuzzy logic controller presented in this study is utilised to track the desired yaw rate by assigning a proper wheel slip ratio to each corner of a vehicle and these wheel slip ratios can then serve as reference inputs to the lower-level wheel dynamics controller. Such a control scheme eliminates the need for conversion from the conventional corrective yaw moment to the required braking torque/pressure at individual wheels. It is shown through simulation that the tracking performance of the proposed controller degrades when the vehicle sideslip angle becomes large. A further study in (Buckholtz, 2002b) refines the controller to include the limit of vehicle sideslip angle in the control logic. Comparative analysis of these two controllers demonstrates the improvement in yaw rate tracking for the refined

one. However, the work does not investigate the robustness of the proposed controllers to parameter variations and disturbances.

Control of vehicle sideslip angle

A DYC controller for vehicle sideslip angle tracking is presented in (Yoshioka *et al.* 1998, 1999) by using sliding mode control. The proposed sliding mode controller directly defines the desired slip ratio of individual wheels and sends these values to ABS/TCS as command inputs. Then the system can choose the wheel for the application of braking actions to stabilise the vehicle. In addition, a brief description of the state and parameter estimation techniques used in this study is also presented. This work is evaluated through both simulations of a full nonlinear vehicle model and field tests. The simulation demonstrates that the SMC is more robust to the change in vehicle yaw inertia than the simple PD controller; there is however no further investigation of the robustness to road friction and vehicle speed variations.

Another vehicle sideslip angle tracking DYC is presented in (Abe *et al.* 1999). This work derives the sideslip angle tracking control law using sliding mode theory and the controller design is based on a 2DOF bicycle model along with a simple nonlinear tyre model on board. The corrective yaw moment computed by the sliding mode controller is the direct control input to the vehicle. Various open- and closed-loop simulations of a nonlinear vehicle model and experiment tests on an actual vehicle are conducted to verify the proposed DYC. Similar studies can be found in (Abe 1999; Abe *et al.* 2001). The main outcome of these studies is to compare the proposed DYC with both 4WS for sideslip angle control and DYC for yaw rate tracking. The proving ground test using an actual vehicle equipped with the developed controllers demonstrates that the sideslip angle tracking control is superior to other control strategies for DYC due to the nonlinear tyre characteristics.

Control of vehicle sideslip angle/sideslip angular velocity

A unique approach to vehicle stability analysis is introduced in (Inagaki *et al.* 1994) by Toyota. In this paper vehicle stability is analysed in the phase plane for vehicle sideslip angle and its angular velocity instead of the conventional state plane for sideslip angle and yaw rate. A control algorithm based on this method is then

developed to confine the vehicle states within the predefined stable region in the phase plane. If the vehicle states go outside the stable region, a corrective yaw moment will be generated through braking one appropriate wheel. A similar study is presented in (Koibuchi *et al.*, 1996). The only difference of this work from the previous study is to extend the one-wheel braking algorithm to four-wheel braking in a fixed proportion for improving course tracking. However the one-wheel algorithm is still used in stability or oversteer correction control. Another work in (Yasui *et al.*, 1996) employs the same method to design a dynamic stability control system to stabilise the vehicle in the event of oversteer. In addition, the brake actuator response criteria which should be satisfied by the brake actuator is also investigated in this study to make sure that the real implementation of such a system on an actual vehicle is effective and reliable.

Control of the combination of yaw rate and sideslip angle

Alberti and Babbel (1996) propose a driving stability control system to correct critical course deviations through braking individual wheels. The proposed control system consists of two independent control strategies: one is to track the desired yaw rate using a simple PD regulator and the other is to limit the sideslip angular velocity through a proportional regulator, respectively. Whilst the lane change simulation on slippery road surfaces demonstrates the effectiveness of the developed control system, the possible conflict or interference between two independent control strategies is not investigated as such conflict may degrade the stabilisation capacity of the whole control system. In addition, no description of appropriate vehicle model and yaw moment generation scheme is presented in this study.

A model following control strategy for DYC is presented in (Park and Ahn, 1999). In this study a H_∞ controller is designed based on the 2DOF linear bicycle model. The required corrective yaw moment is generated through brake torque applied at one wheel using a switching control scheme. The main difference of this work from others is that the control input from the proposed H_∞ controller is the brake torque to be applied at a specific wheel rather than the corrective yaw moment. The μ-analysis helps to achieve robust performance and robust stability of the developed control system. Whilst simulation results of a nonlinear vehicle model show good state

tracking and robustness to parameter variations, the effect of the proposed control system on the longitudinal vehicle dynamics is not considered.

Uematsu and Gerdes (2002) propose two new schemes to control yaw rate and sideslip angle simultaneously for maintaining vehicle stability. This study first derives two sliding mode controllers for both yaw rate and sideslip angle tracking using a dynamic sliding surface and a single sliding surface with a weighted combination of yaw rate and sideslip angle, respectively. These two controllers are then compared with those for controlling either sideslip angle or yaw rate alone. It is demonstrated through simulations that the two proposed sliding controllers with combined yaw rate and sideslip angle as the control objective is better than those using only one of them as the control objective. However, this work is only demonstrated on a simple 2DOF vehicle model and therefore the justification of such an approach is relatively weak.

Summary

The brake based dynamic stability control systems reviewed above have concentrated on the selection of controlled variables and the development of control algorithms. Some studies have used a two-step approach: firstly, the DYC controller is designed using various control design methods such as linear quadratic optimal control, sliding mode control or fuzzy logic control to demand a corrective yaw moment; then the brake torques/forces or slip ratios of individual wheels required to generate the corrective yaw moment are derived through a second control loop. Nevertheless, other researchers have only emphasised the development of the control logic and ignored how the corrective yaw moment is generated.

Brake based dynamic stability control systems on one hand have been shown to be a commercially viable technique for improving vehicle limit stability. Among various controlled variables presented in the literature, the control of vehicle sideslip angle and its angular velocity at the handling limit may be the most effective scheme since when the vehicle sideslip angle has the same sign as its angular velocity, even for small sideslip angles, large sideslip angular velocity may lead to vehicle spinning. On the other hand, the inherent drawback of the brake based dynamic stability control system, interference with the longitudinal vehicle dynamics and hence disturbance to

the driver when they intervene, limits its application to only extreme driving situations. This effect is significant from the driver point of view, especially during high speed driving since it conflicts with the driver actions. Therefore, the brake intervention should be avoided as much as possible (Smakman, 2000; Selby, 2003).

Driveline based dynamic stability control systems

For driveline based dynamic stability control systems, in order to correct the undesired and unpredictable vehicle motion in the yaw plane, either the front/rear or left/right torque distribution can be actively controlled to generate a corrective yaw moment. In the case of front/rear torque distribution control for 4WD vehicles, a corrective yaw moment is generated indirectly by utilising the tyre property that the lateral tyre force is reduced with increase in the corresponding longitudinal tyre force. For left/right torque distribution control, a significant corrective yaw moment is generated directly through the difference in the longitudinal forces between left and right wheels of the same axle. There are four typical left/right torque split mechanisms as shown in Figure 2.3.

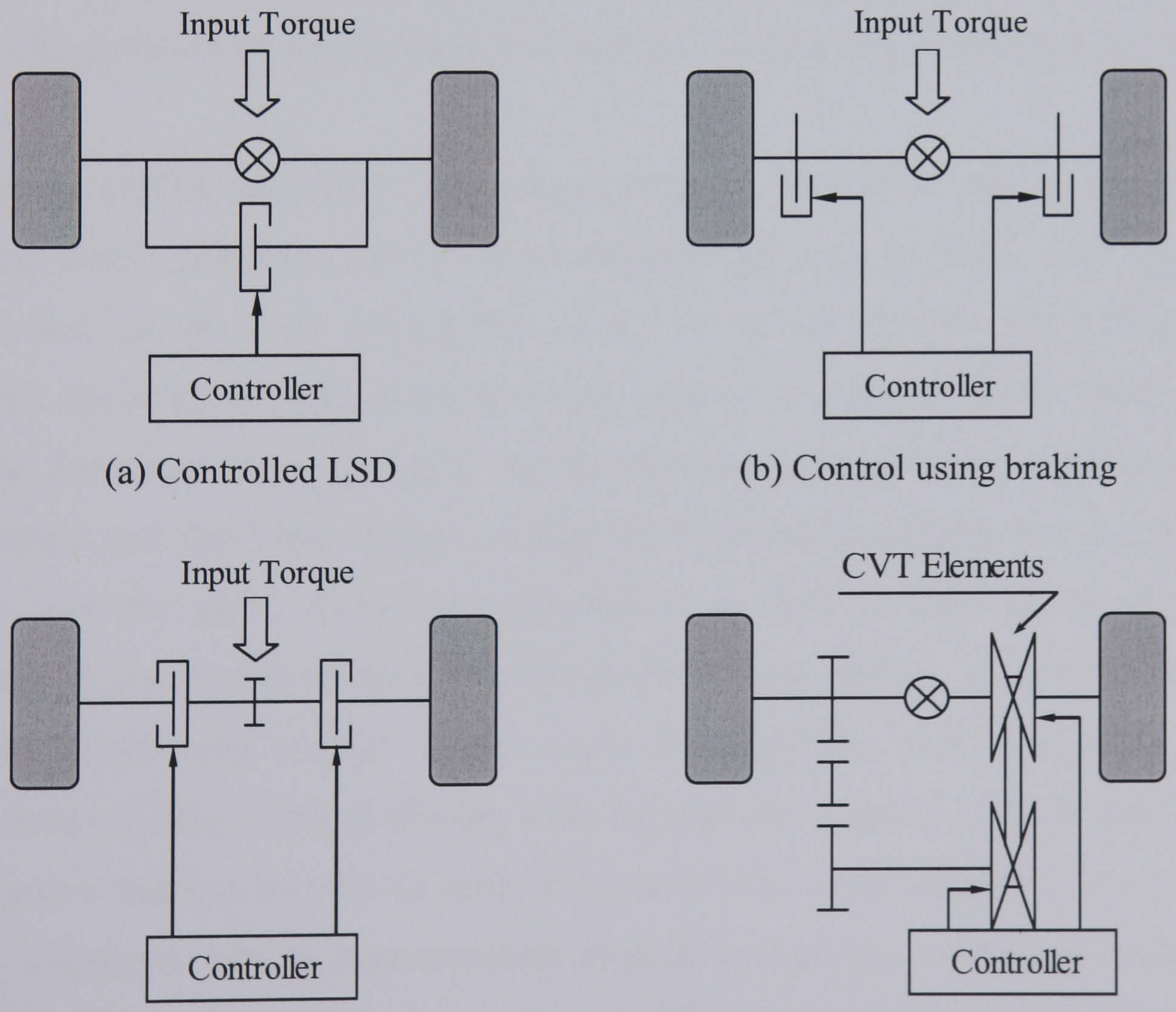

Figure 2.3 Schematics of typical left/right torque split mechanisms

- **Controlled LSD (Limited Slip Differential)**

In the case of LSD, due to the locking effect of the differential, torque can only be transferred from the faster spinning wheel to the slower spinning one, namely in one direction.

- **Control using braking**

In this case braking one wheel on a conventional differential can produce different speed and torque between left and right wheels of the same axle.

- **Control using driving torque**

This mechanism can split the desired value of torque between two wheels using two multi-disc clutches at each wheel.

- **Torque bypass**

Through arranging an additional gearbox across the conventional differential, torque can be transferred between left and right wheels of the same axle. This can be achieved by using either a continuously variable transmission (CVT) as shown in Figure 2.3(d) or a fixed-ratio gearbox with controlled clutches as adopted in this thesis. The direction of torque transfer is therefore controllable in this mechanism.

Naito *et al.* (1990) investigate a front/rear torque split control system in which the front/rear torque split ratio can be varied continuously from the RWD to a rigid 4WD mode based on the input information of the lateral acceleration and difference in rotational speed between the front and rear wheels. Simulation results show that the optimum front/rear torque split ratio should vary according to the level of longitudinal acceleration and the road surface conditions. Final tests suggest that the proposed system provides good cornering performance as well as high level of traction performance comparable to that of a rigid 4WD system. Naito *et al.* (1992) propose a right/left torque split control system using electronically controlled Limited Slip Differentials (LSD). Various driving tests suggest that right/left torque split control can improve traction as well as cornering performance and stability during various driving situations. Whilst improvements in both traction and cornering performance are shown in these studies, no details of appropriate vehicle model and control algorithm are presented.

Motoyama *et al*. (1993) compare the contributions of left/right and front/rear torque distribution control to vehicle handling performance. Figure 2.4 shows the simulation model of a drivetrain with a front, a rear and a centre differential. The torque distribution ratios for the front, rear and centre differentials are identified by α_F, α_R and α_C, respectively. A simple PD control law is derived to achieve a neutral steering characteristic by tracking the reference yaw rate. Both simulations and vehicle tests show that the left/right torque split control is more powerful and effective over even wider range of lateral accelerations than the front/rear counterpart in terms of affecting vehicle handling performance.

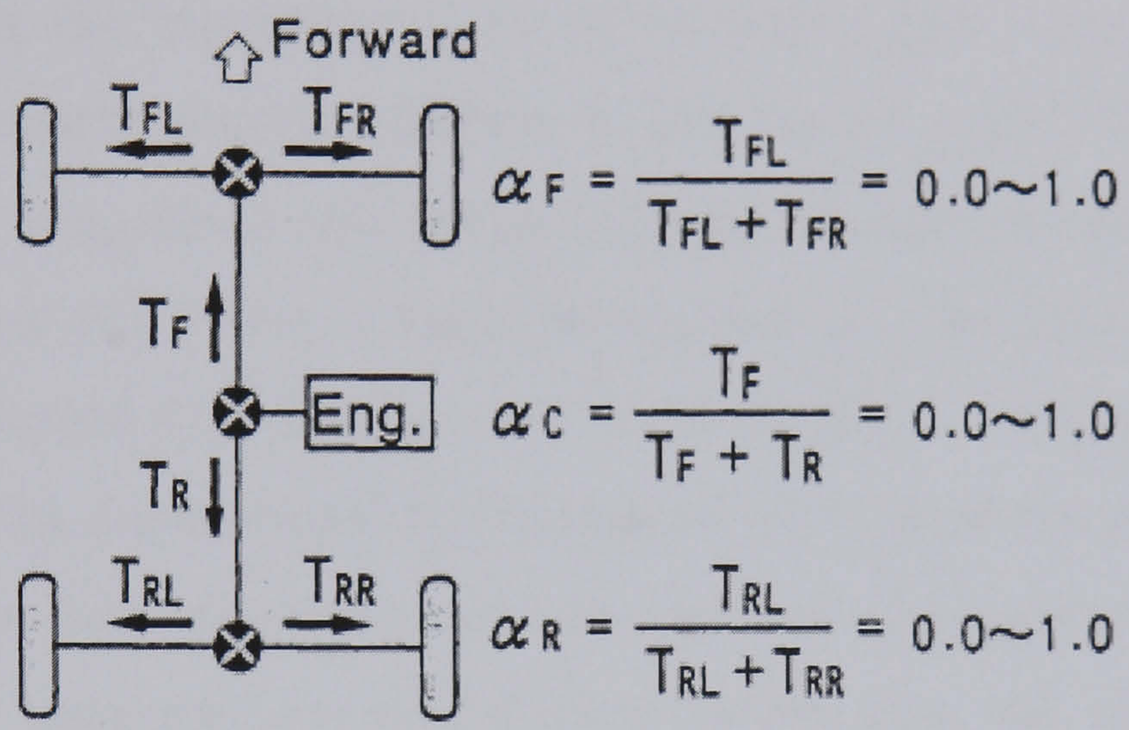

Figure 2.4 Simulation model of drivetrain used in (Motoyama *et al*., 1993)

Doniselli *et al*. (1993) investigate the left/right torque distribution using an ideal controlled differential. A theoretical analysis of various mechanical approaches for splitting the torque between left and right driving wheels of the same axle is presented. A nonlinear control law is proposed and shown to improve vehicle stability as well as the steady state and transient properties of vehicle handling. A number of simulations of a nonlinear vehicle model are carried out and the results suggest that a vehicle with the controlled differential has the potential to be more efficient in enhancing active safety and handling performance compared to that with the conventional one at both low and high lateral accelerations.

An intelligent four-wheel drive system which consists of a centre differential, a hydraulic multi-disc clutch and an electronic control unit for distributing the torque between front and rear axles is developed by Matsuo *et al*. (1993). This 4WD system

attempts to achieve a good balance of handling performance and stability without interfering with the handling limit predictability through torque distribution using a yaw rate model following control strategy. Similar to Naito's work (1990), the ideal torque distribution ratios for this 4WD system are calculated according to the lateral acceleration and road friction conditions based on a 2DOF nonlinear vehicle model. The front/rear torque distribution is then varied so that the actual yaw rate of the vehicle follows the desired one. Simulation results show the effectiveness of the proposed system during acceleration while cornering under different road friction conditions.

Mitsubishi presents the implementations of an active yaw control (AYC) system through left/right torque transfer (Ikushima and Sawase, 1995; Sawase and Sano, 1999). The former proposes a new torque transfer mechanism using a continuously variable transmission (CVT) for minimal energy loss and the latter develops a novel torque transfer differential by adding a set of two friction clutches and a three-gang gearing system to the conventional differential so that the lateral torque transfer can be implemented in both directions and the amount of transferred torque can be actively controlled independently of the input torque from the engine. A yaw rate model following control strategy is applied to the first study and a feedforward control scheme with μ estimation is adopted in the second one. In addition, the combination of the proposed AYC system with a brake based DSC system is also investigated in the second study to improve vehicle stability when the safety limit is reached. A number of simulations are carried out using a nonlinear 4WD vehicle model and the results suggest improvements in both cornering performance and vehicle stability.

Shibahata *et al.* (1992) develop the so-called β-method to analyse the vehicle dynamic characteristics throughout the handling region and the effects of longitudinal acceleration/deceleration on vehicle handling performance. This method relates the vehicle sideslip angle to vehicle stability and is used to predict the required stabilising yaw moment to compensate for changes in vehicle handling behaviour due to longitudinal acceleration/deceleration during cornering. The required corrective yaw moment is then generated by actively distributing torque between left and right sides of the vehicle. The technique is found to significantly increase the vehicle handling performance envelope in combined cornering and acceleration/braking manoeuvres.

The commercial product, Active Torque Transfer System (ATTS) developed by Honda is presented in (Kuriki and Shibahata, 1998). The effect and performance of ATTS is discussed through implementing this system on an actual FWD vehicle. The main breakthrough of this implementation is the zero torque steer achieved by a special suspension.

Matsuno *et al.* (2000) propose an experimental study of a variable torque distribution control system which splits torque between front and rear axles based on the μ estimation. Parameter identification law in adaptive control theory is used to estimate the road friction coefficient through identifying the actual cornering stiffness of tyres. The controller sets the torque to be transferred according to the estimated μ and the deviation between the actual and reference yaw rates. Different experimental tests show that the proposed system improves vehicle handling performance and stability under various road/operating conditions over the system with fixed torque distribution ratio. However, the control law of the proposed controller is not clear.

In contrast to the conventional internal combustion (IC) engine vehicles with axles, transmission and differential units, electric vehicles can make the dynamic stability control to be performed in a simpler and quite exact manner, especially with the use of in-wheel motors which enable the torque applied at individual wheels to be controlled independently and fast (Fujioka and Yanase, 1994; Sakai *et al.*, 1999; Shino *et al.*, 2000; Esmailzadeh *et al.*, 2002). In this study, as electric vehicles are not of interest, the review in this respect will not be detailed.

Summary

The studies reviewed above show the potential of the driveline based dynamic stability control systems for affecting vehicle handling behaviour. The general principles of such systems with respect to handling control are similar to those of the brake based ones and control theory is however not rigorously applied compared with the brake based schemes. In addition, the characteristics of the torque split devices with regard to the amount and rate at which torque can be transferred has rarely been presented in the literature. Furthermore, most papers are concentrated on the implementation of the proposed system and the discussion of controllers is mostly

qualitative, and so is the discussion of the improvements in vehicle handling behaviour.

As the amount of driving torque that can be applied to a given wheel of the driving axle depends on both engine capacity and driving situations, and in addition, the driving torque commonly has a lower limit than braking torque, the available corrective yaw moment generated by the driveline based system may not be comparable to that generated by the brake based one. However the driveline based systems do offer the advantage of not interfering with the longitudinal vehicle dynamics present in brake based systems when they intervene, and then no additional pitch motions are generated. In fact, during some extreme manoeuvres, the coordination of driveline and brake schemes may be required.

2.2.3 Comparative studies

In order to achieve integrated vehicle dynamics control, the effects of individual systems and the regions in which they are effective need to be clarified. A few papers have been devoted to comparing the relative merits of different stand-alone vehicle dynamics control systems.

Yamamoto (1991) analyses and compares three different control categories for improving vehicle handling and stability, i.e. active steering control, driving/braking force distribution control and roll stiffness distribution control. A feedforward plus feedback control law for 4WS is first proposed to enhance steering response and disturbance rejection in the linear region of tyre characteristics. When the vehicle approaches the limit of tyre adhesion, the other two control methods should be utilised. The work applies a yaw rate model following control strategy to the latter two systems. Both simulation studies and test results verify the effects of the three control methods in corresponding effective regions, as shown in Figure 2.5 where G_x and G_y denote longitudinal and lateral acceleration, respectively.

Shimada and Shibahata (1994) make a similar comparison of three different vehicle dynamics control systems: torque distribution control, active roll stiffness distribution control and active rear steering control through the analysis of vehicle dynamics. The

study compares the ability of each system to generate a stabilising yaw moment and hence the ability to improve vehicle handling performance during combined cornering and acceleration/deceleration manoeuvres using the previously developed β-method by (Shibahata *et al.*, 1992). The effect and effective regions of different control methods are summarised as:

- The active rear steering control is only effective for a small sideslip angle and can compensate for the change in vehicle dynamics at lateral accelerations of up to $7m/s^2$. When the sideslip angle increases, the effects of such systems decline.
- The active roll stiffness distribution control is only effective at a higher lateral acceleration ($4m/s^2$ or above) and the effect highly depends on the longitudinal weight distribution of the vehicle.
- The torque distribution control is effective throughout the vehicle handling regime.

Therefore, the work is concluded that the torque distribution control has the greatest capability to compensate for the changes in vehicle cornering characteristics induced by acceleration and deceleration.

Control factors \ Region	Gx, Gy Small	Gx Large	Gy Large	Gx, Gy Large
① Steer angle control	L	S	S	S
② Driving/braking force control between left and right	M	M	M	M
③ Roll stiffness distribution control for front/rear	S	S	L	L
④ Driving/braking force distribution control for front/rear	S	S	S	L

Notations (Effective / L : Large, M : Medium, S : Small)

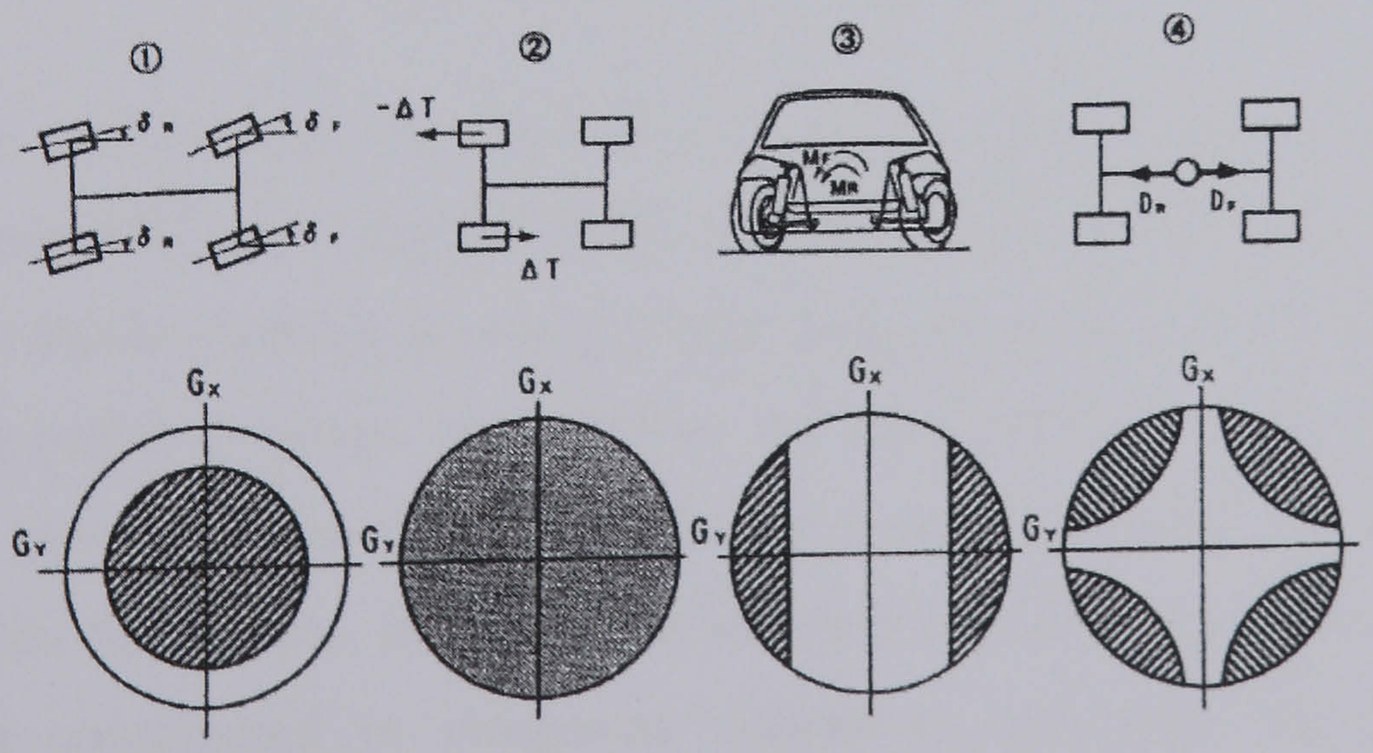

Figure 2.5 Effective region of each control form (Yamamoto, 1991)

A detailed review and comparison of 4WS and DYC is presented in (Furukawa and Abe, 1997). The study points out that 4WS approaches or even reaches its functional limit when the rear lateral tyre force is saturated. At this point, no matter how advanced the control theory used is, it is difficult or impossible for 4WS to make a breakthrough. On the other hand, DYC can be used as a promising technique to improve vehicle handling further and to overcome the limitation of 4WS at or close to the handling limit. In addition, the study states that the nonlinearities of vehicle and tyre should be taken into account when deriving control laws for DYC. The work does not include actuation issues but mentions the potential of coordination/integration of 4WS and DYC.

Summary

The above comparative studies confirm that different vehicle dynamics control subsystems have functional limitations and effective regions of their own within the entire handling regime of the vehicle. The functional limitations are closely related to the nonlinear tyre characteristics and the effective regions can be specified in terms of the level of vehicle lateral acceleration. More specifically, active steering systems are most effective at low to mid-range lateral accelerations; roll moment distribution control systems are only effective at high lateral accelerations since the effect of lateral load transfer increases with lateral acceleration; torque distribution control is seen to be effective over the entire handling regime of the vehicle and the brake based DYC is only desirable at the handling limit.

2.3 Integrated Vehicle Dynamics Control Systems

The literature reviewed so far has focused on the stand-alone vehicle dynamics control systems which are independently developed and individually optimised to affect lateral vehicle handling by using different aspects of the vehicle dynamics. The potential functional overlaps or conflicts between different stand-alone control systems have not been exploited in these studies. Actually, there is still much scope to further enhance the vehicle handling performance by controlling these stand-alone systems in a coordinated or integrated manner to overcome the drawbacks of individual systems and to achieve an improved overall vehicle performance. In

addition, one can also expect commercial benefits such as cost reduction, hardware and space saving through sharing sensor information and coordinating subsystems. Two design approaches to integrated vehicle dynamics control, bottom-up and top-down will be examined in this section.

2.3.1 Bottom-up approach

The first stage of integrated vehicle dynamics control is the coordination of stand-alone control systems which is referred to in this thesis as *bottom-up* design approach. In the bottom-up approach the integrated control is designed based on two or more existing controllable subsystems to minimise or avoid their interferences. The subsystem controllers are designed independently to achieve their own control objectives and then to influence specific aspects of the vehicle dynamics with no prior knowledge of how other control systems affect the same aspect of the vehicle dynamics. This approach is now predominantly studied in the literature, and is relatively simple in terms of control design and implementation. Figure 2.6 shows the typical structure of this approach to integrated vehicle dynamics control.

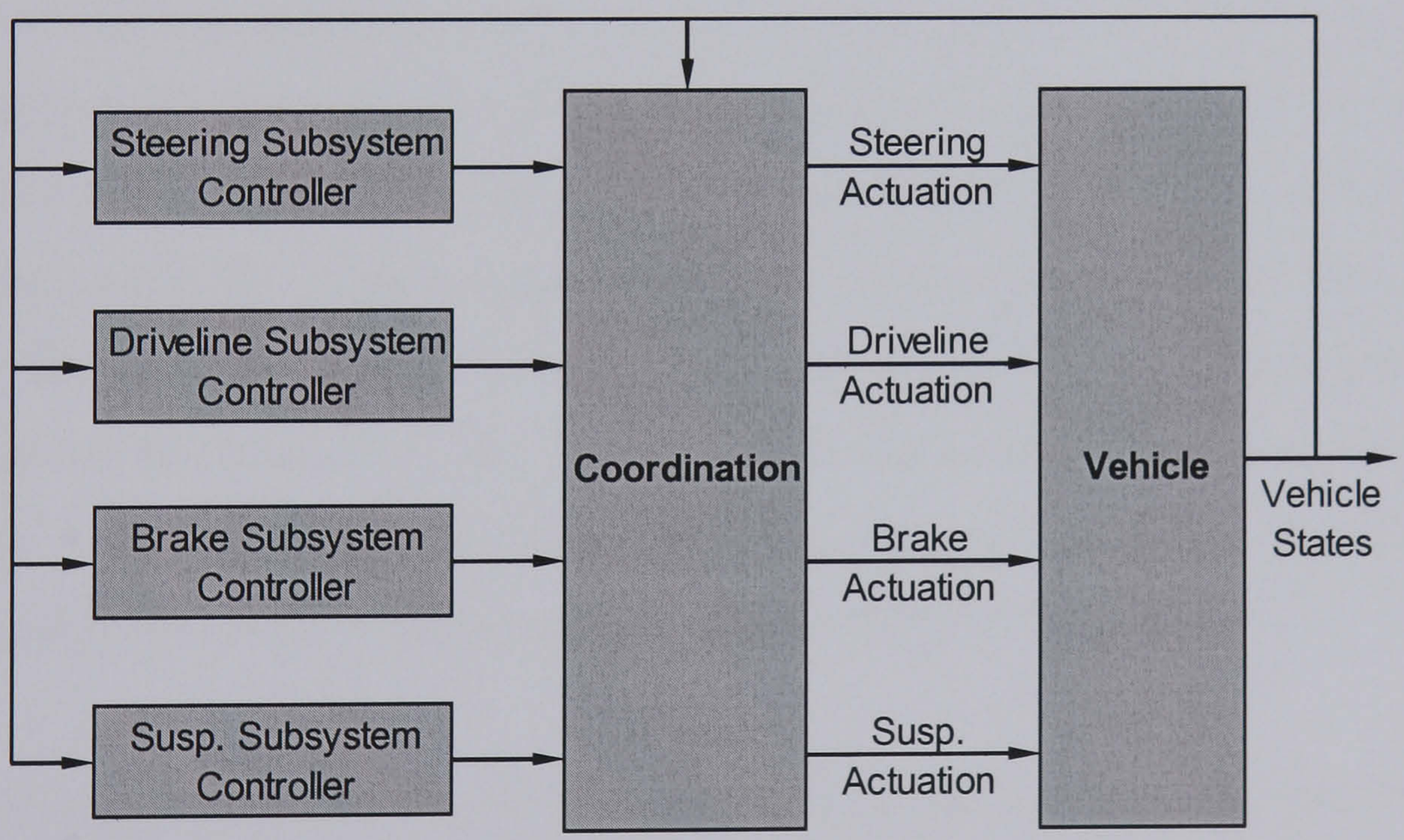

Figure 2.6 General structure of the bottom-up approach to integrated vehicle dynamics control

A cooperative control scheme for 4WS and DYC is presented in (Furukawa and Abe, 1996). The work derives a sliding mode-like control law for DYC to make the vehicle sideslip angle to converge to zero using a linear 2DOF bicycle model. In order to

determine the direct yaw moment, a simple tyre model on board is utilised to estimate the lateral tyre forces. The DYC then cooperates with a simple feedforward zero-sideslip angle 4WS to compensate for its drawback due to the saturation of lateral tyre forces. Both open and closed-loop computer simulations of a nonlinear vehicle model confirm the effectiveness of the proposed control system and its robustness to road friction variations. However the interactions between the two actuation schemes, braking and rear wheel steering is not examined in this work.

Lakehal-ayat and Diop (2002) propose a similar configuration to coordinate the stand-alone active braking and active suspension systems. The control system is designed to achieve the multivariable regulation of the longitudinal velocity, lateral acceleration and yaw rate to the reference values by using a decoupled suspension model. Whilst good yaw rate tracking is demonstrated through simulations, the results are so limited that it is difficult to draw useful conclusions about the quality of the proposed control system.

Hac and Bodie (2002) propose another similar integrated vehicle dynamics control algorithm which coordinates active control of brake and suspension with magneto-rheological (MR) dampers to improve vehicle stability and emergency handling. An analysis of vehicle stability is first performed on a 2DOF nonlinear bicycle model and the control authority of each stand-alone control system in terms of the ability to generate the required corrective yaw moment is evaluated. The integrated control algorithm which is based on the yaw rate model following control strategy is then designed. Test results demonstrate that the proposed integrated control system significantly reduces the brake usage compared with DYC only.

The most detailed description and example of the bottom-up approach can be found in (Smakman 2000a, 2000b) of BMW. An Internal Model Controller for the suspension based system and a simple PD control law for the single-wheel DYC system are proposed in this study based on a thorough analysis of the vehicle dynamics. The work reports that these stand-alone control systems interfere with each other due to different control objectives and actuation concepts when they are present on a vehicle simultaneously. Then a simple rule is proposed to prevent these interactions. Moreover, the interference with the longitudinal vehicle dynamics observed in DYC

is also significantly reduced through distributing the required control effort between two individual actuators. This work demonstrates the potential to improve the performances of two stand-alone control systems by complementing each other and understanding interactions between them.

A similar control scheme which coordinates AFS and DYC is presented in (Selby *et al.*, 2001a). The work uses AFS to improve vehicle handling behaviour in low to mid-range lateral acceleration and employs DYC to maintain vehicle stability at the handling limit. Due to the interference between AFS and DYC, a rule based switching control scheme is proposed to keep the vehicle under control throughout the handling region. In addition, the required corrective yaw moment demanded by the DYC controller is shared between DYC and AFS through proper selection of these rules to delay the intervention of braking actions and consequently to reduce interference with the longitudinal vehicle dynamics. A comparative study of AFS and ARS when coordinated with DYC is presented in (Selby *et al.*, 2001b). The authors come to a conclusion that AFS is more suitable to be coordinated with DYC than ARS in terms of assisting DYC in maintaining vehicle stability.

Summary

The work reviewed in this section aims to integrate two stand-alone vehicle dynamics control systems in a cooperative or coordinative way. However, few authors except Smakman (2000) investigate the integration issue through a detailed analysis and understanding of the vehicle dynamics and interactions between subsystems. Therefore, the vehicle dynamics and the interactions between different stand-alone control systems have to be fully understood before the final integration is achieved. Though the bottom-up approach seems to be the one which is now followed in industry such as BMW and Robert Bosch, a detailed description of the methodology is not available. In addition, this approach is a local but not a global integrated vehicle dynamics control solution.

2.3.2 Top-down approach

A more sophisticated approach to integration design is called the *top-down* design. In comparison with the bottom-up design, the top-down approach is a true global vehicle

dynamics control solution. In the top-down approach, a global or central controller which is responsible for making all control decisions is usually designed using multivariable control techniques. Such a controller produces generic control inputs to available actuation schemes. The design process is attractive due to its analytic nature and the fact that a quantitative framework for controller evaluation is inherent. However, the potential improvement is restrained by the substantial increase in complexity of the design process and the need for accurate state or parameter estimations and reliable sensors in the implementation. The general structure of this approach to integrated vehicle dynamics control is illustrated in Figure 2.7. This section will briefly review the studies in this field and identify the profile of this approach.

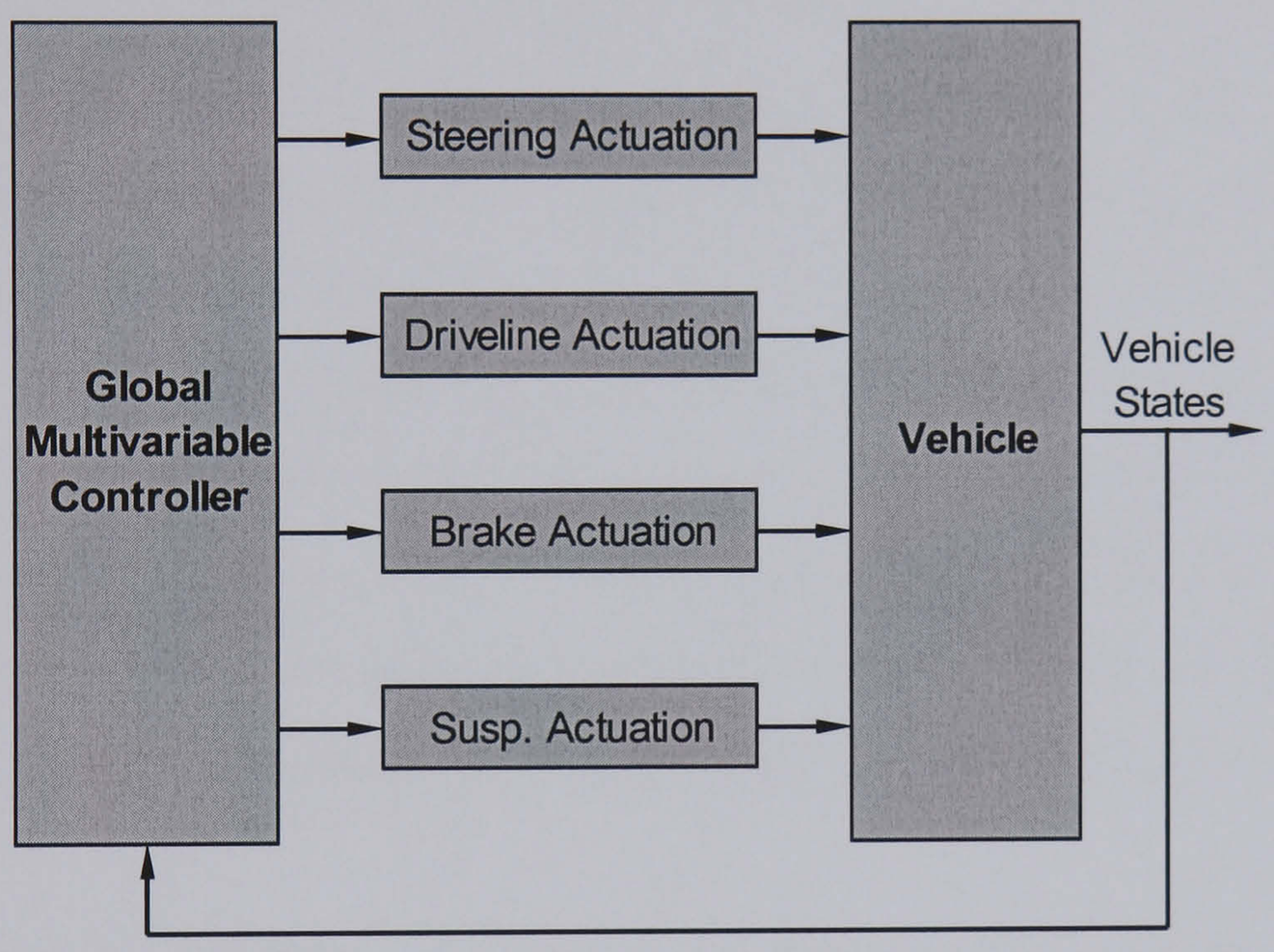

Figure 2.7 General structure of the top-down approach to integrated vehicle dynamics control

Hirano *et al.* (1992, 1993) propose a 2DOF yaw rate tracking control strategy to integrate 4WS and 4WD by modulating the rear wheel steer angle and the front/rear torque split ratio. The feedforward compensator deals with the fast steering response within the linear region of tyre characteristics and the feedback H_∞ controller augments the rear wheel steer angle and determines the torque split ratio to stabilise the vehicle in the nonlinear region of tyre characteristics. It is reported that the tracking of the original reference yaw rate is not realistic and easy to cause the vehicle to spin at the handling limit. This problem is addressed through the addition of an adaptive control algorithm that reduces the desired yaw rate when the estimated

sideslip angle becomes large. This implies the coupling of yaw motion and sideslip motion of the vehicle and suggests that such an interaction needs to be dealt with, especially during limit handling. A refined control law is presented in (Hirano, 1994; Ono *et al.*, 1994) where the μ-synthesis is used to design the feedback compensator so that both robust stability and robust performance can be ensured. The controller is evaluated through simulations and actual vehicle tests.

Yu and Moskwa (1994) study a model based technique for integrated control of 4WS and individual wheel torque control (IWTC) using input-output linearisation and sliding model control theory. A 3DOF vehicle dynamics model along with a simplified Dugoff tyre model is used for controller design. The driver inputs are interpreted as desired longitudinal and lateral forces applied on the vehicle which will be tracked by the controller. Whilst simulation results show that the proposed controller improves vehicle stability compared with zero sideslip angle 4WS alone, the use of the simplified Dugoff tyre model restricts control performance at the limit of handling as it does not completely represent tyre characteristics around this point. This drawback applies to all model based controllers as the control performance is strongly dependent on the accuracy of the model used. Therefore, robustness of the proposed control system is a practical concern. A further paper by Manning *et al.* (2002) investigates how the same SMC is extended to control roll and bounce.

An integrated model following controller for 4WS and DYC is presented in (Wang and Nagai, 1996; Nagai *et al.*, 1997) to track the reference yaw rate and sideslip angle. A 2DOF linear bicycle model is employed for controller design. Simulation results show the improvement in vehicle handling performance and good robustness to road friction and tyre cornering stiffness variations. However, the comparisons are made only between the vehicle with/without the integrated controller and no comparison between the integrated and stand-alone controllers is presented. Therefore, it is difficult to draw conclusions that the proposed controller is superior to the corresponding stand-alone ones. A similar study of integrated control of AFS and DYC is found in (Nagai *et al.*, 2002). In this study, the performance of the integrated control system is compared with that of DYC only. Another comparative study of AFS and ARS when integrated with DYC is presented in (Shino *et al.*, 2002) and

comes to a conclusion that AFS is more suitable to be integrated with DYC than ARS in terms of reducing control action of DYC.

Another model based controller design for the integration of 4WS and IWTC is presented in (Horiuchi *et al.*, 1998, 1999) using nonlinear predictive control theory. The model used for controller design in this work is quite similar to that in (Yu and Moskwa, 1994) with load transfer effects included. The controller is designed to track the desired yaw rate, desired forward speed and desired lateral velocity which are calculated based on driver steer and braking inputs. Simulation results of the proposed controller show improved vehicle stability and good robustness to road friction variations in comparison with the zero sideslip angle 4WS. However, the need for all states and tyre vertical load feedback requires expensive sensors and time-consuming estimation which are unrealistic in real implementation. Although the controller is shown to be robust to road surface friction variations, no discussion of the required accuracy or upper limits on noise for such sensors and estimators is provided.

Hattori *et al.* (2002) propose a concept called VDM (Vehicle Dynamics Management) which aims to achieve seamless vehicle steerability and stability anytime by making the most of tyre performance through the integration of all stand-alone vehicle dynamics control systems. This concept uses the global integration scheme to form a hierarchical control algorithm and enables each subsystem or layer to cooperate with others through both-way communications. One of two core technologies of this concept is the feedforward force/moment control by translating the driver inputs into desired vehicle forces/moments and the other is the target force/moment distribution among wheels by using nonlinear optimization. Two open-loop simulations are conducted and demonstrate the effectiveness of the proposed concept. However, no details are presented about how the driver inputs are translated into the target forces/moments and how the tyre forces are estimated.

Summary

The reviewed studies present an overview of the multivariable control based top-down hierarchical design approach. Whilst most of the papers demonstrate excellent control performance, the work to date is dominated by theoretical studies and there are no

practical examples in which the potential benefits of integration have been exploited on production vehicles. The model based multivariable controller needs full states measurement/estimation which will lead to commercially expensive applications and computationally complex control algorithms. Although many papers assume that all required state and parameter information is available, no investigation with respect to sensor noise and estimation accuracy is presented.

In addition, most works reviewed here use inappropriately simple or even linear tyre models for controller design and evaluation, therefore, the quality of vehicle modelling, especially in the nonlinear region of tyre characteristics is questionable.

2.4 Discussion

Two distinct sorts of stand-alone vehicle dynamics control systems for affecting vehicle handling: active steering systems and dynamic stability control systems and comparative studies of these systems have been covered in this literature review. In addition, two potential approaches to integrated vehicle dynamics control: the bottom-up approach and the top-down approach have also been reviewed. The review clearly shows the need for active control of vehicle handling, the improvements induced by these active control systems and the development trend of active vehicle dynamics control.

Active steering systems have first received much attention as steering is traditionally the primary input to the vehicle from drivers and the most direct means to affect vehicle handling. The concept of active steering was first studied in the form of ARS and more recently AFS has attracted more commercial interest. These systems affect vehicle handling through actively steering front or/and rear wheels and then directly controlling the amount of generated lateral tyre forces. Whilst a large number of papers in this area have been published, it has not meant that this field is the most developed with respect to practical solutions to the vehicle handling control problem. In addition, most papers have indeed only designed open-loop control systems without drivers included in the control loop and therefore it is as yet unclear what the subjective improvement induced by these systems is from the driver point of view. It

is recognised that active steering is a highly effective approach to affect vehicle handling behaviour as long as the vehicle lateral acceleration is small and the lateral tyre forces show approximately proportional characteristics with respect to tyre slip angles, however, quite few papers have considered limit handling situations in which it is most likely for normal drivers to lose control of the vehicle. Actually this is one of the main shortcomings of studies reviewed here: the lateral acceleration range used is not wide enough for assessing the proposed control systems.

As an alternative to active steering, the dynamic stability control systems, including brake based and driveline based ones have been extensively studied since the 1990's. These two categories of systems can actually be grouped as one more general form – active torque distribution system (ATDS). The study of the brake based DSC systems dominates in this field as it is more powerful in terms of the amount of achievable corrective yaw moment and more flexible because of the ability to brake individual wheels. In contrast, the driveline based DSC systems have received relatively little interest and control laws have not been so rigorously applied to such systems as in the area of brake and steering systems. The primary reason for limiting a widespread application of such a technique appears to be the cost of extra hardware required and the amount of achievable corrective yaw moment which is largely limited by the engine capacity and driving tasks. Nevertheless, it is a favourable tool for the developing electric vehicles on which the individual mounted motors are available for independently controlling the torque applied at each wheel.

The major advantage of the brake based systems is that they can make the most of existing ABS hardware and only require a small number of additional sensors. One of the main disadvantages of the brake based systems mentioned in the literature is the interference with the longitudinal vehicle dynamics and therefore they are only acceptable at the limit of handling from the driving 'pleasure' point of view. However, this effect does not exist in the driveline based systems and hence these systems can be applied over a wide range of vehicle operating conditions. In addition, though different approaches have been proposed to evaluate vehicle stability in the literature relating to the brake based systems, the relative merits of these approaches have not yet been fully quantified.

Regarding the stand-alone control systems reviewed here, each has its own characteristic and limitation, thereby no one is completely effective in all driving situations nor are they absolutely essential for vehicle handling control at all times. The goal of integrated vehicle dynamic control is to achieve the optimum vehicle dynamic performance with minimum cost and energy consumption through integrating an optimum number of stand-alone control systems on a vehicle.

Two approaches to this, bottom-up and top-down have been presented in the published papers. The bottom-up approach is formulated by adding a level of supervision to the stand-alone control systems to deal with their interactions and the top-down structure is established by using a model based central/global multivariable controller to make all control decisions and to distribute the generic actuations to corresponding actuators.

The bottom-up approach makes the most of previously developed and well-understood stand-alone control systems to improve vehicle performance and to mitigate interactions between subsystems. This modular approach makes the control system design flexible - each subsystem and its controller may be designed separately to achieve desired functional requirements of its own, and consequently reduces design complexity. In addition, subsystems employed can potentially operate even if the coordination level fails and accordingly enables a great degree of fault tolerance. In contrast, the top-down or model based approach tends to be commercially expensive due to the requirement of a number of reliable sensors. Furthermore, there is computational complexity in implementing accurate model based controllers and state estimators. Therefore, given the time and economic constraints, at present it is the view of the author that it is not feasible to synthesise the vehicle control in the form of a fully integrated global controller. Nevertheless, it is valuable to provide insight in this field.

In summary, through the above review, the following common shortcomings in previous work have been identified:

- The use of inappropriately simple models, especially simple tyre models for testing complex controllers;

- The lack of a realistic and sufficiently wide range of handling manoeuvres to fully investigate the performance and limitations of the proposed controllers;
- The lack of clear and well-defined control objectives for improving vehicle handling over the whole range of lateral acceleration;
- The lack of clarity of interactions between systems and approaches to system integration.

The above review and discussion have resulted in an understanding of active control of vehicle handling in both stand-alone and integrated fashions. With the knowledge gained from this review, the following chapters will present the details of vehicle modelling, lateral vehicle dynamics analysis, control system design and evaluation. In particular, a novel integrated control system will be designed and evaluated.

2.5 Research Aims and Objectives

The overall goal of this research is to investigate the current state of integrated vehicle dynamics control and then to develop a generic control structure which ensures a vehicle is safe and pleasurable to drive through making the greatest use of previously developed and well-understood stand-alone vehicle dynamics control systems. More specifically, three levels of active control systems for vehicle handling will be examined and categorised in detail:

- **Stand-alone control systems:** in this thesis a stand-alone control system is defined as the system which is designed to achieve a specific control objective with its own control algorithm and corresponding hardware and without any knowledge of other control systems. The functionality and effective region of each stand-alone control system will first be analysed and defined to identify the possibility of further functional integration. Stand-alone system controllers will then be designed independently.

- **Combined control systems:** a combined control system is defined as being one with multiple stand-alone control systems operating in parallel and without any communication between each other. Such systems will serve as the baseline configuration for further integration analysis.

- **Integrated control systems:** an integrated control system is referred to as being one in which various stand-alone control systems are functionally rather than simply physically superimposed using different design approaches, ranging from local to global integration. These systems aim to improve overall vehicle performance by reducing interactions and conflicts between subsystems to avoid negative or detrimental effects.

As a preliminary study towards the fully integrated vehicle dynamics control, the two stand-alone vehicle dynamics control systems, namely: active steering system and dynamic stability control system are chosen in this thesis to form the integration using the *bottom-up* design approach. In addition, for simplicity, the areas of sensor fusion and state estimation will not be considered in any detail in this thesis and it will be assumed that all controllers to be designed have direct access to sufficient sensor or state information for making control decisions. Furthermore, all the actuator dynamics will be ignored, and thus all control inputs will be directly applied to the vehicle. The following aims and objectives will define the nature of the work undertaken in this thesis and follow directly from the above review and discussion.

2.5.1 Research aims

- Through a thorough analysis of the lateral vehicle dynamics, ranging from linear to nonlinear behaviour, the control objectives for both stand-alone and integrated control systems to be designed will be defined.

- An integrated vehicle dynamics control system which is based on the bottom-up approach and aims to improve overall vehicle performance by coordinating two active subsystems will be designed. It is desired that this integrated control system will allow vehicle handling subsystems to interact more effectively to improve vehicle handling behaviour over a broad range of handling regimes.

- The benefits in overall vehicle handling performance available from the proposed integrated control system will be comprehensively evaluated through computer simulations over the entire range of vehicle handling using a nonlinear vehicle model.

2.5.2 Research objectives

In order to achieve the above aims, the following specific objectives will be met.

- To develop a nonlinear vehicle handling model with appropriate degree of complexity for the study of the lateral vehicle dynamics over the entire range of vehicle handling.

- To define the control objectives in relation to different handling regimes of interest through a thorough analysis of the lateral vehicle dynamics.

- To design the active steering subsystem controllers including AFS and ARS in accordance with the control objective of steerability and to clarify the relative performance properties of AFS and ARS.

- To design the dynamic stability subsystem controller for performing the control task of maintaining vehicle stability in critical driving situations. Both driveline based and brake based DSC subsystems will be developed and the relative merits of these two subsystems will be assessed. This will lead to a new driveline plus brake based DSC subsystem.

- To clarify interactions between the above two subsystems and to propose a structured approach to an integrated control system for these two subsystems; to assess the benefits of the proposed integrated control system with respect to different aspects of vehicle handling behaviour.

2.6 Conclusions

This chapter has presented a broad review of literature relating to active control of vehicle handling, including both stand-alone and integrated control. The specific feature of each stand-alone control system has been discussed and two design approaches to integrated vehicle dynamics control have been introduced. In addition, the relative merits of these two approaches have been briefly compared. A discussion of the reviewed literature has allowed the research aims and objectives of this thesis to be specified.

Chapter 3

Vehicle Modelling

Abstract: *The vehicle modelling for handling analysis is presented in this chapter. This modelling includes the 2DOF linear bicycle model which will be employed for controller design and an 8DOF nonlinear vehicle model which will be used to evaluate the proposed control systems through computer simulations. The test manoeuvres are also described in this chapter.*

3.1 Introduction

To design vehicle dynamics control systems, evaluate control performance and simulate the handling behaviour of a vehicle during a specific manoeuvre, vehicle handling models must be developed. A vehicle handling model should have necessary complexity for a given application but need not be overly complicated for implementation convenience, i.e. the specific application defines the complexity of the model. For normal handling, a relatively simple linear vehicle model with many simplifying assumptions is enough for the purpose of analysis; a more complicated vehicle model however needs to be employed if severe handling is under consideration. Therefore, the ideal model for studying most vehicle handling

scenarios is one with only those degrees of freedom that are relevant and significant nonlinearities should be included when needed.

In this thesis, the vehicle handling model is classified into two different types: a linear model which will be utilised for controller design and generating the reference response to driver steer inputs and a nonlinear one for control system evaluations through computer simulations. In this chapter, a series of analytical and empirical models will be developed to enable the study of basic vehicle handling behaviour from the linear region in normal driving situations to the limit performance region during emergency manoeuvres.

3.2 Vehicle Dynamics Model

The lateral vehicle dynamics can be generally divided into linear and highly nonlinear behaviour. For low levels of lateral acceleration, the 2DOF linear bicycle model is a powerful tool in gaining insight into the basic aspects of vehicle handling. Beyond the low-range lateral acceleration, the effects of nonlinearities on the lateral vehicle dynamics become significant and an appropriate nonlinear handling model will be developed to investigate vehicle behaviour.

3.2.1 Coordinate systems

To derive the equations of motion and measure the position of the vehicle, two coordinate systems are first introduced. The inertial coordinate system, (X,Y,Z) which is fixed on the earth serves as a reference frame for the vehicle motions and defines vehicle attitude and trajectory through the course of a manoeuvre. The vehicle fixed coordinate system, denoted by (x,y,z) with its origin at the vehicle centre of gravity (CG), is employed to define the vehicle motions. Figure 3.1 shows the vehicle coordinate system recommended by SAE when the vehicle is represented as one lumped mass located at its CG with appropriate mass and rotational moments of inertia (Wong, 2001).

Herein, the vehicle fixed axis system (x,y,z) is rotated by a yaw (heading) angle ψ with respect to the inertial system (X,Y,Z) about Z-axis, as shown in Figure 3.2. In

the handling analysis the planar motions of the vehicle are of primary interest. Therefore, the vehicle heading angle ψ and vehicle trajectories X, Y can be calculated on the basis of vehicle motions which are normally described by velocities (yaw, longitudinal and lateral respectively in this thesis) as follows:

$$\dot{\psi} = r \tag{3.1}$$

$$\begin{Bmatrix} \dot{X} \\ \dot{Y} \end{Bmatrix} = \begin{bmatrix} \cos\psi & -\sin\psi \\ \sin\psi & \cos\psi \end{bmatrix} \begin{Bmatrix} \dot{x} \\ \dot{y} \end{Bmatrix} \tag{3.2}$$

The above relationships can be used to perform a numerical integration in time and get the appropriate kinematics parameters.

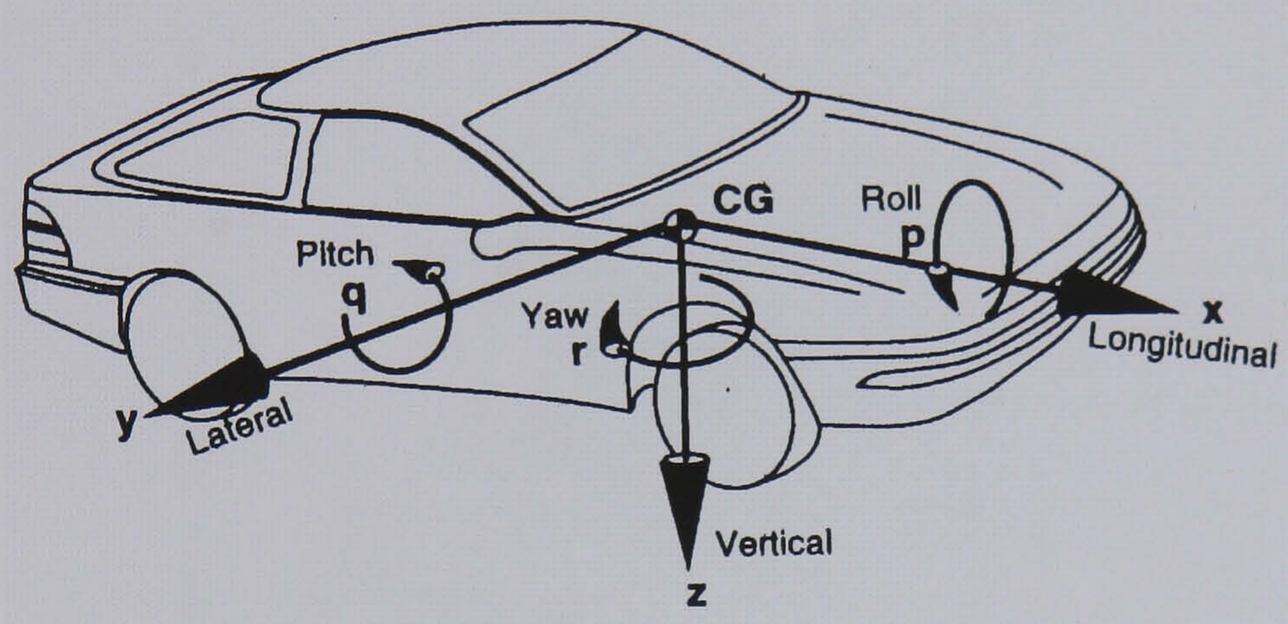

Figure 3.1 SAE vehicle coordinate system and sign convention used to describe vehicle motions

3.2.2 Assumptions to vehicle modelling

A number of simplifying assumptions have been made throughout the study to enable the representation of the lateral vehicle dynamics to be appropriate for the handling analysis undertaken (Crolla, 1992). The main assumptions include:

- The vehicle is running on a flat and smooth road such that there is no vertical motion of the wheels and then the body heave degree of freedom can be neglected.
- The vehicle consists of three rigid bodies: a sprung and two unsprung masses (roll steer can be ignored).
- The steering system is stiff (i.e. there is no compliance steer effect, which means the steering wheel angle input from the driver directly results in a proportional road steered wheel angle).

- The steer angles of both front wheels are the same and so are those of both wheels of the rear axle.
- The vehicle is subject to only small or moderate deceleration (no hard braking is considered and the body pitch degree of freedom is neglected).
- The vehicle is laterally symmetrical (i.e. the centre of gravity is located laterally at the centre of the vehicle).
- The driveline dynamics are neglected (driving/braking torques are thus applied directly to the wheels).
- The effects of aerodynamic lift on the vertical load are negligible.
- Aerodynamic forces are negligible compared with tyre forces.

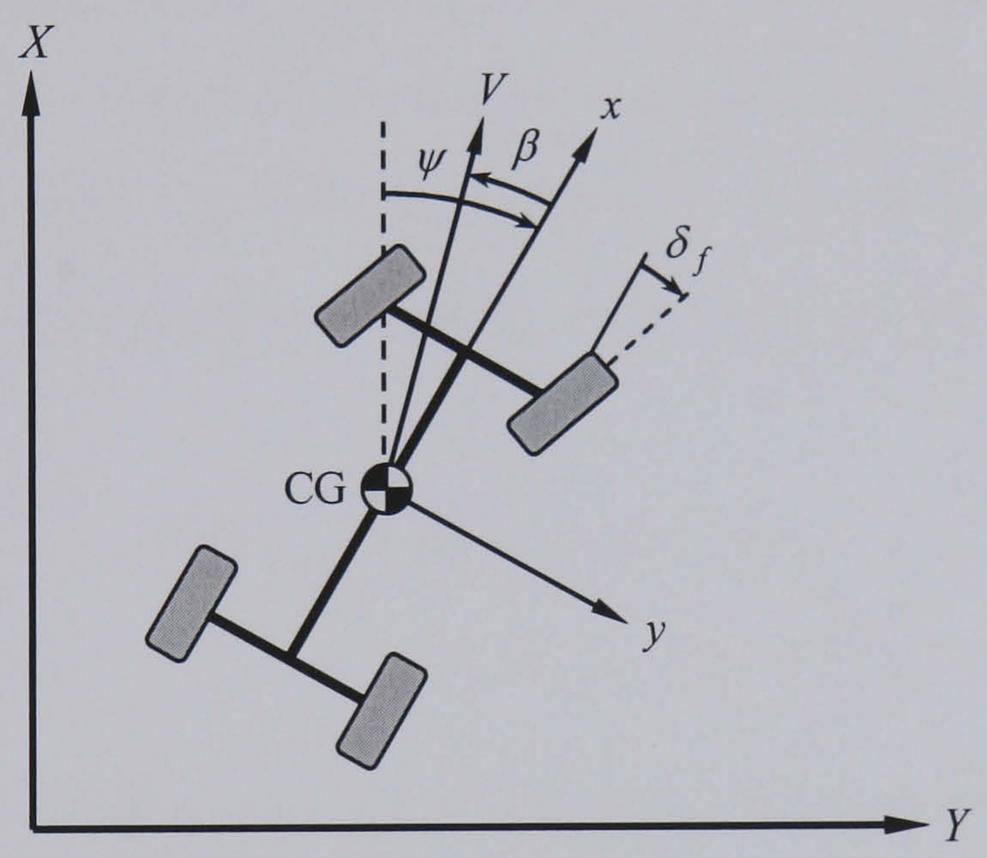

Figure 3.2 Vehicle in an earth fixed coordinate system with negative sideslip angle shown

3.2.3 2DOF linear bicycle model

The linear lateral dynamic behaviour of the vehicle can be described by the so-called bicycle (or single-track) model which has been investigated extensively in the literature. This simplest vehicle handling model possesses only two degrees of freedom: lateral motion and yaw motion, but nevertheless it can be used to demonstrate the basic features of vehicle handling at low lateral acceleration up to 0.3g. For such a model, in addition to the assumptions described in Section 3.2.2, the following set of assumptions is made to further idealise the vehicle motions (Crolla, 1992):

- The left and right wheels on the same axle are laterally lumped into one in the centre-line.

- The vehicle is running at a constant speed V_x (the longitudinal dynamics and forces will not be examined).
- The vehicle structure, including the suspension system, is rigid.
- The vehicle is subject to only small perturbations from a trim condition – for example, straight running or a steady-state turn (i.e. small angle approximations for both tyre slip angles and road wheel steer angles apply). This will lead to fully linear tyre behaviour and equations of motion.
- Both longitudinal and lateral load transfers are neglected.

The illustration of the 2DOF linear bicycle model for conventional front wheel steering vehicles with kinematic quantities and lateral tyre forces is shown in Figure 3.3. The vehicle can be viewed as consisting of a planar (2D) motion described by 2 variables: the lateral speed V_y and the yaw rate r. The equations of motion of the bicycle model can then be expressed as follows by directly applying Newton's Second Law:

$$m(\dot{V}_y + V_x r) = F_{yf}\cos\delta_f + F_{yr} \tag{3.3}$$

$$I_{zz}\dot{r} = l_f F_{yf}\cos\delta_f - l_r F_{yr} \tag{3.4}$$

where F_{yf} and F_{yr} are lateral tyre forces of the front and rear axles, respectively.

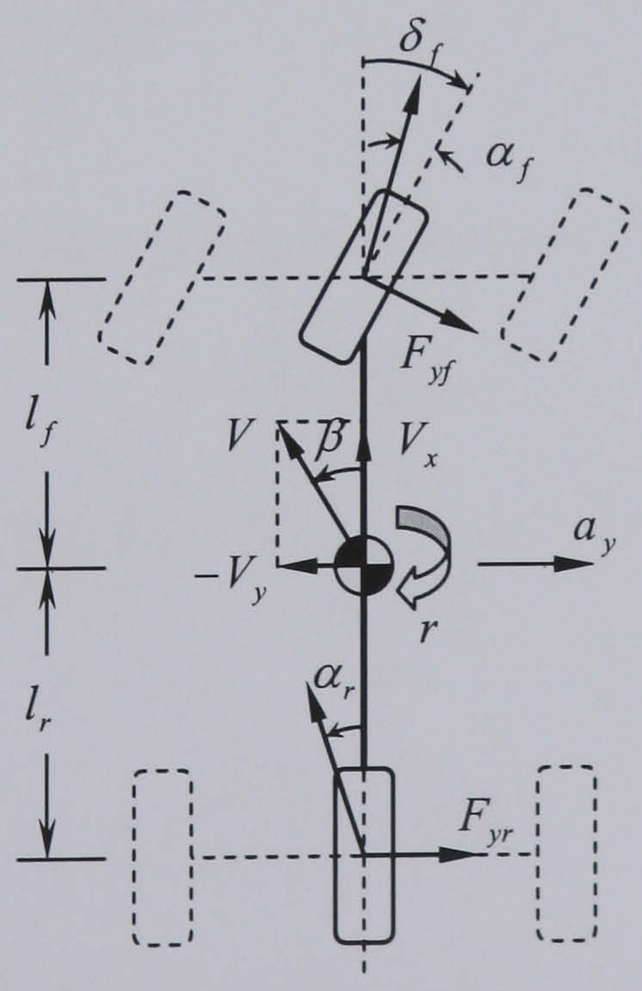

Figure 3.3 Bicycle model for conventional front wheel steering vehicles with kinematic quantities and forces (negative sideslip angle shown)

In line with the small angle assumptions, one can have $\cos\delta_f \approx 1$ and the lateral tyre forces of both axles can be expressed as the product of cornering stiffness C_i and tyre slip angle α_i :

$$F_{yf} = -C_f \alpha_f \tag{3.5}$$

$$F_{yr} = -C_r \alpha_r \tag{3.6}$$

The tyre slip angle is defined as the angle between the plane of the tyre and the tyre's direction of travel, as shown in Figure 3.3 (negative angle shown). It should be noted that the above two equations are written in terms of axles, which means the cornering stiffness is that of the corresponding axle rather than that of the single tyre. In addition, the front and rear tyre slip angles can be approximated as:

$$\alpha_f = \frac{V_y + l_f r}{V_x} - \delta_f \tag{3.7}$$

$$\alpha_r = \frac{V_y - l_r r}{V_x} \tag{3.8}$$

Substituting Eqs. (3.5) to (3.8) into Eqs. (3.3) and (3.4) to give:

$$m(\dot{V}_y + V_x r) = -\frac{(C_f + C_r)}{V_x} V_y - \frac{(l_f C_f - l_r C_r)}{V_x} r + C_f \delta_f \tag{3.9}$$

$$I_{zz}\dot{r} = -\frac{(l_f C_f - l_r C_r)}{V_x} V_y - \frac{(l_f^2 C_f + l_r^2 C_r)}{V_x} r + l_f C_f \delta_f \tag{3.10}$$

Rearranging to give the following state-space representation:

$$\dot{x} = \mathbf{A}x + \mathbf{B}_1 u_1 \tag{3.11}$$

where the state vector x, the input vector u_1, the system matrix $\mathbf{A}$ and the input matrix $\mathbf{B}_1$ are defined by:

$$x = \begin{pmatrix} V_y \\ r \end{pmatrix}, \; u_1 = [\delta_f]$$

$$\mathbf{A} = \begin{bmatrix} a_{11} & a_{12} \\ a_{21} & a_{22} \end{bmatrix} = \begin{bmatrix} \dfrac{-(C_f + C_r)}{mV_x} & \dfrac{l_r C_r - l_f C_f}{mV_x} - V_x \\ \dfrac{l_r C_r - l_f C_f}{I_{zz} V_x} & \dfrac{-(l_f^2 C_f + l_r^2 C_r)}{I_{zz} V_x} \end{bmatrix}, \; \mathbf{B}_1 = \begin{bmatrix} b_1 \\ b_2 \end{bmatrix} = \begin{bmatrix} \dfrac{C_f}{m} \\ \dfrac{l_f C_f}{I_{zz}} \end{bmatrix}$$

Moreover, the lateral acceleration a_y at the vehicle CG is given as:

$$a_y = \dot{V}_y + V_x r \tag{3.12}$$

The vehicle sideslip angle β at the CG which is defined as the angle between the vehicle longitudinal axis and the local direction of travel takes the form:

$$\beta = \tan^{-1}\left(\frac{V_y}{V_x}\right) \tag{3.13}$$

For small angles, β can be approximated as:

$$\beta = \frac{V_y}{V_x} \tag{3.14}$$

2DOF linear bicycle model for 4WS vehicles

As discussed in Chapter 2, the vehicle handling characteristics can be tuned by actively steering the rear axle in the opposite or same direction as the front one. Figure 3.4 illustrates the same-direction case for the 4WS bicycle model with the rear wheel steer angle δ_r included. From the mathematical modelling point of view, the equations of motion of the 4WS bicycle model can be directly derived by modifying the expression of the rear lateral tyre force in the above 2WS model, i.e. by modifying the expression of the rear tyre slip angle α_r. The rear tyre slip angle α_r can be obtained in the similar way to the front one and expressed as:

$$\alpha_r = \frac{V_y - l_r r}{V_x} - \delta_r \tag{3.15}$$

Thus the following equations of motion of the 4WS bicycle model can be derived:

$$m(\dot{V}_y + V_x r) = -\frac{(C_f + C_r)}{V_x} V_y - \frac{(l_f C_f - l_r C_r)}{V_x} r + C_f \delta_f + C_r \delta_r \tag{3.16}$$

$$I_{zz}\dot{r} = -\frac{(l_f C_f - l_r C_r)}{V_x} V_y - \frac{(l_f^2 C_f + l_r^2 C_r)}{V_x} r + l_f C_f \delta_f - l_r C_r \delta_r \tag{3.17}$$

Similarly, the state-space representation of the 4WS bicycle model is given as:

$$\dot{x} = \mathbf{A}x + \mathbf{B}u \tag{3.18}$$

where

$$u = \begin{bmatrix} \delta_f \\ \delta_r \end{bmatrix}, \quad \mathbf{B} = \begin{bmatrix} b_{11} & b_{12} \\ b_{21} & b_{22} \end{bmatrix} = \begin{bmatrix} \dfrac{C_f}{m} & \dfrac{C_r}{m} \\ \dfrac{l_f C_f}{I_{zz}} & \dfrac{-l_r C_r}{I_{zz}} \end{bmatrix}$$

x and $\mathbf{A}$ are the same as those in Eq. 3.11 for the same vehicle.

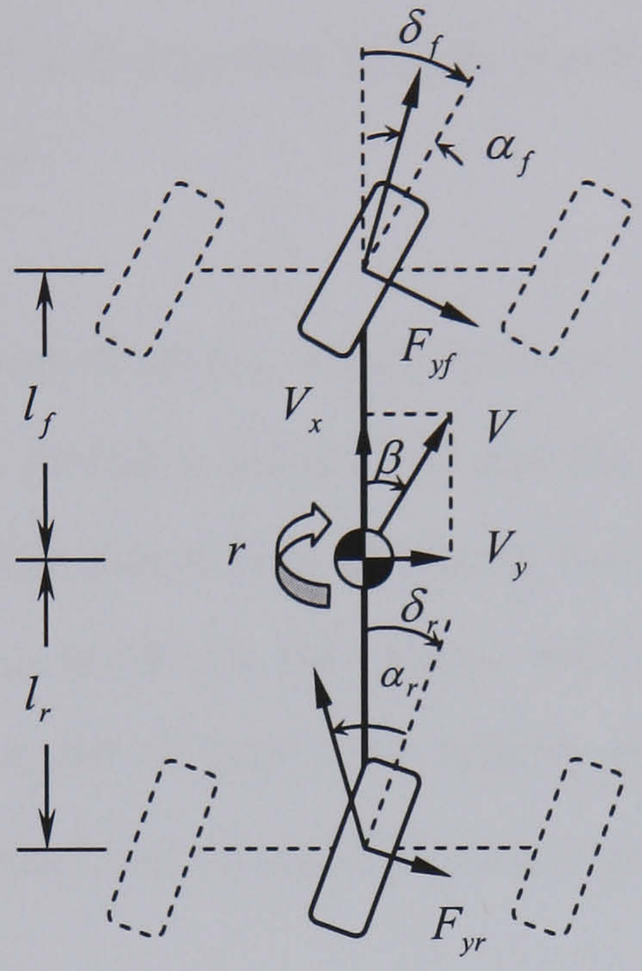

Figure 3.4 Bicycle model for 4WS vehicles with kinematic quantities and forces

Parameter set

With the linear bicycle model described above, the basic handling characteristics of the vehicle can be analysed. The parameter set for the linear bicycle model representing an average passenger car is listed in Table 3.1.

Table 3.1 Vehicle parameters for the 2DOF linear bicycle model

Vehicle Parameter	Symbol	Value	Unit
Vehicle mass	m	1704.7	kg
Distance from CG to front axle	l_f	1.035	m
Distance from CG to rear axle	l_r	1.655	m
Vehicle yaw moment of inertia	I_{zz}	3048.1	kgm^2
Front axle cornering stiffness	C_f	105850	N/rad
Rear axle cornering stiffness	C_r	79030	N/rad
Vehicle forward speed	V_x	27.8	m/s

3.2.4 Nonlinear vehicle model (NLVM)

The above simple description of the lateral vehicle dynamics is a useful tool for understanding the key features of vehicle handling. However, it can only accurately represent the vehicle dynamics up to 0.3g of lateral acceleration. With increasing lateral acceleration, it cannot capture the full vehicle dynamic behaviour. Therefore, in order to enable handling analysis even in the nonlinear region of the lateral vehicle dynamics, a more complicated and accurate vehicle model with appropriate degrees of freedom needs to be developed.

As stated previously, the planar motions which include longitudinal, lateral and yaw motions of the vehicle are of primary interest in handling analysis. However, during transient manoeuvres the suspension which connects the sprung mass to the unsprung masses introduces a phase lag between the planar motions of the vehicle unsprung mass and the instantaneous vertical tyre load which is one of the major elements determining the tyre-road contact forces and then the planar motions of the vehicle.

Therefore, in order to model transient behaviour of the vehicle, it is necessary to introduce additional degrees of freedom. The primary effect of the suspension with respect to the lateral handling behaviour is the roll mode which has a great influence on the lateral load transfer and then lateral force generation capability. In addition, the dominant nonlinearities in the vehicle dynamics result from the tyres which dominate in generating forces affecting vehicle handling behaviour. Thus, by employing a vehicle dynamics model with appropriate degrees of freedom and a nonlinear tyre model, a good representation of vehicle handling behaviour can be produced. In accordance with the assumptions in Section 3.2.2, the nonlinear vehicle handling model developed in this section has the following eight degrees of freedom and the associated variables are shown in Figure 3.5:

1. Translation in the longitudinal direction (V_x: vehicle forward speed);
2. Translation in the lateral direction (V_y: vehicle lateral speed);
3. Yaw motion about the vertical axis (r: vehicle yaw rate);
4. Body roll motion relative to the chassis about the roll axis (ϕ: body roll angle);
5. Rotation of the front left wheel (ω_1: 1st wheel angular velocity);

6. Rotation of the front right wheel (ω_2 : 2nd wheel angular velocity);
7. Rotation of the rear left wheel (ω_3 : 3rd wheel angular velocity);
8. Rotation of the rear right wheel (ω_4 : 4th wheel angular velocity).

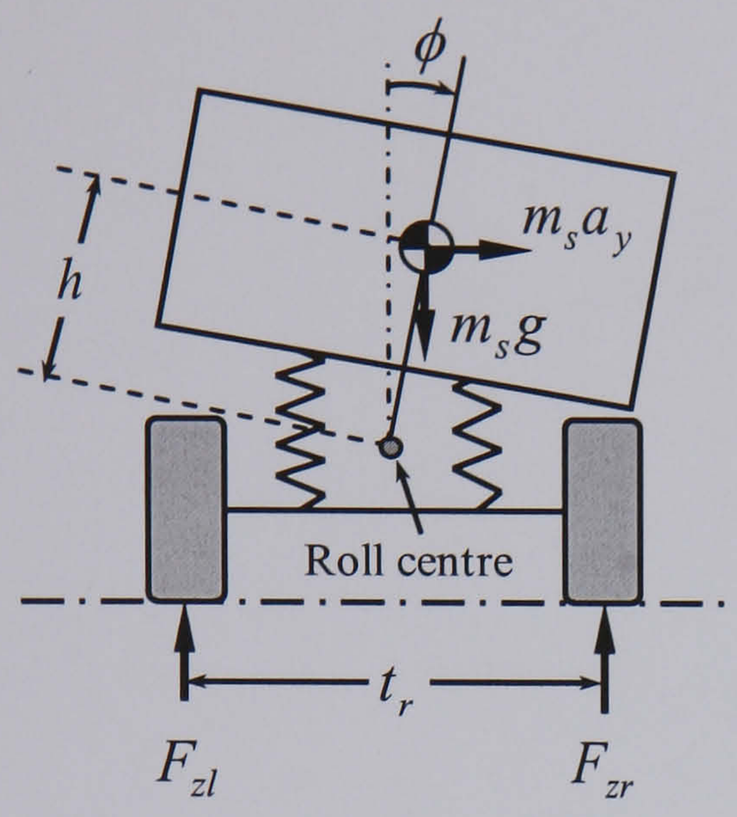

Rear view

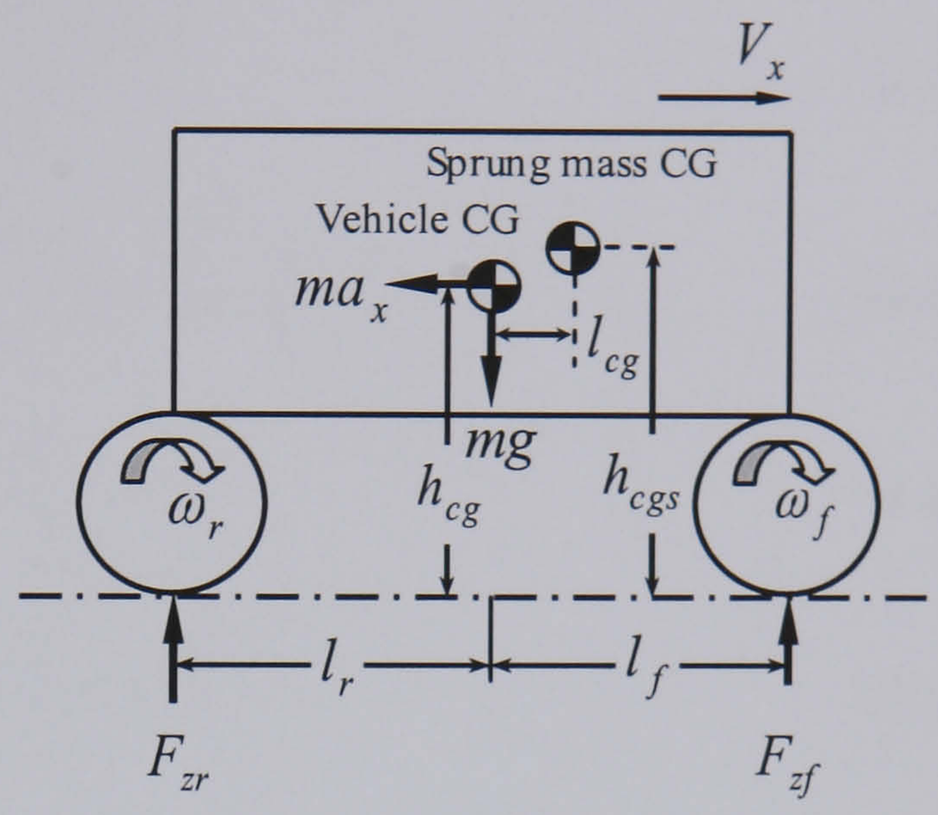

Side view

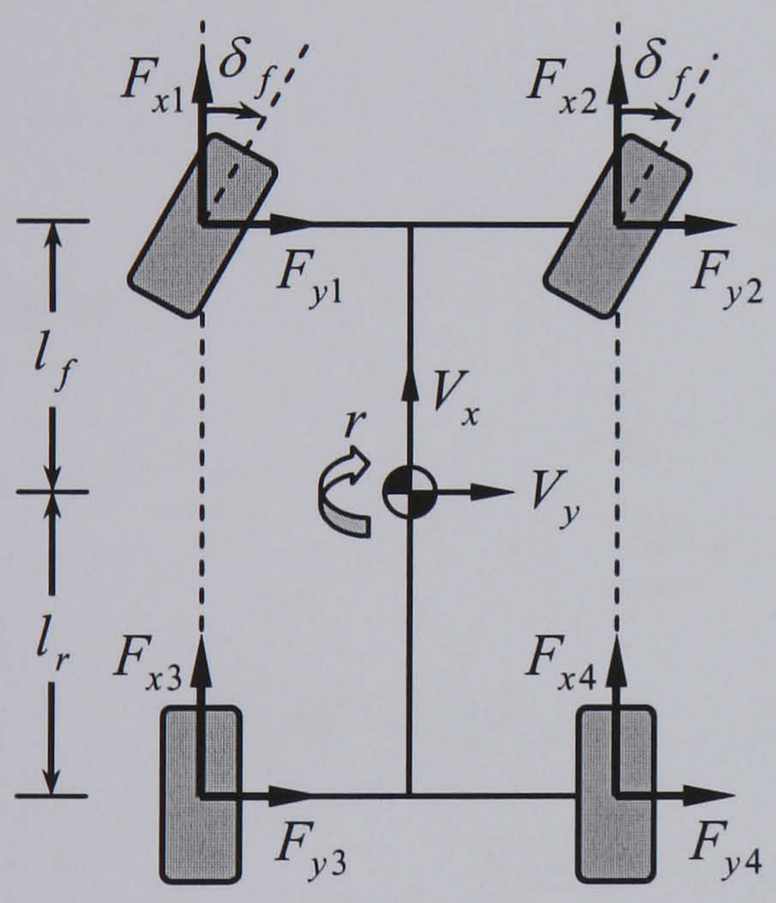

Top view

Figure 3.5 Schematic diagrams of the NLVM with degrees of freedom and external forces

Equations of motion

All equations of motion of the NLVM are generated in the vehicle fixed reference frame and local wheel fixed coordinate system. The detailed derivation of the equations of motion can be referred to Appendix A and the complete list of vehicle parameters and variables used in the equations is in the Notations section. The eight equations of motion of the NLVM are given as:

$$\dot{V}_x = \frac{\sum F_x + m_s h \dot{r} \phi}{m} + V_y r \tag{3.19}$$

$$\dot{V}_y = \frac{\sum F_y - m_s h \ddot{\phi}}{m} - V_x r \tag{3.20}$$

$$\dot{r} = \frac{\sum M_z + I_{xz} \ddot{\phi}}{I_{zz}} \tag{3.21}$$

$$\ddot{\phi} = \frac{\sum M_x - m_s h(\dot{V}_y + V_x r) + I_{xz} \dot{r}}{I_{xx}} \tag{3.22}$$

$$\dot{\omega}_1 = \frac{-R_{w1} F_{xw1} + T_1}{I_w} \tag{3.23}$$

$$\dot{\omega}_2 = \frac{-R_{w2} F_{xw2} + T_2}{I_w} \tag{3.24}$$

$$\dot{\omega}_3 = \frac{-R_{w3} F_{xw3} + T_3}{I_w} \tag{3.25}$$

$$\dot{\omega}_4 = \frac{-R_{w4} F_{xw4} + T_4}{I_w} \tag{3.26}$$

where

$$\sum F_x = F_{x1} + F_{x2} + F_{x3} + F_{x4} - F_r$$

$$\sum F_y = F_{y1} + F_{y2} + F_{y3} + F_{y4}$$

$$\sum M_z = l_f (F_{y1} + F_{y2}) - l_r (F_{y3} + F_{y4}) + \frac{t_f}{2}(F_{x1} - F_{x2}) + \frac{t_r}{2}(F_{x3} - F_{x4})$$

$$\sum M_x = [m_s g h - (K_{\phi f} + K_{\phi r})]\phi - (C_{\phi f} + C_{\phi r})\dot{\phi}$$

$$m = m_s + m_{uf} + m_{ur}$$

Eqs. (3.23) to (3.26) are used to model the rotational dynamics of four road wheels and to predict the wheel angular velocity. Solutions of the above four equations allow the computation of the corresponding longitudinal slip ratio and then the longitudinal tyre forces. The single wheel dynamics model is illustrated in Figure 3.6.

External forces

The external forces acting on the vehicle are primarily the tyre forces generated at the tyre-road contact patches. In the above equations, F_{xi} and F_{yi} are the resultant

longitudinal and lateral forces acting on the i th wheel in the vehicle fixed coordinate system. Tyre forces F_{xwi} and F_{ywi} are however defined in the local wheel axis system. Therefore, the resultant force components along the vehicle axes, F_{xi} and F_{yi} have the following relationships with the tyre forces along the wheel axes, F_{xwi} and F_{ywi}, as shown in Figure 3.6.

$$\begin{Bmatrix} F_{xi} \\ F_{yi} \end{Bmatrix} = \begin{bmatrix} \cos\delta_i & -\sin\delta_i \\ \sin\delta_i & \cos\delta_i \end{bmatrix} \begin{Bmatrix} F_{xwi} \\ F_{ywi} \end{Bmatrix}, \ (i = 1,...,4) \tag{3.27}$$

where δ_i is the steer angle of the i th wheel and is assumed to have the following relationships:

$$\delta_1 = \delta_2 = \delta_f, \ \delta_3 = \delta_4 = \delta_r \tag{3.28}$$

The rolling resistance F_r is given as (Gillespie, 1992):

$$F_r = f_r W \tag{3.29}$$

where

f_r : Rolling resistance coefficient

W : Weight of the vehicle

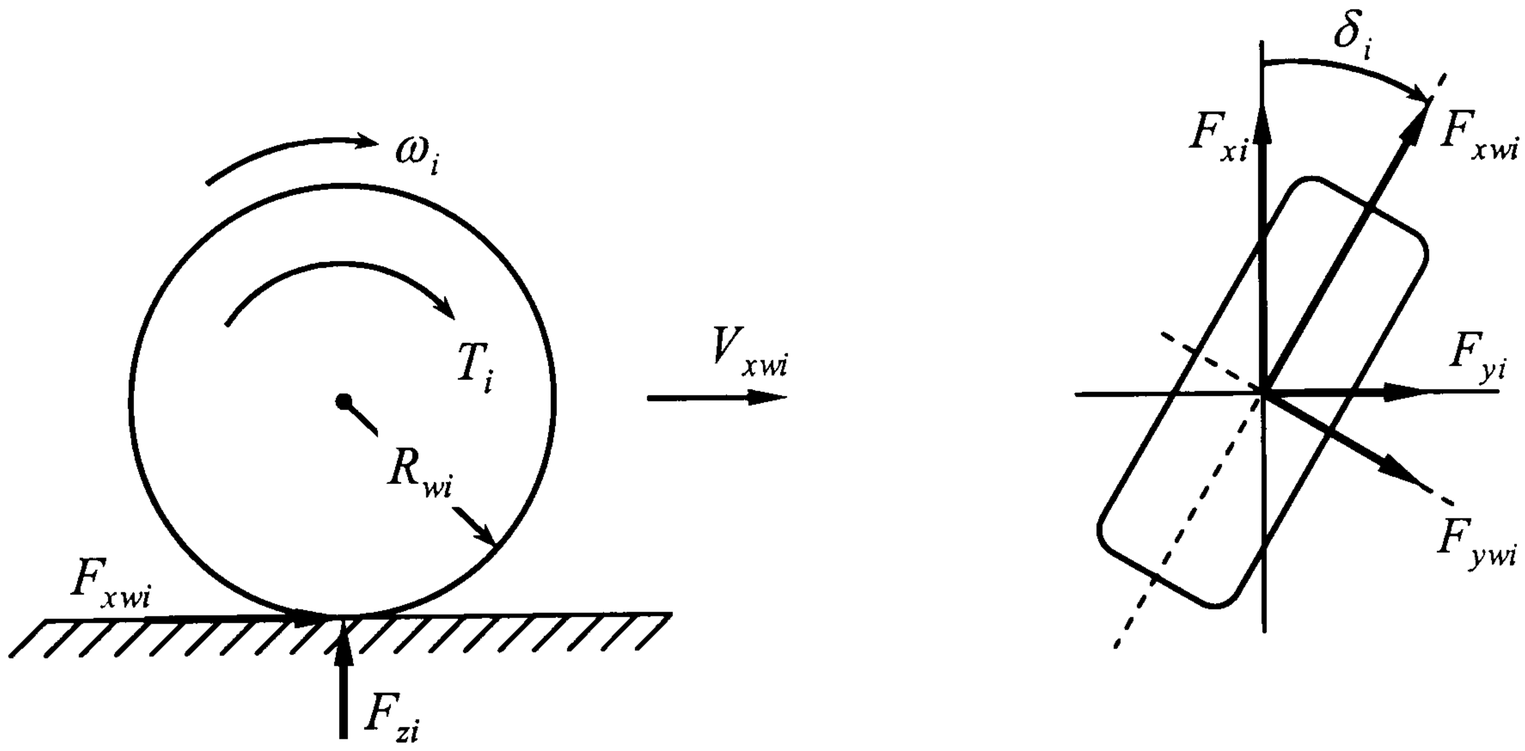

Single wheel dynamics model Tyre force relationship

Figure 3.6 Single wheel dynamics model and tyre force relationship

3.2.5 Calculation of tyre loads

The amount of vertical load on a tyre determines the available tyre forces. The vertical tyre loads are normally given by the weight of the vehicle and the position of the

centre of gravity. Nevertheless, vertical tyre loads vary with dynamic load transfer which results from inertial forces generated by the acceleration of vehicle masses. Therefore the vehicle handling model must also accommodate such load transfer and account for differential roll stiffness between front and rear axles. The load transfer effects are especially critical in modelling vehicle limit performance under extreme driving conditions. During dynamic manoeuvres, the instantaneous tyre load is the sum of static load plus load transfer that is due to longitudinal acceleration, lateral acceleration and body roll motion, respectively, i.e.

$$F_{zi} = F_{z0i} + F_{zaxi} + F_{zayi} + F_{z\phi i} \tag{3.30}$$

Herein, the quasi-static balance equations will be employed to calculate the vertical load for each corner of the vehicle.

Static loads on level ground

When the vehicle is at rest or travels at constant forward speeds on a straight and level road, the static loads on the front and rear axles are:

$$F_{zf0} = mg\frac{l_r}{l} \tag{3.31}$$

$$F_{zr0} = mg\frac{l_f}{l} \tag{3.32}$$

Load transfer due to longitudinal acceleration

When the vehicle accelerates, load transfer from the front axle to the rear axle takes place due to inertia, thereby the load on the front is reduced and the load on the rear is increased by the same amount. During deceleration or braking, the opposite is the case. With the assumption of moderate longitudinal acceleration and no body pitch, the vehicle can be treated as one lumped mass m located at its CG. With reference to the side view of the vehicle model in Figure 3.5, taking moment about the centre of contact for rear tyres gives the load on the front axle:

$$F_{zf} = mg\frac{l_r}{l} - ma_x\frac{h_{cg}}{l} = F_{zf0} - F_{zax} \tag{3.33}$$

Similarly, the load on the rear axle is given as:

$$F_{zr} = mg\frac{l_f}{l} + ma_x\frac{h_{cg}}{l} = F_{zr0} + F_{zax} \tag{3.34}$$

Thus the total longitudinal load transfer is:

$$F_{zax} = \frac{ma_x h_{cg}}{l} \tag{3.35}$$

The change in the vertical load for each wheel on the same axle due to longitudinal acceleration is assumed to be equal, i.e. $F_{zax}/2$.

Load transfer during cornering

During cornering, the centrifugal force developed at the CG due to inertia tends to pull the vehicle away from the turn and causes lateral load transfer, resulting in the increased outer wheel load and decreased inner wheel load. Actually, load transferred in the lateral direction results from both lateral acceleration and the vehicle body roll motion about the roll axis. The lateral load transfer model for a full vehicle negotiating a left hand turn is illustrated in Figure 3.7. The SAE definition is used for the roll centre and it is assumed to lie on the vehicle centreline. In addition, the inclination of roll axis is ignored and the lateral acceleration for both sprung and unsprung masses is assumed to be the same for analysis convenience.

The centrifugal forces, $m_{uf}a_y$ and $m_{ur}a_y$, associated with the front and rear unsprung masses, cause separate lateral load transfer terms across each axle. The amount of corresponding load transfer can be calculated in the same way as the longitudinal one and is given as:

$$F_{zayf(1)} = \frac{m_{uf}a_y h_{uf}}{t_f} \tag{3.36}$$

$$F_{zayr(1)} = \frac{m_{ur}a_y h_{ur}}{t_r} \tag{3.37}$$

The forces, $m_s a_y$ and $m_s g$, cause a total load transfer which is distributed in the same way between the front and rear axles. These two forces may be treated as one

force at the point of A which is the projection of the sprung mass CG on the roll axis plus a roll moment, i.e.

$$M_{xs} = m_s a_y h \cos\phi + m_s g h \sin\phi \tag{3.38}$$

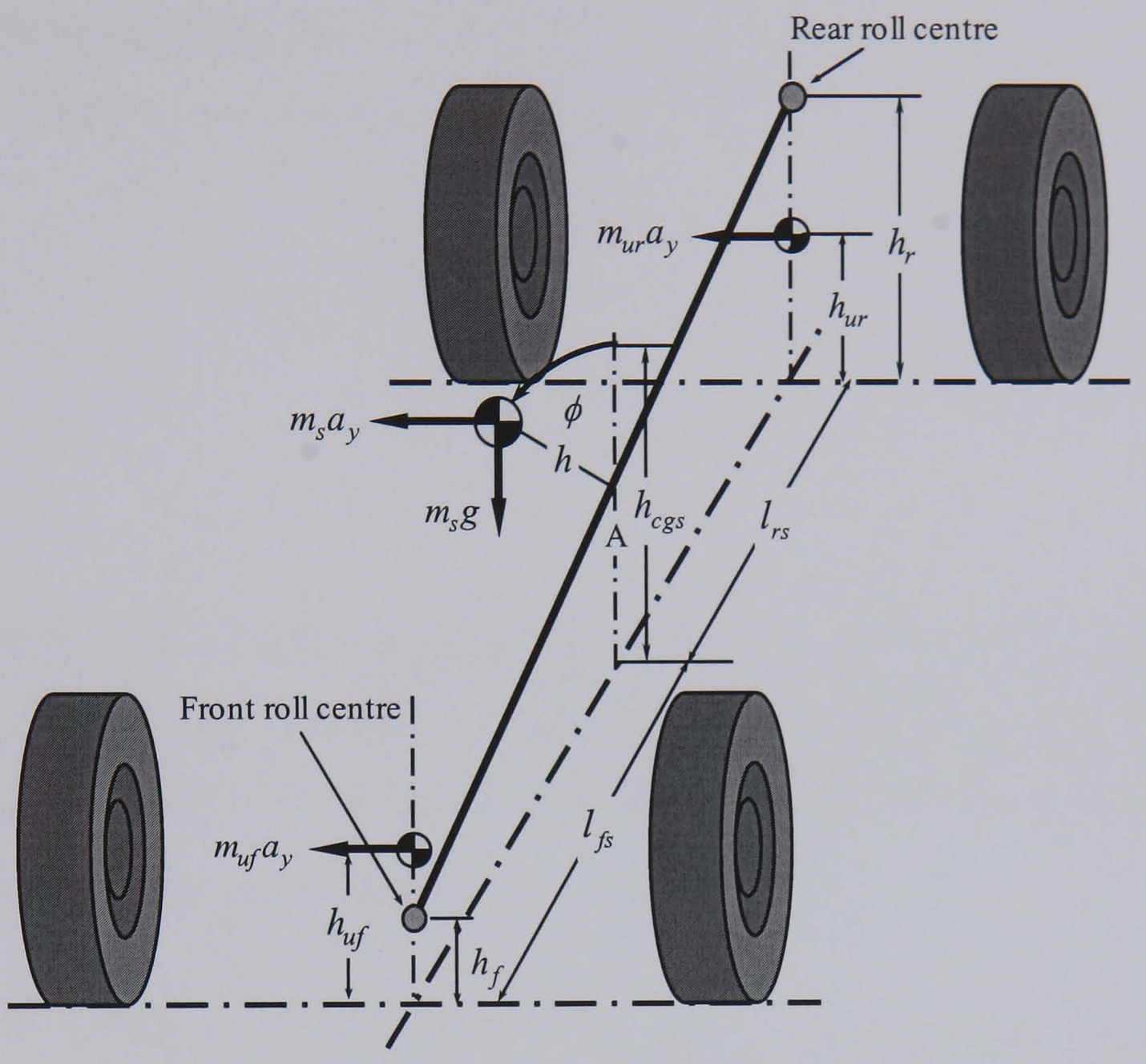

Figure 3.7 The lateral load transfer model for a full vehicle

This moment must be reacted by the suspension springs and anti-roll bars. If the vehicle body can be assumed to be torsionally stiff, then the above roll moment may be distributed according to the ratio of the roll stiffness between the front and rear axles. The active roll moment distribution control systems indeed utilise this property to determine the load transfer balance between front and rear and thus affect the vehicle handling performance. The roll moments reacted at front and rear axles are given by:

$$M_{xsf} = -K_{\phi f}\phi - C_{\phi f}\dot{\phi} \tag{3.39}$$

$$M_{xsr} = -K_{\phi r}\phi - C_{\phi r}\dot{\phi} \tag{3.40}$$

Thus load transfer terms due to the body roll motion are:

$$F_{z\phi f} = \frac{M_{xsf}}{t_f} \tag{3.41}$$

$$F_{z\phi r} = \frac{M_{xsr}}{t_r} \tag{3.42}$$

The lateral force, $m_s a_y$, which acts at point A can be distributed between the front and rear suspension along the roll axis, i.e. acting at the front and rear roll centres, respectively. The amount of corresponding lateral load transfer is given as:

$$F_{zayf(2)} = \frac{m_s a_y l_{rs}}{l} \cdot \frac{h_f}{t_f} \tag{3.43}$$

$$F_{zayr(2)} = \frac{m_s a_y l_{fs}}{l} \cdot \frac{h_r}{t_r} \tag{3.44}$$

The total lateral load transfer for both front and rear is the sum of the above three components. The vehicle negotiating a right hand turn results in positive values for all of the three components. Therefore, the vertical tyre load acting on each wheel F_{zi} during manoeuvres can be expressed as:

$$F_{z1} = \frac{mgl_r}{2l} - \frac{ma_x h_{cg}}{2l} + \frac{a_y}{t_f}\left(\frac{m_s l_{rs} h_f}{l} + m_{uf} h_{uf}\right) + \frac{1}{t_f}\left(-K_{\phi f}\phi - C_{\phi f}\dot{\phi}\right) \tag{3.45}$$

$$F_{z2} = \frac{mgl_r}{2l} - \frac{ma_x h_{cg}}{2l} - \frac{a_y}{t_f}\left(\frac{m_s l_{rs} h_f}{l} + m_{uf} h_{uf}\right) - \frac{1}{t_f}\left(-K_{\phi f}\phi - C_{\phi f}\dot{\phi}\right) \tag{3.46}$$

$$F_{z3} = \frac{mgl_f}{2l} + \frac{ma_x h_{cg}}{2l} + \frac{a_y}{t_r}\left(\frac{m_s l_{fs} h_r}{l} + m_{ur} h_{ur}\right) + \frac{1}{t_r}\left(-K_{\phi r}\phi - C_{\phi r}\dot{\phi}\right) \tag{3.47}$$

$$F_{z4} = \frac{mgl_f}{2l} + \frac{ma_x h_{cg}}{2l} - \frac{a_y}{t_r}\left(\frac{m_s l_{fs} h_r}{l} + m_{ur} h_{ur}\right) - \frac{1}{t_r}\left(-K_{\phi r}\phi - C_{\phi r}\dot{\phi}\right) \tag{3.48}$$

These expressions will be used to calculate the instantaneous vertical load inputs to the nonlinear tyre model to be developed in the following section.

3.3 Tyre Model

As mentioned in preceding sections, the dominant forces acting on a road vehicle are generated in the tyre-road contact patch. The tyre serves as a component of the whole vehicle system to support the vehicle load and absorb the road irregularities, to

develop longitudinal forces for acceleration and braking, and to generate lateral forces necessary to control the direction of the vehicle. Therefore, in order to simulate and analyse the complete vehicle handling region, ranging from linear perturbation to large transient performance limit, it is important to accurately predict tyre forces. These forces are generally dependent on so many parameters. But for a given tyre-road friction pair they can be fairly accurately estimated through the instantaneous tyre load, the longitudinal slip ratio and the lateral slip angle.

3.3.1 Definitions

To enable precise description of the forces and moments generated on a tyre, the standard SAE tyre axis system is used (Gillespie, 1992), as shown in Figure 3.8. The forces on a tyre are developed through the deflection or more accurately - shear mechanism across the tyre-road contact patch. Both longitudinal and lateral forces come from some amount of slip occurring at the tyre-road interface, which are known as the longitudinal slip ratio λ and lateral slip angle α, respectively.

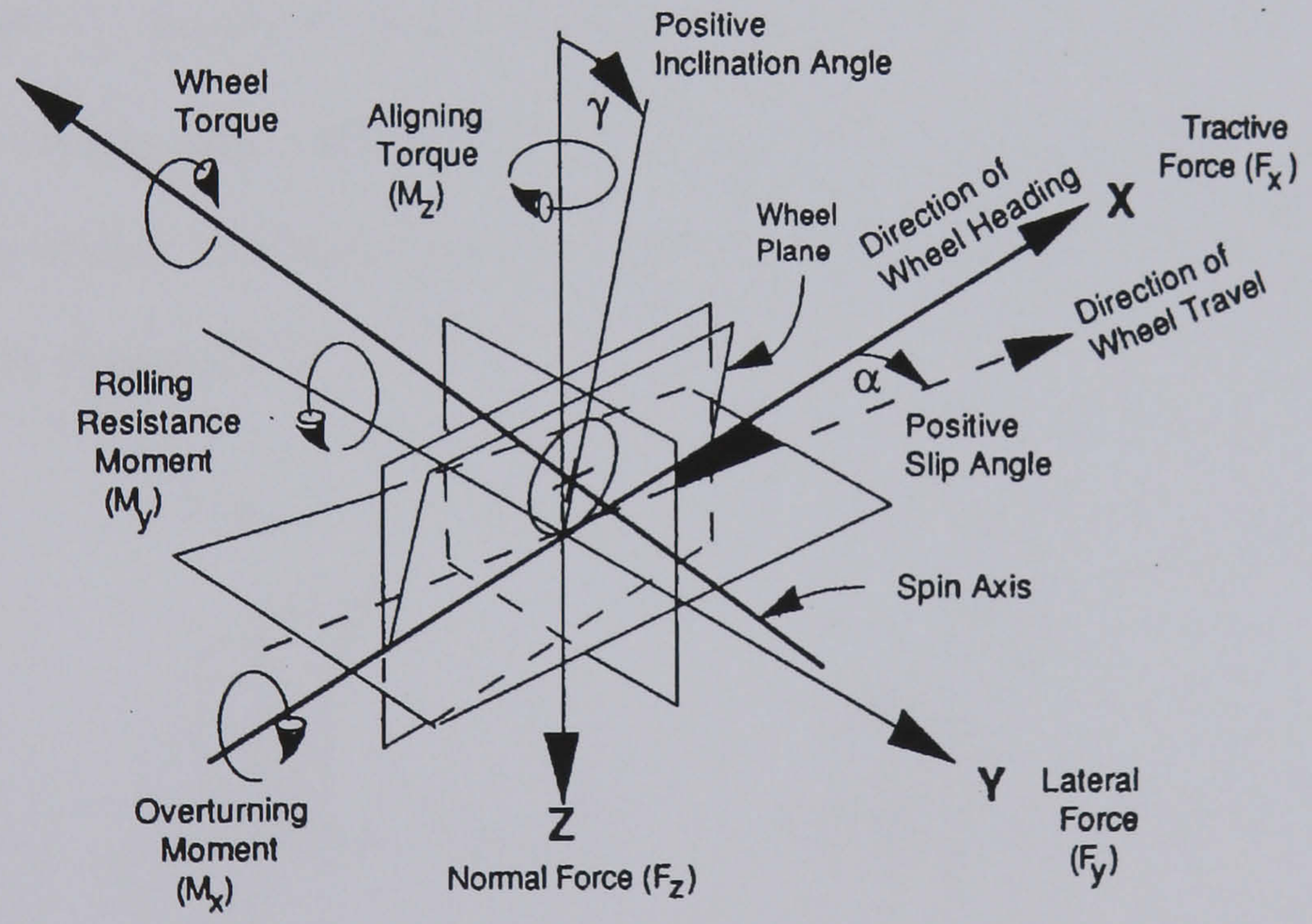

Figure 3.8 SAE tyre axis system

The longitudinal slip ratio λ is defined as the ratio of the difference between the tyre rolling speed and the wheel centre speed in the direction of wheel heading to the tyre rolling speed or the wheel centre speed in the direction of wheel heading depending on acceleration or braking. The definition is given as:

$$\lambda = \begin{cases} \dfrac{R_w\omega - V_{xw}}{R_w\omega}, & \text{if } R_w\omega \geq V_{xw} \text{ (acceleration)} \\ \dfrac{R_w\omega - V_{xw}}{V_{xw}}, & \text{if } R_w\omega < V_{xw} \text{ (braking)} \end{cases} \tag{3.49}$$

The variables used in the above equations can be referred to Figure 3.6. For a pure rolling tyre, $V_{xw} = R_w\omega$, hence $\lambda = 0$; when a tyre is spinning on slippery roads, $\lambda = 1$, and for complete wheel lock, $\lambda = -1$.

The tyre slip angle α is defined as the angle between the direction of wheel heading and the direction of wheel travel. The tyre slip angle is illustrated in Figure 3.9 and can be expressed as:

$$\alpha_i = \tan^{-1}\left(\frac{V_{yi}}{V_{xi}}\right), \text{(unsteered wheel, } i = 3,4) \tag{3.50}$$

$$\alpha_i = \tan^{-1}\left(\frac{V_{yi}}{V_{xi}}\right) - \delta_i, \text{(steered wheel, } i = 1,\ldots,4) \tag{3.51}$$

where V_{xi} and V_{yi} represent longitudinal and lateral speed components of the ith wheel centre along the vehicle fixed axes, and δ_i is the steer angle of the corresponding wheel. The calculation of individual tyre slip ratio λ_i and slip angle α_i can be found in Appendix B.

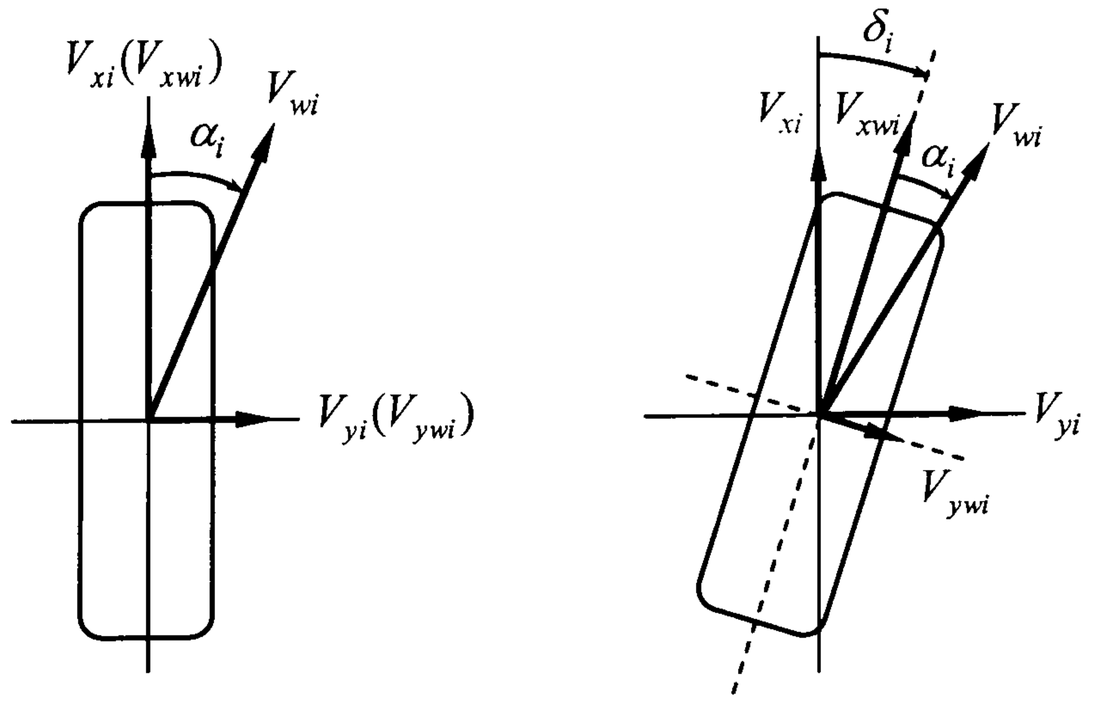

Figure 3.9 Definition of tyre slip angle for unsteered and steered wheels

3.3.2 Pacejka tyre model

Various tyre models have been developed to predict tyre forces. The linear tyre model, which is often used for the basic analysis of vehicle handling, as in the 2DOF

linear bicycle model presented previously, only considers the lateral force as a linear function of the tyre slip angle and does not include the effect of the longitudinal force. This model is simply expressed in the form of Eqs. 3.5 and 3.6. Such an expression actually is the linear representation of the tyre cornering properties. However, this is only appropriate for low levels of lateral acceleration and it is not capable of simulating the effect of lateral tyre force saturation under critical driving conditions. A more comprehensive nonlinear model which can reasonably estimate both longitudinal and lateral tyre forces over the entire range of vehicle handling manoeuvres up to the performance limit is therefore essential. In this thesis, the tyre model developed by Pacejka and Besselink (1997) (referred to as *Pacejka Tyre Model* or *Magic Formula Tyre Model*) is used to characterise the tyre nonlinear behaviour. The Pacejka Tyre Model coefficient values are included in Appendix C.

This model employs an empirical formula known as "Magic Formula" to express the longitudinal tyre force F_{xw}, the lateral tyre force F_{yw} and the self-aligning moment M_{zw} as a function of slip ratio λ and slip angle α, respectively. It can be used to describe the pure slip condition under which only the longitudinal or lateral force is produced at a time and can also be modified to cope with the combined slip condition under which the longitudinal and lateral forces are generated simultaneously. The general form of the formula which holds for a given vertical load is given as:

$$Y(X) = D\sin\{C\arctan[B(1-E)(X+S_h)+E\arctan[B(X+S_h)]]\}+S_v \quad (3.52)$$

where the output $Y(X)$ represents F_{xw}, F_{yw} or M_{zw}, and the input X denotes λ or α, respectively. The coefficients in the formula are obtained from experimental tests and do not have any direct physical meaning but just define the shape of the force curves:

B : Stiffness factor

C : Shape factor

D : Peak factor

E : Curvature factor

S_h : Horizontal shift

S_v : Vertical shift

Pure longitudinal and lateral slip

For pure longitudinal slip, the slip ratio λ and vertical tyre load F_z are used as the model inputs. The typical pure longitudinal force characteristic curves produced by the Pacejka Tyre Model for the tyre that will be used in this thesis are shown in Figure 3.10. It can be seen that for a given tyre load and small values of slip the longitudinal force generation is approximately proportional to slip. As the slip increases the longitudinal force reaches a maximum at about 10% to 20% slip after which it decreases. Actually, this property is of primary importance and usually utilised by ABS and TCS to maintain tyres near the peak value of the longitudinal force and to prevent tyres from lockup or spinning.

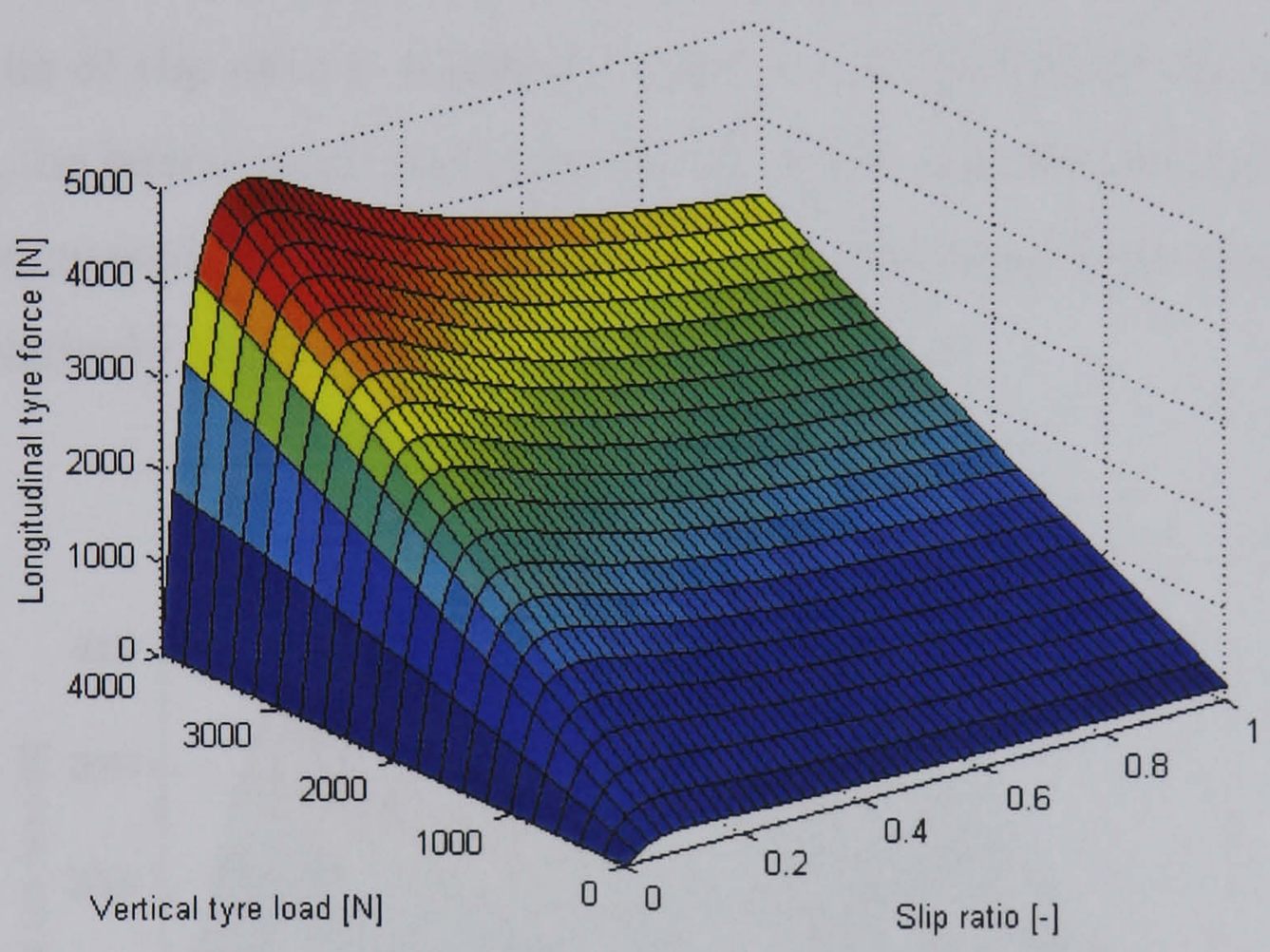

Figure 3.10 Pure longitudinal tyre force as a function of slip ratio and vertical tyre load calculated by the Pacejka Tyre Model

In the case of pure lateral slip, the model inputs consist of the slip angle α and the vertical load F_z. The typical pure lateral tyre force characteristics based on the Pacejka Tyre Model are shown in Figure 3.11. Similarly, for a given tyre load and small values of slip angle, the lateral force increases approximately linearly with the slip angle and saturates at around $10^\circ - 15^\circ$ slip angle after which it declines as the slip angle increases. In addition, the lateral force at a given slip angle increases with the vertical tyre load, but it does not go up proportionally with load. This characteristic plays an important role in lateral load transfer which leads to a reduction in the lateral force of the corresponding axle during cornering.

Combined longitudinal and lateral slip

The pure slip conditions apply only to the case in which lateral and longitudinal forces are generated separately such as during steady-state cornering and straight ahead driving. When a tyre generates lateral and longitudinal forces simultaneously, the situation will be different as the force developed in one direction generally tends to reduce that available in the other direction, i.e. interaction between forces exists. Figure 3.12 shows the longitudinal and lateral forces calculated by the Pacejka Tyre Model under combined slip conditions. It can be clearly seen that at zero slip angle the longitudinal force is at its maximum and maximum lateral force occurs when slip ratio is zero. In addition, at a certain value of slip ratio, the longitudinal force declines as slip angle increases and the reduction in the longitudinal force is more significant when the value of slip ratio is relatively small. For the lateral force, at a certain value of slip angle, the lateral force decreases slowly at first and then increasingly fast when slip ratio is increased. At wheel lock or spinning the lateral force practically reduces to zero for relatively small values of slip angle.

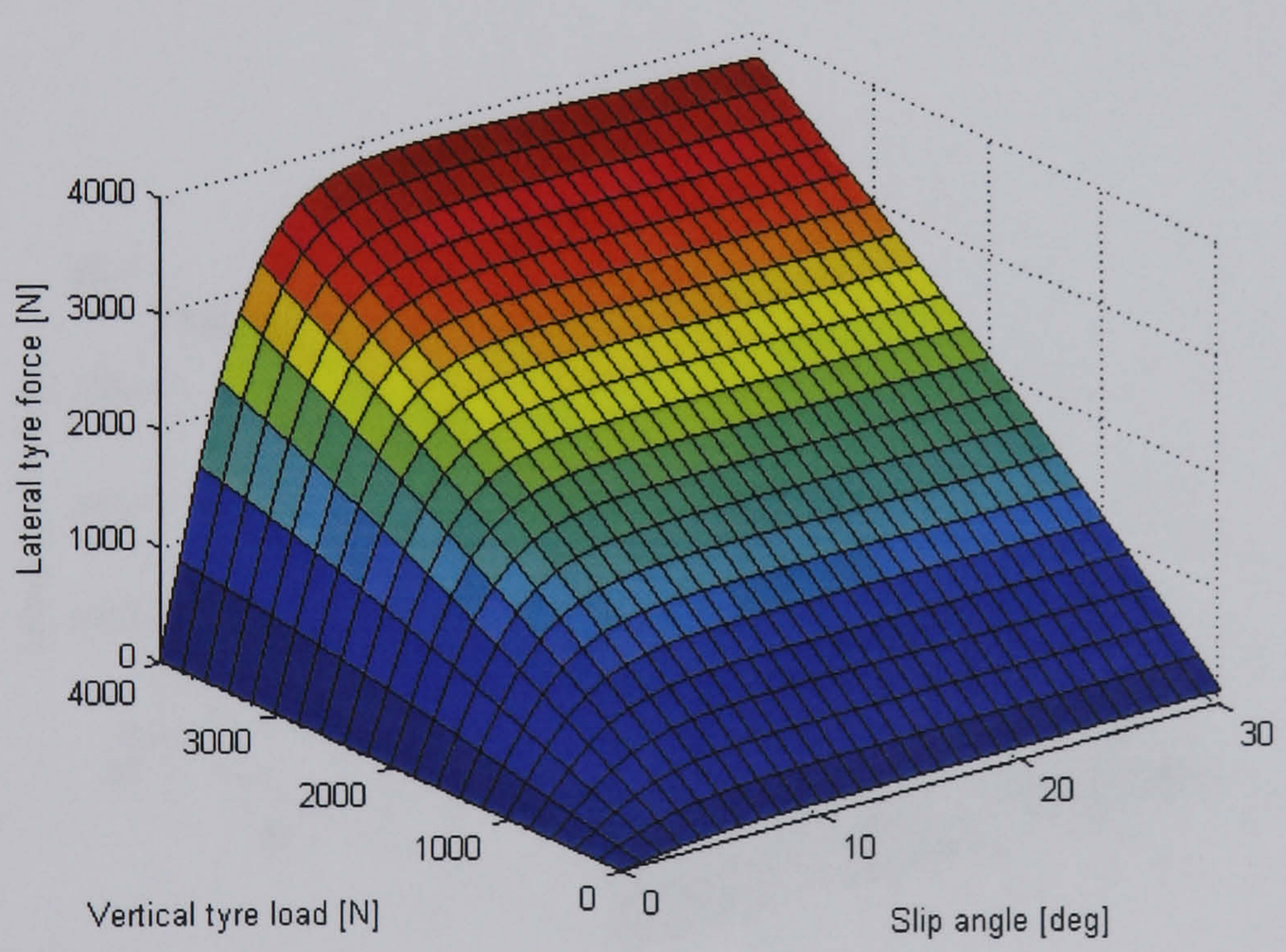

Figure 3.11 Pure lateral tyre force as a function of slip angle and vertical tyre load calculated by the Pacejka Tyre Model

Tyre lags

The empirical tyre model introduced above is a steady-state model and does not possess any transient properties. As noted in Pacejka (1997), steady-state tyre models are only accurate for steady or slow varying motions. When tyre slip angle and

vertical loads vary quickly during high lateral acceleration and rapid transient manoeuvres, the transient effect on the tyre dynamics must be taken into consideration as the tyre takes a finite time to react to these changes and reach a new steady state. Many studies have stated that a first order lag is sufficient to model this effect (Crolla, 1992; Dixon, 1996; Esmailzadeh *et al.*, 2001).

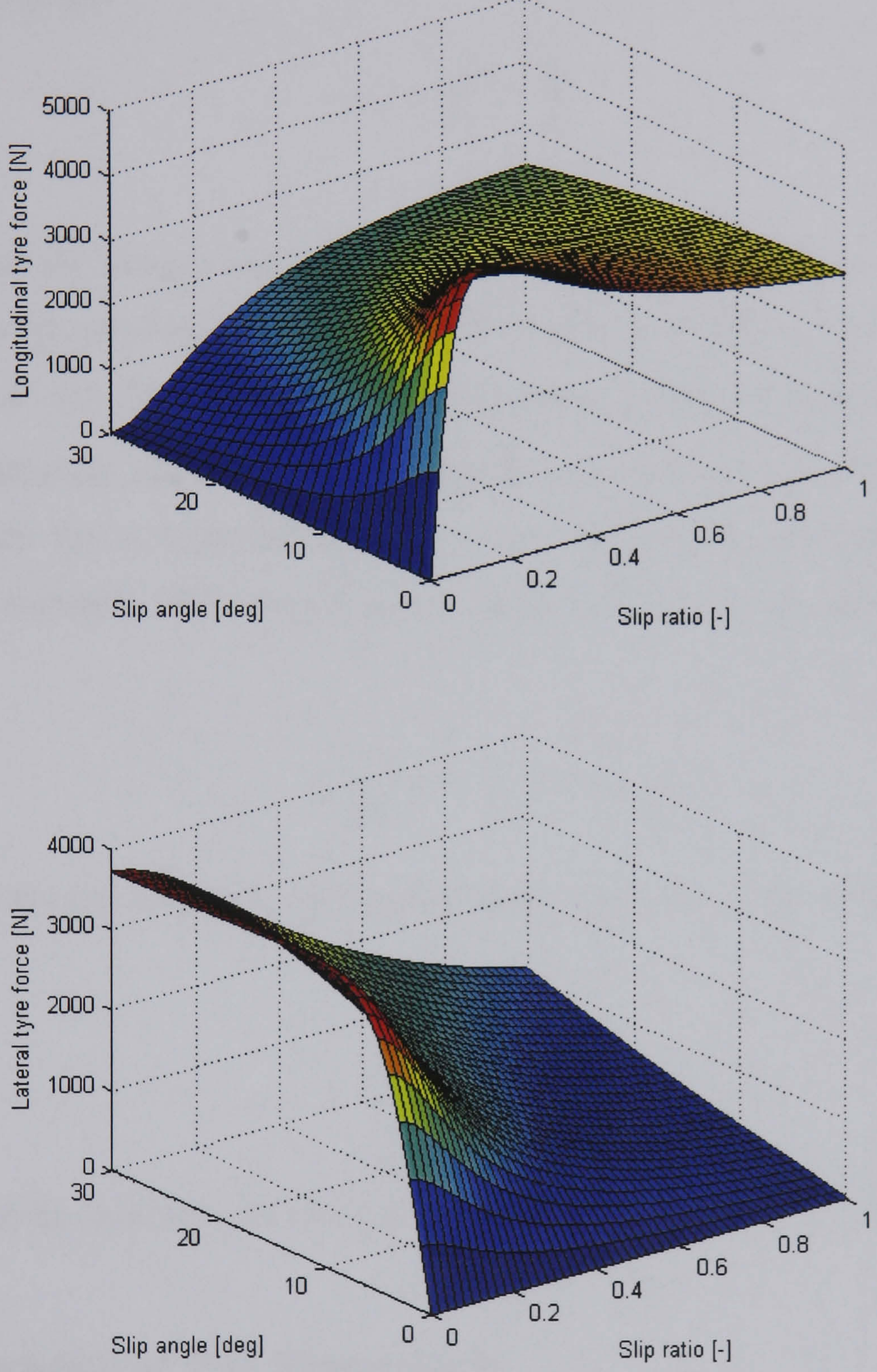

Figure 3.12 Longitudinal and lateral tyre forces calculated by the Pacejka Tyre Model under combined slip conditions ($F_z = 4000\text{N}$)

For the lateral tyre force, the lag has a time constant equal to the time taken by the tyre to roll through a distance known as the lateral relaxation length RL_y. This length

is approximately equal to the tyre rolling radius (Crolla, 1992; Dixon, 1996). Therefore the lateral tyre force is finally modelled as:

$$\tau_{yl}\frac{d}{dt}F_{yw}+F_{yw}=F_{ywss} \tag{3.53}$$

where τ_{yl} is the time constant for the lateral tyre force and takes the following approximated form:

$$\tau_{yl}=\frac{RL_y}{V_x}=\frac{R_w}{V_x} \tag{3.54}$$

In the case of the longitudinal tyre force, as the tyres are stiffer in the longitudinal direction, the longitudinal relaxation length is of lesser effect (Clover and Bernard, 1998). Clover and Bernard define the longitudinal relaxation length RL_x to be the ratio of longitudinal slip stiffness to longitudinal carcass stiffness. The recommended value, 0.091m for a 0.3m radius tyre for the longitudinal relaxation length from (Clover and Bernard, 1998) is used in this thesis. Similarly, the longitudinal tyre force is given as:

$$\tau_{xl}\frac{d}{dt}F_{xw}+F_{xw}=F_{xwss} \tag{3.55}$$

where τ_{xl} is the time constant for the longitudinal tyre force and can be approximated as:

$$\tau_{xl}=\frac{RL_x}{V_x} \tag{3.56}$$

The self-aligning moment is neglected in this study due to its very small magnitude.

3.4 Description of Test Manoeuvres

There are a number of test procedures that can be simulated to determine the effectiveness of a particular control system. The following represents time based analysis of the vehicle. In this thesis, the driver steer inputs refer to the steer angle applied at the front wheels by the driver and have the following relationship with the steering wheel angle δ_{sw}:

$$steer\ angle = \frac{\delta_{sw}}{n_s} \tag{3.57}$$

where n_s is the steering ratio.

The evaluation of the controller performance will be performed on the NLVM within Matlab/Simulink® environment. All the test manoeuvres except steady-state cornering will be examined in an open-loop manner and no driver model or course tracking controller is included in the control loop, i.e. the driver does not apply any steering corrections after applying an initial steer input for negotiating a specific manoeuvre. This is because no single driver is the same in the first place, and secondly, any real driver will adapt himself to the vehicle during driving. Therefore the performance of the driver-vehicle closed-loop system cannot be evaluated through the simulations conducted in this thesis. The definition of the manoeuvres is referred to the ISO/SAE standards.

Steady-state cornering

The steady-state cornering manoeuvre is the classical method to measure the steady-state handling characteristics of the vehicle. There are various ways to study the steady-state handling properties of the vehicle and the constant radius method is employed in this thesis (Gillespie, 1992; Dixon, 1996). In this test the vehicle is initially driven around a constant 33m radius path at a low speed and the vehicle forward speed is then increased in steps, thus increasing the amount of lateral acceleration produced by the vehicle. A simple PI course tracking controller will be used in this manoeuvre to force the vehicle to follow the desired circular curve. The understeer gradient can thus be examined against the lateral acceleration.

Constant speed J-Turn

The constant speed J-Turn is a simple handling procedure that consists of straight running for a set time before commencing a turn that eventually results in steady-state cornering at a specific level of lateral acceleration. This manoeuvre is a common method to evaluate both steady-state response and transient behaviour of the vehicle. As the name implies, in this test, the vehicle forward speed is kept constant at 100km/h. The steer input for this manoeuvre is illustrated in Figure 3.13 and the

amplitude of the steer input is the steer angle required to produce a lateral acceleration of 0.4g.

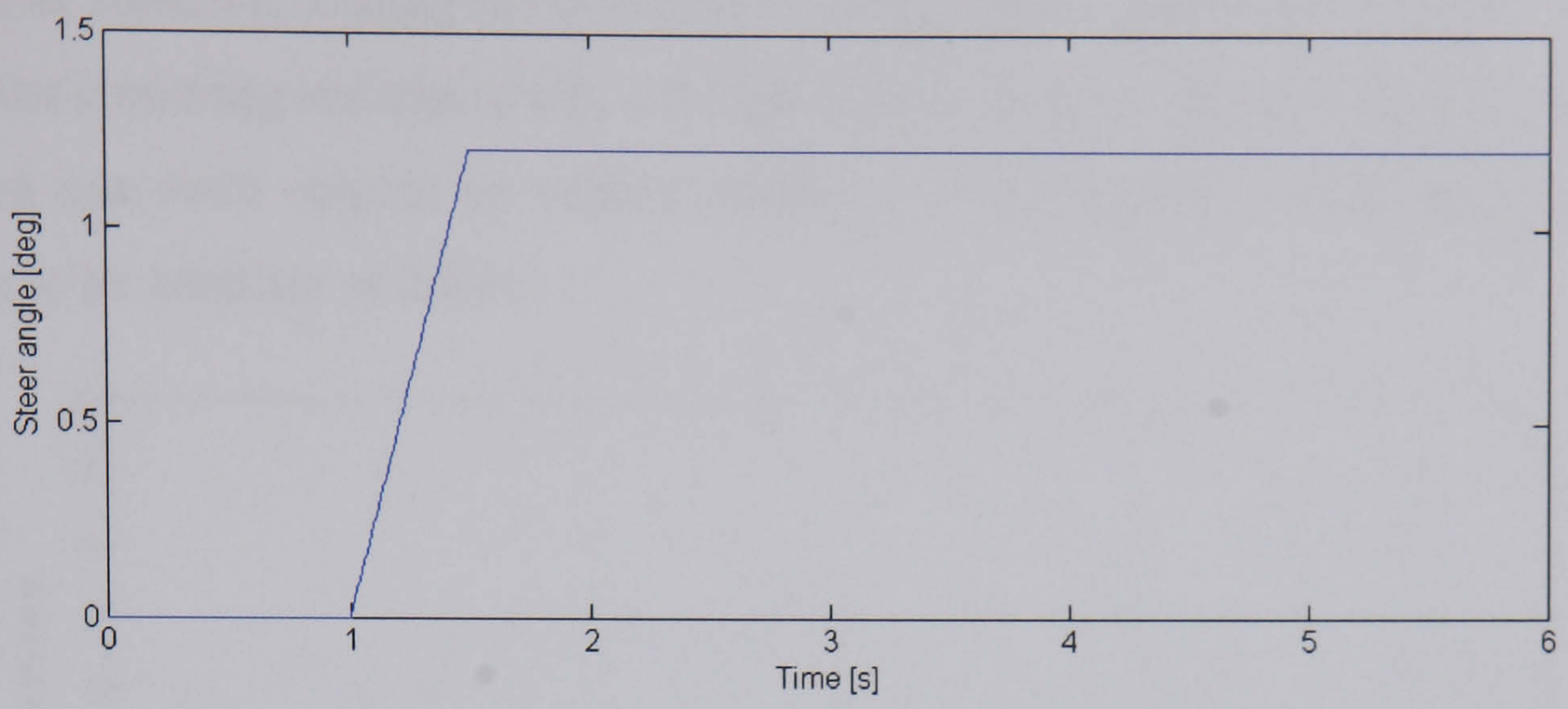

Figure 3.13 Steer angle for constant speed J-Turn

Single sine steer input

The single sine steer input is used to simulate the response of the vehicle to a single lane change manoeuvre. This manoeuvre is a good way to evaluate the transient handling behaviour of the vehicle and to determine vehicle stability. The test is conducted at a speed of 100km/h and the steer input is applied at various amplitudes with a constant frequency of 0.5Hz. The steer inputs that are required to produce peak lateral acceleration of 0.5g, 0.7g and to push the vehicle towards the handling limit for such manoeuvres are shown in Figure 3.14.

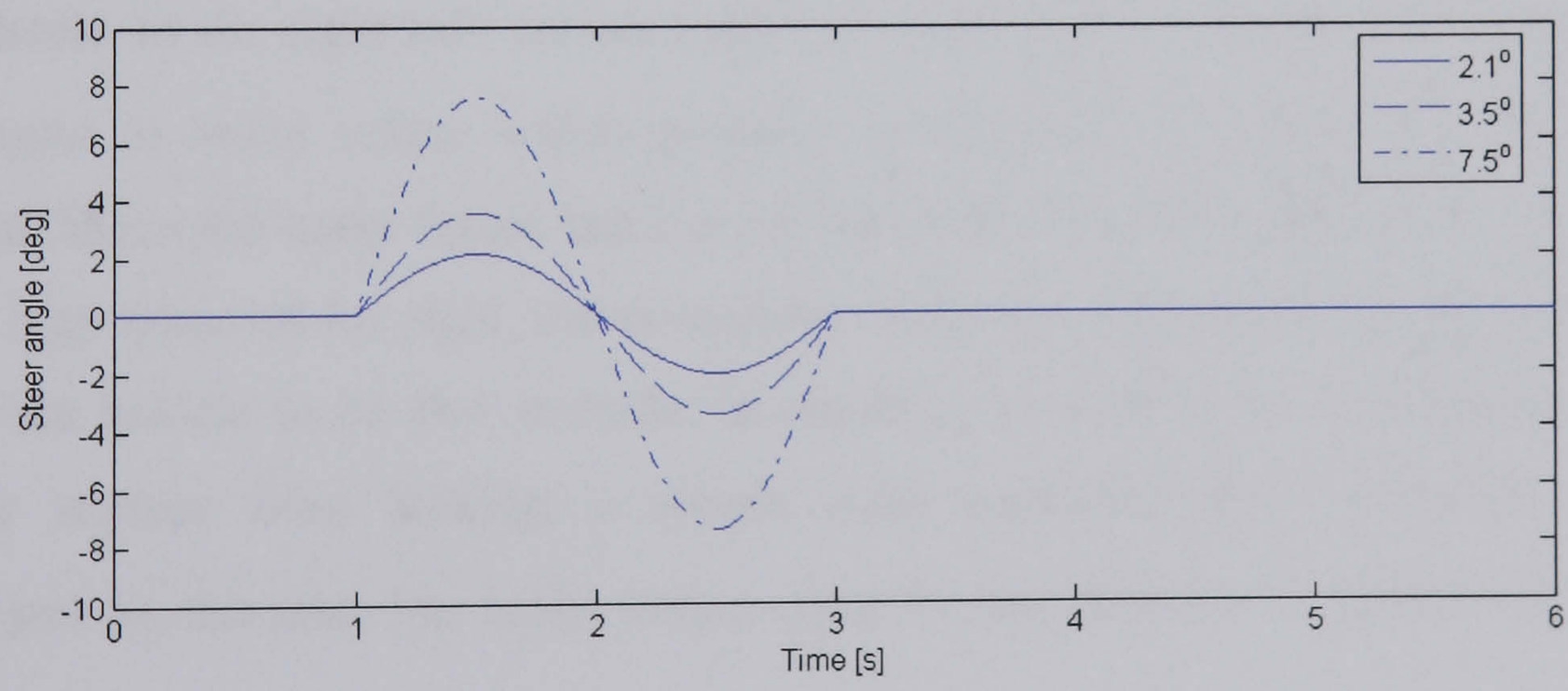

Figure 3.14 Steer angles for single sine steer input

Sine steer input with increasing amplitude

This manoeuvre is used to examine the vehicle dynamics from the linear handling region up to the performance limit. The steer input for this manoeuvre is shown in

Figure 3.15. The amplitude of the steer input is increased gradually until the vehicle reaches the limit of handling. The initial forward speed of the vehicle is once again chosen as 100km/h. During the manoeuvre the driving torque is held constant and as a result the cornering resistance will slow the vehicle down. This manoeuvre is the most extreme one with respect to vehicle stability. The frequency of the steer input is chosen to be constant at 0.6Hz.

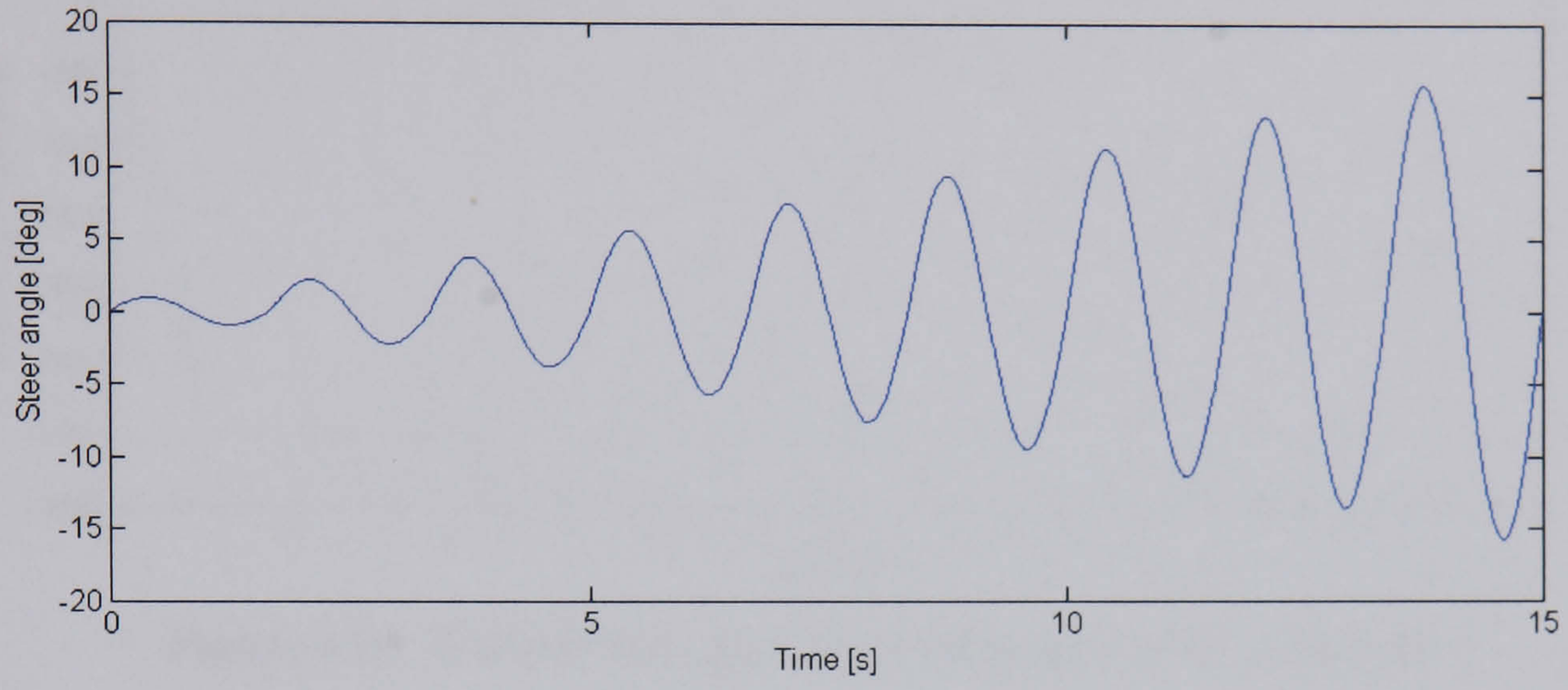

Figure 3.15 Steer angle for sine steer input with increasing amplitude

Braking on split-μ surfaces

This manoeuvre is utilised to examine vehicle straight ahead driving stability. In the test the vehicle is driven straight ahead at a speed of 100km/h on a split-μ surface where the wheels on the left side of the vehicle are on an icy ($\mu = 0.2$) surface and the wheels on the right side are on a dry ($\mu = 1.0$) surface and then an approximate step input in brake torque which produces a longitudinal acceleration of -0.4g is applied. Since the brake forces that can be achieved on the left side of the vehicle are lower than those on the right, the asymmetric braking will generate a yaw moment to cause the vehicle to be yaw instable. In addition, in order to prevent wheels on the low-μ surface from locking, a simple ABS controller (PD controller) is also employed for this test. The brake torque input for this manoeuvre is shown in Figure 3.16.

Overview of manoeuvres

Due to the nature of the manoeuvres described above, it is not necessary to test all the designed controllers on each one. The allocations of manoeuvres for evaluating

different control systems are listed in Table 3.2. All the manoeuvres can be applied to the passive vehicle and the active steering subsystems, AFS and ARS whereas DSC is examined only when stability control is required. Combined and integrated controls are evaluated for those manoeuvres where both stand-alone controllers are activated simultaneously.

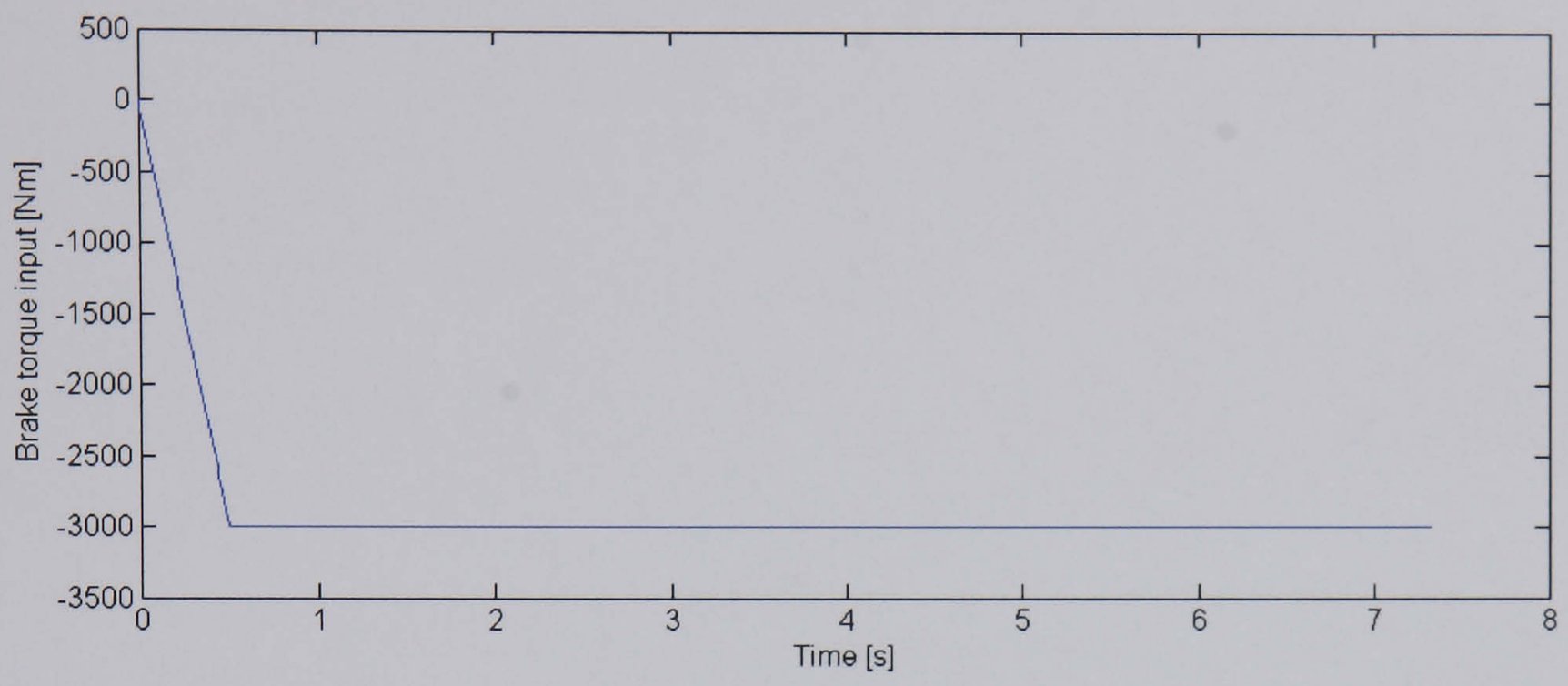

Figure 3.16 Brake torque input for braking on a split-μ surface

Table 3.2 Overview of test manoeuvres for controller evaluation

$\sqrt{}$= Evaluated; - = Not evaluated

Vehicle and Active Control / **Test Manoeuvres**	Passive vehicle	AFS	ARS	DSC	Combined control	Integrated control
Steady-state cornering	$\sqrt{}$	$\sqrt{}$	$\sqrt{}$	-	-	-
Constant speed J-Turn	$\sqrt{}$	$\sqrt{}$	$\sqrt{}$	-	-	-
Single sine steer input	$\sqrt{}$	$\sqrt{}$	$\sqrt{}$	$\sqrt{}$	$\sqrt{}$	$\sqrt{}$
Sine steer input with increasing amplitude	$\sqrt{}$	$\sqrt{}$	$\sqrt{}$	$\sqrt{}$	$\sqrt{}$	$\sqrt{}$
Braking on split-μ surfaces	$\sqrt{}$	$\sqrt{}$	$\sqrt{}$	$\sqrt{}$	-	-

3.5 Conclusions

This chapter has presented the details of vehicle modelling for handling analysis. Two vehicle handling models, a 2DOF linear bicycle model for controller design and an 8DOF nonlinear vehicle model for final control performance evaluation have been

developed. The features of each model have been discussed and justified with respect to the study to be performed. In addition, the Pacejka tyre model has also been introduced to simulate the nonlinear tyre characteristics. Finally the test manoeuvres which will be used to evaluate the performance of the proposed controllers have been described.

Chapter 4

Analysis of Vehicle Dynamics and Definition of Control Objectives

Abstract: *This chapter first examines the basic handling behaviour which includes both steady-state characteristics and transient dynamics of passive vehicles with respect to varying forward speed and lateral acceleration. The definition of control objectives for both stand-alone and integrated vehicle dynamics control systems is then presented.*

4.1 Introduction

Corresponding to the linear and nonlinear behaviour of the tyres, the lateral vehicle dynamics can also be separated into linear and highly nonlinear behaviour, respectively. The vehicle handling behaviour including steady-state characteristics and transient dynamics varies significantly in the linear and nonlinear regions, and with changes in driving situations and external environments. Therefore, before designing the active control systems for vehicle handling, the lateral dynamics of passive vehicles needs to be first analysed. In addition, in order to define the control objectives for both stand-alone and integrated control systems, the entire handling

regime of the vehicle is broken down into three distinct sub-regions with respect to the magnitude of lateral acceleration.

4.2 Lateral Dynamics of Passive Vehicles

Since handling in this thesis specifically refers to the lateral vehicle dynamics, this section will investigate this aspect of the vehicle dynamics in both linear and nonlinear handling regions. The primary variables which are of interest and are used to describe the lateral vehicle dynamics are the lateral acceleration a_y, the yaw rate r and the sideslip angle β.

4.2.1 2DOF nonlinear vehicle model (2NVM)

As discussed in Chapter 3, the 2DOF linear bicycle model can only be used to predict the vehicle handling behaviour for relatively low levels of lateral acceleration up to 0.3g. In order to extend the validity of the linear bicycle model and examine the lateral vehicle dynamics over the entire handling regime, a 2DOF nonlinear vehicle model (2NVM) is developed by substituting the pure lateral slip "Pacejka Tyre Model" for the linear tyre model and taking the quasi-static lateral load transfer effect into account. Consequently, in this nonlinear model, the left and right wheels on both front and rear axles are separated, which is the reverse case of the 2DOF linear bicycle model described in Chapter 3. The detailed description of the 2NVM can be found in Appendix D.

4.2.2 Steady-state handling characteristics

The steady-state handling refers to a steady or trim cornering condition in which the vehicle is driven at a constant speed and steer angle, resulting in a constant radius of turn (Crolla, 1992). Cornering of a bicycle model at both low and high speeds is illustrated in Figure 4.1 where CT_l and CT_h represent the centre of turn at low speeds and high speeds, respectively.

When a vehicle negotiates a turn at a very low speed, the tyres need not develop lateral forces and thus they roll with no slip angle, i.e. the tyres' direction of heading

and direction of travel are identical. Therefore the centre of turn CT_l must lie on the projection of the rear axle. The low-speed average steer angle of the front wheels (against small angle assumption) is defined as the *Ackerman Angle* (Gillespie, 1992) or the *Kinematic Angle* (Dixon, 1991), as shown in Figure 4.1:

$$\delta_A = l/R \tag{4.1}$$

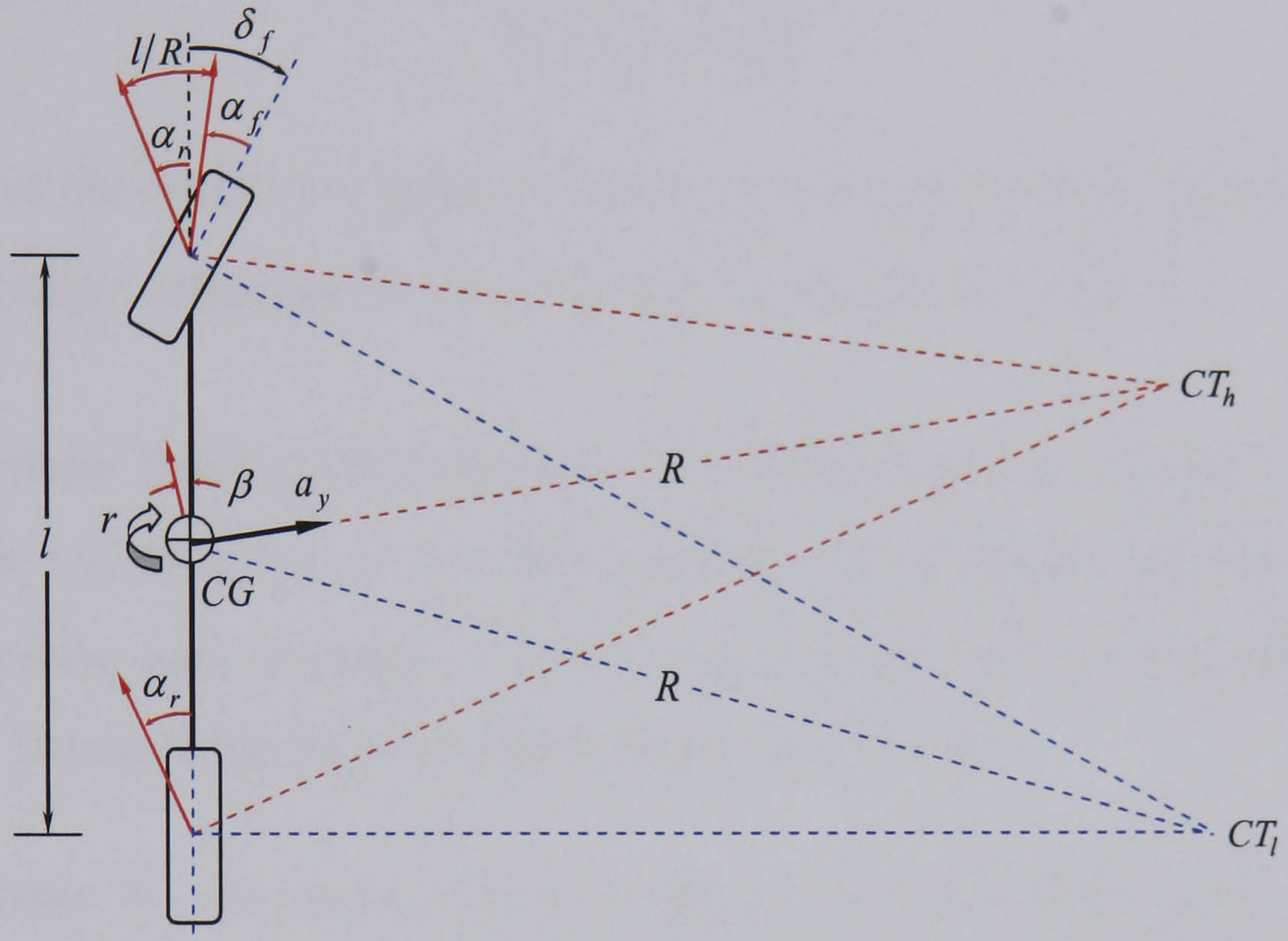

Figure 4.1 Schematics of cornering of a bicycle model

At high speeds, lateral acceleration will be present during cornering. To counteract the inertia force induced by the lateral acceleration the tyres must develop lateral forces, and slip angles will be present at each wheel, i.e. the tyre will experience lateral slip as it rolls and its direction of travel will deviate from its direction of heading. The centre of turn CT_h has now moved forward from the rear axle line. The sideslip angle at the CG is defined as the angle between the vehicle longitudinal axis and the local direction of travel (Gillespie, 1992). When the lateral acceleration is negligible, the sideslip angle is positive. At high speeds the slip angle on the rear wheels causes the sideslip angle at the CG to become negative, as shown in Figure 4.1.

Under steady-state cornering conditions, the trajectory of the vehicle CG is circular and thus the steady-state yaw rate and lateral acceleration can be expressed as:

$$r_{ss} = \frac{V_x}{R} \tag{4.2}$$

$$a_{yss} = \frac{V_x^2}{R} \tag{4.3}$$

For the linear bicycle model, the steady-state handling solution can be obtained by setting the dynamic terms on the left hand side of Eq. (3.11) to zero and solving for the two outputs V_y and r. Therefore one can have (Crolla, 1992):

$$\delta_f = \frac{l}{R} + K_u \frac{V_x^2}{R} \tag{4.4}$$

where K_u is the *understeer gradient* which is defined as the gradient of the front wheel steer angle demanded by the driver against lateral acceleration.

The steady-state handling characteristics of a vehicle can be measured through the steady-state cornering test on a constant radius. The understeer gradient K_u is the most commonly used measure of vehicle performance under steady-state handling conditions. Normally the following three cases are of interest:

- Understeer: $K_u > 0$, the steer angle needs to be increased with speed;
- Neutral steer: $K_u = 0$, the steer angle remains constant as the speed varies;
- Oversteer: $K_u < 0$, the steer angle will decrease as the speed is increased.

The understeer gradient of a passive vehicle described by the NLVM is plotted as a function of lateral acceleration as illustrated in Figure 4.2.

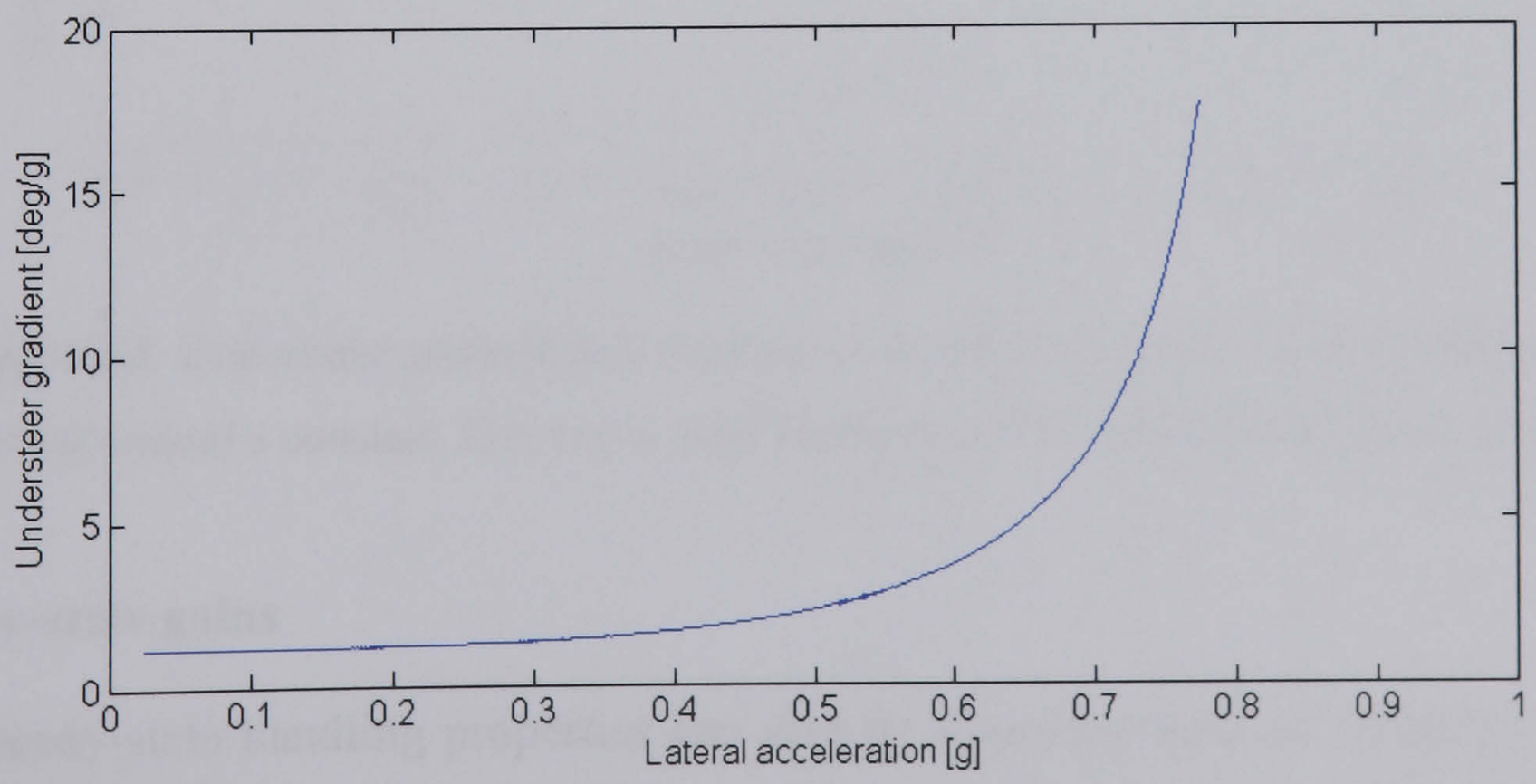

Figure 4.2 Understeer gradient as a function of lateral acceleration during steady-state cornering around a constant 33m radius path for the NLVM

As can be seen from Figure 4.2, the understeer gradient of the vehicle examined here remains almost the same up to around 0.3g of lateral acceleration and increases progressively towards the performance limit which is referred to as the *handling limit*. Therefore, at low levels of lateral acceleration up to 0.3g, the vehicle responds to steer inputs quite linearly. This is indeed the region that the 2DOF linear bicycle model is typically used to describe. Above this level the required steer angle for maintaining the cornering radius increases progressively.

The location of the handling limit largely depends on the friction between the tyre and road surface. The value of friction is dependent on many factors such as inflation pressure of tyres, condition of the road surface (dry, wet or icy) and condition of the tyre tread (worn or new), etc. (Smakman, 2000b). The road surface condition however is the dominant factor and this influence is shown in Figure 4.3. The basic shape of the curves remains unchanged for different values of the road surface coefficient of friction while the road friction does determine the range of the linear region and the location of the handling limit. Increasing road friction generally leads to wide linear region and high handling limit in terms of the level of lateral acceleration.

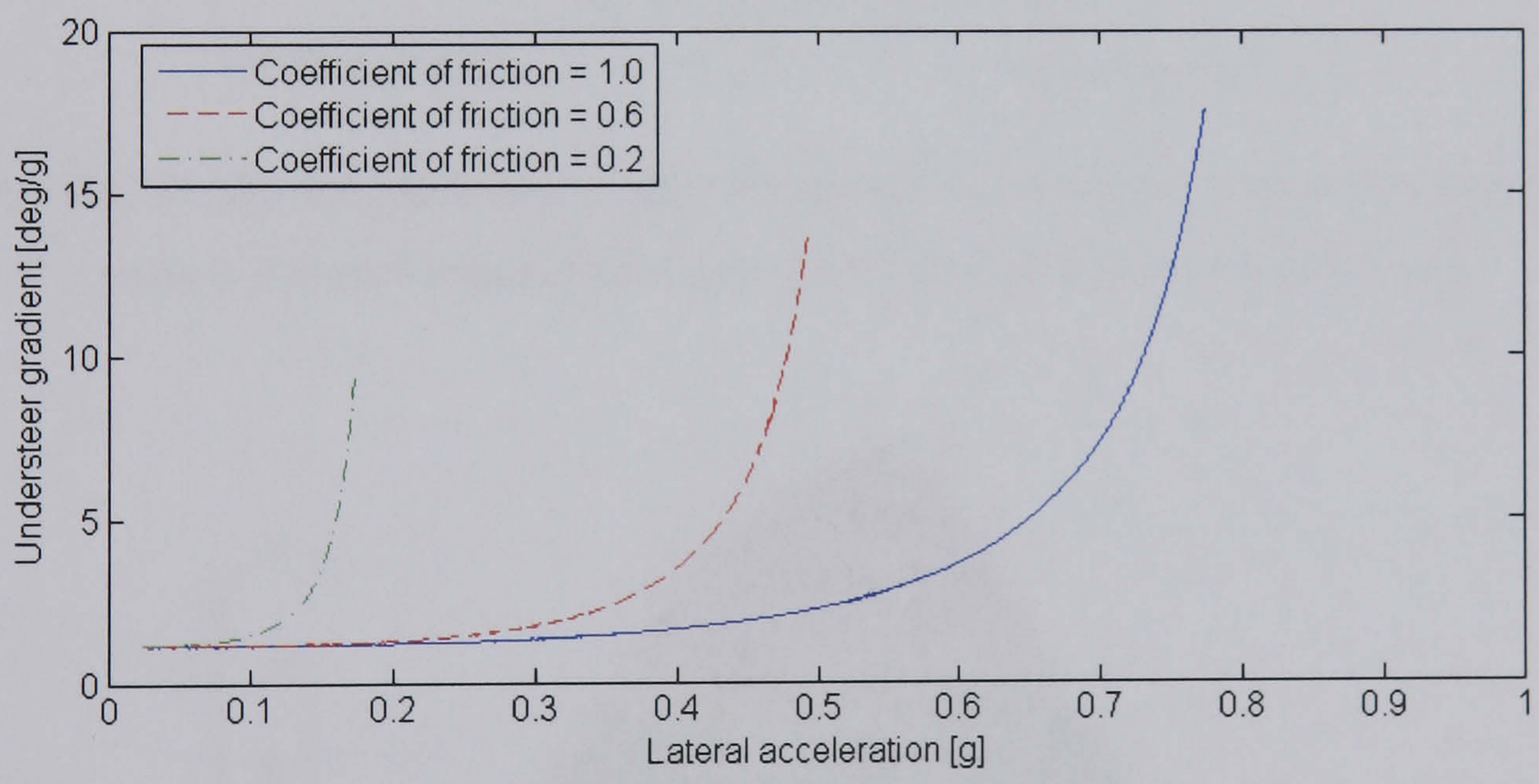

Figure 4.3 Understeer gradient as a function of lateral acceleration during steady-state cornering around a constant 33m radius path for the NLVM under different road conditions

Steady-state gains

The steady-state handling properties can also be examined through investigating the steady-state gains of the vehicle outputs with respect to the driver steer inputs. In order to show the influence of both the vehicle forward speed and lateral acceleration

on the steady-state gains of yaw rate, lateral acceleration and sideslip angle with regard to the driver steer inputs, the 2NVM introduced in Section 4.2.1 is employed. The 2NVM needs to be linearised around certain operating points for the purpose of analysis. Here, different levels of lateral acceleration are chosen as the points of linearisation. The linearisation process is explained in Appendix D. The road surface friction however is assumed to be constantly high in this case. The linearised models at different levels of lateral acceleration represent different driving conditions up to the handling limit. The resultant steady-state gains are shown in Figures 4.4 to 4.6.

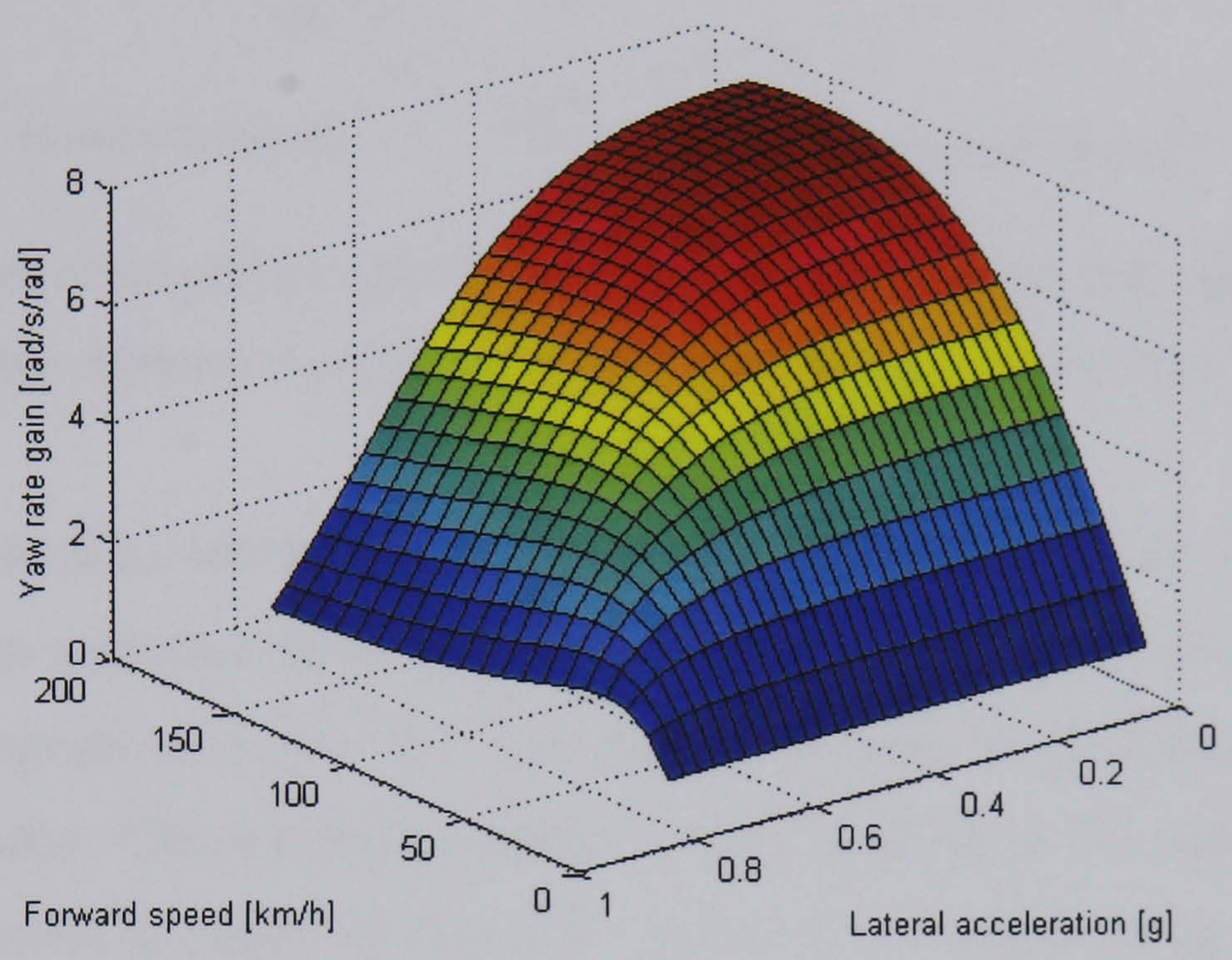

Figure 4.4 Steady-state gain of yaw rate with respect to driver steer inputs as a function of vehicle forward speed and lateral acceleration for the linearised 2NVM

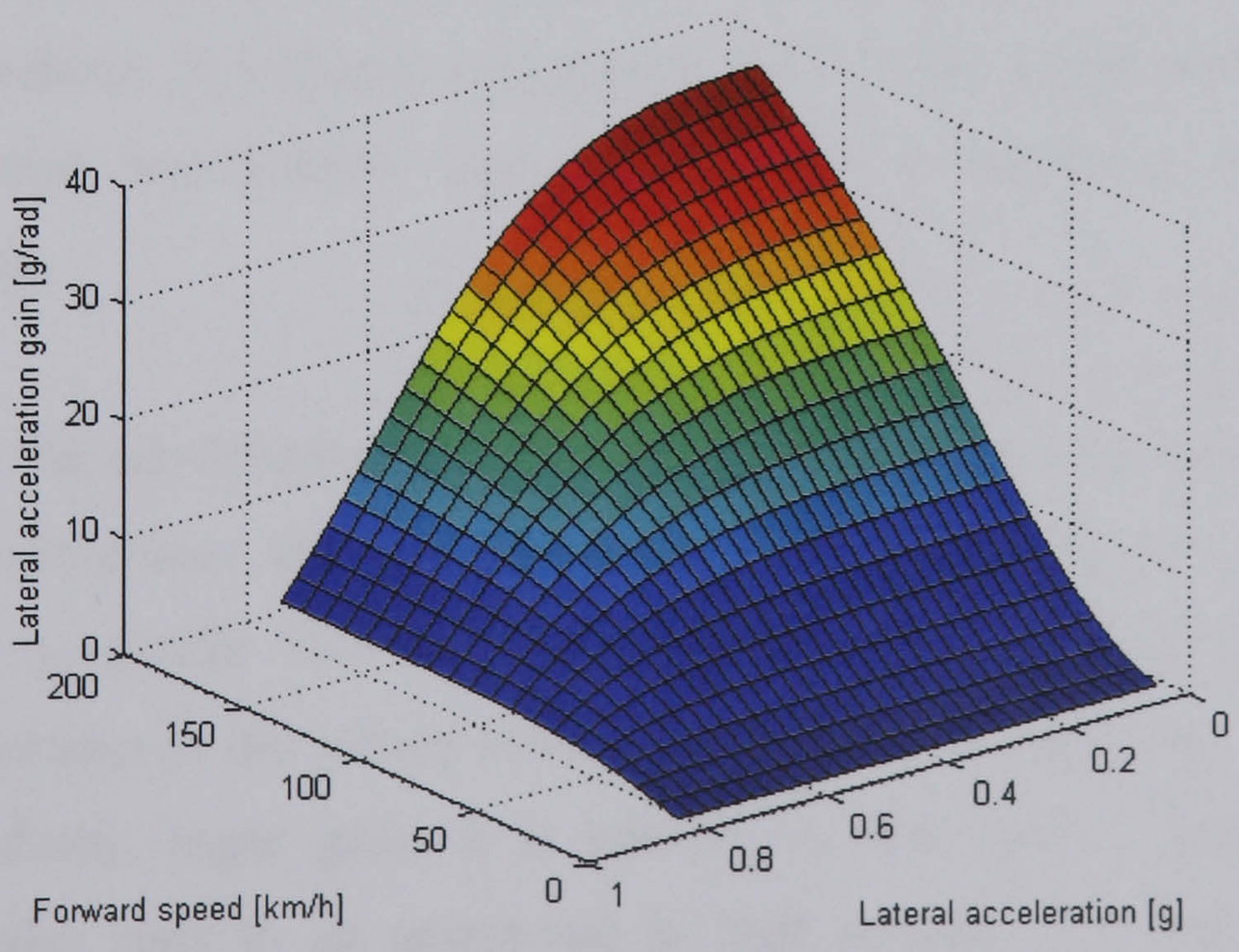

Figure 4.5 Steady-state gain of lateral acceleration with respect to driver steer inputs as a function of vehicle forward speed and lateral acceleration for the linearised 2NVM

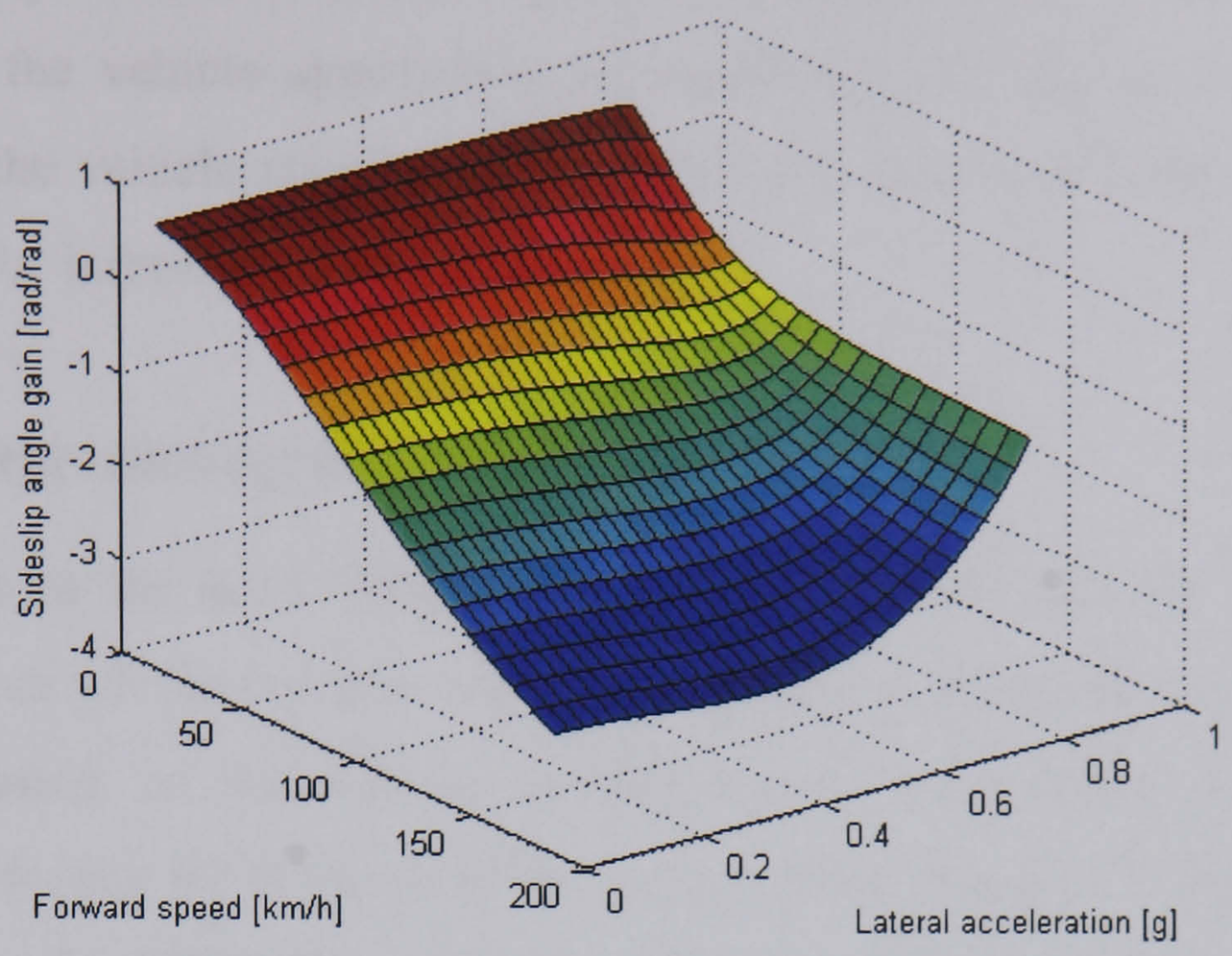

Figure 4.6 Steady-state gain of sideslip angle with respect to driver steer inputs as a function of vehicle forward speed and lateral acceleration for the linearised 2NVM

Once again these diagrams are typical for an understeering vehicle. The steady-state yaw rate gain, at a specific level of lateral acceleration, increases with speed up to the *characteristic speed* at which the yaw rate gain reaches its peak, and begins to decrease thereafter. Characteristic speed is simply defined as the speed at which the steer angle required to negotiate any turn is twice the Ackerman Angle. The level of lateral acceleration does not influence the basic shape of the yaw rate gain curve, but increasing lateral acceleration does lead to progressive reduction in the yaw rate gain and consequently less responsive yaw motion, especially when the vehicle is close to the limit of handling. In addition, progressive decrease in the characteristic speed for increasing lateral acceleration also demonstrates progressive increase in the understeer level.

In the case of the steady-state lateral acceleration gain, at a certain level of lateral acceleration, it increases continuously with speed and finally reaches a horizontal asymptote. At a specific forward speed, increasing lateral acceleration results in progressive decrease in the steady-state gain of lateral acceleration. Finally, for the steady-state sideslip angle gain, it is positive at low speeds, gradually becomes negative and also runs to an asymptote at high speeds. The influence of lateral acceleration on the sideslip angle gain is relatively complex. The steady-state sideslip angle gain increases slightly for increasing lateral acceleration up to around 0.6g,

which means the vehicle sideslip angle is more responsive to steer inputs in this region. When the vehicle approaches the handling limit, due to the highly strong understeer of the vehicle response, the steady-state gain of sideslip angle decreases progressively for increasing lateral acceleration.

4.2.3 Transient handling characteristics

With reference to the linear bicycle model introduced in Chapter 3, the dominant lateral dynamics of the vehicle can be described as a second-order system. The transient dynamics of the vehicle in response to steer inputs can therefore be examined by plotting the location of the system poles. Figure 4.7 shows the location of the poles for the 2DOF linear bicycle model as a function of the vehicle forward speed in the upper half of the complex plane. Increasing forward speed can be seen to lead to progressively less damped vehicle dynamics as the poles have an increasing imaginary part and move towards the imaginary axis with speed.

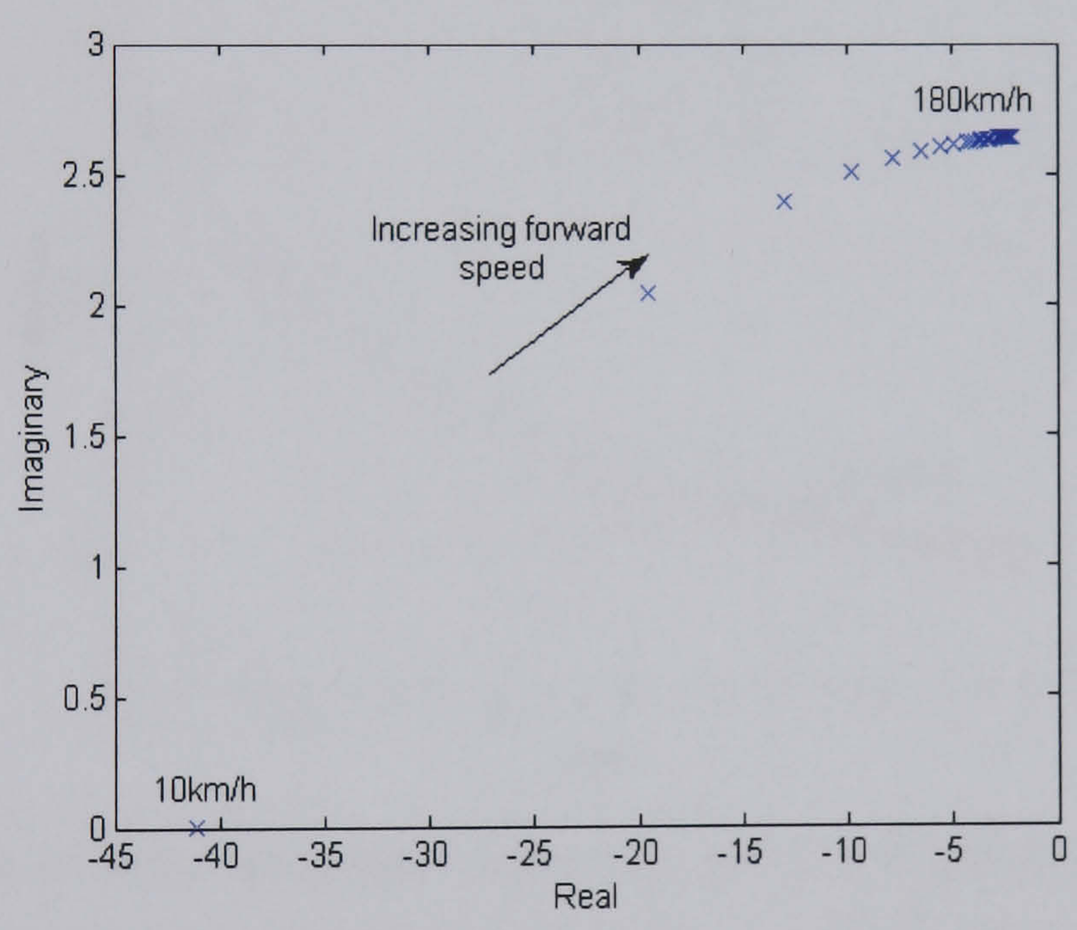

Figure 4.7 Location of poles with positive imaginary part for the 2DOF linear bicycle model as the vehicle forward speed is increased from 10km/h to 180km/h

The transient handling properties of the passive vehicle can also be examined by plotting the pole positions of the linearised 2NVM. The linearised 2NVM, as described in Appendix D, has two dominant poles which belong to the yaw and sideslip motions of the vehicle. Figure 4.8 shows the location of the two dominant poles with positive imaginary part at different levels of lateral acceleration and vehicle forward speeds (from 50km/h to 180km/h). Here the linearised 2NVM for

0.1g of lateral acceleration can be compared with the 2DOF linear bicycle model. As can be seen, at low speeds, the poles of the linearised 2NVM lie far away from the corresponding poles of the 2DOF linear bicycle model. This is mainly due to the tyre lag which has a large effect at low speeds. As the vehicle speed increases, the tyre dynamics become fast and have little influence on the dominant vehicle dynamics. Hence the poles of the linearised 2NVM approach those of the 2DOF linear bicycle model. In addition, at a certain level of lateral acceleration, the poles of the linearised 2NVM shift towards the imaginary axis as the speed is increased. At a specific speed, the poles of the linearised 2NVM are seen to move towards the origin and the imaginary axis for increasing lateral acceleration. In other words, increasing lateral acceleration results in less damped and slower vehicle dynamics. The effect of reduced damping can also be illustrated in Figure 4.9 where the damping factor is plotted as a function of vehicle forward speed and lateral acceleration.

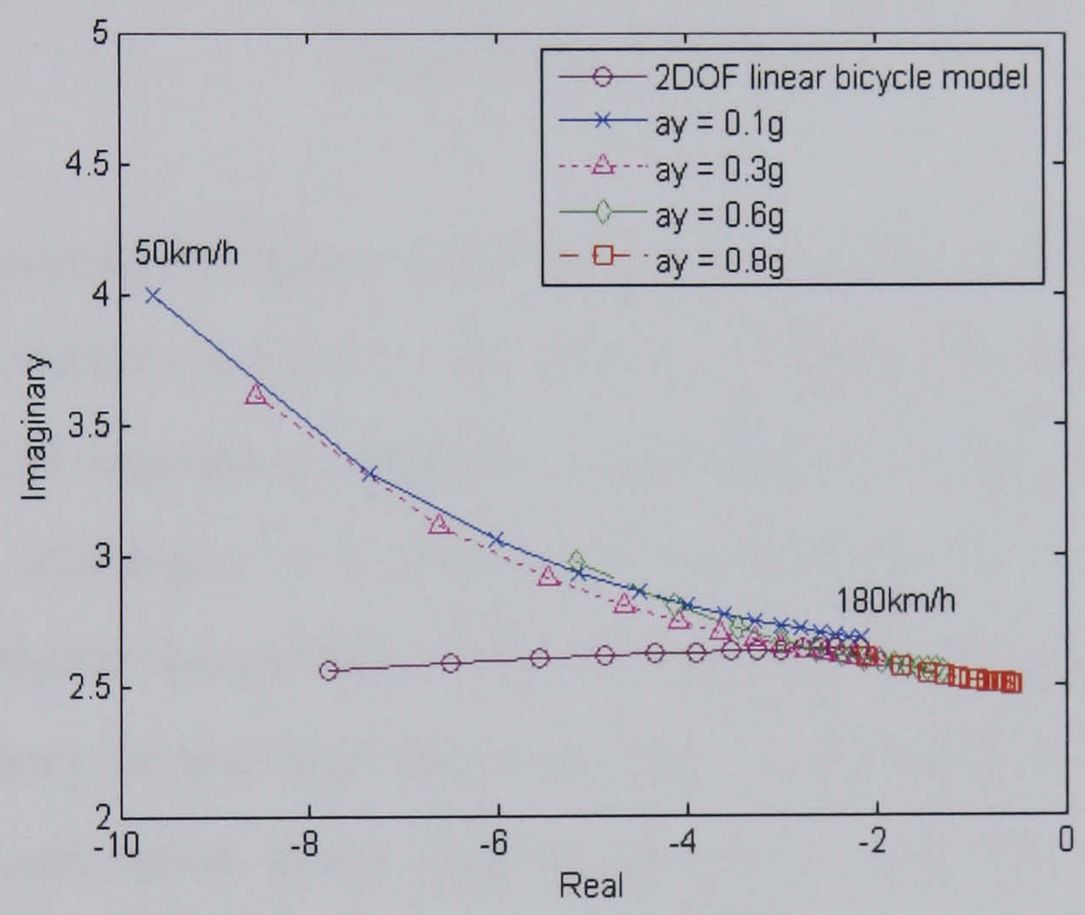

Figure 4.8 Location of dominant system poles with positive imaginary part for the linearised 2NVM as a function of vehicle forward speed and lateral acceleration

Frequency response

The frequency response gives a full description of the small perturbation and dynamic behaviour of the vehicle. The steady-state response is the limiting case of frequency response at zero or low frequency (Crolla, 1992). The vehicle response to driver steer inputs in the frequency domain can be analysed through the Bode diagram. Figure 4.10 (based on the 2DOF linear bicycle model) shows frequency responses of the yaw

rate, lateral acceleration and sideslip angle to the steer angle at four different values of the vehicle forward speed.

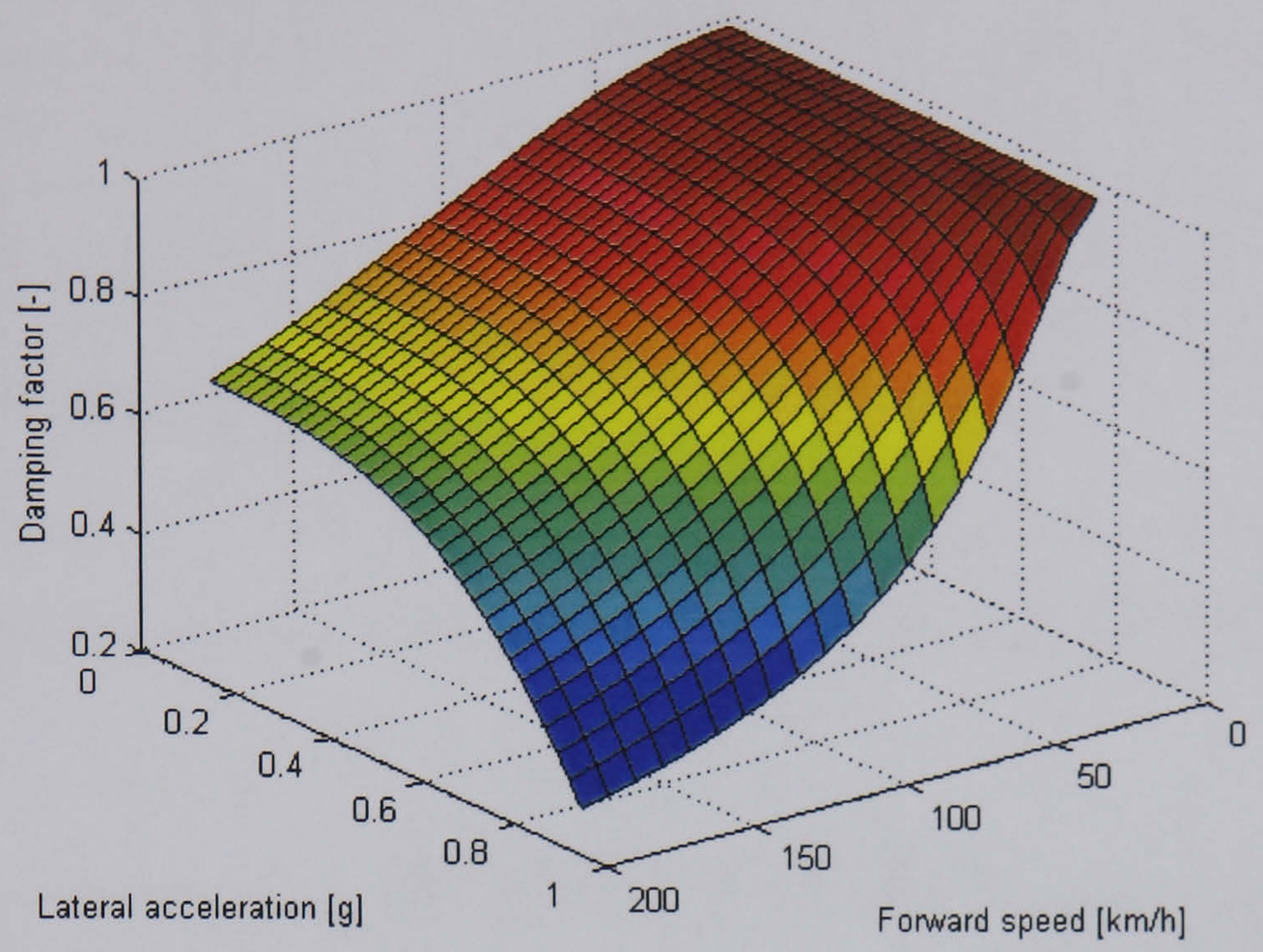

Figure 4.9 Damping factor as a function of vehicle forward speed and lateral acceleration for the linearised 2NVM

The frequency responses in Figure 4.10 reinforce some of the information previously obtained about the vehicle used here. At very low frequencies they are the same as the steady-state handling responses analysed in Section 4.2.2. The less damping as speed increases is quite noticeable as a peak at around 0.5Hz for the yaw motion of the vehicle. This highlights the problem that the response of understeering vehicles may feel highly oscillatory during high speed driving. In addition, the increase in the yaw rate and lateral acceleration phase lags at relatively high frequencies as the speed increases implies that the vehicle behaviour becomes slower, resulting in a reduction in the steering response and controllability of the vehicle from the handling point of view.

The influence of lateral acceleration on the vehicle handling behaviour can be examined in the frequency domain by using the linearised 2NVM as well. The frequency responses of the yaw rate, lateral acceleration and sideslip angle to driver steer inputs for four different levels of lateral acceleration at a specific forward speed ($V_x = 100\text{km/h}$) are plotted in Bode diagrams as illustrated in Figure 4.11. Once again the responses of the linearised 2NVM for 0.1g of lateral acceleration are compared with those of the 2DOF linear bicycle model.

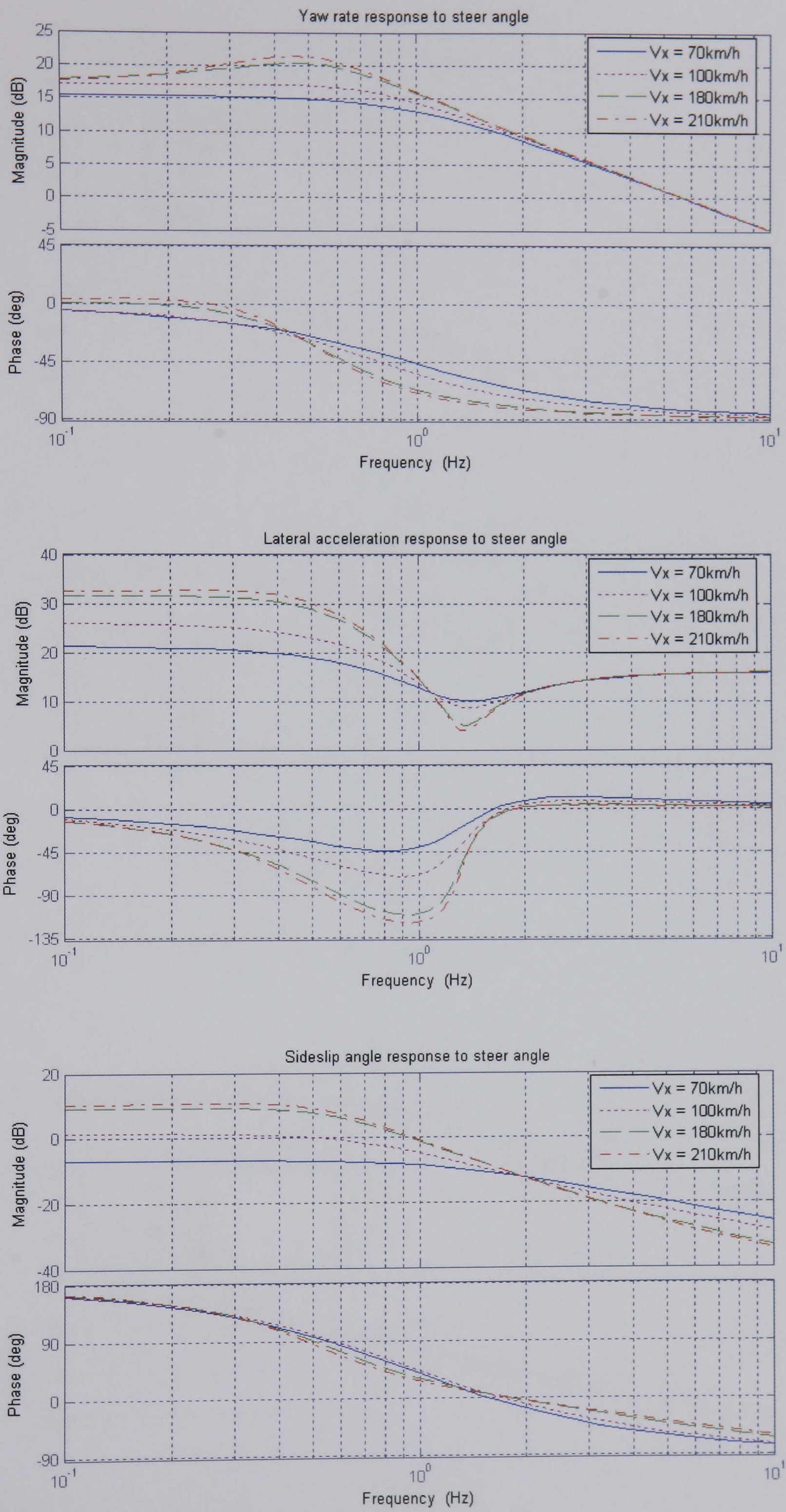

Figure 4.10 Frequency response of the 2DOF linear bicycle model to driver steer inputs at four different forward speeds

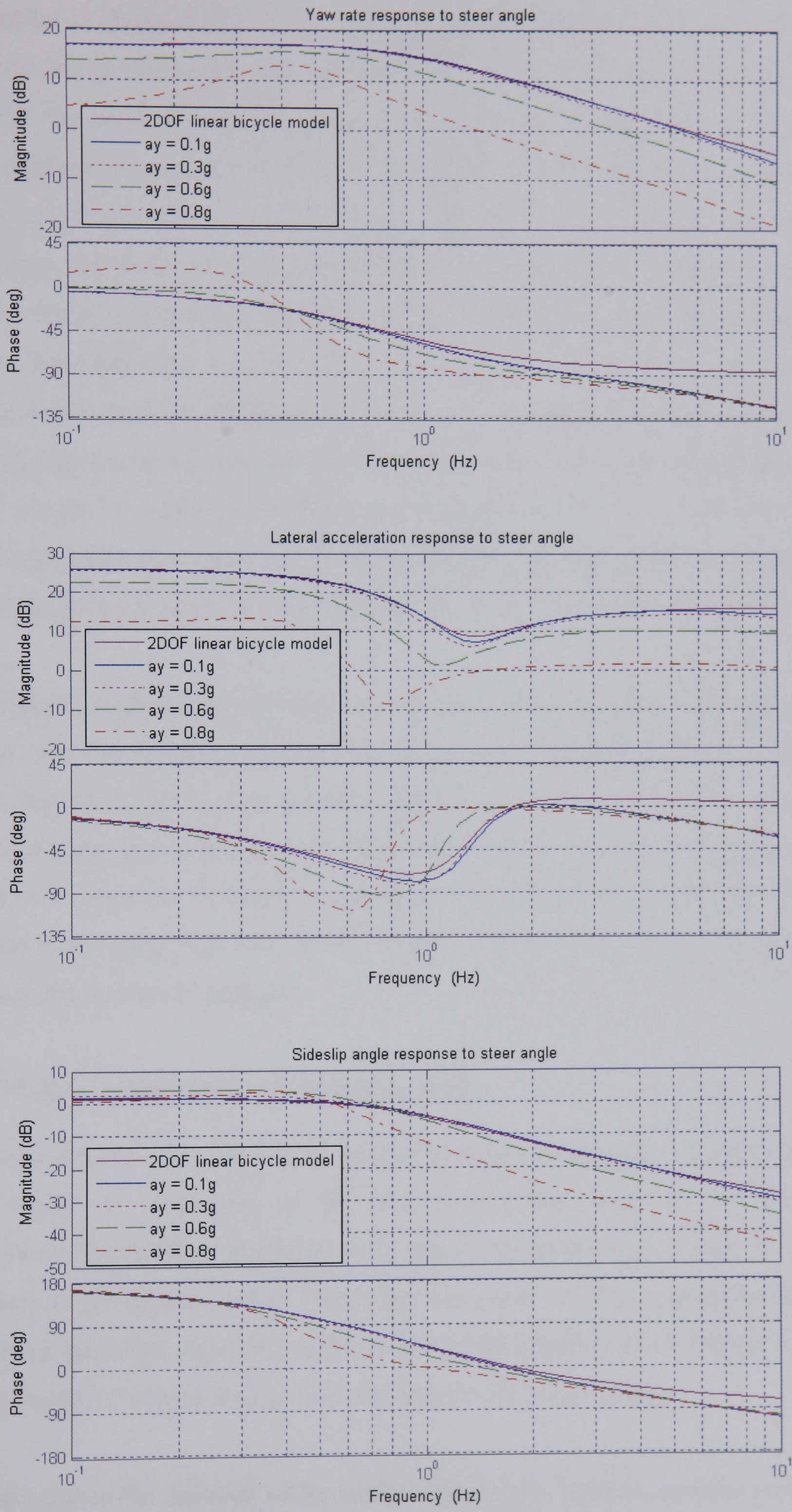

Figure 4.11 Frequency response of the linearised 2NVM to driver steer inputs for four levels of lateral acceleration at 100km/h

The responses of the linearised 2NVM for 0.1g lateral acceleration are seen to be quite similar to those of the 2DOF linear bicycle model. The only big difference is that due to the additional tyre force lag the linearised 2NVM has more phase lag than the 2DOF linear bicycle model at high frequencies. The responses in Figure 4.11 further confirm the previous analyses of the influence of lateral acceleration on the lateral vehicle dynamics. A reduction in gain can be observed for yaw rate and lateral acceleration responses for increasing lateral acceleration. The sideslip angle gain is increased slightly at low to mid-range lateral acceleration and finally declines again when the handling limit is approached. The damping of the system can be seen to decrease significantly as lateral acceleration increases, especially at the handling limit. This is mainly the case for the yaw motion of the vehicle and relatively slightly for the sideslip motion. In addition, for all responses, one can observe that increasing lateral acceleration leads to a reduction in the bandwidth, an increase in the phase lag at relatively high frequencies and consequently slow vehicle dynamic behaviour.

The conclusions which can therefore be reached through the above investigations are that both the steady-state and transient lateral vehicle dynamics can be influenced dramatically by the level of lateral acceleration as well as the vehicle forward speed. The vehicle response with respect to driver steer inputs becomes less responsive, less damped and slower as the lateral acceleration increases. It is indeed such changes in the vehicle response that the active steering subsystems to be designed in the following chapter aim to mitigate.

4.2.4 Vehicle behaviour at the handling limit

As discussed previously, the lateral vehicle dynamics is dominated by the lateral tyre forces which are generated at the tyre road contact patches. At low lateral accelerations, the vehicle response with respect to driver steer inputs is relatively linear due to the approximately linear tyre behaviour in this region. As the lateral acceleration increases, especially close to and at the handling limit, the tyre dynamics becomes highly nonlinear and so does the lateral vehicle dynamics.

Therefore, due to the inherent saturation property of the lateral tyre force with respect to the corresponding slip angle, the lateral vehicle dynamics may exhibit abrupt

behaviour in response to driver steer inputs when the tyre reaches its performance limit. Herein, the handling limit is of primary interest. Such behaviour is indeed determined by which one of front and rear axles saturates first at the handling limit. If the lateral tyre forces of the rear axle pass the saturation point before those of the front axle, further increase in sideslip motion and then in tyre slip angle will result in increase in front tyre forces and decrease in rear tyre forces. The resulting yaw moment will therefore accelerate the yaw motion and lead to vehicle instability and spin.

However, if the front tyre forces are saturated first, the opposite situation will happen and the yaw moment generated by the lateral tyre force balance between the front and rear axles will counteract the yaw motion. This case indeed leads to limit understeer. From the system stability point of view, the limit understeer mode is stable. However at this point, the authority of front axle steering in controlling the directional behaviour of the vehicle is reduced to zero, which means the driver can no longer control the vehicle direction through turning the steering wheel.

4.3 Definition of Control Objectives

4.3.1 Lateral vehicle dynamics regimes

As reviewed in Chapter 2, different vehicle dynamics control subsystems have their own basic functions and effective regions over the entire range of vehicle handling regimes. Therefore, in order to formulate the control tasks for both stand-alone and integrated control systems, three distinct regions with respect to the level of lateral acceleration of the vehicle may be identified as:

- **Low** lateral acceleration: 0 - 0.3g, mild or normal cornering;
- **Mid** lateral acceleration: 0.3g - 0.6g, moderate to vigorous cornering;
- **High** lateral acceleration: 0.6g - limit, severe cornering approaching limit or safety critical conditions.

The low lateral acceleration region is usually characterised by low vehicle sideslip angle and small phase lag between yaw rate and lateral acceleration; the moderate

cornering region is generally accompanied by relatively rapid driver steer inputs, with potentially increased vehicle sideslip angle and lateral acceleration; the severe cornering region involves extremely large and rapid steer inputs and either a rapid transition from throttle to brake, or simply no pedal inputs at all following an initial release and normally generates large vehicle sideslip angle (Gillespie, 1992).

Generally, one can refer to the **low** lateral acceleration region as linear regime and the **mid** and **high** lateral acceleration regions are definitely related to the nonlinear handling regime. These three regimes on high-μ $(=1)$ road surfaces are illustrated in Figure 4.12 and listed in ascending order of difficulty for active systems to control. Examples of stand-alone control systems which work in a particular region would be active steering in A and B, roll moment distribution control in B and C, and dynamic stability control in C. Therefore it can be stated that the control tasks of active systems are closely related to the vehicle operating conditions.

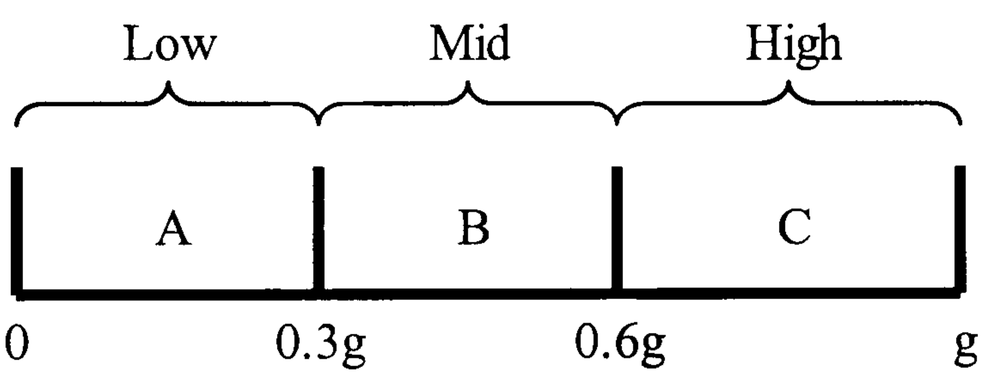

Figure 4.12 Schematics of the lateral vehicle dynamics regions with respect to the level of lateral acceleration on high-μ $(=1)$ road surfaces

One should note here that the choice of the boundaries between regions A, B and C in Figure 4.12 is fairly flexible, and will be influenced by subjective judgements and conditions of the road surface (μ). There are clearly three phases which can be identified as low, moderate and severe cornering but there is inevitably a degree of individual choice in selecting exactly where the boundaries occur (Crolla, 1992).

4.3.2 Control objectives

The first step in any control design is the definition of control objectives which is important in order to clearly define the control tasks for individual control algorithms. As reviewed in Chapter 2, most previous studies just focus on one specific vehicle handling regime and the lack of well-defined control objectives for improving vehicle

handling over the complete range of lateral vehicle dynamics is one of the common shortcomings. In this thesis, the control objectives are closely related to different aspects of the vehicle handling behaviour to be improved. With reference to the analysis of the lateral vehicle dynamics in Section 4.2, two aspects which represent the major desired vehicle characteristics in relation to handling behaviour are identified as:

- Steerability
- Stability

Steerability as a control objective

Steerability refers to the general response of the vehicle to driver steer inputs in normal driving situations. It indeed represents the ability of the vehicle to follow the driver steer commands and consists of aspects such as the speed of response, the damping and the gain from steer inputs to vehicle response. It is however important to recognise that the evaluation of steerability or handling quality of a vehicle is a highly subjective issue.

Some studies have been carried out to find the relationship between subjective and objective measures of vehicle handling performance (Weir and DiMarco, 1978; Higuchi *et al.*, 1996). The yaw rate response of a vehicle with respect to driver steer inputs has been shown to have the highest correlation to the subjective evaluation of handling quality of a vehicle (Weir and DiMarco, 1978). The work suggests that a range of values of steady-state yaw rate gain and equivalent time constant which are highly regarded by typical drivers. Higuchi *et al.* also suggest that the yaw rate gain, yaw natural frequency and yaw rate phase lag are major factors that affect the results of driver subjective evaluation of vehicle handling performance, and reductions in gain and natural frequency of yaw rate and increase in phase lag of yaw rate will lead to a reduction in steering response.

A typical driver spends the majority of his time operating the vehicle in the low lateral acceleration region, i.e. in the linear handling region. As a result, a typical driver is familiar with handling a vehicle under such conditions whilst inexperienced in controlling the vehicle during critical manoeuvres, i.e. in the nonlinear handling

regimes. Therefore, as a favourable objective, the vehicle should respond linearly to steer inputs with little phase lag and in a well-damped fashion, and such vehicle response should remain unchanged, predictable and consistent over a wide range of operating conditions, even in the presence of system parameter variations and subject to external disturbances. Hence the control task relating to this aspect of the lateral vehicle dynamics is to improve vehicle steering response, i.e. steerability. In addition, it is desirable to choose the yaw rate of the vehicle to be the controlled variable for this purpose.

Stability as a control objective

With reference to the discussion in Section 4.2.4, when the handling limit is approached, vehicle stability may be in question. Therefore, from the active safety point of view, the vehicle should be kept stable at all times, i.e. vehicle stability should be treated as another control objective. Herein, only vehicle stability close to and at the limit of handling will be examined. The control task concerning stability of the lateral vehicle dynamics is hence to maintain vehicle stability under such critical driving conditions. In addition, the controller designed for this purpose should also have the ability to cope with the situation of limit understeer in which the vehicle almost has no response to driver steer inputs.

According to the review of DSC systems in Chapter 2, vehicle stability can be determined in the phase plane for the vehicle sideslip angle and its angular velocity, and bounding the sideslip motion of the vehicle within a predefined stable region in the phase plane can maintain vehicle stability. The vehicle sideslip angle and its angular velocity will therefore be adopted as the variables to be controlled in this thesis for the purpose of maintaining vehicle stability.

Coordination of control objectives over the entire range of vehicle handling

The two control objectives, steerability and stability described above cover the entire range of vehicle handling from normal driving situations to the limit of handling. However, the boundary between these two objectives is not distinct and different individual control objectives may conflict with each other in certain driving situations. Having a good steerability often means not to have good stability, especially in

critical driving situations as the two controlled vehicle motions, yaw and sideslip are strongly coupled which can be seen by inspecting Eqs. (3.9), (3.10) and (3.14).

It is therefore important that such conflict must be treated carefully in the design of the integrated vehicle dynamics control system. The solution to this problem is indeed closely related to the design of the final integration scheme and can be formulated as follows:

- The objective of steerability has the priority at low to mid-range lateral acceleration and stability is not in question in these regions.
- Stability dominates the objective close to and at the limit of handling whilst steerability is not the primary concern in this region.

This scheme can be explained further by using the fuzzy membership function as illustrated in Figure 4.13. These membership functions can achieve smooth transition from one objective to the other and become a feature for the designer to tune. As can be seen clearly, the steerability objective is abandoned at high levels of lateral acceleration in favour of the stability objective. Hence the related control tasks and actions will follow the similar transition scheme and the detailed description of such a scheme can be referred to Chapter 7.

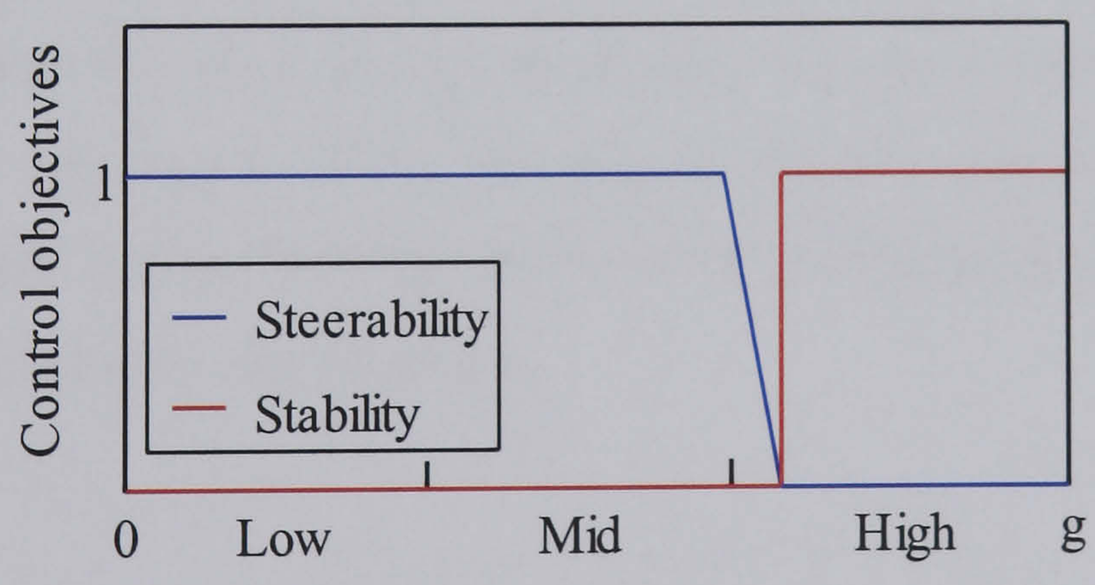

Figure 4.13 Schematics of the coordination of control objectives

In addition to the objectives mentioned above, from the driving pleasure point of view, the driver should not experience being taken over from controlling the vehicle by the active control systems. In other words, any feedback of the control actions (e.g. braking actions of the brake based DSC system) to the driver through the vehicle

dynamics should be minimised as much as possible if it is regarded as being unnatural by the driver.

4.4 Conclusions

This chapter has analysed the basic handling behaviour of passive vehicles in both linear and nonlinear handling regimes. A 2DOF nonlinear vehicle model (2NVM) has been introduced to enable the analysis of the influence of lateral acceleration on the handling characteristics of the vehicle. The vehicle response to driver steer inputs generally becomes less responsive, less damped and slower as the lateral acceleration increases. In addition, the vehicle behaviour at the limit of handling is a big concern as the vehicle may become unstable around this point. All these aspects of the passive vehicle dynamics are indeed what the active controls aim to improve.

In order to formulate the control tasks for stand-alone active subsystems and the integrated vehicle dynamics control system, the entire handling region of the vehicle has been broken down into three distinct sub-regions with respect to the level of lateral acceleration. The individual control objectives which are based on the practical preferred vehicle dynamics have been identified primarily as steerability and stability. The task of improving vehicle steerability at low to mid-range lateral acceleration has been shown to be related to the control of vehicle yaw rate. The task of maintaining vehicle stability under critical driving conditions has been linked to bounding the sideslip motion of the vehicle. The coordination of these two control objectives has also been introduced to cope with the potential conflict between them and to allow a new control configuration to be proposed.

Chapter 5

Design of Active Steering Subsystem Controllers

Abstract: *In this chapter, the design of active steering subsystem controllers for both AFS and ARS is presented. The reference model which produces the desired vehicle response to driver steer inputs is introduced first and is then followed by the design and evaluation of the AFS and ARS controllers, respectively. In addition, the functional difference between AFS and ARS is also examined with respect to the ability to generate the required corrective yaw moment. The chapter finally ends with conclusions.*

5.1 Introduction

As stated in Chapter 1, the final integrated vehicle dynamics control system will be based on two stand-alone active control systems which will be developed and optimised independently. Therefore, before the final integration is investigated, the stand-alone subsystem controllers introduced for vehicle handling need to be studied first. The design of active steering subsystem controllers will be performed in this chapter and the dynamic stability subsystem controller will be designed in the following chapter.

The literature review in Chapter 2 shows that whilst a variety of control algorithms have been applied to different active steering systems to improve steering response of the vehicle, no comparison has yet been given to show the relative performance properties of these systems. Therefore, in order to investigate the benefits of different active steering systems as a part of the final integration strategy to affect the lateral vehicle dynamics, the functional difference between the two active steering subsystems, AFS and ARS will also be examined in this chapter.

5.2 Design of Active Steering Subsystem Controllers

For the purpose of controller design, the control objective of steerability can be translated into a reference behaviour which is represented in a reference model and stands for the ideal or desirable behaviour of the vehicle in response to driver steer inputs. This is indeed consistent with the definition of the steerability objective presented in Chapter 4. The reference or desired response which is produced by the reference model can be compared with the actual vehicle response. Hence the task of the active subsystem controllers is to minimise the deviation between the actual vehicle response and the reference response. In other words, in this thesis AFS and ARS controllers are designed based on the model tracking control strategy. This control strategy is a very efficient and systematic scheme that allows the designer to specify design objectives in terms of a reference model rather than a performance index. The design objectives are therefore met by forcing the actual controlled system to follow the response of the reference model (Ro and Kim, 1996).

Different control design methods can be utilised to achieve the goal of tracking reference models. The model-based design method is a sophisticated and powerful way and can incorporate system requirements and information in the design process. Internal model control theory, linear optimal control theory and sliding mode control theory are all examples of model-based design techniques.

5.2.1 Reference model

As discussed in Chapter 4, the driver attempts to control the yaw rate of the vehicle during normal and moderate cornering from the steerability point of view. The

reference model therefore reflects the desired relationship between the driver steer inputs and vehicle yaw rate. In accordance with the steerability objective, the reference model is expected to produce a constant yaw response with respect to steer inputs, regardless of the level of lateral acceleration. The 2DOF linear bicycle model has this feature and is used as the reference model. The yaw rate generated by the reference model is chosen as the reference signal to be tracked by the active steering subsystem controllers. Here the reference yaw rate is a function of the vehicle forward speed and driver steer inputs. One should however note that the detrimental effect of the vehicle forward speed on damping is still present in this reference model.

The active steering subsystem controllers are therefore designed to track the reference yaw rate intended by the driver through driving the tracking error between the actual and desired yaw rate to zero. In this way, they make contributions to the steerability improvement by assisting the driver in steering the vehicle and helping the driver to avoid extreme handling situations. In this thesis the AFS acts as a steering correction system by applying an additional steer angle to that demanded by the driver and the ARS actively demands a steer angle at the rear wheels.

5.2.2 Sliding mode control (SMC)

With regard to the model tracking problem identified above, the feedback control approach can be used to achieve this. Since the vehicle is a highly nonlinear system operating under uncertainty conditions, the steerability controllers to be designed are therefore expected to provide robustness to parameter variations and external disturbances. Hence the sliding mode control (SMC) technique which possesses a good robustness characteristic or invariance property will be used in this thesis to cope with system uncertainties inherent in the vehicle dynamics (Ro and Kim, 1996).

The SMC which is a form of variable structure control (VSC) theory was developed in the Soviet Union in the 1950s (Itkis, 1976). It is indeed a simple approach to robust control. The purpose of robust control is to make explicit consideration of modelling uncertainties in the control design process in order to achieve the desired control objective. The SMC design provides a systematic approach to the problem of maintaining stability and consistent performance in the face of modelling imprecision.

Furthermore, by allowing the trade-offs between modelling error and performance to be quantified in a simple fashion, it can illuminate the whole design process. Practical implementations of SMC have been found in underwater vehicles, robot manipulators, high-performance electric motors and power systems (Slotine and Li, 1991). In the field of vehicle dynamics control, SMC has been applied to ABS (Kazemi *et al.*, 2000; Buckholtz, 2002), active suspension control (Alleyne and Hedrick, 1995; Kim and Ro, 1998) and dynamic stability control (Yoshioka *et al.*, 1998; Yi *et al.*, 2003).

The basic idea behind the SMC design is to choose a suitable surface which is a well-behaved function of the tracking error and then derive a feedback control law using Lyapunov stability theory to force the system trajectories to reach and remain on the surface, in spite of the presence of model imprecision and of disturbances. Once the system trajectories are on the surface, the closed-loop dynamics of the system are completely governed by the equations that define the surface. Since the parameters defining the surface are chosen by the designer, the closed-loop dynamics of the system will be dependent neither on perturbations in the parameters of the system nor on disturbances and hence robustness is achieved.

The approach can be briefly explained as follows. Consider the single-input dynamic system:

$$x^{(n)} = f(\mathbf{x}) + b(\mathbf{x})u \tag{5.1}$$

where the scalar x is the output of interest, the scalar u is the control input and $\mathbf{x} = [x \;\; \dot{x} \;\; \ldots \;\; x^{(n-1)}]^{\mathrm{T}}$ is the state vector. In Eq. (5.1), the function $f(\mathbf{x})$ (in general nonlinear) is not exactly known, but the extent of the imprecision on $f(\mathbf{x})$ is upper bounded by a known continuous function of $\mathbf{x}$; similarly, the control gain $b(\mathbf{x})$ is not exactly known, but is of known sign and is bounded by known, continuous functions of $\mathbf{x}$. The control problem is to get the state $\mathbf{x}$ to track a specific time-varying state $\mathbf{x}_d = [x_d \;\; \dot{x}_d \;\; \ldots \;\; x_d^{(n-1)}]^{\mathrm{T}}$ in the presence of model imprecision on $f(\mathbf{x})$ and $b(\mathbf{x})$ (Slotine and Li, 1991).

For the tracking task to be achievable using a finite control u, the initial desired state $\mathbf{x}_d(0)$ must satisfy:

$$\mathbf{x}_d(0) = \mathbf{x}(0) \tag{5.2}$$

This condition states that in a second-order system, for instance, any desired trajectory feasible from time $t = 0$ necessarily starts with the same position and velocity as those of the plant. Otherwise, tracking can only be achieved after a transient.

Let $e = x - x_d$ be the tracking error in the variable x, and let

$$\mathbf{e} = \mathbf{x} - \mathbf{x}_d = [e \;\; \dot{e} \;\; \ldots \;\; e^{(n-1)}]^{\mathrm{T}} \tag{5.3}$$

be the tracking error vector. Furthermore, let a time-varying surface $S(t)$ in the state space $\mathbf{R}^{(n)}$ be defined by the scalar equation $s(\mathbf{x}; t) = 0$, where

$$s(\mathbf{x}; t) = \left(\frac{d}{dt} + \kappa \right)^{n-1} e \tag{5.4}$$

in which κ is a strictly positive constant. Given initial condition in Eq. (5.2), the problem of tracking $\mathbf{x} \equiv \mathbf{x}_d$ is equivalent to that of remaining on the surface $S(t)$ for all $t > 0$; indeed, $s \equiv 0$ represents a linear differential equation whose unique solution is $e \equiv 0$, with initial condition given in Eq. (5.2). Thus, the problem of tracking the n-dimensional vector $\mathbf{x}_d$ can be reduced to that of keeping the scalar quantity s at zero. More precisely, the problem of tracking the n-dimensional vector $\mathbf{x}_d$ can in effect be replaced by a first-order stabilization problem in s. Furthermore, bounds on s can be directly translated into bounds on the tracking error vector $\mathbf{e}$, and therefore the scalar s represents a true measure of tracking performance. The corresponding transformations of performance measures assuming $\mathbf{e}(0) = \mathbf{0}$ is:

$$\forall\, t \geq 0,\ |s(t)| \leq \varepsilon \quad \Rightarrow \quad \forall\, t \geq 0,\ \left|e^{(i)}(t)\right| \leq (2\kappa)^i \Phi, \quad (i = 0, \ldots, n-1) \tag{5.5}$$

where $\Phi = \varepsilon / \kappa^{n-1}$. ε and Φ are the thickness and width of a thin boundary layer around the above surface $s = 0$, respectively.

The simplified first-order problem of keeping the scalar s at zero can now be achieved by choosing the control law u in Eq. (5.1) such that outside of $S(t)$:

$$\frac{1}{2}\frac{d}{dt}s^2 \leq -\eta |s| \tag{5.6}$$

where η is a strictly positive constant. Essentially, Eq. (5.6) states that the squared distance to the surface, as measured by s^2, decreases along all system state trajectories. Thus, it constrains trajectories to point towards the surface $S(t)$, as illustrated in Figure 5.1. In particular, once on the surface, the system trajectories do not leave the surface. In other words, satisfying condition in Eq. (5.6), called *sliding condition*, makes the surface an invariant set. Furthermore, Eq. (5.6) also implies that some disturbances or dynamic uncertainties can be tolerated while still keeping the surface an invariant set. Graphically, this corresponds to the fact that in Figure 5.1 the trajectories off the surface can move while still pointing towards the surface. $S(t)$ verifying Eq. (5.6) is referred to as a *sliding surface* (*sliding manifold*), and the system's behaviour once on the surface is called *sliding mode*. As mentioned previously, once on the sliding surface $S(t)$, the system trajectories are defined by the equation of the surface itself, namely:

$$\left(\frac{d}{dt}+\kappa\right)^{n-1} e = 0 \tag{5.7}$$

In other words, the surface $S(t)$ is both a 'place' and a dynamic response.

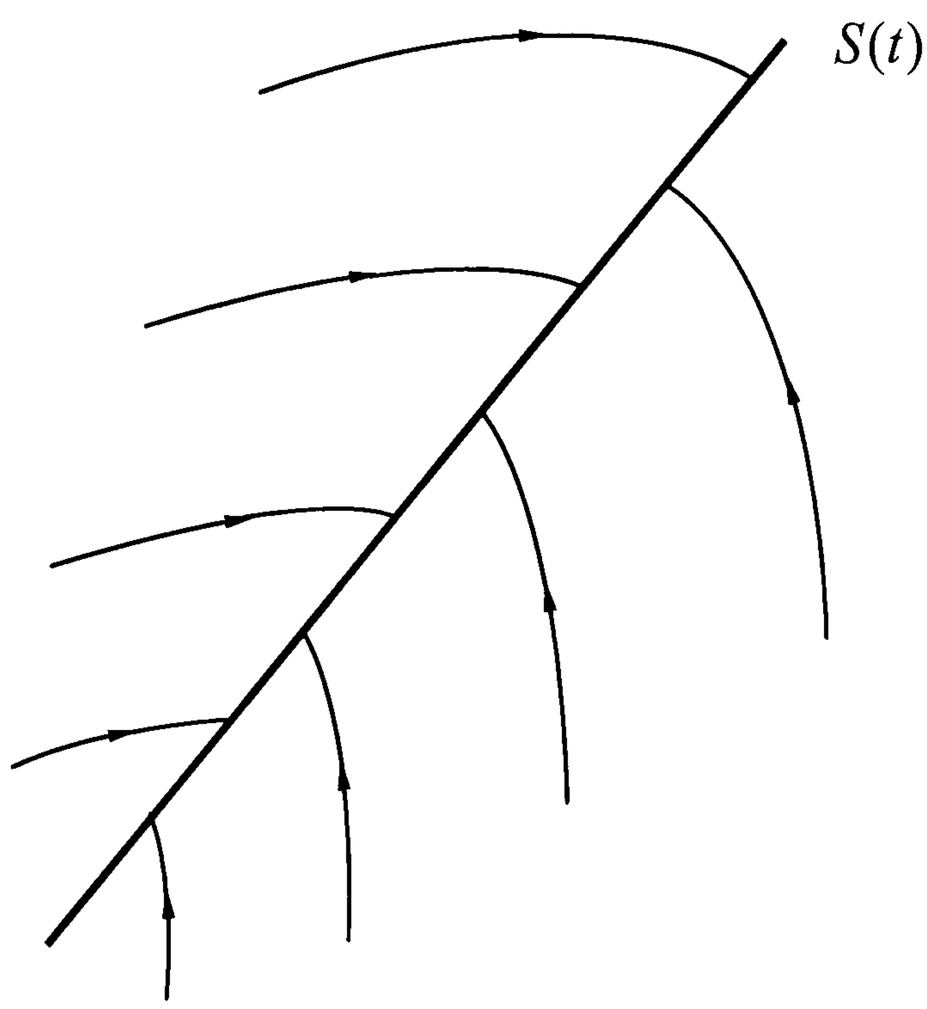

Figure 5.1 The sliding condition

The SMC design approach is therefore a two-stage approach involving the selection of an appropriate sliding surface to yield desirable performance and the derivation of

a control law to ensure the sliding mode is attained. Normally the following control law is employed:

$$u(t) = u_e(t) + u_r(t) \tag{5.8}$$

where $u_e(t)$ is the equivalent control that may be obtained from a conventional method of the linear system theory applied to the nominal system, and the term $u_r(t)$ is the robust control, which is switching in nature and used to deal with model uncertainty.

5.2.3 Active Front Steering (AFS) controller design

In the case of AFS, the yaw motion of the vehicle can be expressed as the following single-input-single-output (SISO) affine system, i.e. nonlinear systems with right-hand side in the equation of motion as a linear function of the control input:

$$\dot{r} = f + d + bu \tag{5.9}$$

where u is the control input - front wheel steer angle δ_f, r is the output of interest - yaw rate, f is not exactly known (mainly due to the nonlinear tyre dynamics and nonlinear suspension conditions) but estimated as $\hat{f}$ and disturbance d is assumed to be uniformly bounded as $|d| \le D$. The estimation error on f is assumed to be bounded by some known function $F = F(r,t)$:

$$\left|\hat{f} - f\right| \le F \tag{5.10}$$

For the yaw rate tracking task, the difference between the actual and reference yaw rate defines the tracking error and its derivative:

$$e = r - r_d \tag{5.11}$$

$$\dot{e} = \dot{r} - \dot{r}_d \tag{5.12}$$

The sliding surface is then selected as:

$$s = e \tag{5.13}$$

Here, the sliding surface can be interpreted as the surface of the yaw rate error between the vehicle and the reference model. As s goes to zero, the AFS can track the reference yaw rate perfectly. The solution $s=0$ is rigorous but difficult to use for controller design. A better approach for controller design is to introduce the so-called *equivalent control* method for defining the system behaviour in the course of sliding mode, i.e. the sliding motion can be viewed as an average of the system dynamics on both sides of the sliding surface. The equivalent control is defined by the following equation:

$$\dot{s}=0 \tag{5.14}$$

If there are no dynamic uncertainties or disturbances affecting the system, the equivalent control input can be obtained by solving the above equation formally. Therefore one can have:

$$\dot{s}=\dot{r}-\dot{r}_d=f+bu-\dot{r}_d \tag{5.15}$$

Assuming b is non-singular, thus the best approximation of the continuous equivalent control law that would achieve $\dot{s}=0$ is given as:

$$\hat{u}=b^{-1}(-\hat{f}+\dot{r}_d) \tag{5.16}$$

In order to satisfy the sliding condition in spite of uncertainty on the dynamics f and disturbances, a term which is discontinuous across the surface $s=0$ needs to be added to $\hat{u}$ and the following switching control law is obtained:

$$u=\hat{u}-b^{-1}k\,\mathrm{sgn}(s)=b^{-1}[-\hat{f}+\dot{r}_d-k\,\mathrm{sgn}(s)] \tag{5.17}$$

where k is a positive parameter to be tuned in the controller design and sgn( ) is the sign function, respectively.

Stability of the closed-loop AFS system and tracking of the reference yaw rate can be manifested by examination of the candidate Lyapunov function. The Lyapunov candidate is chosen as:

$$V(t)=\frac{1}{2}s^2(t) \tag{5.18}$$

Differentiation of $V(t)$ along the system trajectories in Eq. (5.9) under control in Eq. (5.17) yields:

$$\begin{aligned}\dot{V}(t) &= \frac{1}{2}\frac{d}{dt}s^2 = \dot{s}s \\ &= [f - \hat{f} + d - k\,\mathrm{sgn}(s)]s \\ &= (f - \hat{f})s + ds - k|s| \end{aligned} \tag{5.19}$$

so that, for $k \geq F + D + \xi/\sqrt{2}$ with constant $\xi > 0$:

$$\dot{V}(t) \leq -\xi V^{1/2}(t) \tag{5.20}$$

i.e. the value of $\dot{V}(t)$ is negative, therefore the state will reach the surface $s(t) = 0$. The solution to the above differential inequality $V(t)$ for an arbitrary initial condition $V(0) > 0$ is nonnegative and is bounded by:

$$V(t) < \left(-\frac{\xi}{2}t + \sqrt{V_0}\right)^2, \quad V_0 = V(0) \tag{5.21}$$

Since the solution vanishes after some $t_s < 2\sqrt{V_0}/\xi$, the scalar s vanishes as well and consequently sliding mode starts after a finite time interval smaller than $2\sqrt{V_0}/\xi$. Subsequently the system is invariantly confined to the sliding surface $s(t) = 0$ defined in Eq. (5.13) despite parametric uncertainty on f and unknown disturbance d. In fact let $k \geq F + D + \eta$ with constant $\eta = \xi/\sqrt{2} > 0$, the sliding condition in Eq. (5.6) is satisfied. Furthermore, definition in Eq. (5.4) implies that once on the surface, the tracking error tends exponentially to zero or in other words, the state trajectory slides along the surface towards $\mathbf{x}_d$ exponentially, with a time constant equal to $1/\kappa$.

The uncertainty on the control gain b is not taken into consideration in the above analysis. Here the control gain b is further assumed to be unknown but bounded as:

$$0 < b_{\min} \leq b \leq b_{\max} \tag{5.22}$$

The control gain and its bounds can be time-varying or state-dependent. Since the control input enters multiplicatively in the dynamics, it is natural to choose the estimate of gain b as the geometric mean of the above bounds (Slotine and Li, 1991):

$$\hat{b} = (b_{\min} b_{\max})^{1/2} \tag{5.23}$$

Bounds (5.22) can then be written in the form:

$$\beta^{-1} \leq \frac{\hat{b}}{b} \leq \beta \tag{5.24}$$

where

$$\beta = (b_{\max}/b_{\min})^{1/2} \tag{5.25}$$

Since the control law will be designed to be robust to the bounded multiplicative uncertainty (5.24), β is called the *gain margin* of the design, by analogy to the terminology used in linear control.

Therefore, similarly, one can derive the following switching control law:

$$u = \hat{b}^{-1}[-\hat{f} + \dot{r}_d - k\,\mathrm{sgn}(s)] \tag{5.26}$$

Indeed one can have from Eqs. (5.9), (5.12) and (5.26):

$$\begin{aligned} \frac{1}{2}\frac{d}{dt}s^2 = \dot{s}s &= [(f - b\hat{b}^{-1}\hat{f}) + d + (1 - b\hat{b}^{-1})(-\dot{r}_d) - b\hat{b}^{-1}k\,\mathrm{sgn}(s)]s \\ &= (f - b\hat{b}^{-1}\hat{f})s + ds + (1 - b\hat{b}^{-1})(-\dot{r}_d)s - b\hat{b}^{-1}k|s| \end{aligned} \tag{5.27}$$

so that k must verify:

$$k \geq \left| b^{-1}\hat{b}f - \hat{f} + (b^{-1}\hat{b} - 1)(-\dot{r}_d) \right| + Db^{-1}\hat{b} + \eta b^{-1}\hat{b} \tag{5.28}$$

Since $f = \hat{f} + (f - \hat{f})$, this in turn leads to:

$$k \geq b^{-1}\hat{b}(F + D + \eta) + \left| b^{-1}\hat{b} - 1 \right| \cdot \left| \hat{f} - \dot{r}_d \right| \tag{5.29}$$

and thus

$$k \geq \beta(F + D + \eta) + (\beta - 1) \cdot \left| \hat{f} - \dot{r}_d \right| \tag{5.30}$$

to satisfy the sliding condition in Eq. (5.6). Note that the control discontinuity (the controller parameter) k has been increased in order to account for the uncertainty on the control gain b compared to that without such uncertainty.

As can be seen from above analyses, by choosing k to be large enough, the stability of the sliding mode AFS system can be guaranteed. This design parameter indeed determines the speed at which the system trajectories converge to the sliding surface. The higher the value of k is the faster the convergence of the SMC. In addition, increasing the value of k increases the robustness to parameter uncertainties and external disturbances. In practical applications the design parameter k should be chosen according to many considerations such as power available, system speed of response to input change and input saturation.

For the AFS controller, the control law can therefore be derived by using the conventional 2DOF linear bicycle model described in Eq. (3.11) with nominal values of vehicle parameters. Substituting the second state equation of Eq. (3.11) into Eq. (5.14) gives:

$$a_{21}V_y + a_{22}r + b_2\delta_f - \dot{r}_d = 0 \tag{5.31}$$

The switching control law then takes the form:

$$u = \delta_f = \frac{1}{b_2}\left(-a_{21}V_y - a_{22}r + \dot{r}_d - k\,\mathrm{sgn}(s)\right) \tag{5.32}$$

The sign function, sgn( ) as illustrated in Figure 5.2 satisfies:

$$\mathrm{sgn}(x) = \begin{cases} +1 & \text{if } x > 0 \\ 0 & \text{if } x = 0 \\ -1 & \text{if } x < 0 \end{cases} \tag{5.33}$$

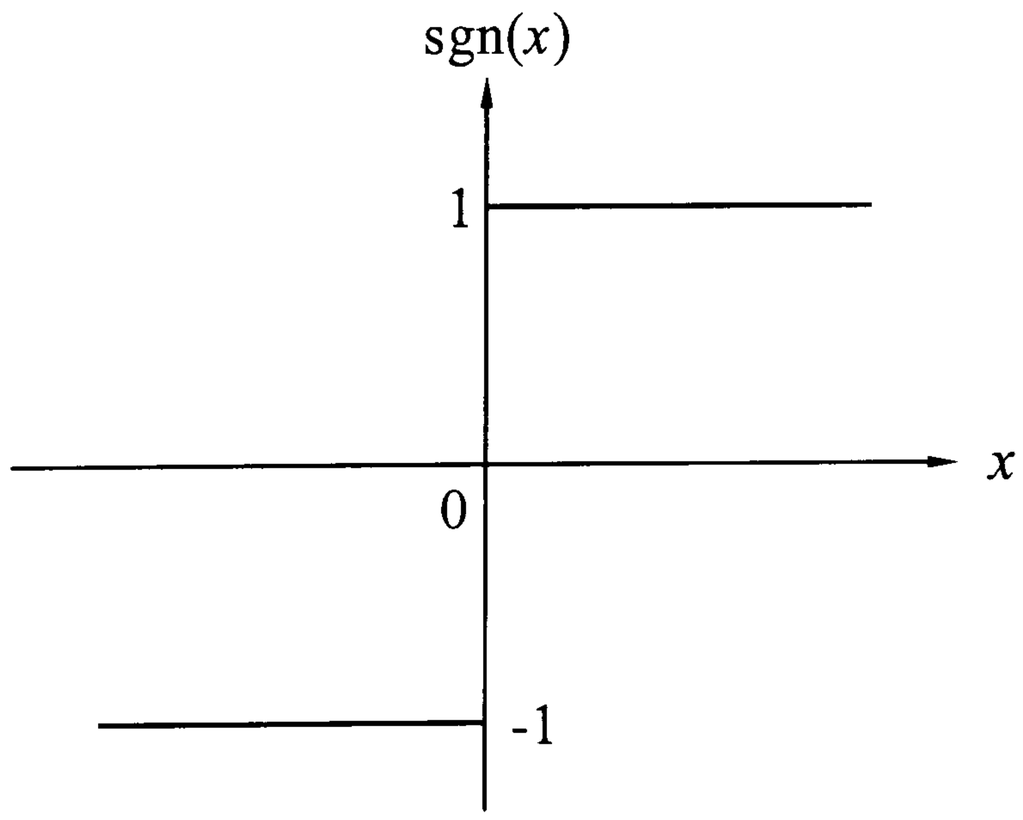

Figure 5.2 Schematics of the sign function

The control law in Eq. (5.32) can be directly applied to the steer-by-wire systems. In the case of steering correction control systems, the control input in Eq. (5.32) is the steer angle at the front wheels, hence the corrective steer angle is the difference between the AFS controller output and the driver steer inputs:

$$\delta_{fc} = \delta_f - \delta_{fd} \tag{5.34}$$

where δ_{fd} is the steer angle at the front wheels demanded by the driver. The block diagram of AFS is shown in Figure 5.3.

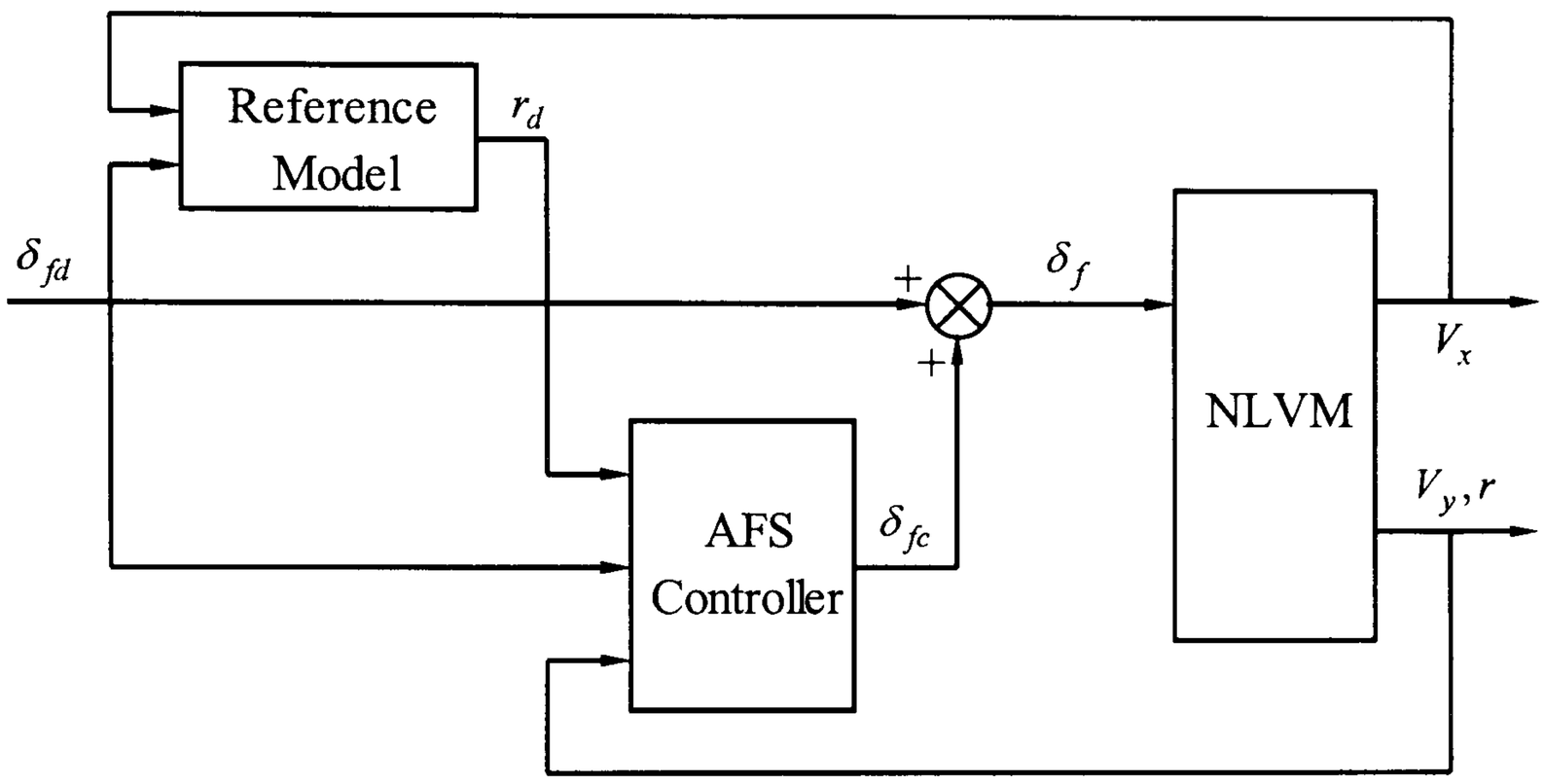

Figure 5.3 Block diagram of AFS

Chattering in sliding control

In the ideal case, the switching action itself in the sliding mode control is intended and its frequency tends to be infinite. However, since in practical systems the implementation of the associated control switching is necessarily imperfect (e.g. switching is not instantaneous due to the presence of finite delays in control computation and actuator response, and it is impossible to switch the control at infinite rate because of the physical limitations of actuators), high-frequency dynamics (such as sensors and actuators) in the closed loop which is neglected in the principal modelling process is excited by the fast switching of a sliding mode controller and chattering always occurs on the sliding surface of a sliding mode control system, as illustrated in Figure 5.4 for second-order $(n = 2)$ systems.

The term *chattering* describes the phenomenon of finite-frequency, finite-amplitude oscillations appearing in many sliding mode implementations. Chattering is generally

undesirable in practice since it involves extremely high control effort and may lead to excessive wear on the actuators. In the case of AFS, chattering will result in a very high-frequency change in the corrective steer angle at the front wheels. Therefore, the chattering effect must be eliminated for the sliding mode controller to perform properly. A sliding mode controller may first be designed under idealised assumptions of no unmodelled dynamics to account for parameter variations and disturbances. In the second design step, possible chattering is to be suppressed by a particular method to achieve robustness with respect to high-frequency unmodelled dynamics.

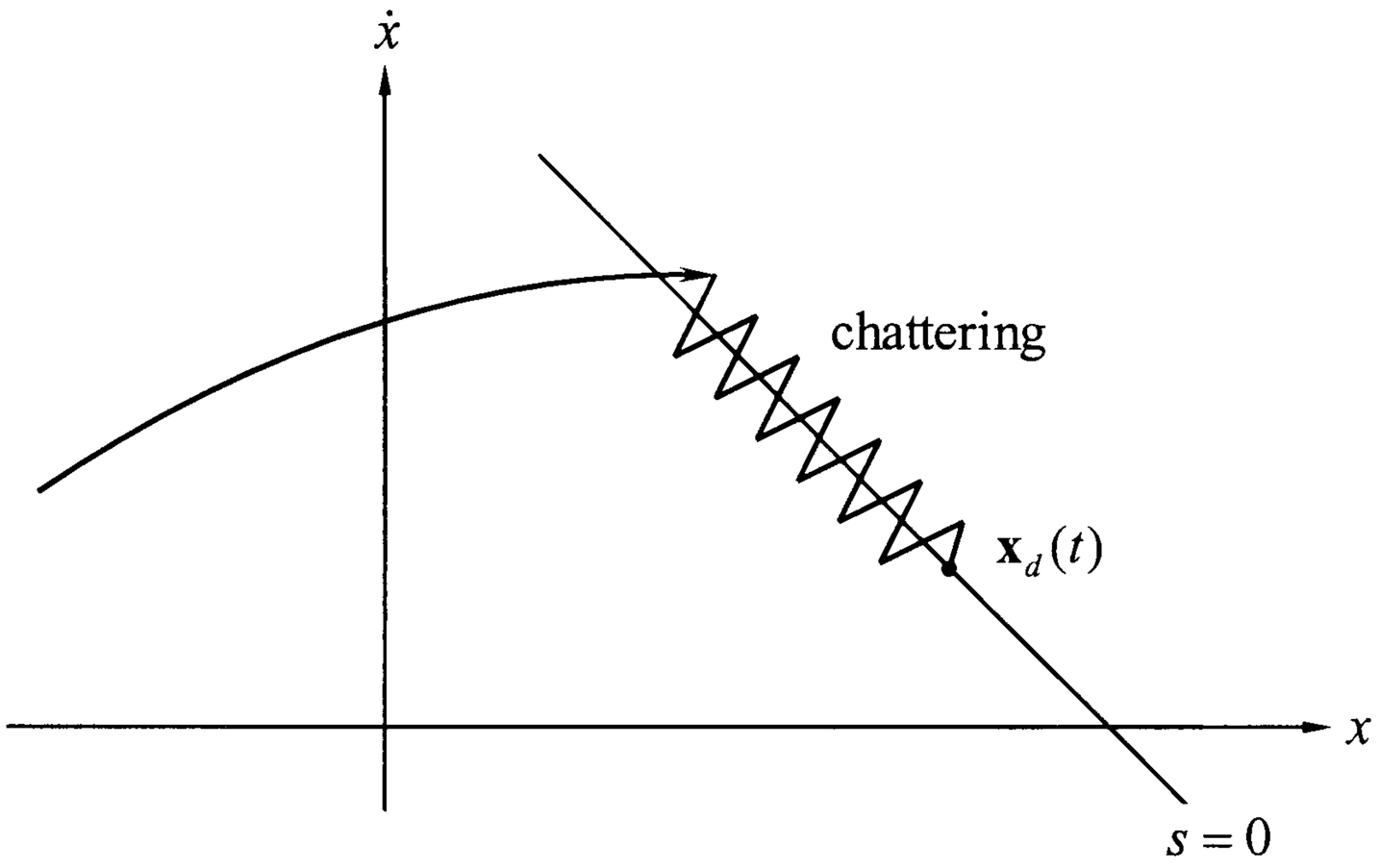

Figure 5.4 Chattering as a result of imperfect control switching

One approach to mitigate the problem of chattering is to relax the requirement that the system trajectories remain on the sliding surface $s=0$. Eventually, by introducing a thin boundary layer around the sliding surface, the switching control can be approximated by a continuous control within the boundary layer. More specifically, the sign function $\text{sgn}(s)$ in Eq. (5.32) is replaced by a saturation function $\text{sat}(s/\varepsilon)$. Thus the continuous approximation of the control law in Eq. (5.32) is given as:

$$\delta_f = \frac{1}{b_2}\left(-a_{21}V_y - a_{22}r + \dot{r}_d - k\,\text{sat}(s/\varepsilon)\right) \tag{5.35}$$

where ε is the boundary layer thickness. The above control law indeed leads to tracking within a guaranteed precision Φ as stated in Eq. (5.5) rather than perfect tracking. The saturation function $\text{sat}(s/\varepsilon)$ illustrated in Figure 5.5 is defined as:

$$\text{sat}(s/\varepsilon) = \begin{cases} s/\varepsilon & \text{if } |s| \le \varepsilon \\ \text{sgn}(s/\varepsilon) & \text{if } |s| > \varepsilon \end{cases} \tag{5.36}$$

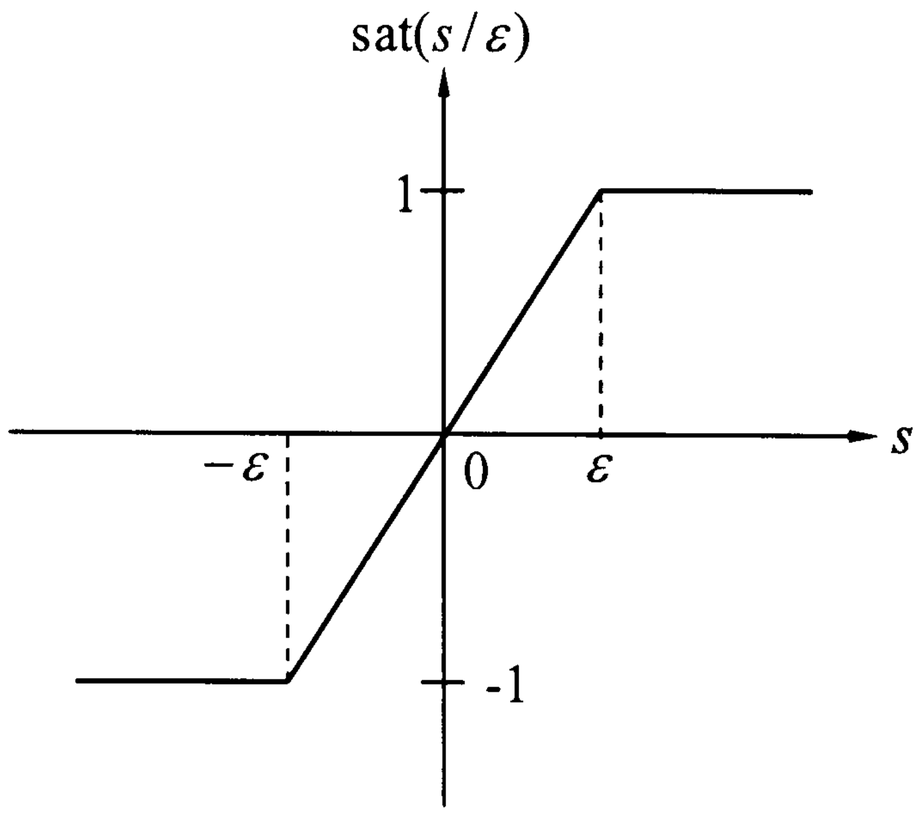

Figure 5.5 Schematics of the saturation function

5.2.4 Active Rear Steering (ARS) controller design

The design process of the ARS controller is the same as that of the AFS controller except that the nominal bicycle model described in Eq. (3.18) will be used to derive the control law. Thus similarly, substituting the second state equation of Eq. (3.18) into Eq. (5.14) and applying the boundary layer solution to eliminate chattering, the following continuous approximation of the switching control law is obtained:

$$\delta_r = \frac{1}{b_{22}}\left(-a_{21}V_y - a_{22}r - b_{21}\delta_f + \dot{r}_d - k_1 \text{sat}(s/\varepsilon)\right) \tag{5.37}$$

where $\delta_f = \delta_{fd}$. The control input in Eq. (5.37) is the steer angle at the rear wheels. The block diagram of ARS is shown in Figure 5.6. The boundary layer thickness ε for both AFS and ARS controllers is chosen to be 0.1 to avoid chattering.

5.2.5 Practical aspects for yaw rate tracking control

As discussed in previous sections, increasing the values of the controller parameters k and k_1 can result in fast convergence rate and good robustness to parametric uncertainty and disturbances. However, exceedingly high values of these parameters may force the corrective steer angle demanded by the AFS controller or the rear wheel steer angle demanded by the ARS controller to repeatedly reach the hardware

saturation limits and easily cause chattering. As a result, it would require a too wide boundary layer which would degrade tracking performance. This problem could be partially solved by tuning the controller parameters to lower values at the expense of the overall controller robustness. Rate limiters may be a good compromise technique to adjust controller sensitivity in order to overcome this kind of saturation (Elbeheiry *et al.*, 2001).

The steering actuator saturation levels and slew rates which are based on current technology in active steer vehicles are given in Table 5.1 (Crolla *et al.*, 2000). The active steer angles of the front and rear wheels can be actuated by either servomotors or hydraulic servo systems (Nagai, 1989; Sato *et al.*, 1991). Here both controller parameters k and k_1 are roughly tuned to be 10.

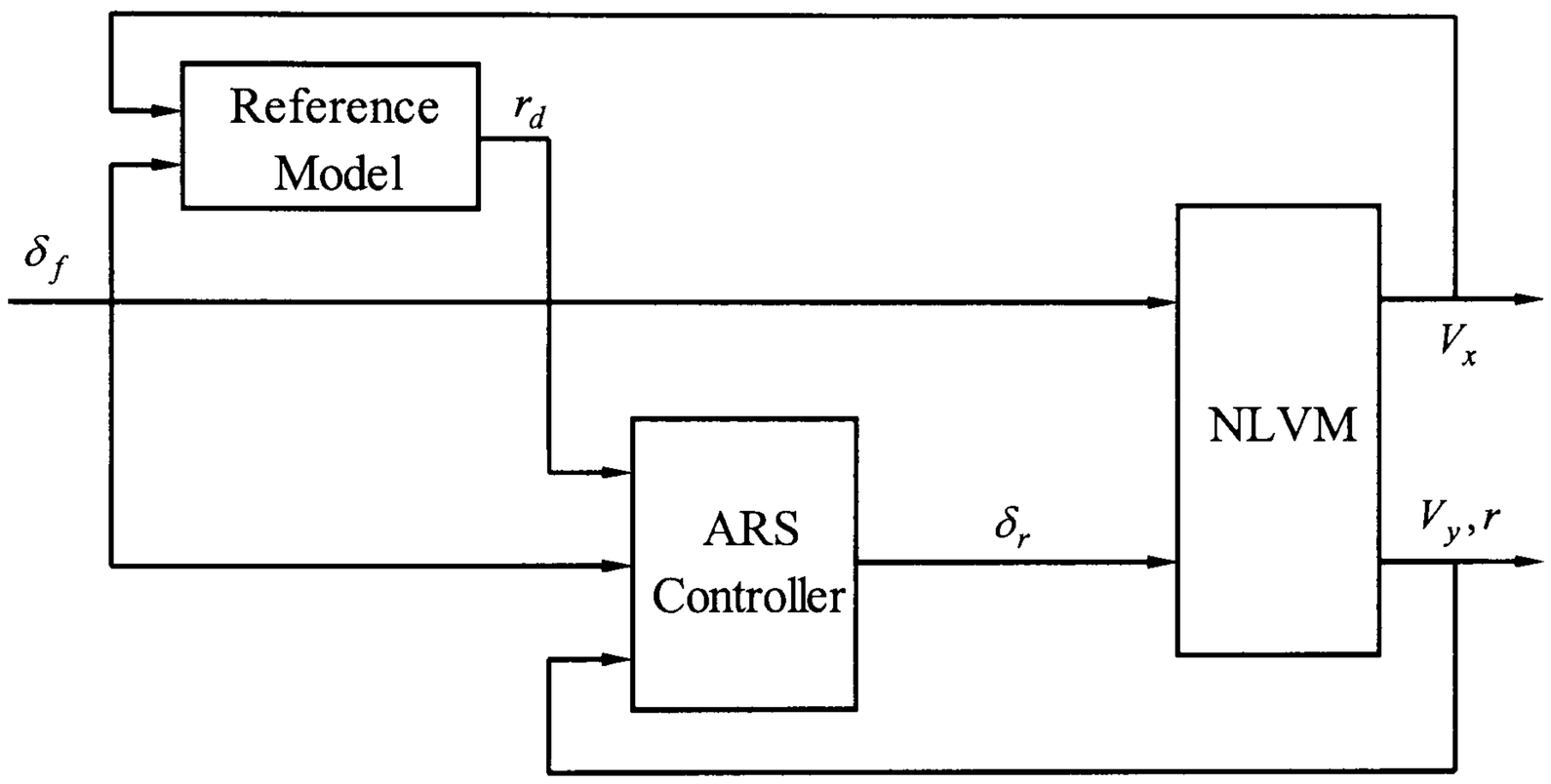

Figure 5.6 Block diagram of ARS

Table 5.1 Steering actuator saturation levels and rate limits

Actuator	Max value	Min value	Max rate	Min rate
Front wheel steer	10°	-10°	25° /sec	25° /sec
Rear wheel steer	3°	-3°	25° /sec	25° /sec

5.3 Analysis of Active Steering Subsystem Controllers

5.3.1 Evaluation of stand-alone steerability controllers on the NLVM

In order to evaluate the stand-alone AFS and ARS controllers designed above, tests of these two controllers will be performed on the NLVM which was described in

Chapter 3. The detailed description of test manoeuvres that will be examined can be referred to Section 3.4.

Steady-state cornering

The simulation results of steady-state cornering around a constant 33m radius path under two different road surface conditions are shown in Figure 5.7. Here the understeer gradient is plotted as a function of lateral acceleration for both passive and controlled vehicles. Under both road surface conditions, the passive vehicle is seen to be slightly understeering at low levels of lateral acceleration and becomes progressively understeering when the vehicle approaches the handling limit.

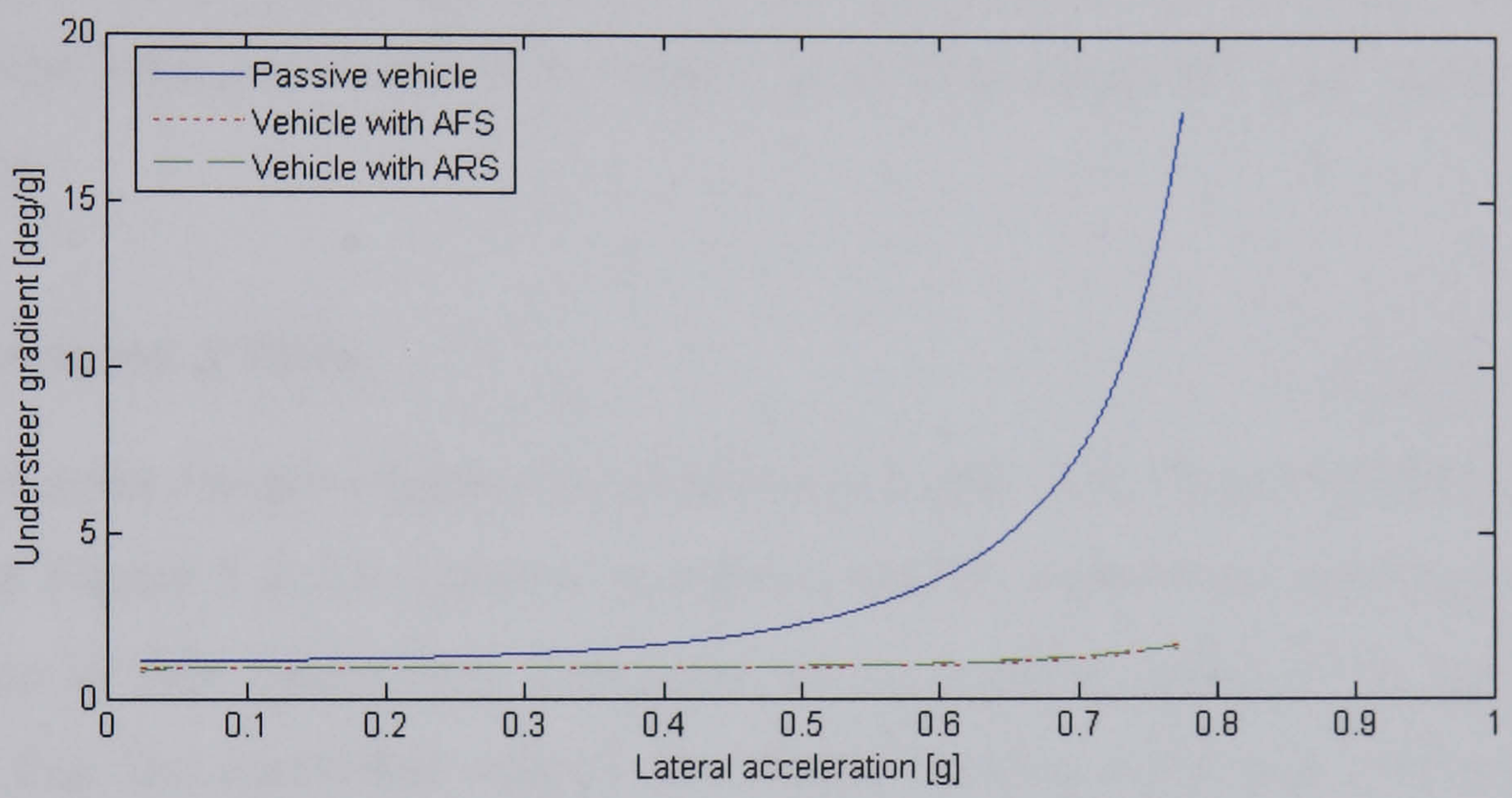

(a) on a high- μ ($=1.0$) road surface

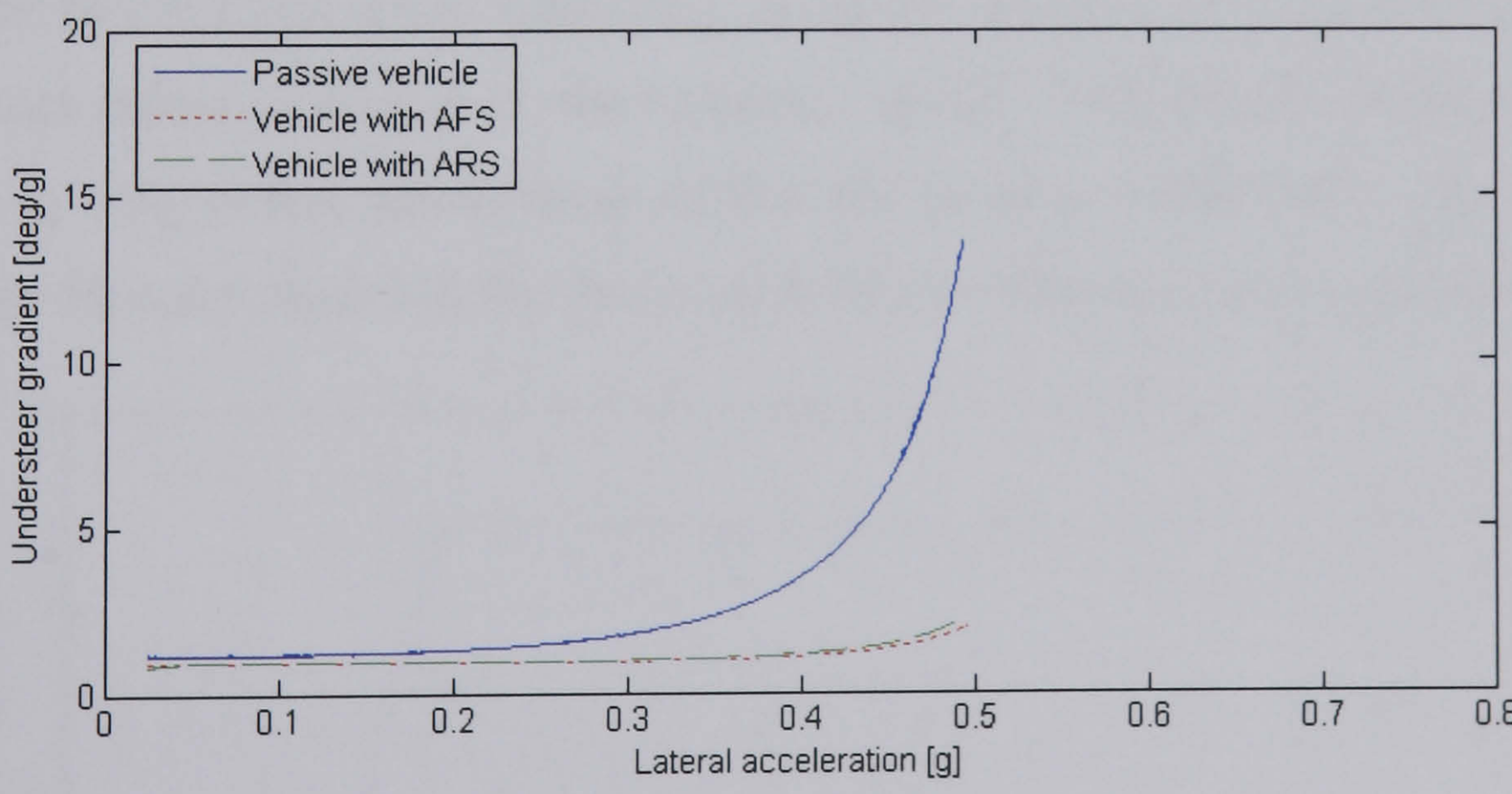

(b) on a low- μ ($=0.6$) road surface

Figure 5.7 Understeer gradient vs. lateral acceleration during steady-state cornering around a constant 33m radius path for the NLVM with and without stand-alone steerability controllers under different road conditions

The vehicle with AFS and ARS controllers is however seen to be linear to much higher levels of lateral acceleration up to the handling limit and consequently behaves in a more predictable manner over an even wider range of handling situations than the passive vehicle under both road surface conditions. This is indeed expected because of the utilisation of the linear reference model which is chosen for the stand-alone steerability controllers and always responds linearly to driver steer inputs.

These results show that the active steering subsystem controllers do offer the prospect of extending the linear handling region of the vehicle and avoiding entering into the nonlinearity. Therefore, from the driver's perspective, the vehicle becomes more controllable. In addition, this specific manoeuvre also demonstrates good robustness of AFS and ARS controllers with respect to vehicle speed and road surface friction variations.

Constant speed J-Turn

The steer input for this manoeuvre is shown in Figure 5.8. The simulation results are shown in Figure 5.9. The passive and the controlled vehicle are seen to show little difference in this manoeuvre. Compared to the passive vehicle, one can however observe that the controlled vehicle has better tracking behaviour and reduces the steady-state tracking error by 99%. The tracking of the passive vehicle is also good due to the fact that the 2DOF linear bicycle model which always responds linearly to driver steer inputs is chosen as the reference model. This specific manoeuvre only goes up to 0.4g lateral acceleration so that the passive vehicle still responds quite linearly to the steer input and the deviation from the reference model remains small.

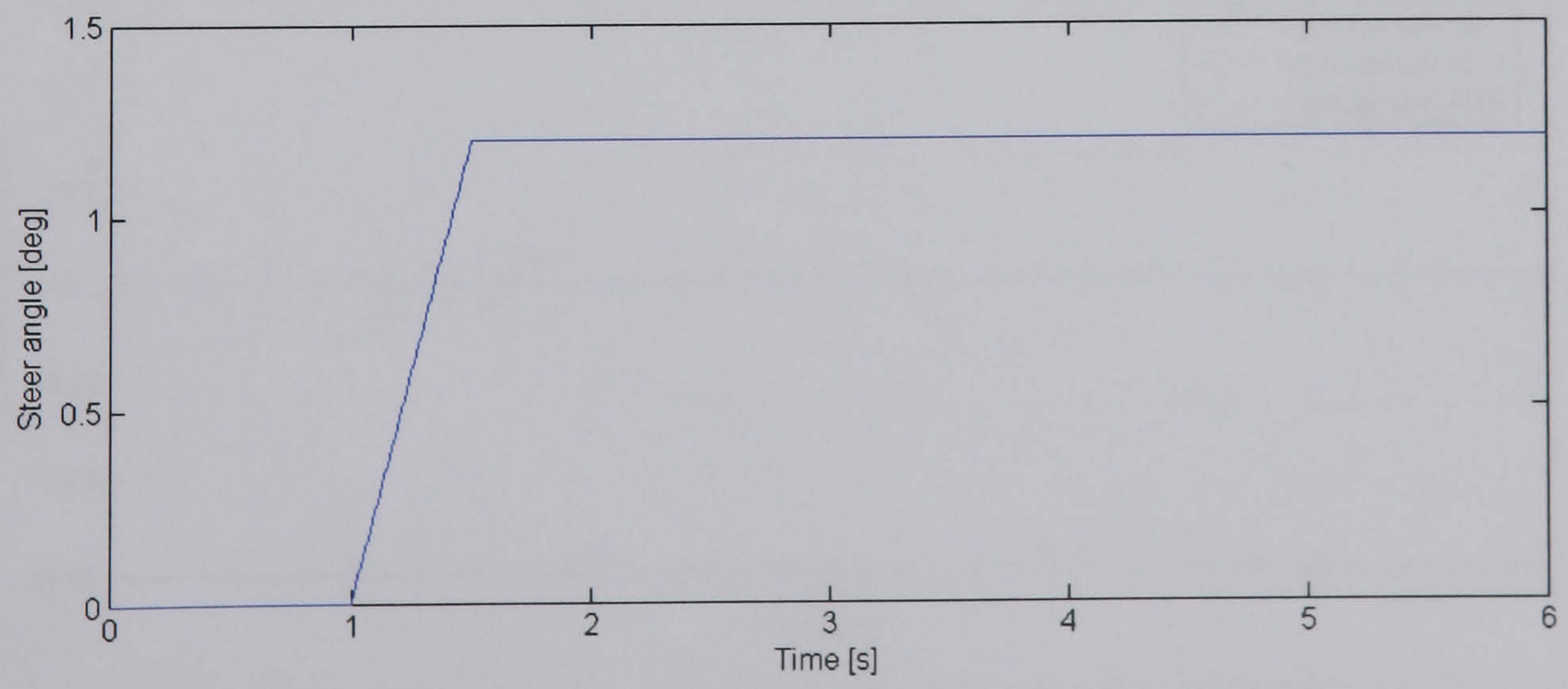

Figure 5.8 Steer angle for constant speed J-Turn

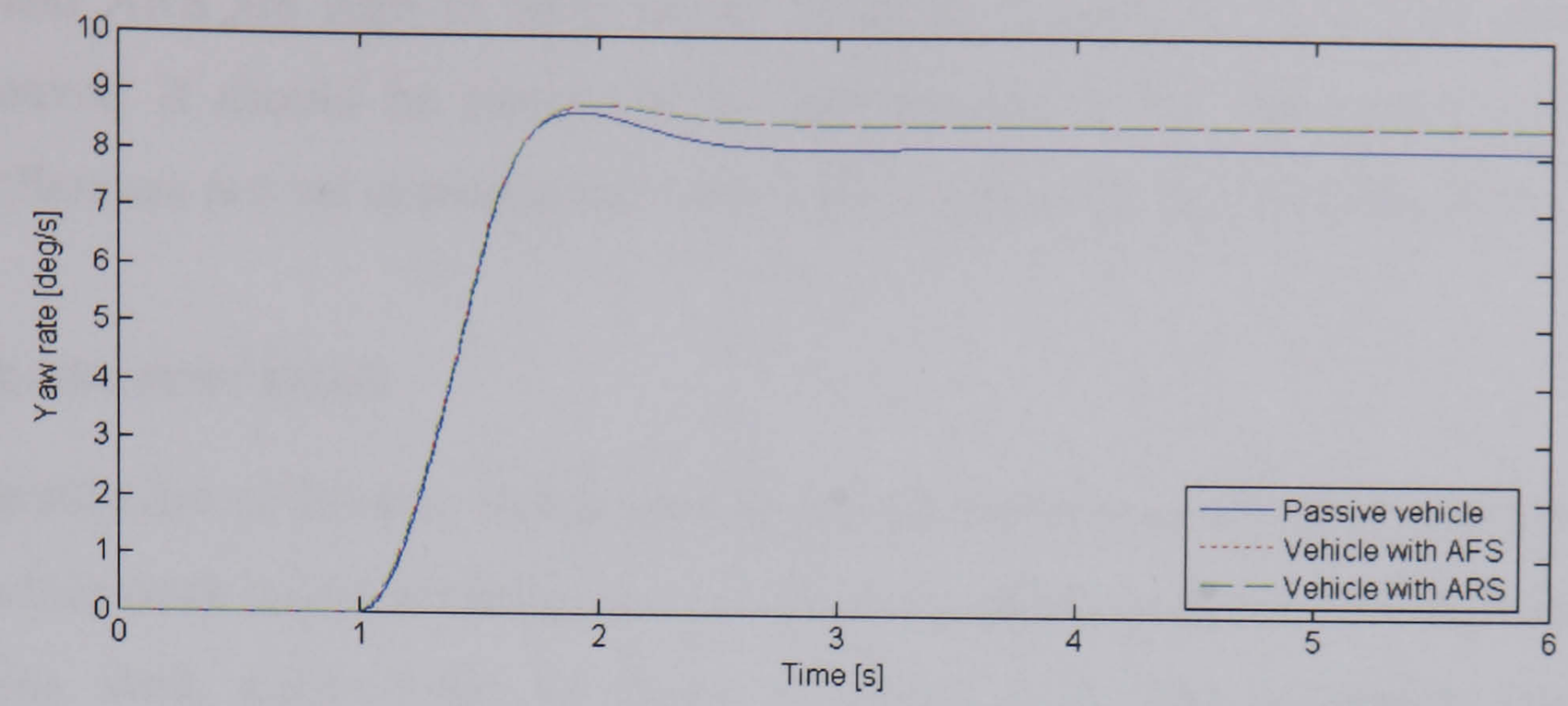

Figure 5.9 Simulation results of constant speed J-Turn for the NLVM with and without stand-alone steerability controllers at 100km/h

AFS and ARS are seen to have nearly identical tracking performance during this manoeuvre. It should be noted that the advantages of the stand-alone steerability controllers are not yet demonstrated very well through this specific manoeuvre.

Single sine steer input

The amplitudes of the steer inputs used in this manoeuvre are the steer angles required to produce peak lateral accelerations of 0.5g, 0.7g and to push the vehicle towards the handling limit, respectively, as shown in Figure 5.10. The simulation results are shown in Figures 5.11 to 5.16.

In the first instance, the vehicle with the AFS controller is seen to have almost the same tracking behaviour as the one with the ARS controller, i.e. AFS and ARS controllers can nearly identically track the reference yaw rate properly and reduce the peak tracking error by 94%. The controlled vehicle is seen to respond to the steer input slightly faster than the passive one.

In the second test, the tracking performance of the ARS controlled vehicle is seen to be slightly poorer than that of the AFS controlled one. A 93% and 67% reduction in the peak tracking error is observed for AFS and ARS, respectively. This is particularly the case when the magnitude of the actual yaw rate is greater than that of the reference yaw rate at high lateral acceleration. When the magnitude of the actual yaw rate is less than that of the reference yaw rate, the tracking performance of the ARS controller is comparable to that of its AFS counterpart. In addition, the active rear wheel steer angle in this critical manoeuvre is seen to be already saturated.

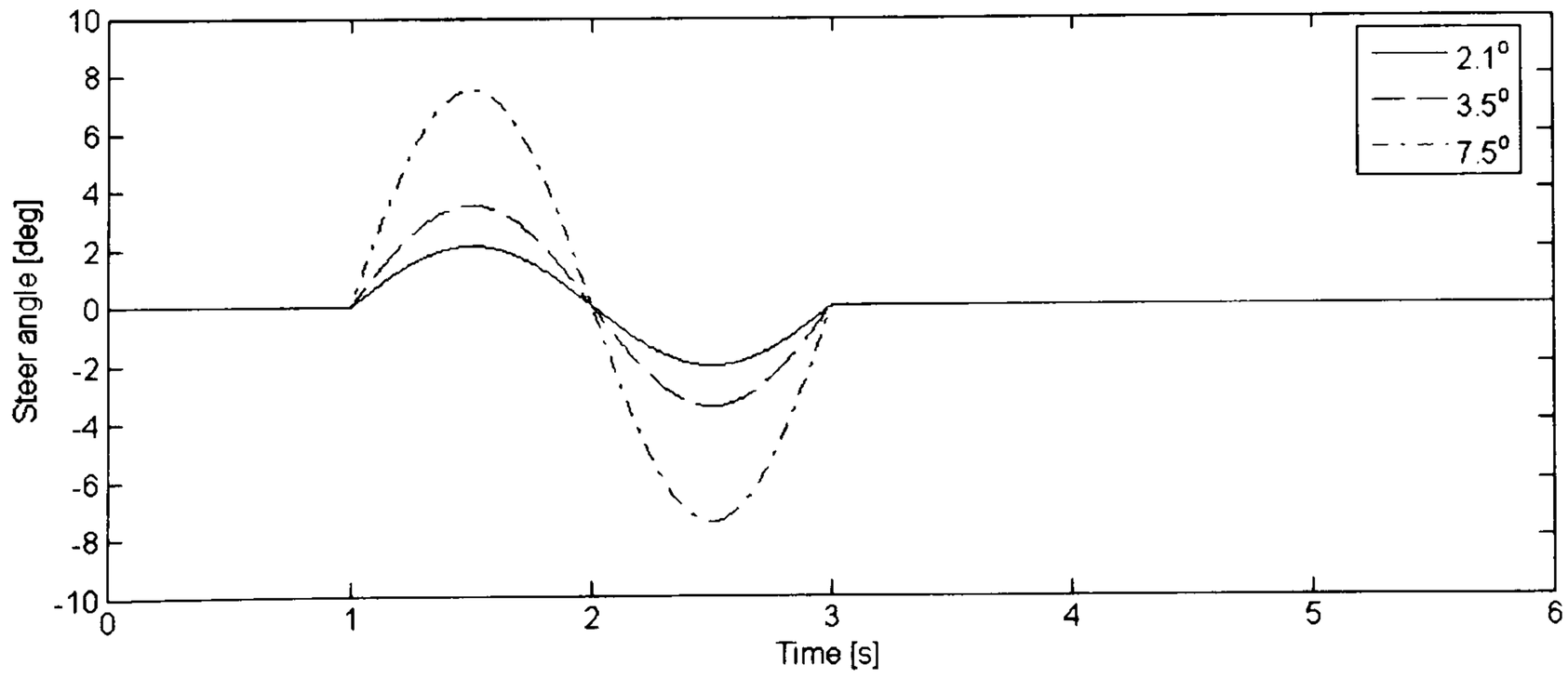

Figure 5.10 Steer angles for single sine steer input

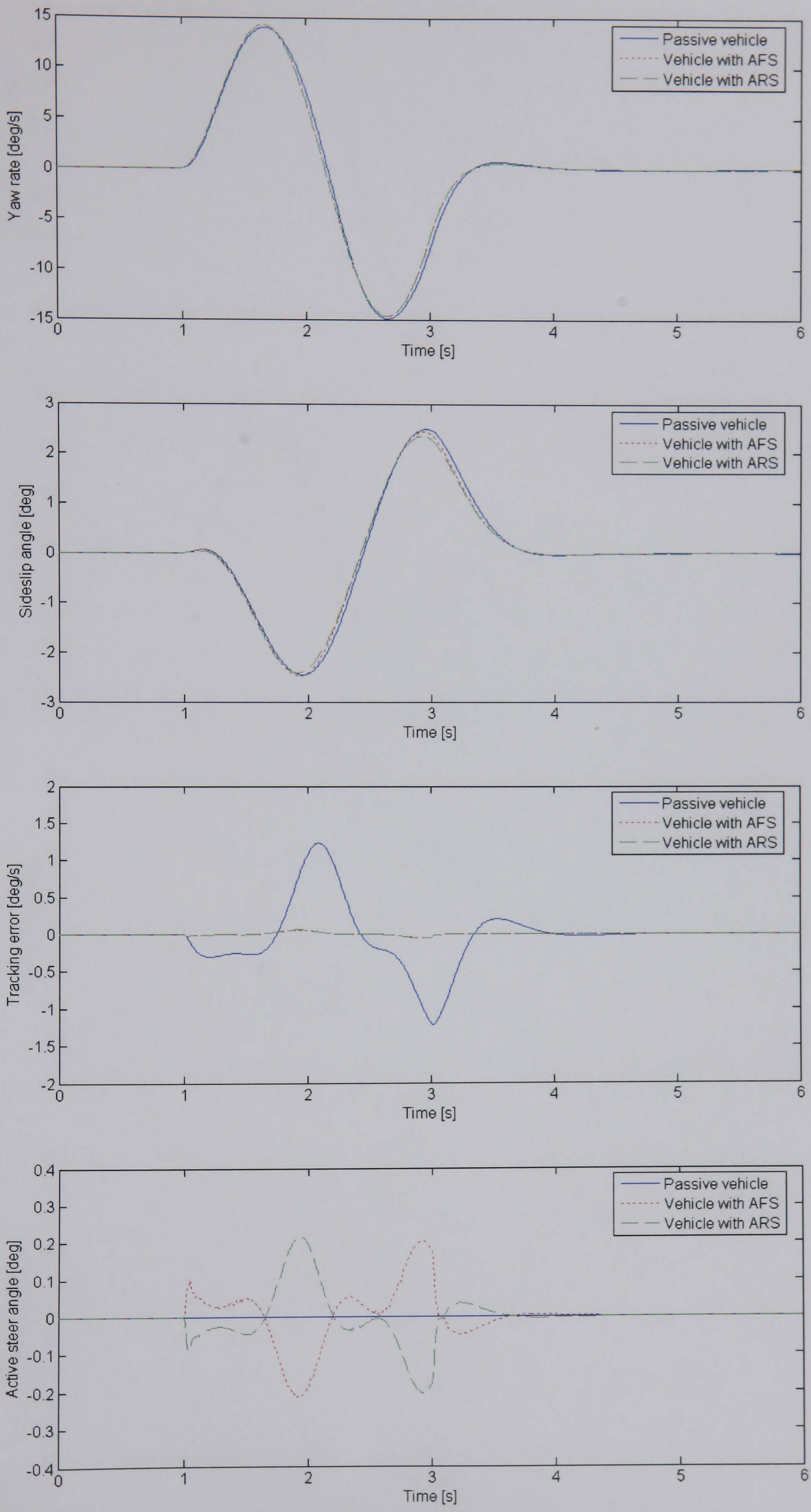

Figure 5.11 Response of the NLVM with and without stand-alone steerability controllers to single sine steer input with amplitude of 2.1° at 100km/h

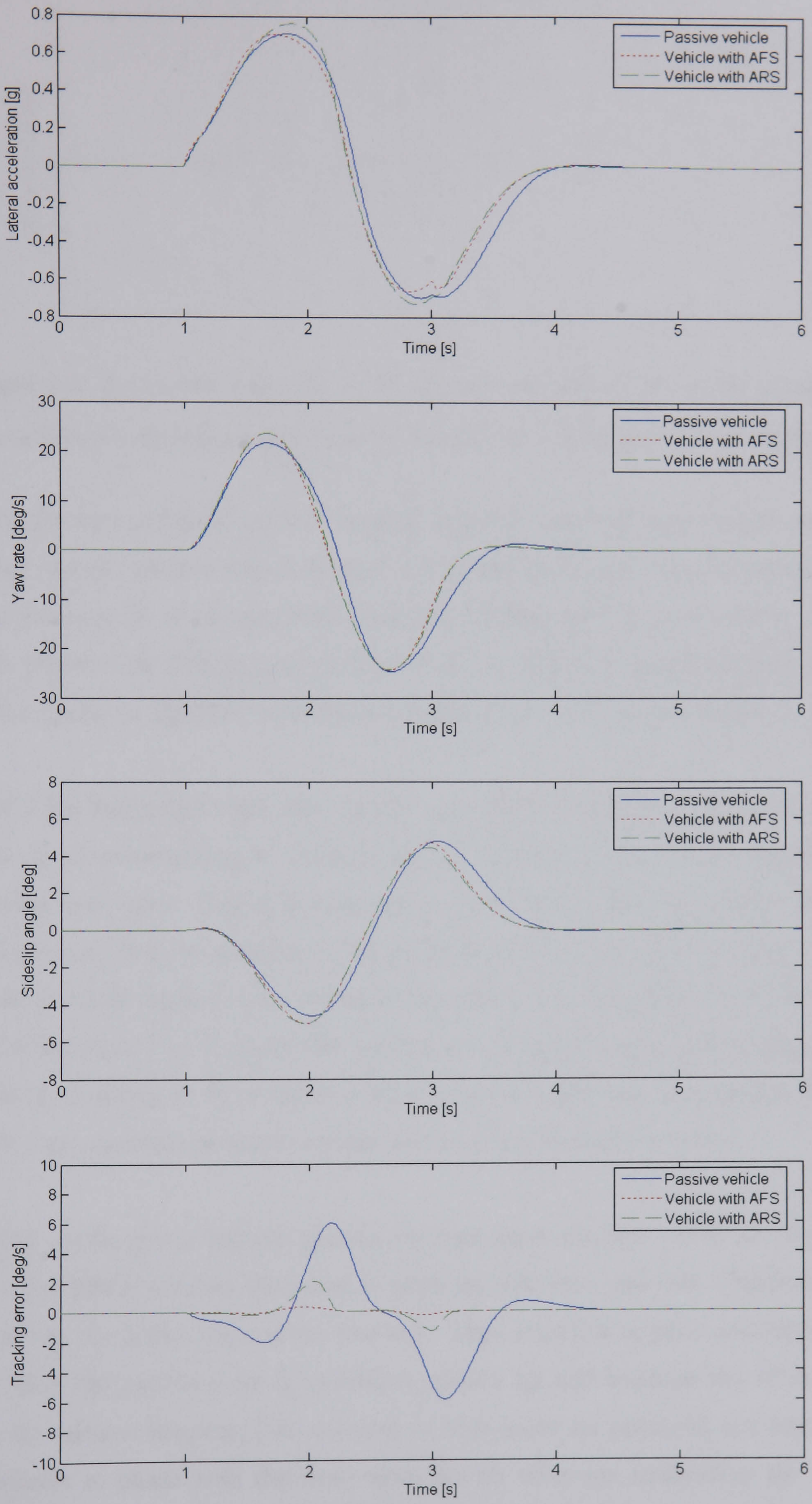

Figure 5.12 Response of the NLVM with and without stand-alone steerability controllers to single sine steer input with amplitude of 3.5° at 100km/h

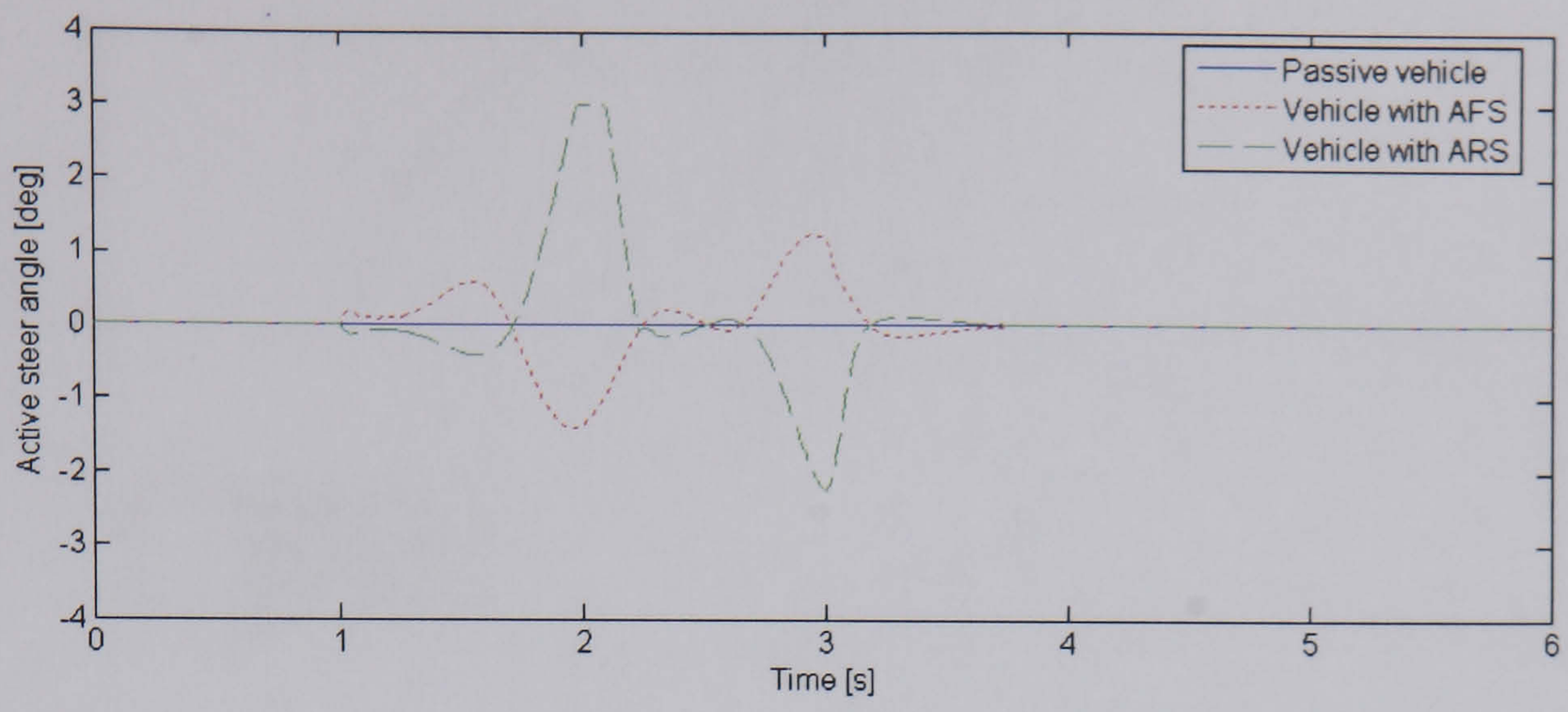

Figure 5.13 Active steer angles for the NLVM with and without stand-alone steerability controllers in response to single sine steer input with amplitude of 3.5° at 100km/h

Finally, the steer amplitude of 7.5° is quite aggressive for both passive and controlled vehicles. In the passive case, whereas the abrupt steer input generates substantial lateral forces at the front tyres, there is a delay before the rear tyres start to generate similar forces. The vehicle reacts with a clockwise rotation around its yaw axis and fails to respond to the driver's attempt to countersteer, resulting in spinout.

In the AFS controlled case, the vehicle can follow the first steer input through effectively countersteering by AFS, it cannot however successfully respond to the following steer input. This is because when the driver rapidly changes the direction of steering and thus the direction of lateral force of the front axle, the lateral force at the rear axle still applies in the opposite direction due to the delay. Therefore a large counterclockwise yaw moment that pushes the vehicle to spin counterclockwise is generated, resulting in large sideslip angle, and the AFS controller cannot keep the vehicle under control any more whereas the actuation limits are reached.

For ARS, as the driver initially applies the steer input, the rear wheels are steered by ARS out of phase with the front ones to track the reference yaw rate. This further lags and reduces the lateral force at the rear axle. Thus a clockwise yaw moment which is larger than the passive case is generated, speeds up and worsens the vehicle spin. When the spinout happens, lateral forces of both axles are saturated and steering the rear wheels in phase with the front ones has no effect on controlling the vehicle. Hence it takes longer for the ARS controlled vehicle to return to the steady-state of straight ahead driving. These effects can be clearly seen in Figures 5.14 to 5.16.

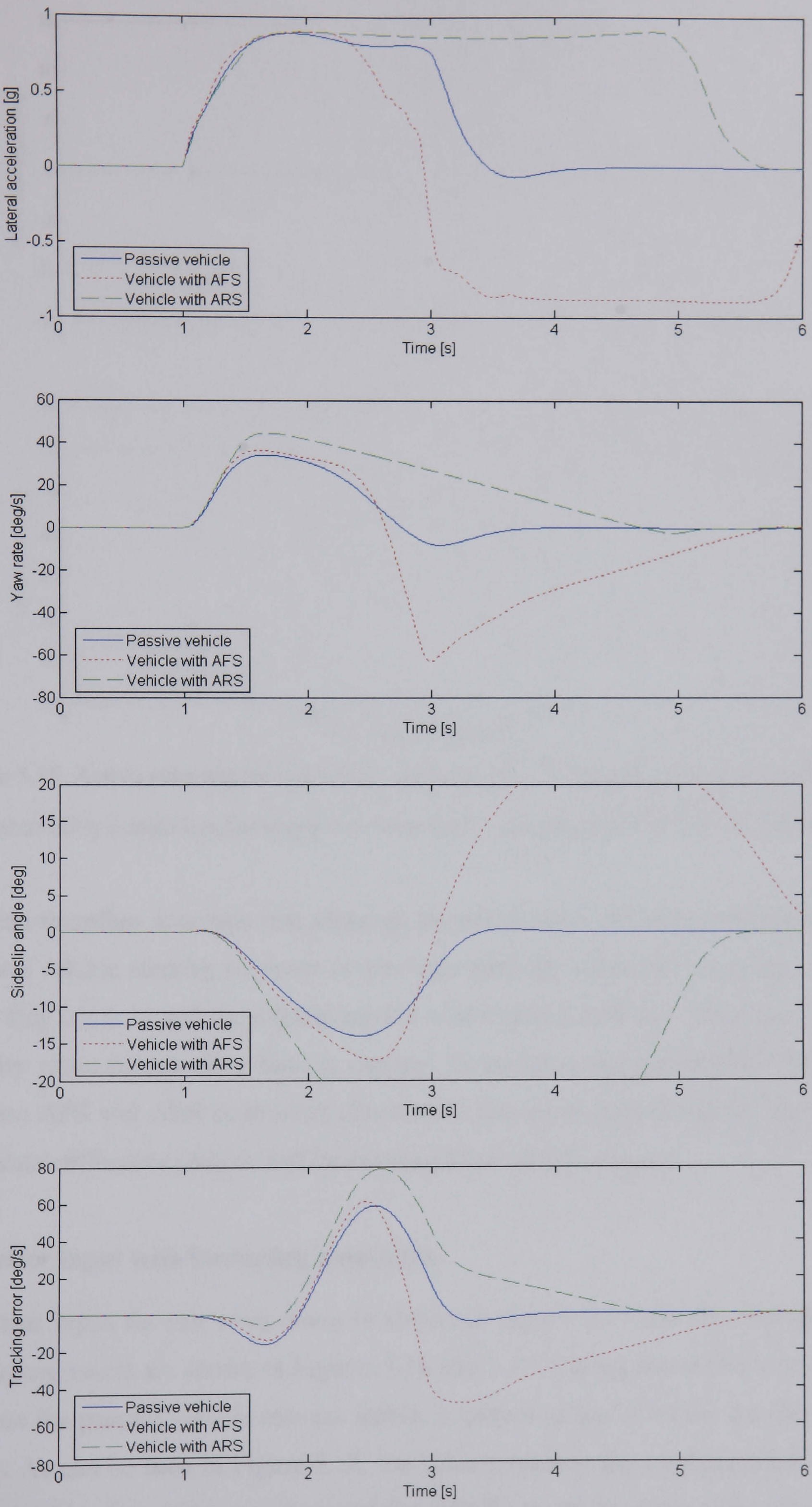

Figure 5.14 Response of the NLVM with and without stand-alone steerability controllers to single sine steer input with amplitude of 7.5° at 100km/h

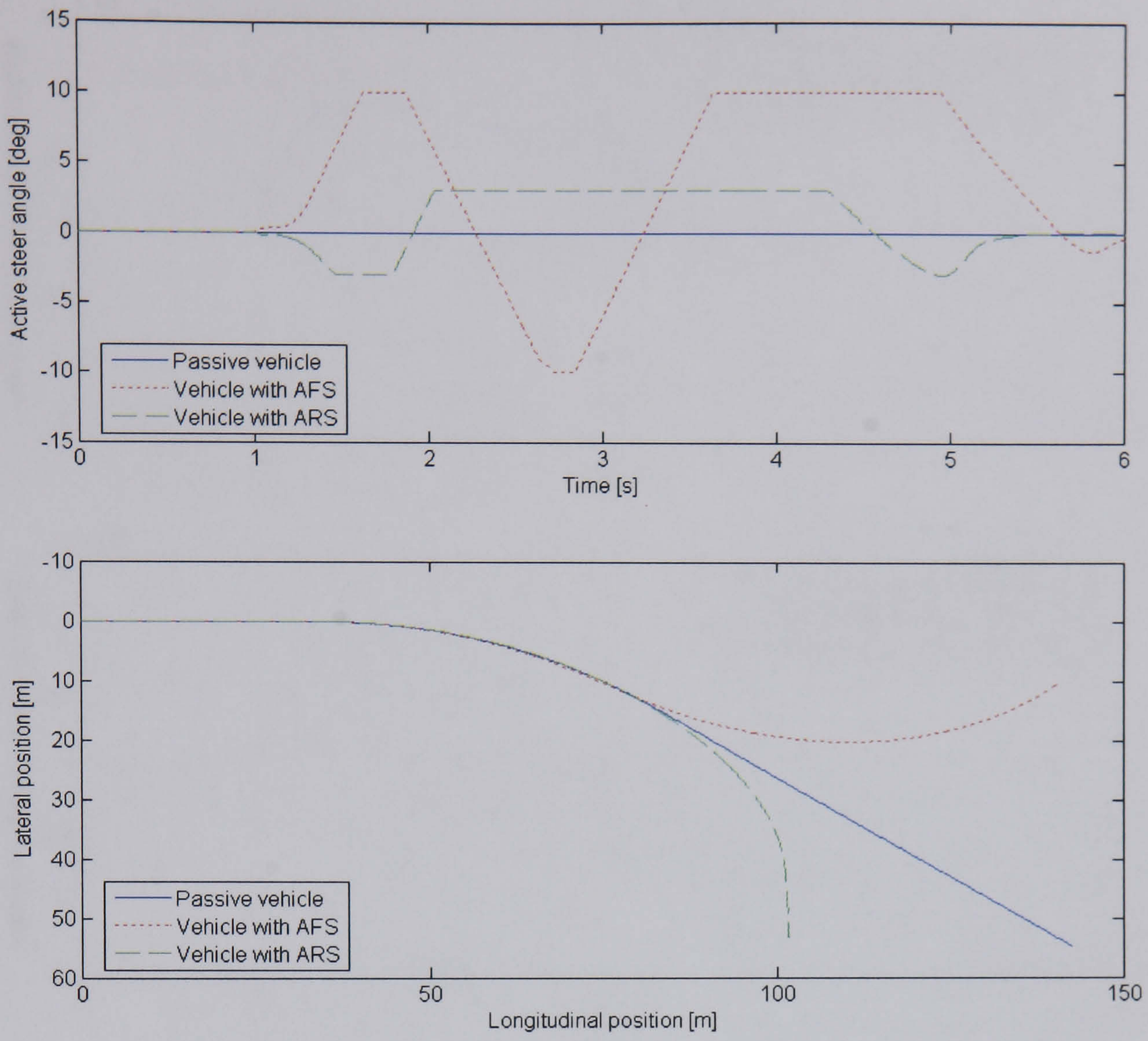

Figure 5.15 Active steer angles and vehicle path for the NLVM with and without stand-alone steerability controllers for single sine steer input with amplitude of 7.5° at 100km/h

One can therefore conclude that although the stand-alone steerability controllers can improve vehicle steering response or yaw rate tracking behaviour up to the handling limit, they fail to bound the sideslip motion of the vehicle and then to maintain vehicle stability when the handling limit is reached. In addition, the performance difference between AFS and ARS controllers observed in the above tests is mainly due to their functional differences which will be examined later in this chapter.

Sine steer input with increasing amplitude

The steer input for this manoeuvre is shown in Figure 5.17 and the corresponding simulation results are shown in Figures 5.18 and 5.19. During this critical manoeuvre, whereas the passive vehicle remains stable, it cannot properly follow the driver steer inputs. As can be seen in Figure 5.18, the vehicle reaches the handling limit at some points in this alternating sequence and the sideslip angle becomes quite large (more than 15°).

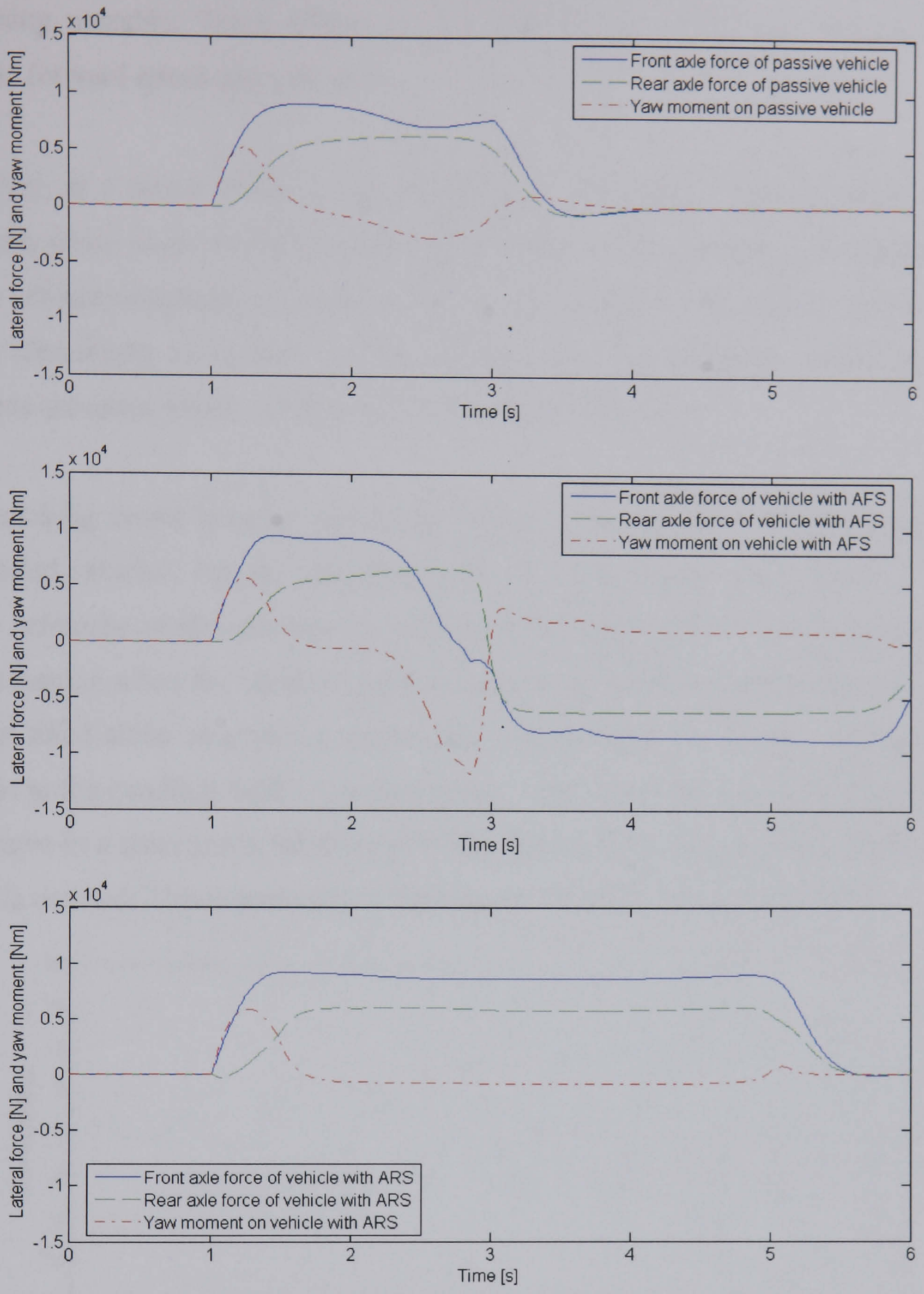

Figure 5.16 Axle forces and yaw moment on the NLVM with and without stand-alone steerability controllers for single sine steer input with amplitude of 7.5° at 100km/h

The reason for the passive vehicle remaining stable in this test is that at such high steer inputs, the lateral tyre forces of the front axle have a significant component in the longitudinal direction. This longitudinal component rapidly slows the vehicle down and also applies a contra-cornering yaw moment on the vehicle as there is more load at the outside wheel due to lateral load transfer and therefore the corresponding longitudinal component of the lateral tyre force is greater than that at the inner wheel. This will reduce the overall yaw moment on the vehicle to prevent the vehicle from

becoming unstable. These effects can be clearly seen in the time response of the vehicle forward speed and yaw rate.

However, at a certain point in this sequence the AFS and ARS controlled vehicles suddenly cease to respond to the steer inputs and break into a slide. The sideslip angle of the vehicle rises radically and the simulation is stopped. The vehicle with the stand-alone steerability controllers cannot properly track the reference model any more whereas actuation limits of AFS and ARS are both reached.

The tracking errors become very large at the handling limit for both passive and controlled vehicles. For the controlled case, this is partially due to the fact that the linear reference model produces a reference yaw rate which is not achievable in a stable fashion when the handling limit is reached. In addition, the functional limitation of the stand-alone steerability controllers in bounding the sideslip motion of the vehicle at the handling limit is another reason. The controlled vehicle is however seen to behave in a more predictable manner than the passive vehicle before the instability point is reached. This is particularly the case for the AFS controlled vehicle.

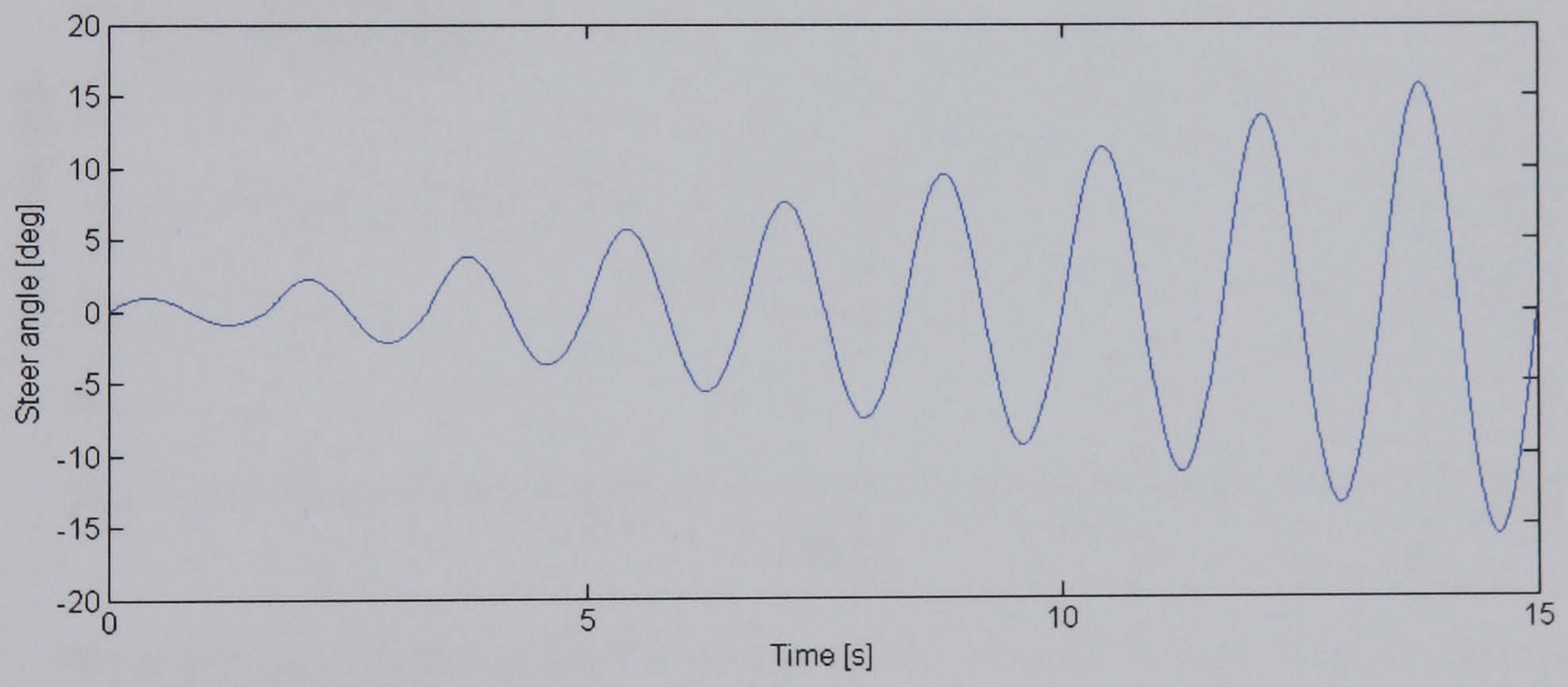

Figure 5.17 Steer angle for sine steer input with increasing amplitude

Braking on split-μ surfaces

In this test the vehicle is driven straight ahead at a speed of 100km/h on a split-μ surface where the wheels on the left side of the vehicle are on an icy ($\mu = 0.2$) surface and the wheels on the right side are on a dry ($\mu = 1.0$) surface and then an approximate step input in brake toque which produces a longitudinal acceleration of -0.4g is applied.

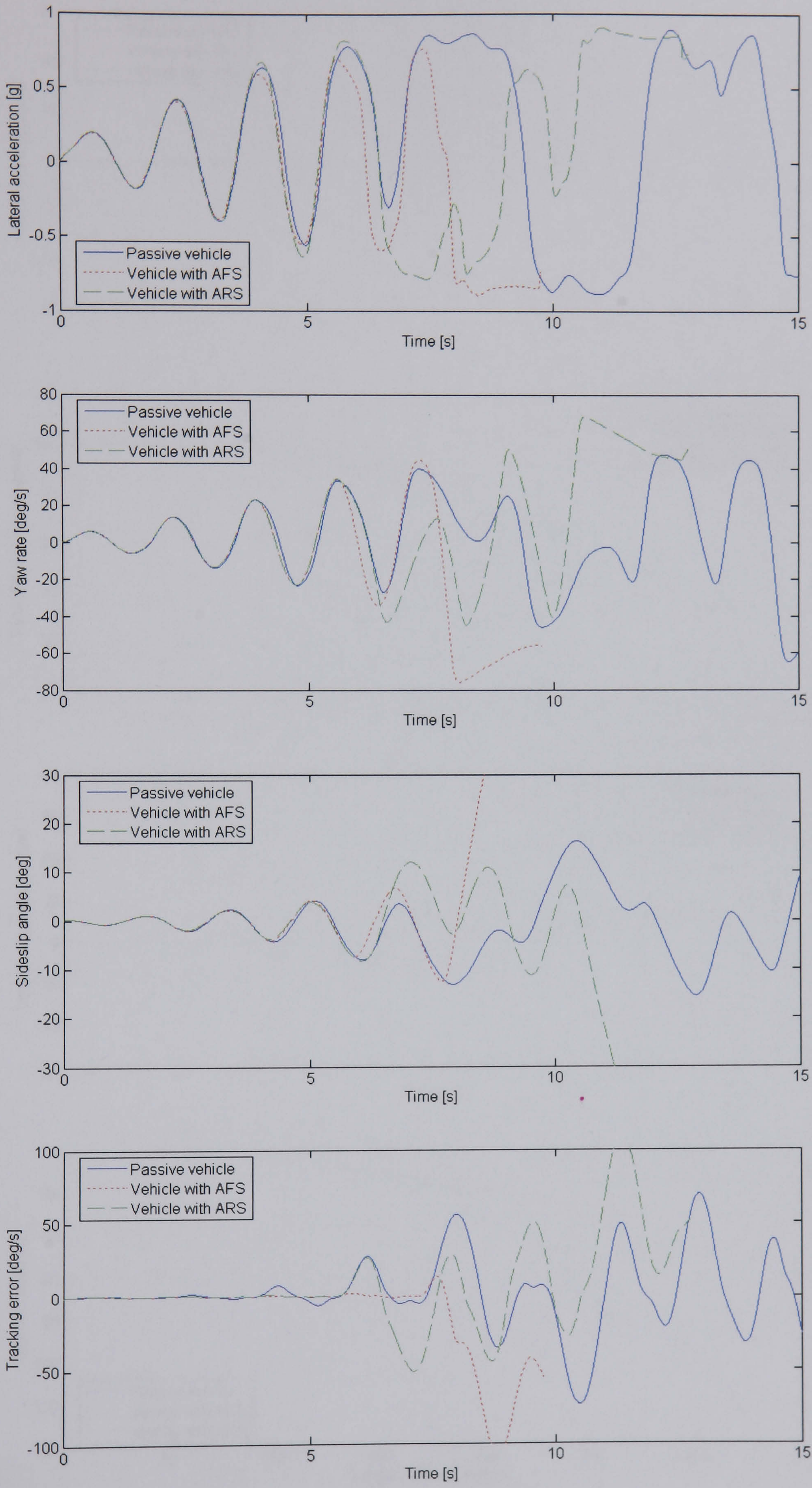

Figure 5.18 Response of the NLVM with and without stand-alone steerability controllers to sine steer input with increasing amplitude at 100km/h

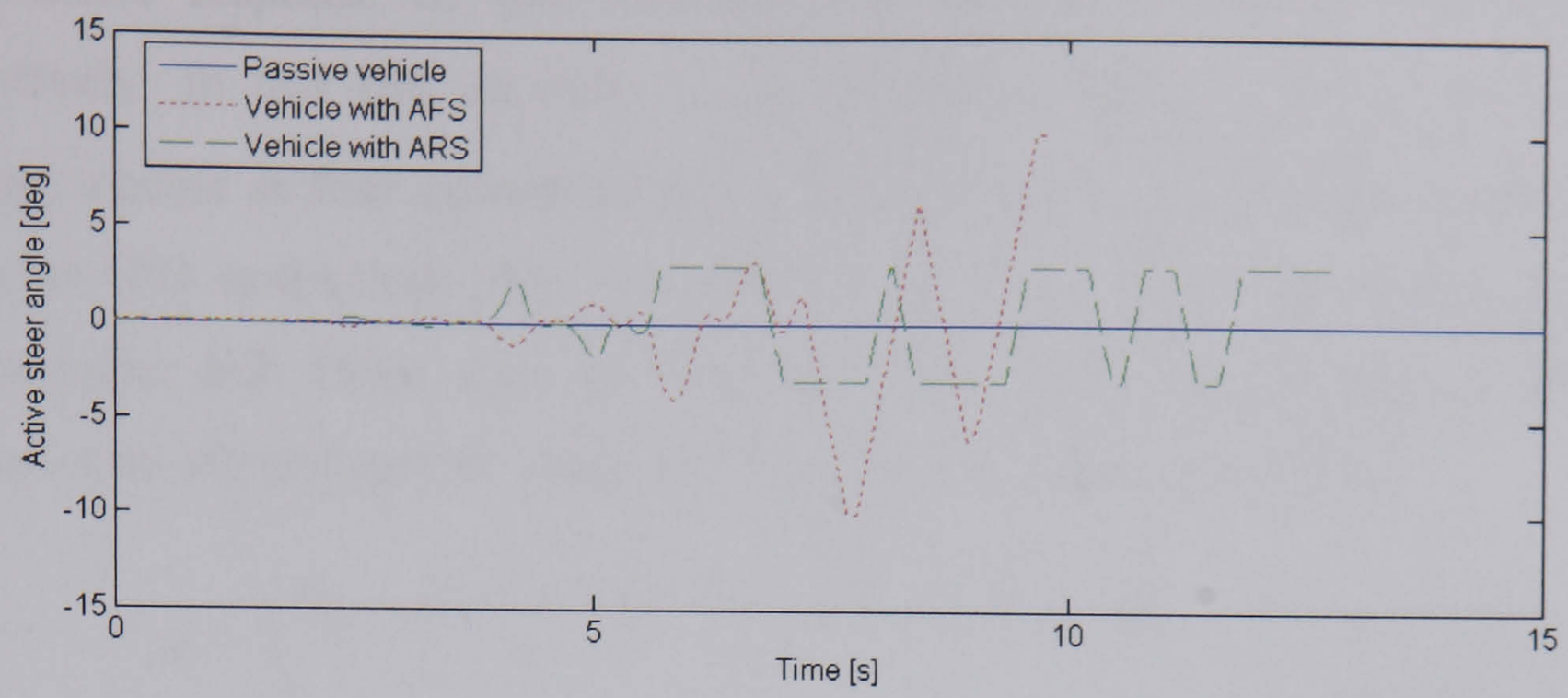

Figure 5.19 Active steer angles, vehicle speed and path for the NLVM with and without stand-alone steerability controllers for sine steer input with increasing amplitude at 100km/h

The vehicle response in this manoeuvre is shown in Figures 5.20 and 5.21, respectively. In this test, in order to prevent wheels on the low-μ surface from locking, wheels at four corners of the vehicle are all equipped with a simple ABS controller (PD controller). This controller aims to limit wheel slip ratio to above the desired value -0.2. There is no requirement for wheel slip ratio to settle at this value and hence an integral action is ignored. Therefore the controller acts as:

$$T_{ABS} = \begin{cases} K_{p\_ABS}(-0.2-\lambda) + K_{d\_ABS}\, d(-0.2-\lambda)/dt & \text{if } \lambda \le -0.2 \\ 0 & \text{if } \lambda > -0.2 \end{cases} \tag{5.38}$$

The controller was tuned empirically with the following result:

$$K_{p\_ABS} = 200000, \quad K_{d\_ABS} = 20000 \tag{5.39}$$

In addition, the brake torque is distributed to each axle in a fixed ratio which is the same as the vehicle weight distribution ratio to improve braking performance. The vehicle with the stand-alone ABS controller is seen to become unstable and spin. The AFS and ARS controlled vehicles however remain stable, leading to a 85% and 50% reduction in lateral deviation for AFS and ARS, respectively. This test demonstrates that the stand-alone AFS and ARS controllers have good disturbance rejection capabilities and can successfully maintain straight ahead driving stability of the vehicle. In addition, by using the ABS controller, the wheels on the low-μ surface are prevented from locking, as can be seen in Figure 5.20.

5.3.2 Robustness of stand-alone steerability controllers

In this thesis the stand-alone AFS and ARS controllers are designed by using the SMC technique in order to achieve robustness with respect to vehicle parameter variations and external disturbances. The disturbance rejection property of the stand-alone steerability controllers has been examined in Section 5.3.1 through the split-μ braking manoeuvre. In this section robustness of the stand-alone AFS and ARS controllers to parameter variations, specifically to vehicle forward speed and road surface friction variations will be investigated through open-loop simulation tests of the NLVM. Vehicle response to single sine steer input on nominal road surfaces ($\mu = 1.0$) at a speed of 140km/h is shown in Figure 5.22.

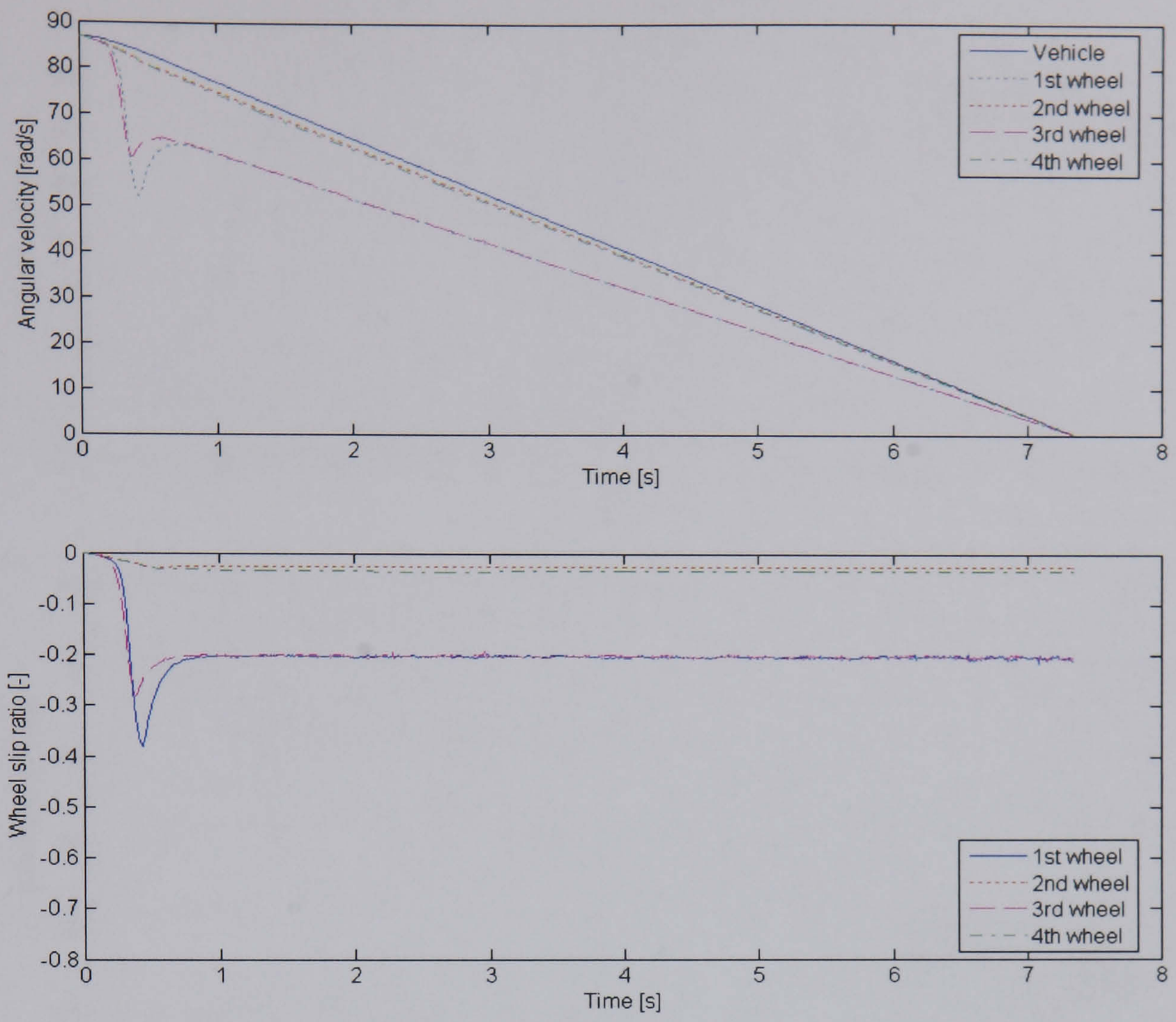

(a) Vehicle with AFS+ABS

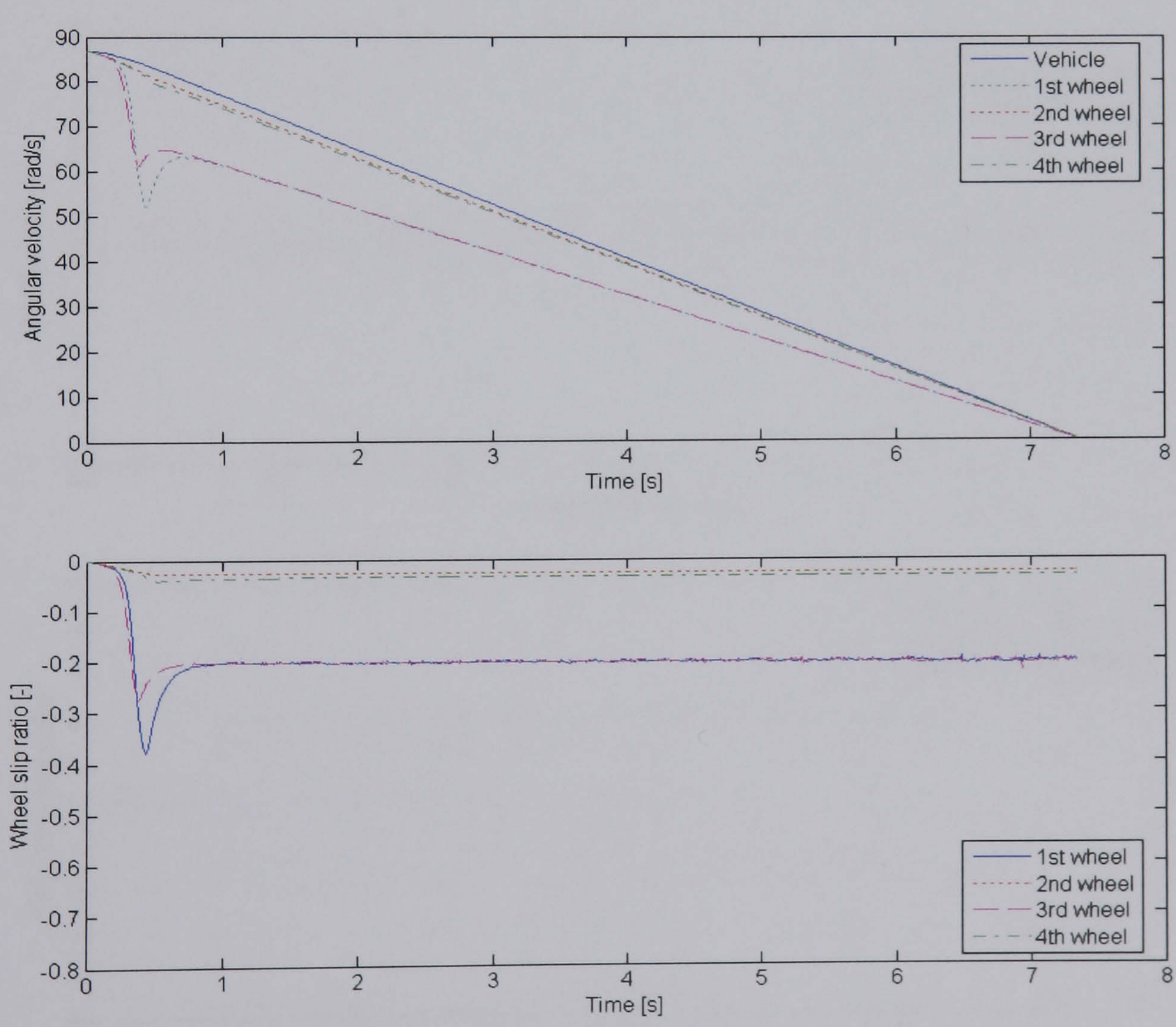

(b) Vehicle with ARS+ABS

Figure 5.20 Velocity and wheel slip ratio responses of the NLVM with steerability controllers and ABS controller to braking on a split-μ surface

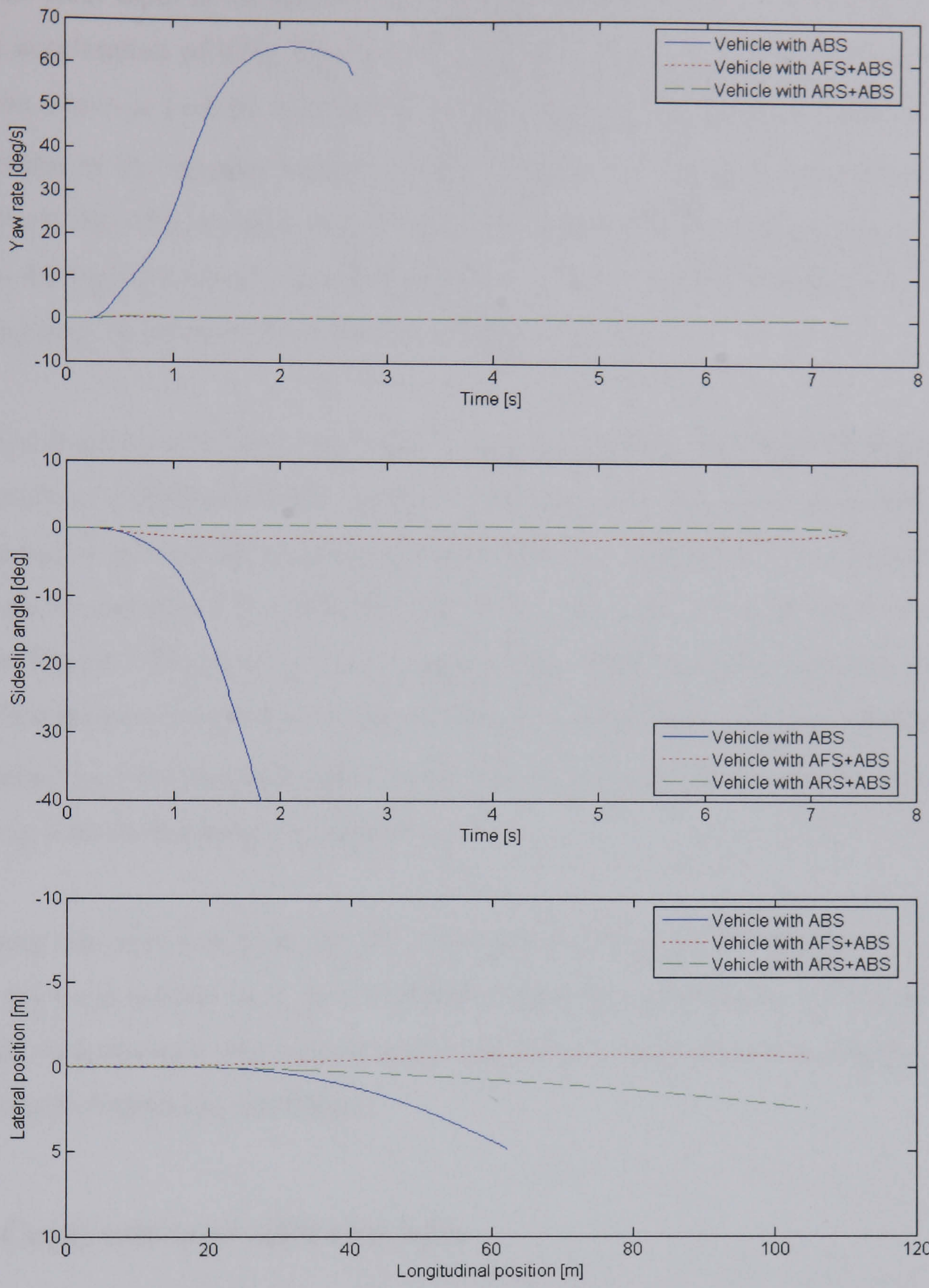

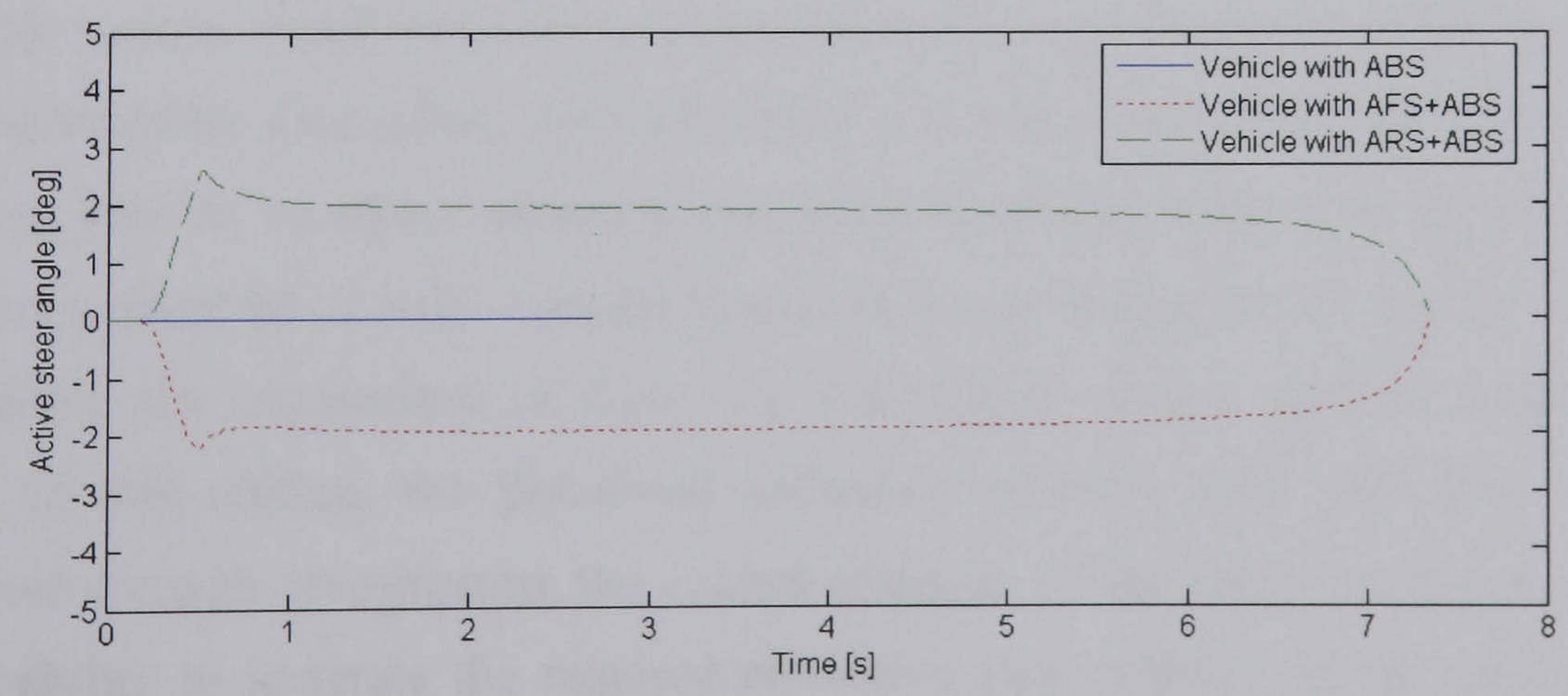

Figure 5.21 Response of the NLVM with and without stand-alone steerability controllers to braking on a split- μ surface

Here the steer input is the same as the one used in Section 5.3.1 for producing a peak lateral acceleration of 0.5g. Figure 5.23 shows the vehicle response to the same steer input on a low-μ $(=0.6)$ road surface at nominal speed of 100km/h. In the first case, a variation in the vehicle forward speed will lead to a change in the reference yaw rate. Both the AFS controlled and ARS controlled vehicles are seen to be able to follow the varied reference yaw rate properly. A 92% and 91% reduction in the peak tracking error is observed for AFS and ARS, respectively.

For road friction variations, a decrease in the road surface coefficient of friction may also result in a decrease in the reference yaw rate. However, due to the difficulty in measuring or estimating the road surface coefficient of friction, the reference model will remain unchanged for different road surface conditions in this thesis. As can be seen in Figure 5.23, both the AFS controlled and ARS controlled vehicles can track the reference yaw rate properly even on low-μ road surfaces. The peak tracking error is reduced by 94% for AFS and 87% for ARS as the vehicle is already close to the handling limit in this specific manoeuvre.

One may therefore conclude that the stand-alone AFS and ARS controllers designed in the previous section have good robustness with respect to parameter variations and external disturbances and consequently can provide consistent performance over a wide range of operating conditions.

5.4 Comparison of AFS and ARS

Through various simulation tests conducted above, the performance of the two stand-alone steerability controllers, AFS and ARS in terms of reference yaw rate tracking has been seen to be almost identical and some functional differences between them have been observed as well. In order to choose the most appropriate one for the final integration, the comparison of these two stand-alone control systems needs to be made. In this section, the functional difference between AFS and ARS will be explained through investigating the control authority of the two subsystems in terms of the ability to generate the required corrective yaw moment on the vehicle. The analysis of corrective yaw moment generation can be referred to Appendix E.

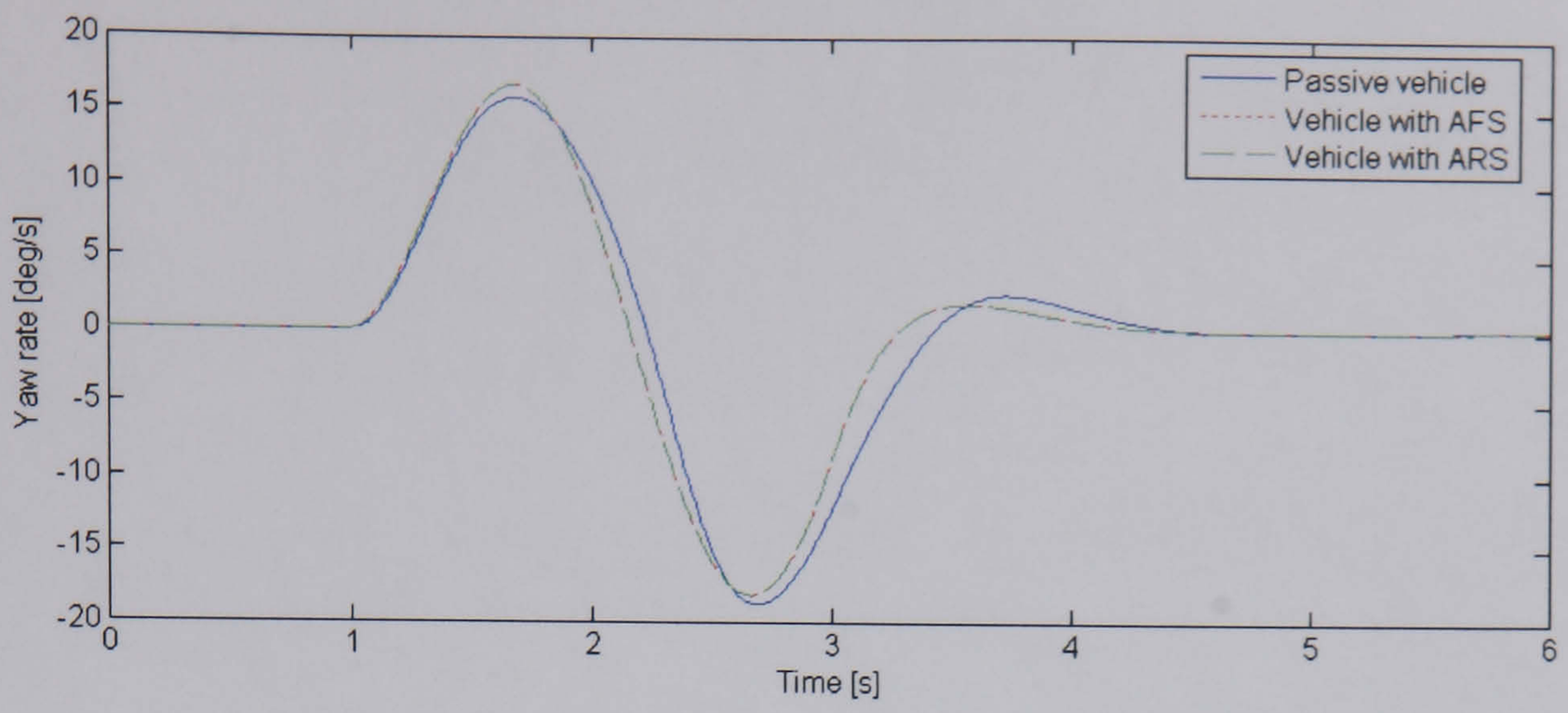

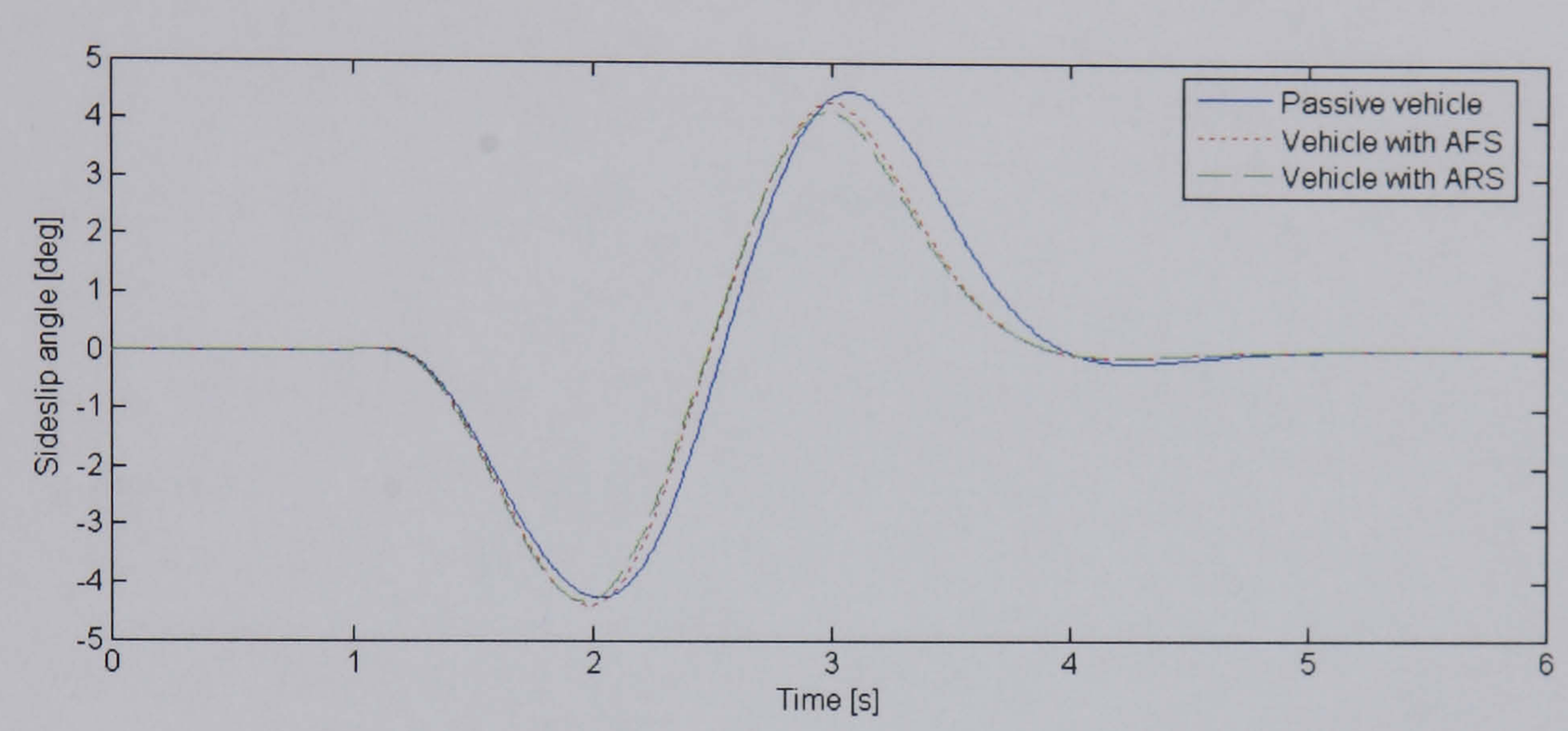

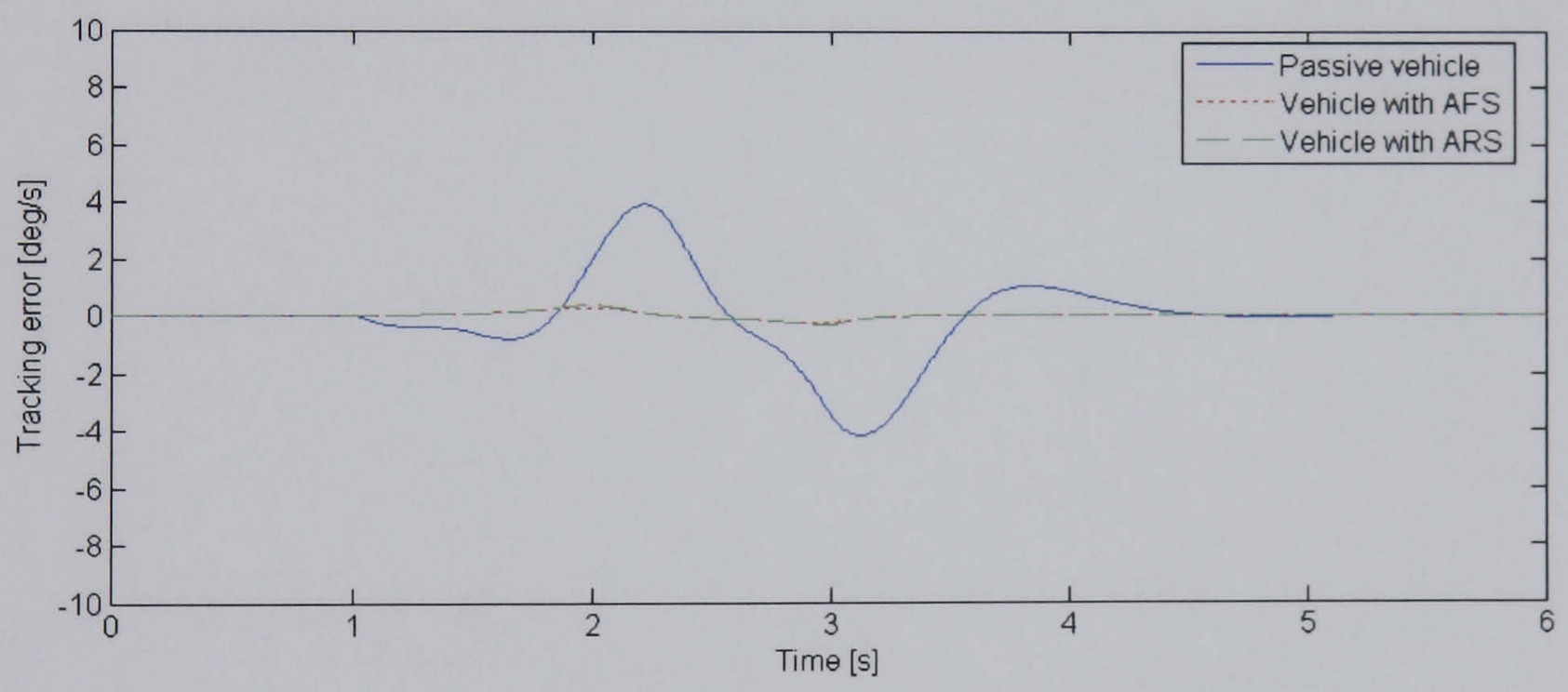

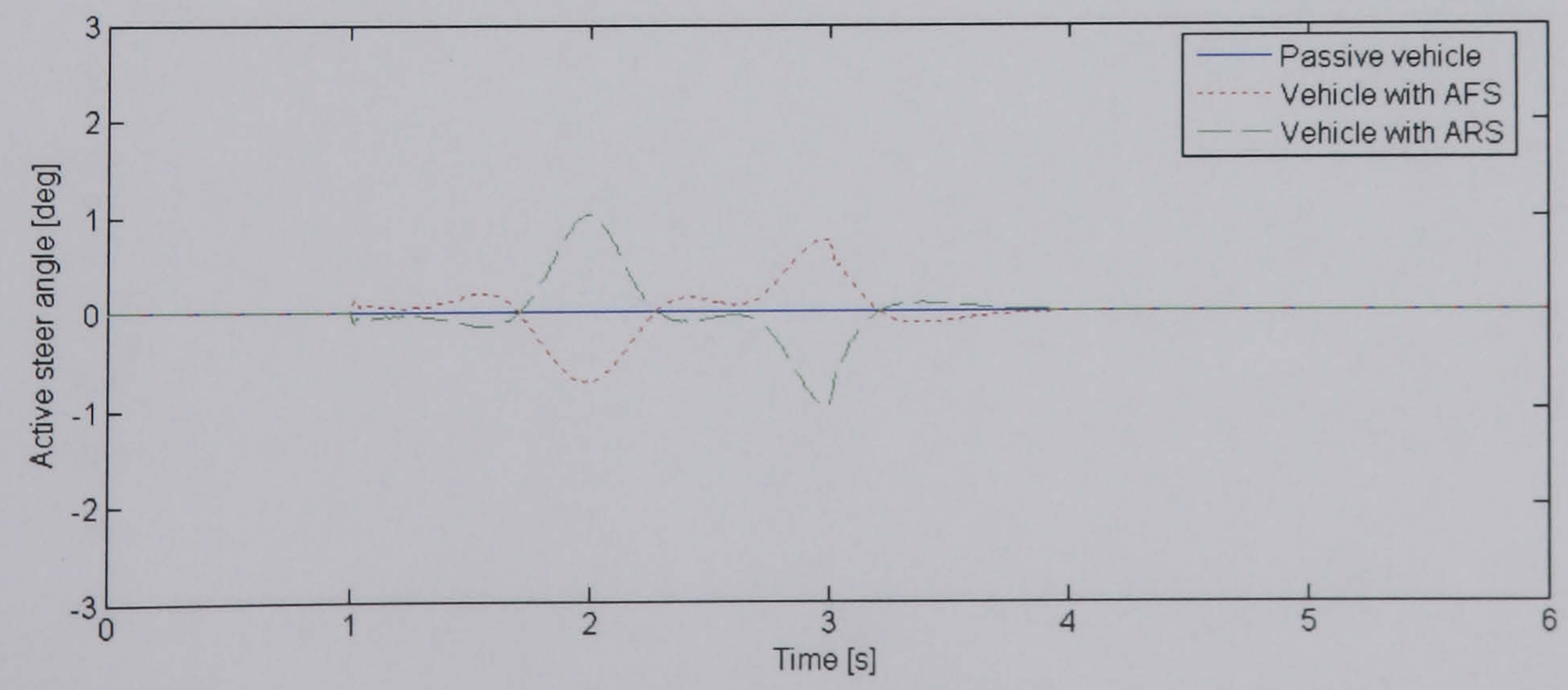

Figure 5.22 Response of the NLVM with and without stand-alone steerability controllers to single sine steer input on a nominal road surface at 140km/h

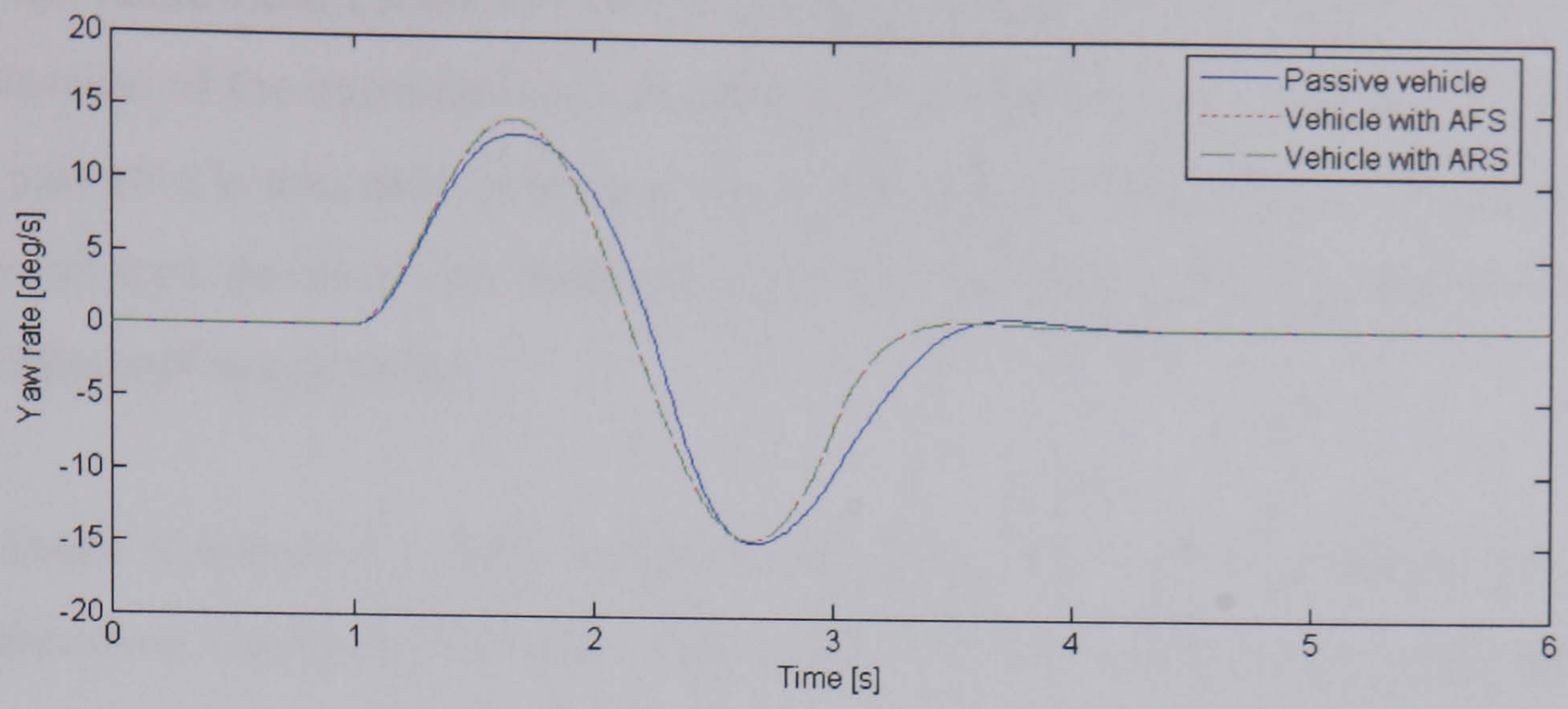

Figure 5.23 Response of the NLVM with and without stand-alone steerability controllers to single sine steer input on a low-μ ($=0.6$) road surface at nominal speed of 100km/h

Here, the achievable corrective yaw moment generated by each subsystem is plotted as a function of the corresponding control input and lateral acceleration of the vehicle. If the yaw rate is assumed to be positive or the vehicle is assumed to be negotiating a right hand turn, positive yaw moment means pro-cornering and negative yaw moment represents contra-cornering.

The results obtained for AFS is shown in Figure 5.24. AFS is seen to be able to generate equal amount of pro and contra-cornering yaw moment during straight ahead driving (zero lateral acceleration). At moderate lateral accelerations, the contra-cornering yaw moment generated by AFS through reducing the driver steer inputs or countersteering is larger than the pro-cornering yaw moment as this steering action can substantially reduce the slip angle, and consequently the lateral force at the front axle, creating a large change in the yaw moment. When the vehicle reaches the handling limit, both the achievable pro and contra-cornering yaw moments are relatively small. This is because at the handling limit, the front wheel steer angle is usually large and the front axle reaches the saturation point around which relatively small changes in the steer angle and consequently in the tyre slip angle have little effect on the lateral forces.

The corrective yaw moment exerted by ARS is shown in Figure 5.25. Similar to AFS, the pro and contra-cornering yaw moments achieved by actively steering the rear wheels are the same when the vehicle is driven straight ahead. However, when the handling limit is approached, the achievable pro-cornering yaw moment is even larger than that in the opposite direction. This is because at the handling limit, the rear tyre slip angle is quite large and the corresponding lateral tyre force reaches its maximum, therefore by steering the rear wheels out of phase with the front ones the slip angle and lateral force at the rear axle can be dramatically reduced, resulting in a large pro-cornering yaw moment. In contrast, the lateral force at the rear axle cannot be increased further by simply increasing the tyre slip angle through steering the rear wheels in phase with the front ones as the lateral tyre force is already saturated.

Therefore there is an obvious difference between AFS and ARS in generating the corrective yaw moment and influencing vehicle handling behaviour. Generally, with the increase of lateral acceleration, ARS is more powerful in generating pro-cornering

yaw moment. Once vehicle instability occurs, it is quite difficult for ARS to correct. By contrast, AFS is more effective in generating contra-cornering yaw moment even close to the handling limit, especially when the driver steer inputs are relatively small. This analysis further explains the performance difference between AFS and ARS observed in the previous simulation results.

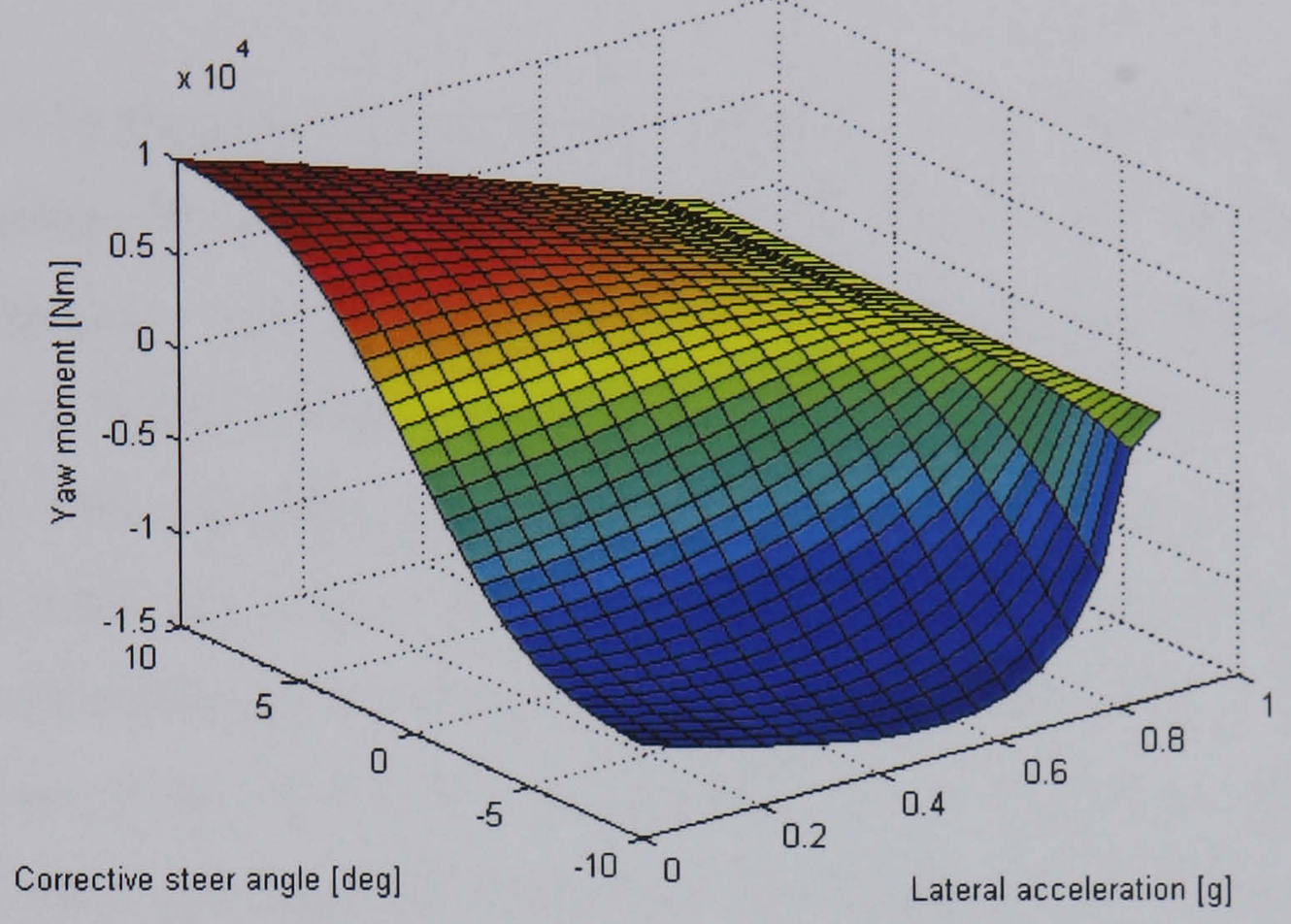

Figure 5.24 Corrective yaw moment generated by AFS

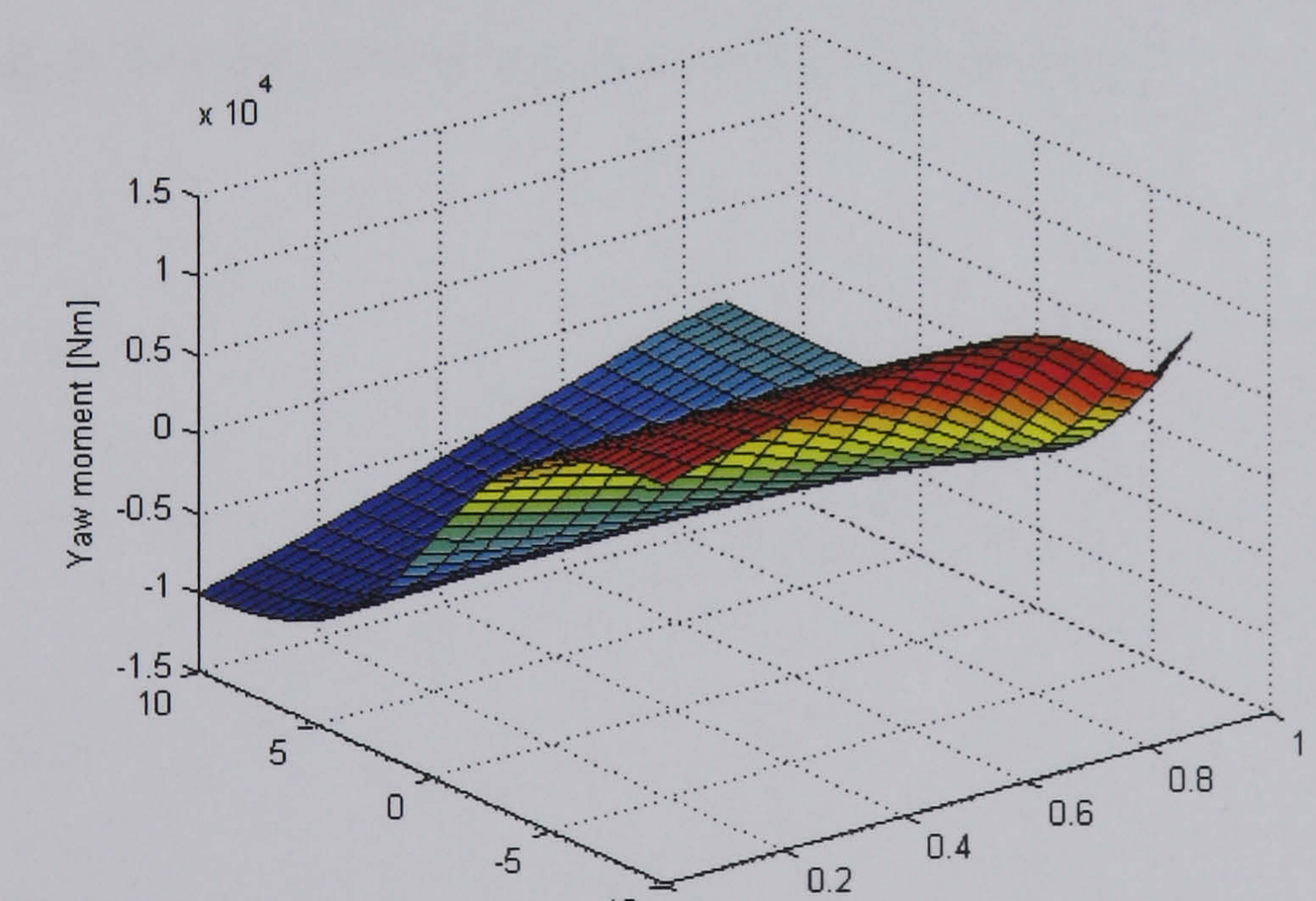

Figure 5.25 Corrective yaw moment generated by ARS

5.5 Conclusions

This chapter has presented the design of active steering subsystem controllers. The reference model tracking control strategy has been proposed and the corresponding

reference model has been introduced. This strategy enables the vehicle to follow the response of the reference model and to behave in a desired manner. Based on this strategy, both stand-alone AFS and ARS controllers have been designed to perform the control task of improving vehicle steerability by using the SMC technique which possesses inherent robustness with respect to system parameter variations and external disturbances.

In order to verify the effectiveness of the proposed stand-alone steerability controllers, various computer simulation tests on the NLVM have been carried out over a wide range of handling conditions. New results clarifying the relative performance properties of AFS and ARS have been presented. Simulation studies demonstrate that the designed AFS and ARS controllers can improve vehicle steering response up to the handling limit and achieve good robustness. However, it has been found that the stand-alone steerability controllers designed for yaw rate tracking fail to bound the sideslip motion of the vehicle and to maintain vehicle stability at the handling limit. This indeed raises the demand for the DSC subsystem which will be examined in the following chapter. Finally, the control authority of AFS and ARS in terms of the achievable corrective yaw moment acting on the vehicle have been compared to show the functional difference between the two active subsystems.

Chapter 6

Design of Dynamic Stability Subsystem Controller

Abstract: *This chapter presents the design of the dynamic stability subsystem controller. Vehicle stability is first analysed in the phase plane of the vehicle sideslip angle and its angular velocity. The dynamic stability subsystem controller is then designed by using the phase-plane method to perform the control task of maintaining vehicle stability. Both driveline based and brake based dynamic stability subsystems are investigated to show the relative merits. A new dynamic stability subsystem based on a combination of the two actuation concepts is also proposed. The controller is finally evaluated through computer simulations.*

6.1 Introduction

Due to the inherent saturation properties of lateral tyre forces with respect to tyre slip angles, AFS and ARS described in Chapter 5 cannot keep the vehicle under control when the handling limit is reached and consequently vehicle stability is in question. In order to maintain vehicle stability during critical driving situations, both driveline

based and brake based dynamic stability control (DSC) systems have been widely developed in the literature. These two systems aim to influence vehicle handling through exploiting the interactions between longitudinal and lateral tyre forces. However, as reviewed in Chapter 2, no comparison has yet been given to assess the relative merits of these two systems in previous studies. In this chapter the stand-alone stability controller, which is aimed at maintaining vehicle stability close to and at the handling limit, will be designed. The corresponding driveline based and brake based DSC subsystems will be analysed and compared. This analysis will allow a new driveline plus brake based DSC subsystem to be proposed.

6.2 Analysis of Vehicle Stability

6.2.1 Stability of nonlinear systems

The general n-dimensional nonlinear continuous dynamic systems can be described by a set of first-order nonlinear differential equations of the form:

$$\dot{\mathbf{x}} = \mathbf{f}(\mathbf{x}, t) \tag{6.1}$$

where $\mathbf{x}$ is the $n\times 1$ state vector and $\mathbf{f}$ is a $n\times 1$ nonlinear vector function of the states. A nonlinear system is said to be autonomous if $\mathbf{f}$ does not depend explicitly on time. A solution $\mathbf{x}(t)$ of the equations (6.1) usually corresponds to a curve in state space as t varies from zero to infinity. This curve is generally referred to as a *state trajectory* or a *system trajectory*. One should note that although Eq. (6.1) does not explicitly contain the control input as a variable, it is directly applicable to feedback control systems since Eq. (6.1) can represent the closed-loop dynamics of a feedback control system, with the control input being a function of state $\mathbf{x}$, and therefore 'disappearing' in the closed-loop dynamics (Slotine and Li, 1991).

In order to analyse stability of nonlinear systems of (6.1), the equilibrium points need to be defined first since many stability problems are naturally formulated with respect to equilibrium points. The term *equilibrium point* of a dynamic system is used for a state of the system that does not change in the course of time, i.e. $\dot{\mathbf{x}} = 0$. Therefore, the point $\mathbf{x}_e$ is said to be an equilibrium point of the system if and only if $\mathbf{f}(\mathbf{x}_e, t) = \mathbf{0}$. That is, if the initial state of the differential equations of (6.1) is $\mathbf{x}_e$, i.e., $\mathbf{x}(t_0) = \mathbf{x}_e$,

then the state of the equations remains $\mathbf{x}_e$ for all $t \geq t_0$. Nonlinear systems can normally have multiple equilibrium points.

There are several mathematical definitions of the term *stability*. The one based on the Lyapunov theory is introduced here (Slotine and Li, 1991). In addition, various concepts of stability need to be defined in order to accurately characterise the complex and rich stability behaviour exhibited by nonlinear systems.

- An equilibrium point $\mathbf{x}_e$ is
  - **Stable** if for any $\varepsilon > 0$, $t_0 \geq 0$, there exists $\mathrm{E}(\varepsilon, t_0) > 0$, such that

$$\|\mathbf{x}(t) - \mathbf{x}_e\| < \varepsilon, \quad \forall t \geq t_0 \quad \text{if} \quad \|\mathbf{x}(t_0) - \mathbf{x}_e\| < \mathrm{E}(\varepsilon, t_0) \tag{6.2}$$

  - In other words, the definition means that the state can be kept in a ball of arbitrarily small radius ε by starting the state trajectory in a ball of sufficiently small radius E.
  - **Unstable** if the above condition is not satisfied.

- An equilibrium point $\mathbf{x}_e$ is **asymptotically stable** if it is stable and for any $t_0 \geq 0$, there exists $\mathrm{E}(t_0) > 0$, such that

$$\lim_{t \to \infty} \|\mathbf{x}(t) - \mathbf{x}_e\| = 0 \quad \text{if} \quad \|\mathbf{x}(t_0) - \mathbf{x}_e\| < \mathrm{E}(t_0) \tag{6.3}$$

- An equilibrium point $\mathbf{x}_e$ is **globally asymptotically stable** if it is stable and for any $\mathbf{x}(t_0) \in \Re^n$

$$\lim_{t \to \infty} \|\mathbf{x}(t) - \mathbf{x}_e\| = 0 \tag{6.4}$$

That is, asymptotic stability holds for any initial states.

For linear systems, asymptotic stability and global asymptotic stability are equivalent, therefore the distinction between local and global stability is not necessary. The definition of stability for nonlinear systems is however not in a general sense and can only be applied to individual equilibrium points.

Linear system analysis with regard to stability can be performed using different techniques such as frequency response and root locus diagrams. For example the

stability of the 2DOF linear bicycle model can be determined by examining the location of the system eigenvalues in the complex plane. However, these approaches are not directly applicable to a nonlinear system. In addition, since analytical solutions of nonlinear differential equations usually cannot be obtained, there is an important need for simulation or a graphical tool to allow nonlinear behaviour of the system to be displayed. This need can be met by phase plane analysis, which can also be used for control analysis and design (Slotine and Li, 1991).

6.2.2 Phase-plane method

The phase-plane method is a graphical method for finding the transient response of second-order systems to initial conditions or simple constant inputs and particularly powerful for the stability analysis. A major class of second-order systems can be described in state space form as follows:

$$\begin{aligned} \dot{x}_1 &= x_2 \\ \dot{x}_2 &= -f(x_1, x_2) \end{aligned} \tag{6.5}$$

where $x_1 = x$ and $x_2 = \dot{x}$ are the states of the system, and f is a nonlinear function of the states. Traditionally, the phase-plane method is developed for the dynamics of (6.5). Stability analysis and control design can then be carried out based on the phase portrait of the system of interest. The detailed description of the phase-plane method can be referred to Appendix G.

6.2.3 Analysis of vehicle stability in the phase plane

Due to the nature of nonlinearity and second-order property of the dominant lateral vehicle dynamics, analysis of vehicle stability can be performed using the phase-plane method. The approach of plotting one vehicle state as a function of another state has been used by a number of researchers to analyse the lateral vehicle dynamics (Ono *et al.*, 1996 and 1998; Mammar and Koenig, 2002, etc.). In these studies yaw rate and sideslip angle of the vehicle have been chosen as the two states of interest. Even though the choice of states in these cases does not strictly comply with the definition of the phase plane in Eq. (6.5), the basic vehicle handling behaviour from linear region to the handling limit can still be examined through this approach.

As analysed in Chapter 4, vehicle stability is naturally related to the sideslip motion of the vehicle. The states for examining vehicle stability in the phase plane are therefore chosen as:

$$\begin{aligned} x_1 &= \beta \\ x_2 &= \dot{\beta} \end{aligned} \tag{6.6}$$

where β and $\dot{\beta}$ are the vehicle sideslip angle and its angular velocity, respectively.

In order to facilitate the analysis of vehicle stability in the β-$\dot{\beta}$ plane, the 2NVM introduced in Chapter 4 is utilised. The vehicle is assumed to be travelling at a constant speed of $V_x = 100\text{km/h}$ on a nominal road surface ($\mu = 1.0$). Vehicle state trajectories corresponding to various initial conditions of β and $\dot{\beta}$ with zero steer inputs are plotted in the β-$\dot{\beta}$ plane as shown in Figure 6.1. The plot is constructed by setting the initial conditions of the states of yaw rate and lateral velocity and then plotting the trajectories of the calculated states of sideslip angle and its angular velocity. Stable trajectories are plotted in solid lines and unstable ones are in dashed lines.

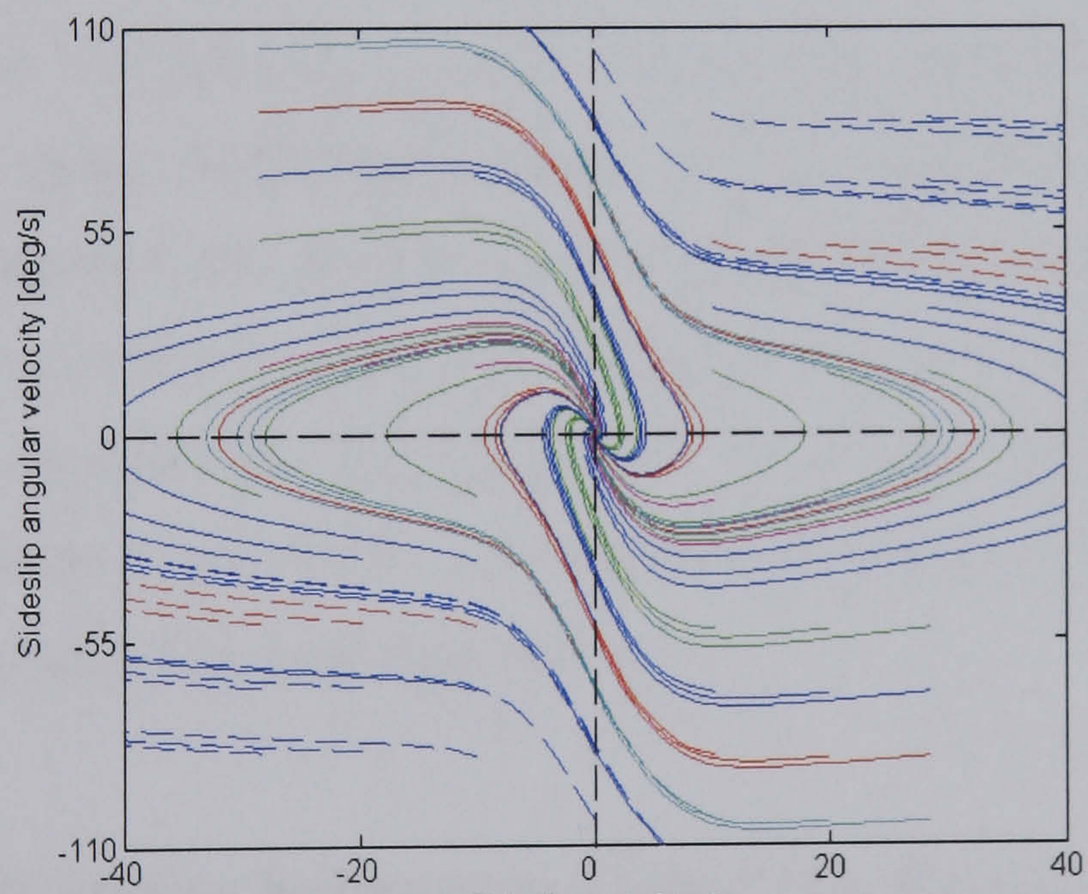

Figure 6.1 Phase portrait of the 2NVM at 100km/h and zero steer input on a nominal road surface

As can be seen from Figure 6.1, for the examined range of initial conditions, there is only one singular point which is the origin for zero steer input and represents straight ahead driving. When the initial conditions of sideslip angle and its angular velocity lie

close to the equilibrium point, the states converge to the origin as time goes to infinity. In addition, for relatively large initial values of sideslip angle and its angular velocity, if they are opposite in sign, the states will also converge to the unique singular point, as those in the second or the fourth quadrant of the phase plane. In other words, from the safety point of view, large sideslip angle is undesirable while it is still stable if the corresponding sideslip angular velocity has opposite sign to the sideslip angle as such velocity will reduce the sideslip angle automatically. However, it is not the case when the initial conditions of these two states lie in the first or third quadrant, i.e. when the sideslip angle and its angular velocity have the same sign. In these two quadrants, even for small sideslip angles, if the sideslip angular velocity is large, the states will not converge to the singular point. The conclusion can therefore be reached that the equilibrium point examined here is asymptotically stable while not globally asymptotically stable.

In order to trace the course or stabilise the vehicle, the driver applies steer inputs to the vehicle during actual manoeuvres. System stability therefore needs to be examined anew under such conditions. Figure 6.2 shows the phase portrait of the 2NVM with a constant steer angle of 5.5° applied for various initial conditions of β and $\dot{\beta}$. One can see from Figure 6.2 that some amount of fixed steer input leads to the shift of the stable equilibrium point and the stable limits in the steered direction (left-half plane) are narrowed compared to the straight ahead driving case in Figure 6.1. That is, some trajectories which converge to the origin for zero steer input become unstable when a certain amount of constant steer input is applied. In addition, system behaviour is seen to be much less-damped around the new equilibrium point, which can be seen from the convergence speed of the state trajectories.

6.3 Dynamic Stability Subsystem Controller Design

The preceding section has shown that the phase-plane method is quite effective in the analysis of vehicle stability with respect to the sideslip motion. Applications of this method in the design of vehicle dynamic stability control systems have been found in (Inagaki *et al.*, 1994; Smakman, 2000; Selby *et al.*, 2001, etc.). In this section the same approach will be employed to design the dynamic stability subsystem controller.

6.3.1 Definition of reference stable region in the phase plane

Similar to the design of active steering subsystem controllers, a reference signal needs to be defined for dynamic stability subsystem controller design. Since vehicle stability is directly related to the sideslip motion of the vehicle, this motion will be chosen as the reference signal for the dynamic stability subsystem controller. In order to maintain vehicle stability, the sideslip motion of the vehicle must be bounded. Thus the task of the stability controller is to bound the reference signal within a region in which the vehicle remains stable. A reference stable region therefore needs to be chosen for the purpose of controller design. Such a reference region will be defined in the β - $\dot{\beta}$ plane.

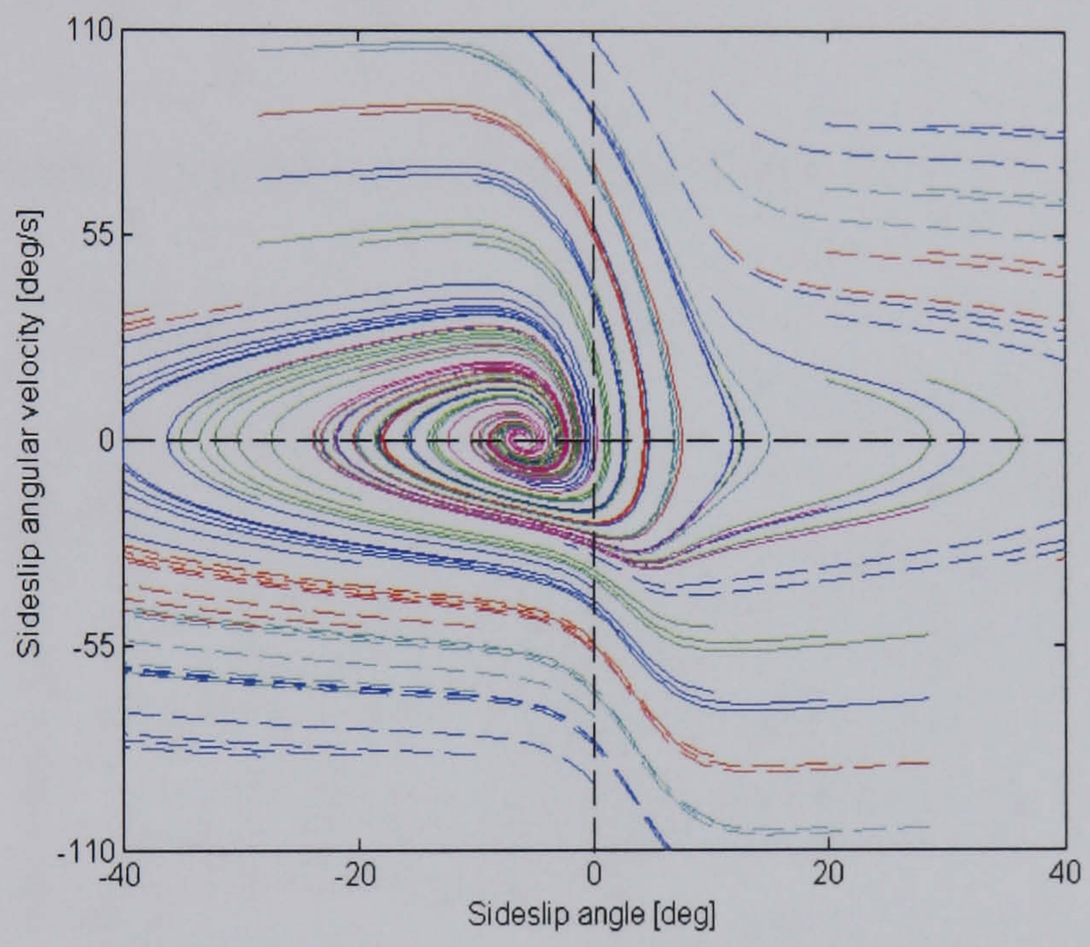

Figure 6.2 Phase portrait of the 2NVM at 100km/h and constant steer angle of 5.5° on a nominal road surface

The choice of the reference region can be based on the resulting phase-plane analysis for zero steer input, as shown in Figure 6.3(a). However, such a region is no longer valid when the driver applies steering action to the vehicle. In addition, the reference region defined in this way allows very high values of sideslip angles, which may make the driver feel unpleasant. Therefore, in order to compensate for the driver steer input and simplify control design, an approximated reference stable region based on Figure 6.3(a) is defined, as shown in Figure 6.3(b). The slope of the reference region boundaries is chosen to be the slope of the phase plane trajectories. By aligning the boundaries in this way, a harmonious control action will be achieved and perceived harshness by the vehicle occupants will be eliminated as the phase plane trajectories

will enter the unstable region at a very blunt angle when instability occurs (Smakman, 2000).

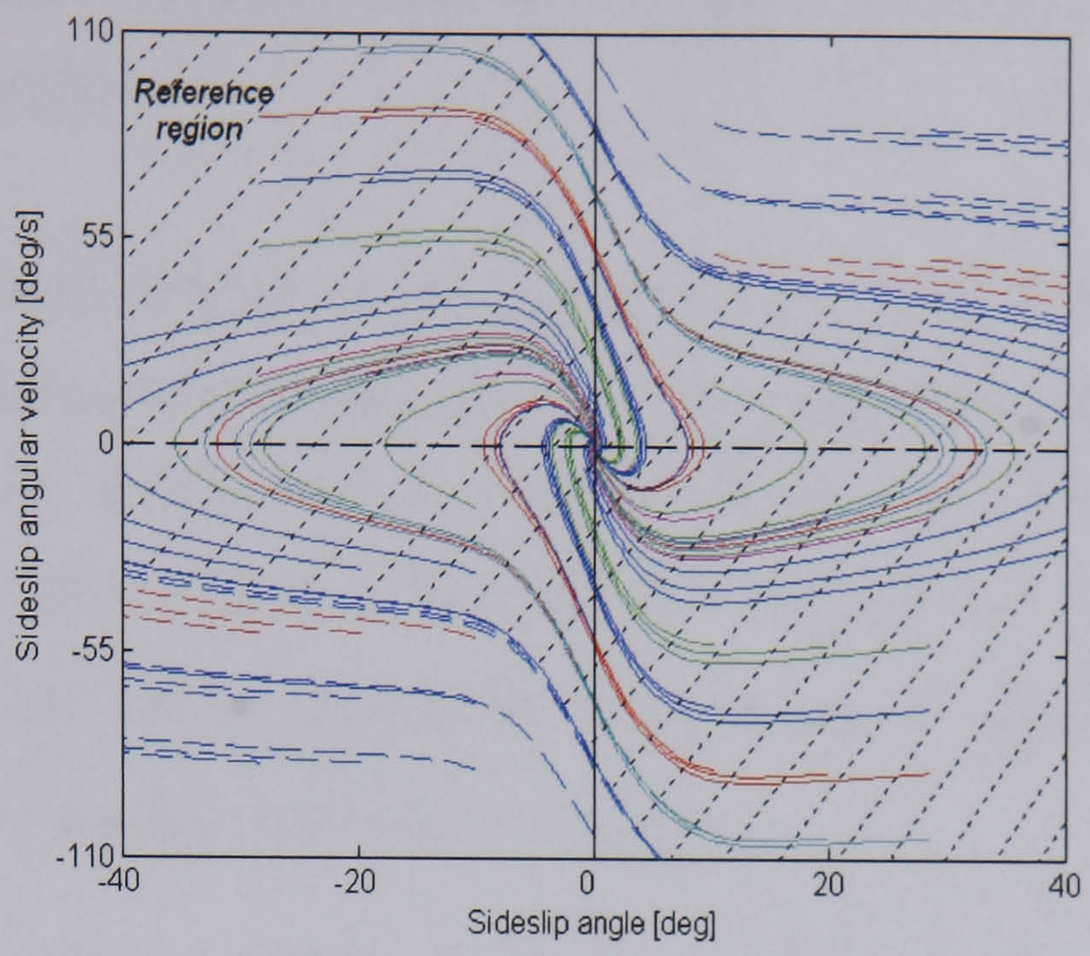

(a) Reference region based on phase-plane analysis with zero steer input

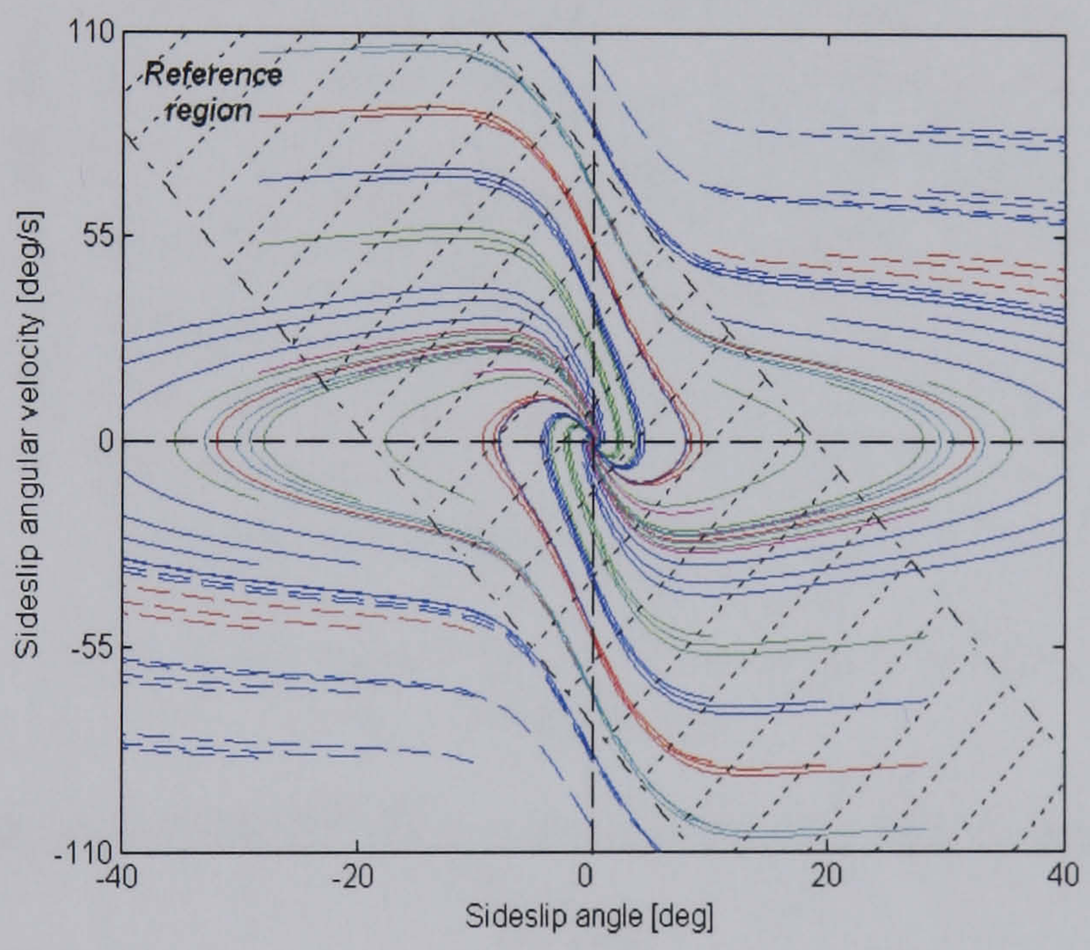

(b) Simplified reference region based on (a)

Figure 6.3 Definitions of different reference regions in the phase plane for the stability controller

With the location of the reference region boundaries on the sideslip motion of the vehicle one can specify how conservative the stability controller is tuned and how much control action is applied. A narrow region implies early and high control action, and more stable vehicle behaviour. A wide region means late and low control action, and less stable vehicle behaviour. When the vehicle states lie inside the reference region, the vehicle is considered to be stable and no control action is required. When

the vehicle states go outside the reference region, a corrective yaw moment will be generated to pull the vehicle back into the stable region. The sign of the corrective yaw moment depends on the location of the vehicle states relative to the reference region in the phase plane.

One of the significant benefits of this approach is that the reference region defined above is largely independent of conditions of the road surface friction and hence the accurate estimation of the road surface coefficient of friction is not required (Shibahata, 1993; Selby, 2003). This effect can be verified by examining the phase portrait of the 2NVM for the same initial conditions of β and $\dot{\beta}$ at zero steer input on a low-μ $(=0.4)$ surface, as shown in Figure 6.4.

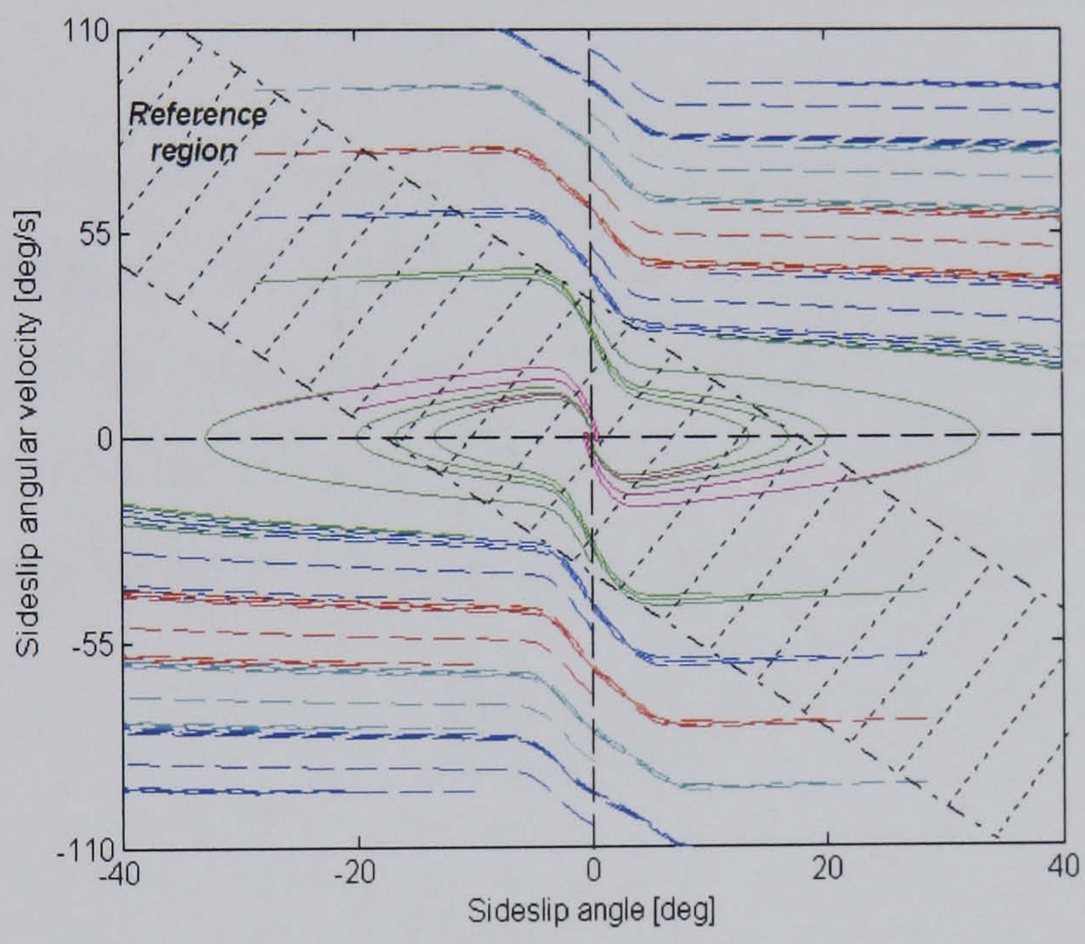

Figure 6.4 Phase portrait of the 2NVM at 100km/h and zero steer input on a low-μ $(=0.4)$ surface

In comparison to Figure 6.3(b), one can see from Figure 6.4 that the achievable sideslip angular velocity on the low-μ surface for the same initial conditions of sideslip angle and its angular velocity become lower. The reference region remains largely unchanged in the direction of sideslip angle, despite the substantial change in the sideslip angular velocity direction. Therefore only one set of reference region boundaries are required for the purpose of controller design, irrespective of friction conditions of the road surface.

6.3.2 Design of dynamic stability subsystem controller

The stand-alone stability controller aims to ensure vehicle stability during critical driving situations by bounding the sideslip states of the vehicle to be within the reference region defined above. The reference region illustrated in Figure 6.3(b) can be described by the following inequality:

$$\left|\dot{\beta} + k_{\beta\dot{\beta}}\beta\right| < b \tag{6.7}$$

where $k_{\beta\dot{\beta}}$ is the slope of the reference region boundaries and $b/k_{\beta\dot{\beta}}$ is the half width of the region. The parameter values which produce the chosen reference region in Figure 6.3(b) are measured as:

$$k_{\beta\dot{\beta}} = 4, \quad b = 72 \tag{6.8}$$

The above reference region is defined based on the phase-plane analysis for zero steer input in the preceding section. However, such a predefined region is no longer valid when the driver applies steer inputs to the vehicle. Therefore, in order to assure vehicle stability in the presence of driver steer inputs, the stability boundaries for controller design are chosen to be more conservative as follows:

$$\left|\dot{\beta} + k_{\beta\dot{\beta}}\beta\right| < b' \tag{6.9}$$

where

$$b' = 24$$

The new reference region of Eq. (6.9) indeed has the same slope as the one of Eq. (6.7) and only the width of the region becomes narrow. In practice, the choice of parameters in Eq. (6.9) means that for steady-state conditions ($\dot{\beta} = 0$) the stability controller does not apply control actions for $|\beta| < 6^\circ$. When the vehicle states move beyond the control boundaries and enter the unstable regions, a corrective yaw moment will be demanded by the stability controller. Herein the perpendicular distance from the vehicle state trajectories to the control boundaries is defined as the stability error and determines the control effort through a simple PD control law (Smakman, 2000), i.e.

$$M_{zc} = K_{p\_DSC} e_{\beta\dot{\beta}} + K_{d\_DSC} \frac{d}{dt} e_{\beta\dot{\beta}} \tag{6.10}$$

where M_{zc} and $e_{\beta\dot{\beta}}$ are the corrective yaw moment command and the stability error; K_{p_DSC} and K_{d_DSC} are controller gains to be tuned, respectively. The definitions of the reference region for stability controller design and the stability error are illustrated in Figure 6.5. The controller tuning was done empirically with the following result:

$$K_{p\_DSC} = 700, \quad K_{d\_DSC} = 100 \tag{6.11}$$

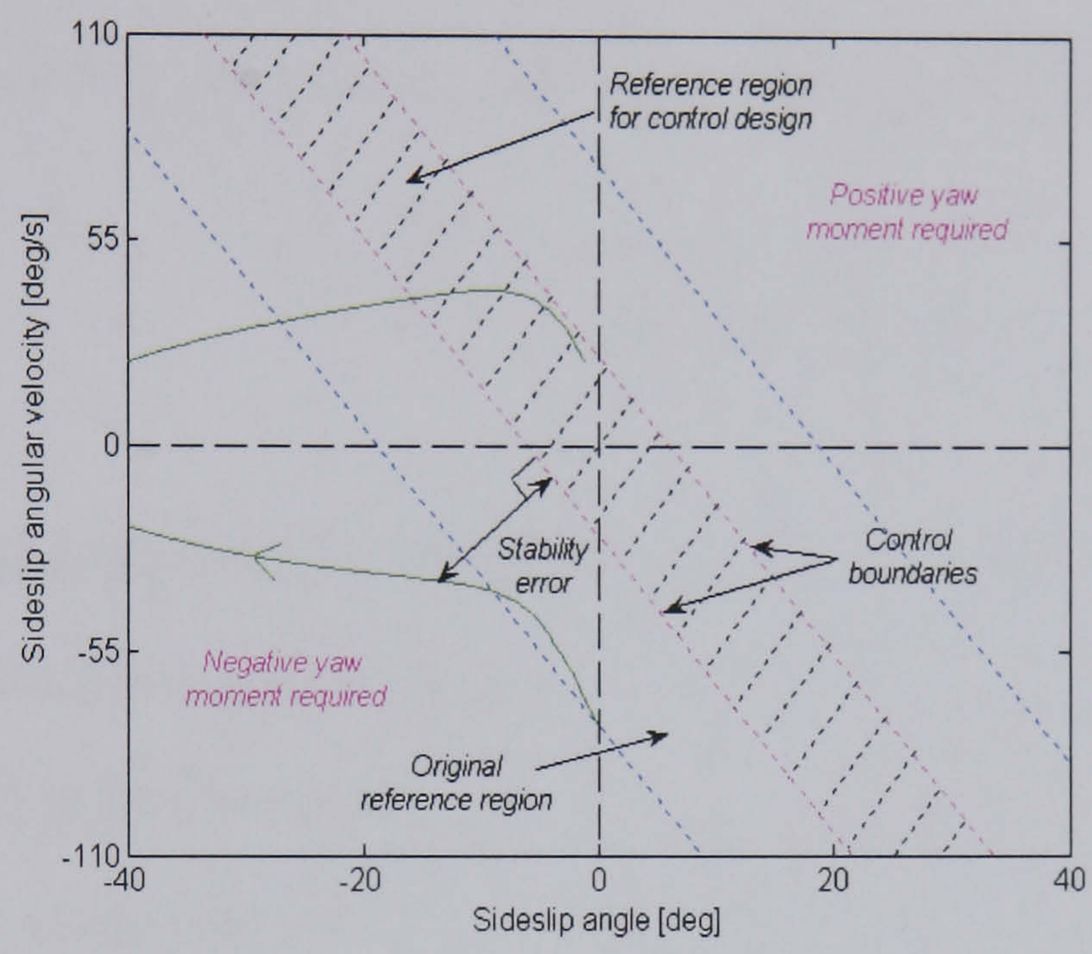

Figure 6.5 Definitions of the reference region and stability error in the phase plane for stability controller design with the required control action

6.4 Description of Dynamic Stability Subsystems

The dynamic stability subsystem controller designed in the preceding section will demand a corrective yaw moment when the vehicle states are located outside the predefined reference region. The required corrective yaw moment can be generated by either distributing driving torque between wheels/axles or selectively braking individual wheels. This section will investigate both actuation concepts and show the relative merits.

6.4.1 Driveline based dynamic stability subsystem

As discussed in Chapter 2, in order to maintain vehicle stability during critical driving situations, the required corrective yaw moment can be generated through actively

controlling either front/rear or left/right torque distribution, i.e. through variable torque distribution (VTD) control. Due to the different mechanisms of yaw moment generation, the effects of left/right and front/rear torque distribution control on vehicle handling behaviour need to be compared. Here the manoeuvre of acceleration during a right hand turn at a fixed steer angle of 5.5° and the NLVM are employed for this purpose. The initial forward speed of the vehicle is chosen to be 40km/h and the constant longitudinal acceleration is set to be 0.2g. The vehicle is assumed to be equipped with a front, a rear and a centre differential, respectively. The torque distribution ratios k_f, k_c and k_r for the front, centre and rear differentials can vary continuously from 0 to 1 (Motoyama, 1993). These ratios are defined as follows:

$$k_f = \frac{T_{fl}}{T_f},\ k_c = \frac{T_f}{T_e},\ k_r = \frac{T_{rl}}{T_r} \tag{6.12}$$

where

T_{fl} : torque applied at the front left wheel

T_{rl} : torque applied at the rear left wheel

T_f : torque applied at the front axle

T_r : torque applied at the rear axle

T_e : input torque from the engine

In order to examine the effect of left/right torque distribution control, the front/rear torque distribution ratio k_c is kept constant at 0.5 by a normal centre differential. The simulation results for left/right torque distribution control are shown in Figure 6.6. As can be seen from Figure 6.6, a relatively large corrective yaw moment can be directly generated by splitting torque between the left and right wheels of the same axle. Two extreme cases can be observed in Figure 6.6: inner wheel drive (IWD) and outer wheel drive (OWD). The former can produce a large contra-cornering yaw moment to push the vehicle away from the corner and the latter can generate a large pro-cornering yaw moment to force the vehicle towards the corner and finally make the vehicle spin. In addition, left/right torque distribution control is seen to be effective over a wide range of lateral acceleration (resulting from changes in the vehicle forward speed and the radius of turn).

In the case of front/rear torque distribution control, the left/right torque distribution on the same axle is maintained at a 50:50 ratio by a normal differential. Figure 6.7 shows the vehicle trajectories under various front/rear torque distribution conditions. In comparison to left/right torque distribution control, actively controlling torque distribution between front and rear axles is seen to have less effect on the vehicle handling behaviour and only understeer characteristic is presented. With the increase in forward speed, the RWD vehicle finally spins due to the insufficiency in lateral tyre forces of the rear axle when the handling limit is reached.

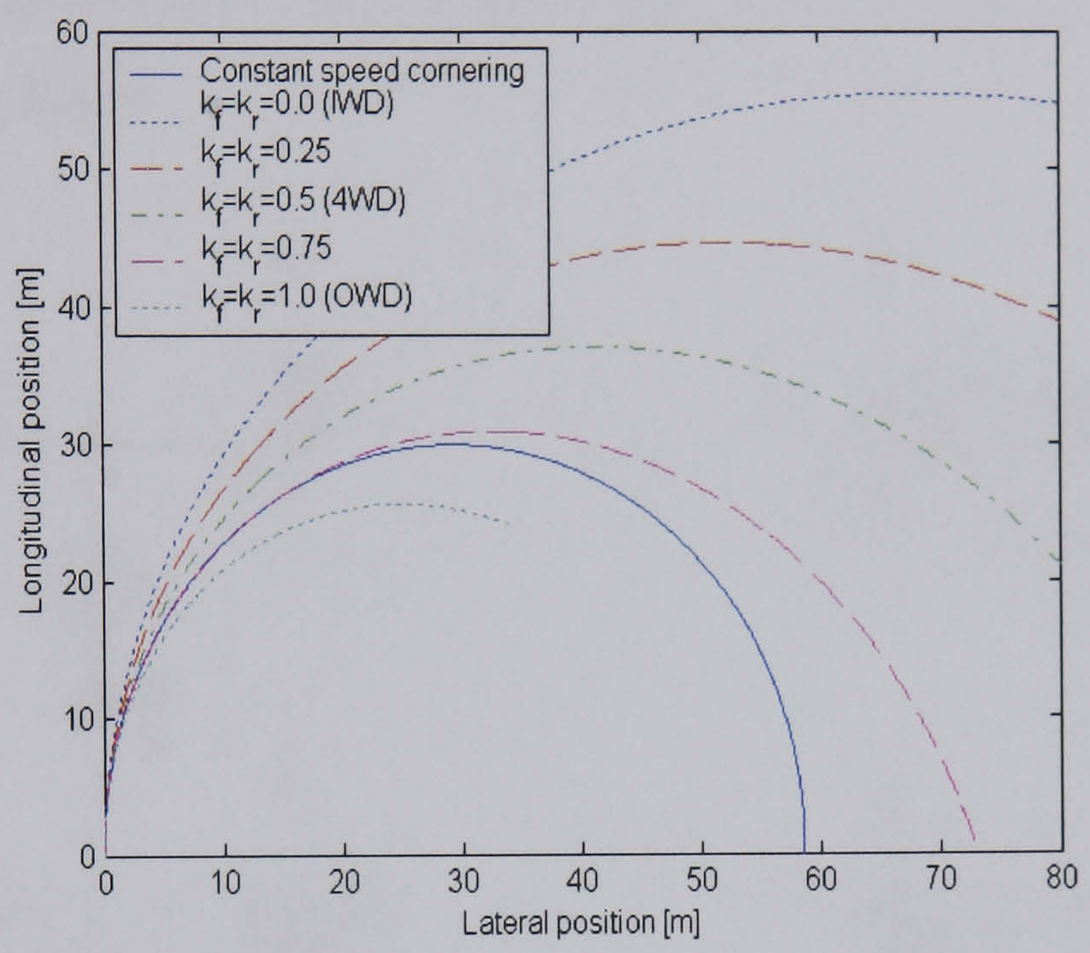

Figure 6.6 Vehicle trajectories under various left/right torque distribution conditions with $k_c = 0.5$

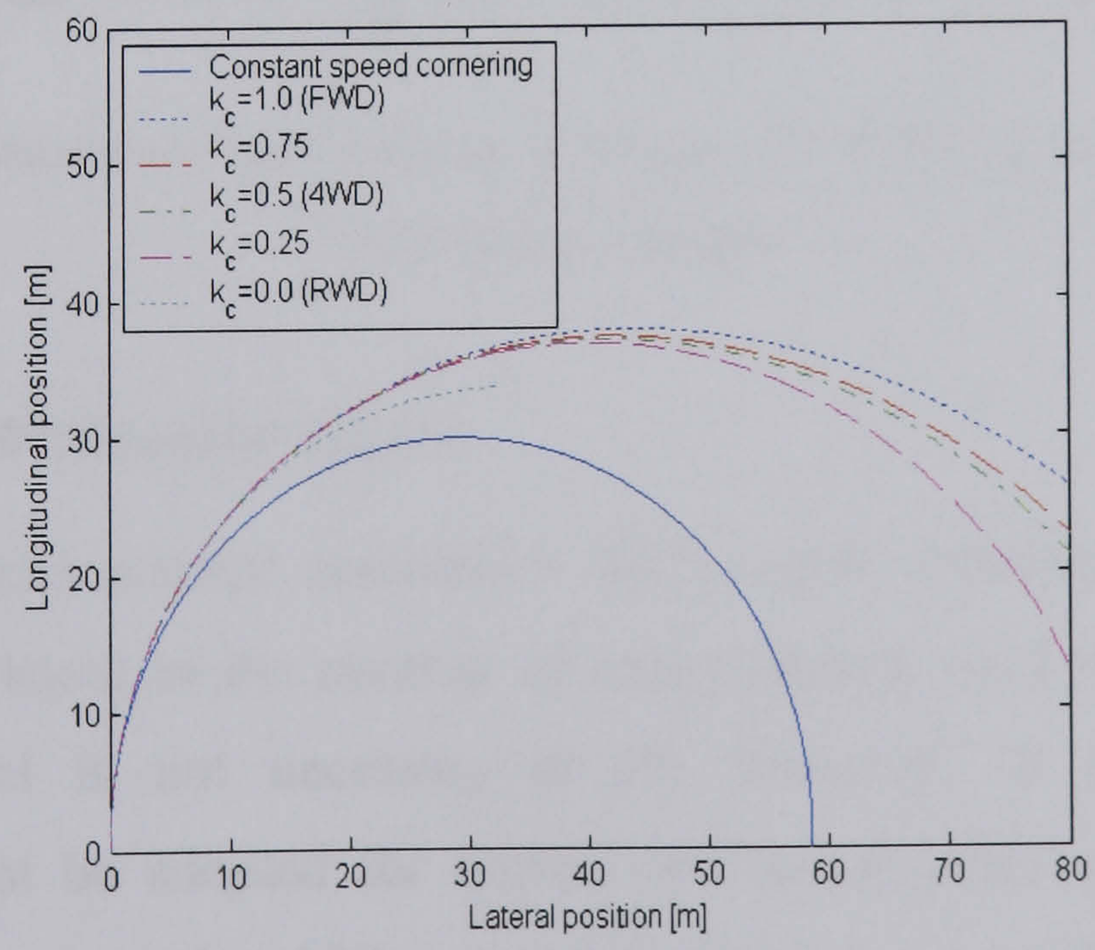

Figure 6.7 Vehicle trajectories under various front/rear torque distribution conditions with $k_f = k_r = 0.5$

For front/rear torque distribution control, the corrective yaw moment is generated indirectly by utilizing the tyre force interaction property, i.e. the lateral tyre force is reduced when the corresponding longitudinal tyre force is increased. The difference in the mechanism of yaw moment generation between left/right torque distribution control and front/rear torque distribution control is illustrated in Figure 6.8 where the vehicle is assumed to be making a right hand turn. One may therefore conclude that the effect of left/right torque distribution control on vehicle handling characteristics is much greater than that of its front/rear counterpart. As a result, only active control of left/right torque distribution for maintaining vehicle stability will be further investigated in this thesis.

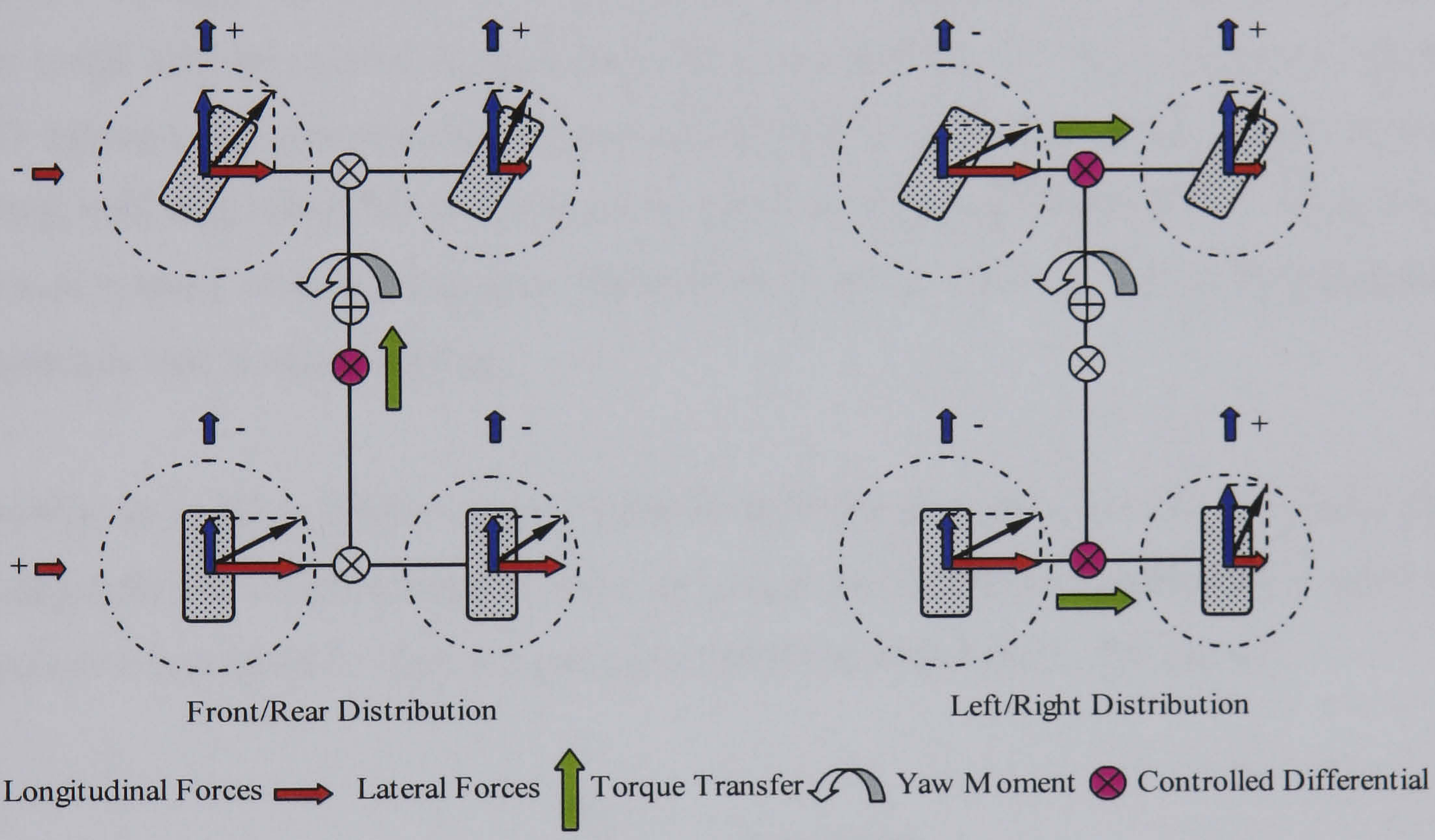

Figure 6.8 Mechanisms of yaw moment generation for front/rear and left/right torque distribution controls

Torque Transfer Differential Model

For the conventional internal combustion (IC) engine vehicles, if the number of driving wheels is equal to the number of independently controlled engines, torque distribution control is not necessary at all. However, to date, this technical arrangement cannot be adopted for normal production vehicles due to high cost. Therefore only the conventional IC engine vehicles with one engine, one transmission system, axles and differential units will be considered in this thesis. In addition, whilst particular attention is devoted to FWD vehicles here and consequently torque transfer

will only take place on the driving axle, i.e. the front axle, the main conclusions of this study can easily be extended to vehicles with other driveline layouts.

For the conventional IC engine vehicles, in order to apply the desired amount of torque at the driving wheels of the same axle, torque biasing devices need to be used. The most common torque biasing device is a non-conventional or controlled differential. There are many examples of controlled differential systems and the vast majority employ a limited slip differential (LSD) in which a friction clutch is employed to provide a connection between the left and right driveshafts (Huchtkoetter and Klein, 1996; Okcuoglu, 1995). LSD systems were originally developed to improve traction performance of the vehicle. More recently it was recognised that they could also be utilised to positively influence the lateral vehicle dynamics. Such LSD systems are characterised by the fact that they can only transfer torque to the slower spinning wheel when the friction clutch is engaged. These systems therefore have no control over the direction of torque transfer and are only able to modulate the magnitude that is being applied.

Thereby, in order to control torque transfer between the left and right wheels of the driving axle without restriction in the direction, a special torque transfer differential of Figure 6.9 developed by Sawase and Sano (1999) is employed in this thesis.

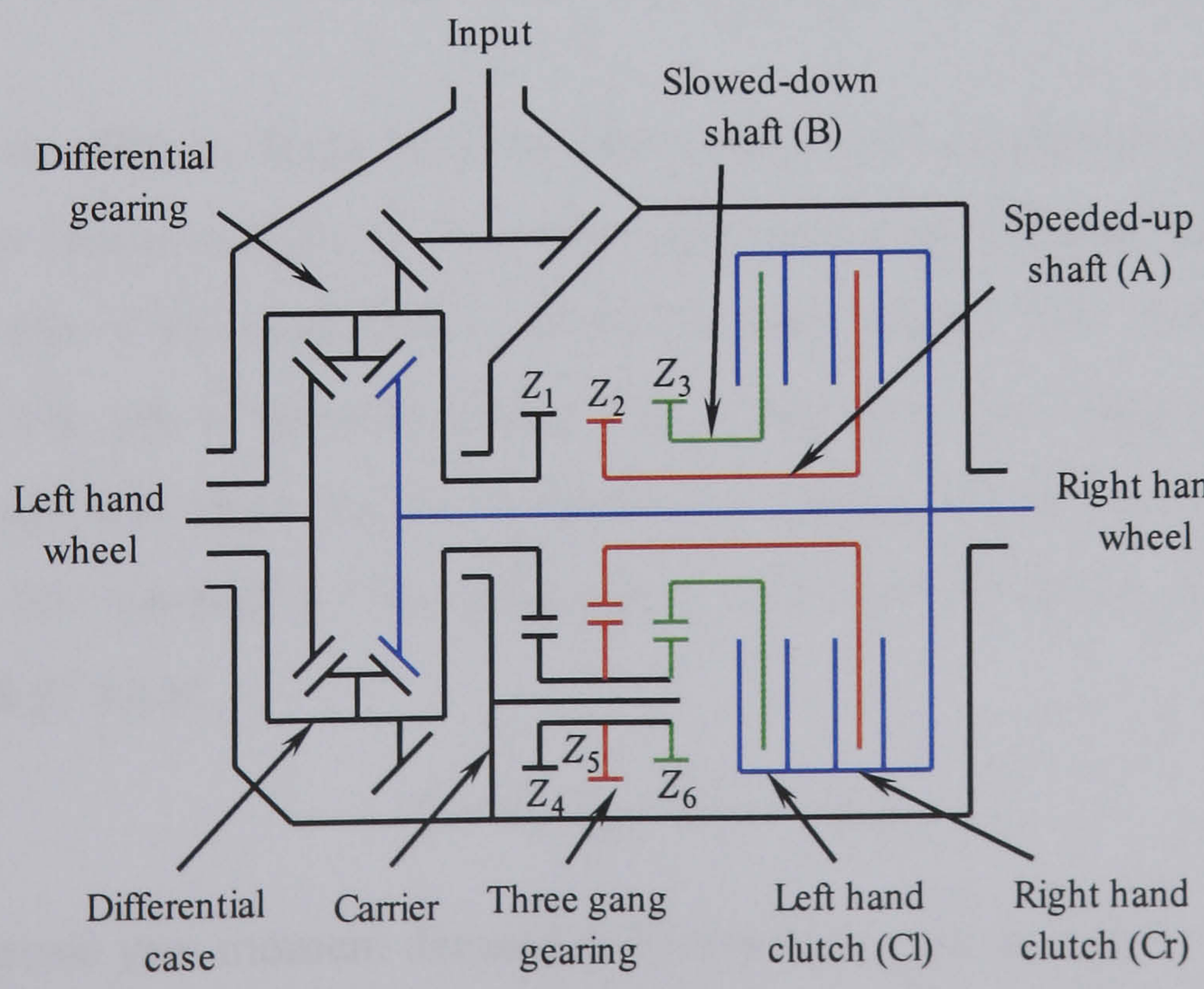

Figure 6.9 Schematics of the torque transfer differential from (Sawase and Sano, 1999)

However, like the LSD, this torque transfer differential still relies on a sufficient speed difference between two clutch plates in order to produce the desired amount of torque transfer. The additional gearing system between the differential case and the clutch plates is designed to guarantee such a speed difference. The gear ratios used in (Sawase and Sano, 1999) ensures that there will be sufficient clutch slip to maintain authority over the direction of torque transfer while the left/right wheel speed difference is less than 25%. The detailed description of this differential can be found in Appendix H.

The relationship between the input torque T_{in}, transferred torques T_{cr}, T_{cl} and wheel torques T_r, T_l during clutch engagement can be expressed as:

$$T_l = \frac{T_{in}}{2} - \frac{Z_1 Z_5}{2 Z_2 Z_4} T_{cr} + \frac{Z_1 Z_6}{2 Z_3 Z_4} T_{cl} \tag{6.13}$$

$$T_r = \frac{T_{in}}{2} + \left(1 - \frac{Z_1 Z_5}{2 Z_2 Z_4}\right) T_{cr} - \left(1 - \frac{Z_1 Z_6}{2 Z_3 Z_4}\right) T_{cl} \tag{6.14}$$

where the numbers of gear teeth are set to be $Z_1 = Z_2 = Z_3 = 42$, $Z_4 = 32$, $Z_5 = 36$ and $Z_6 = 28$ (Sawase and Sano, 1999). Therefore, the lateral torque difference can be controlled regardless of the input torque from the engine. Herein, the differential described above is further assumed to be relatively ideal so that after being transferred, torque applied at two wheels of the same axle may be opposite in sign.

In addition, in order to formulate the final integrated control system, the required corrective yaw moment of Eq. (6.10) rather than the torque difference between the left and right wheels of the same axle is defined as the output of the stability controller. Therefore, in the case of driveline based DSC subsystem, the corrective yaw moment command needs to be converted into the torque difference between the two sides of the vehicle. For simplicity, the quasi-static rotational dynamics of the wheel is employed and given as:

$$T_i = R_w F_{xwi}, \quad (i = 1,\ldots,4) \tag{6.15}$$

and the corrective yaw moment demanded by the stability controller can be expressed as:

$$M_{zc} = \frac{t}{2}\Delta F_x \tag{6.16}$$

where ΔF_x is the longitudinal force difference between the left and right driving wheels of the same axle. Thus the corresponding torque difference takes the form:

$$\Delta T = T_l - T_r = \frac{2M_{zc}R_w}{t} \tag{6.17}$$

For FWD vehicles, $t = t_f$ in above equations.

Upon receiving a torque transfer demand from the stability controller, the appropriate clutch will be engaged to allow the differential to transfer the desired level of torque. The selection of clutches to be engaged can be achieved through a set of simple logic rules according to the sign of the required torque transfer, e.g. if (negative) torque transfer to the right-hand wheel is required, then the right-hand clutch in Figure 6.9 should be engaged. The block diagram of the driveline based DSC subsystem is shown in Figure 6.10.

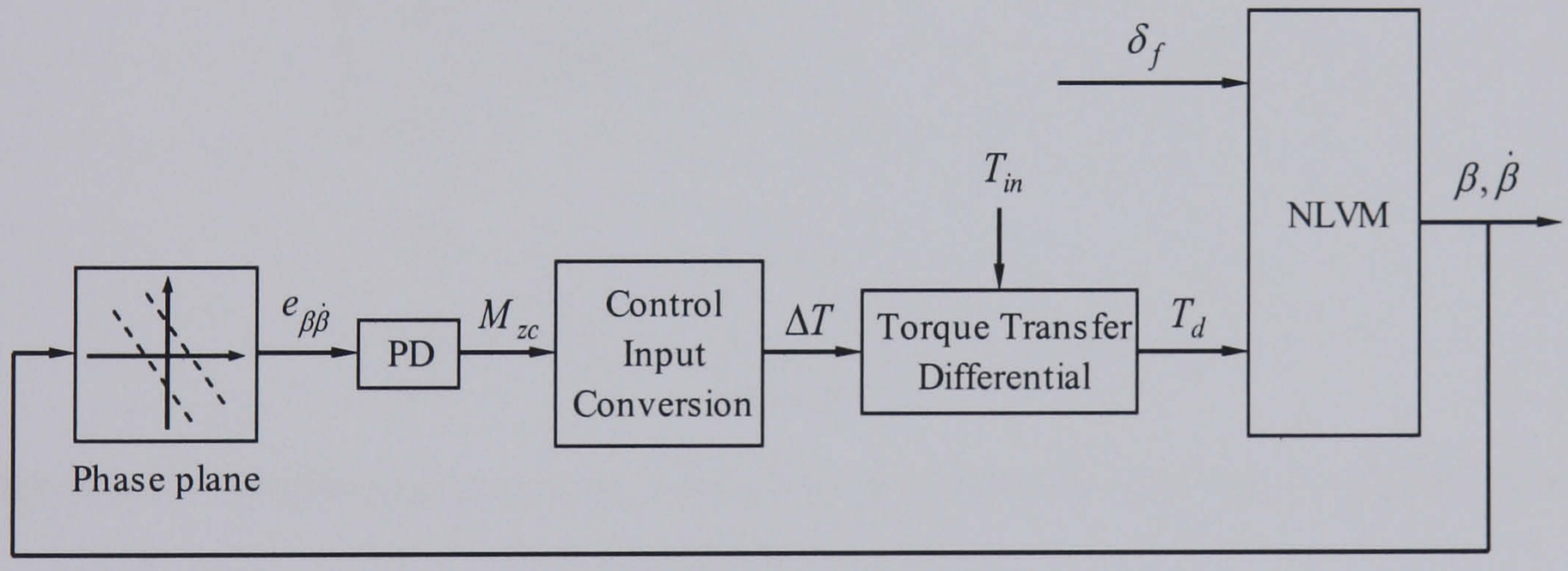

Figure 6.10 Block diagram of the driveline based DSC subsystem

6.4.2 Brake based dynamic stability subsystem

It is well-known that the brake based DSC system is quite powerful in maintaining vehicle stability at the handling limit and is commercially available. However its inherent drawback, the strong influence on the longitudinal vehicle dynamics may limit its utilisation to only highly extreme driving situations. In order to show the relative merits, a brake based DSC subsystem, which employs the same controller as its driveline based counterpart, is introduced in this section. This system selectively

brakes individual wheels to stabilise the vehicle. The selection of individual wheels to be braked is based on the analysis of the yaw moment generation ability of four corners of the vehicle. Similar studies can be found in (Smakman, 2000; Selby, 2003).

Figure 6.11 shows the yaw moment on the vehicle generated by braking individual wheels at the handling limit during a right hand turn. In Figure 6.11, the resulting yaw moment is plotted as a function of the longitudinal slip of the braked wheel and is the sum of two effects: the yaw moment generated directly by the braking force and the yaw moment resulting from the reduction in the corresponding lateral tyre force owing to the increase in the braking force. Depending on the particular wheel these two effects may either add up or act in opposite direction. The difference in absolute magnitude of the yaw moments is due to the dynamic load transfer during cornering.

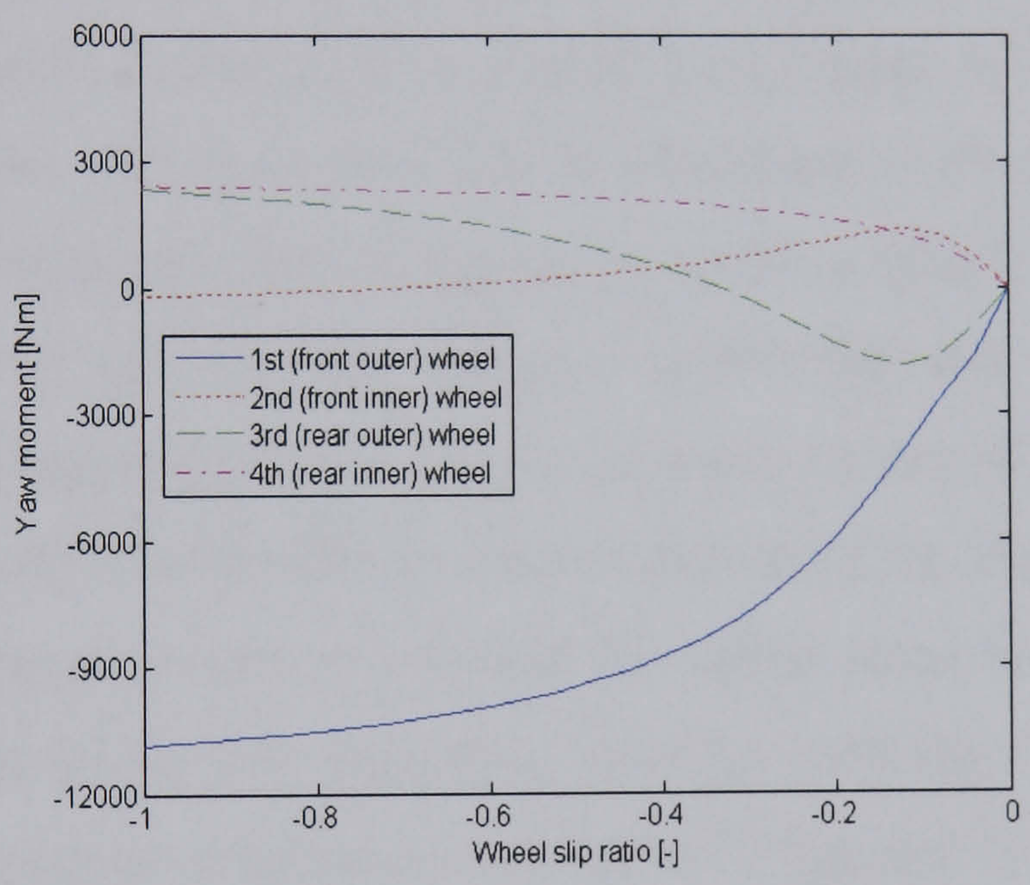

Figure 6.11 Resulting yaw moment through braking individual wheels as a function of the longitudinal slip ratio

The mechanism of yaw moment generation for braking individual wheels is illustrated in Figure 6.12 where the vehicle is negotiating a right hand turn. One can see from Figures 6.11 and 6.12 that the above two effects add up only for the front outer (1^{st}) and rear inner (4^{th}) wheels (monotonous characteristic). Therefore the front outer wheel will be chosen to generate a contra-cornering yaw moment (negative in this case) to correct instability and a pro-cornering yaw moment (positive in this case) will be generated by braking the rear inner wheel to correct limit understeer. The schematics of selectively braking individual wheels is shown in Figure 6.13 for the case of a right hand turn.

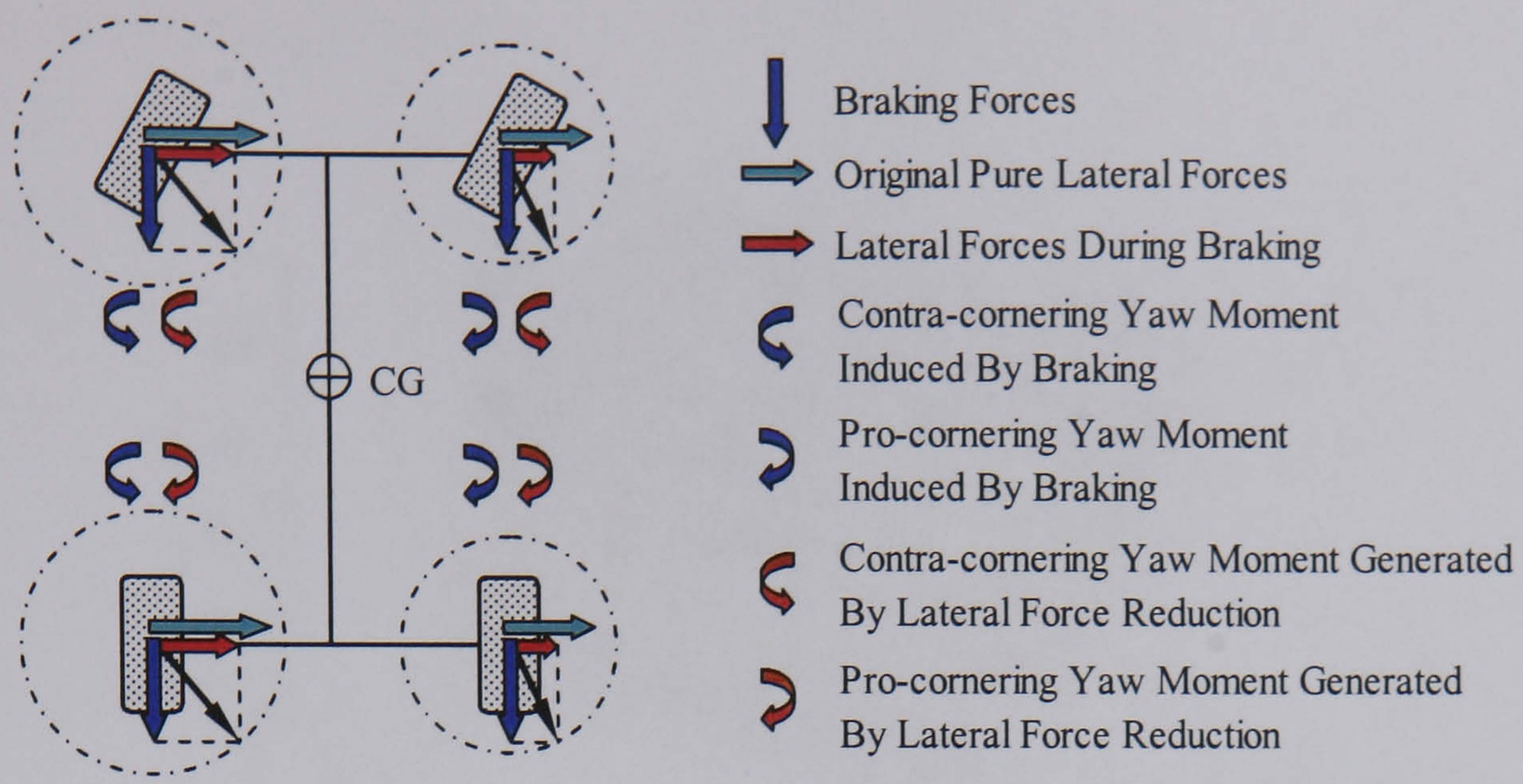

Figure 6.12 Mechanism of yaw moment generation for braking individual wheels

In addition, in this system, the required corrective yaw moment is transformed into the required slip ratio of the corresponding braked wheel through a Brake Intervention Map (Smakman, 2000; Selby, 2003), as shown in Figure 6.14. This map is indeed derived from the yaw moment analysis to be performed in the following section. The wheel slip control task can then be implemented by a simple proportional-type slip controller. The error between the required wheel slip and the actual wheel slip determines the corresponding brake torque that can be actuated by a hydraulic system. The particular wheel to be braked is determined based on the signs of the required corrective yaw moment (contra or pro) and the lateral acceleration (left or right hand turn). Therefore the previously developed stability controller and the slip controller form the cascade control configuration, as shown in Figure 6.15.

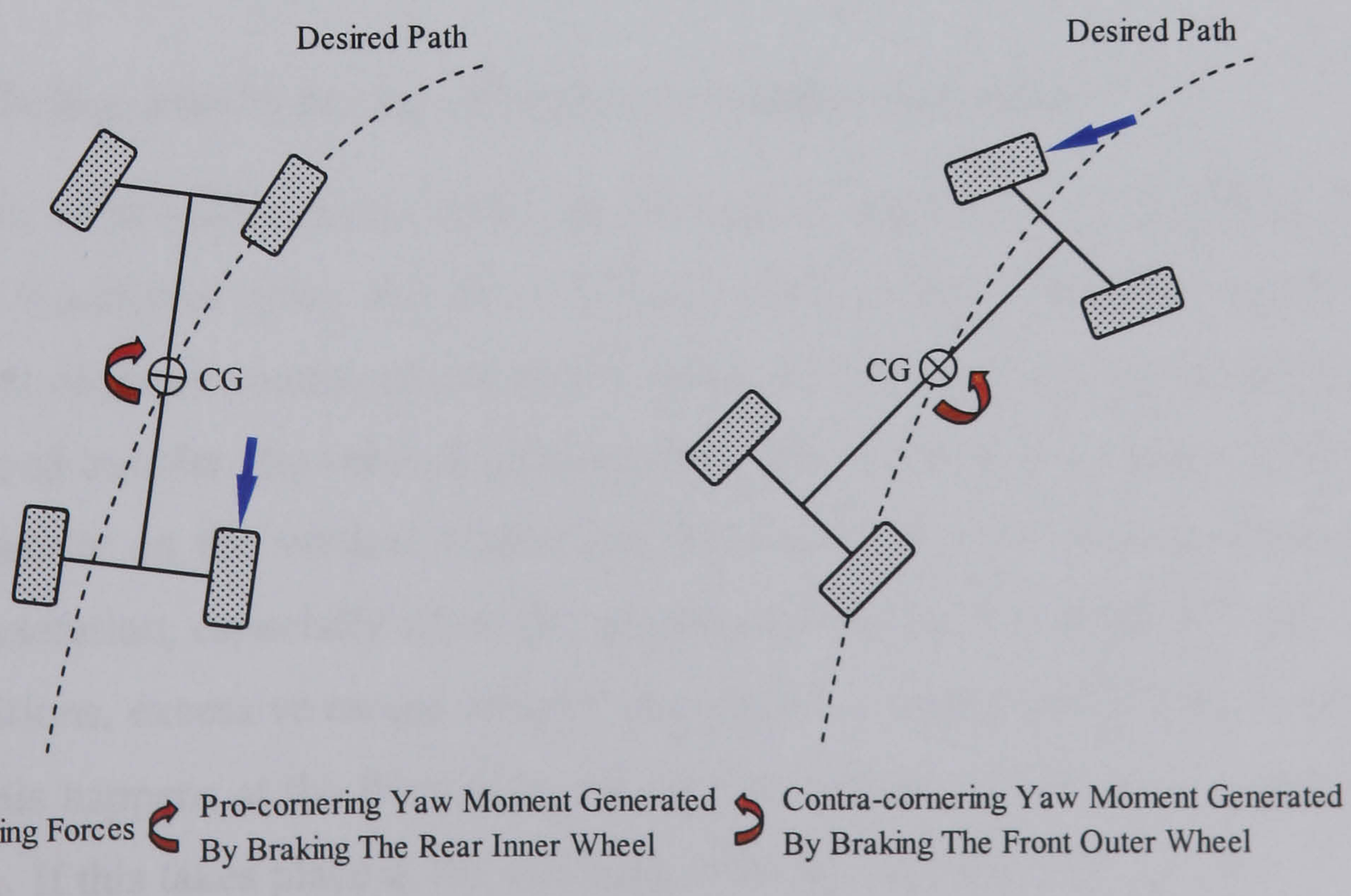

Figure 6.13 Schematics of selectively braking individual wheels in a right hand turn

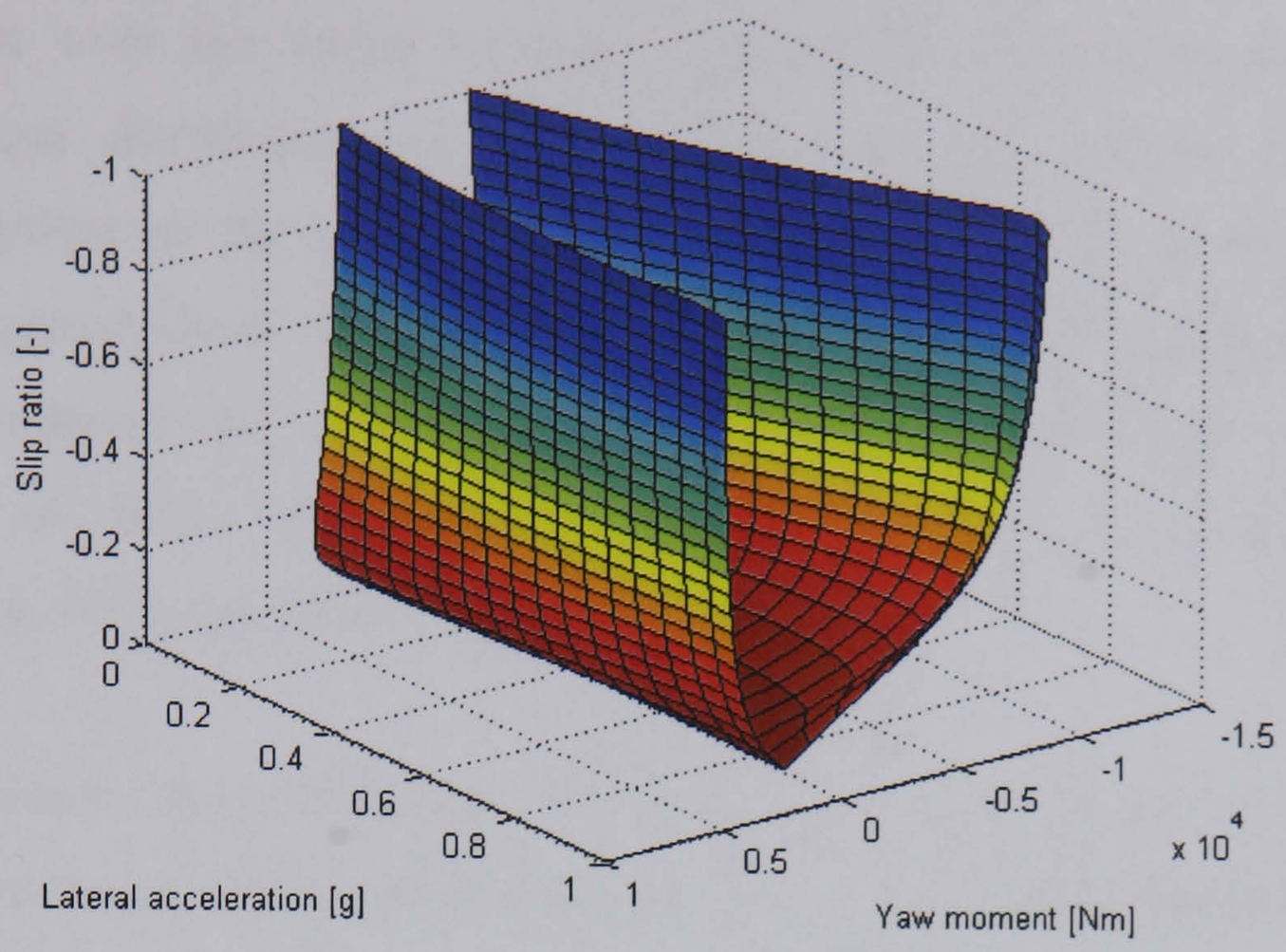

Figure 6.14 Brake intervention map

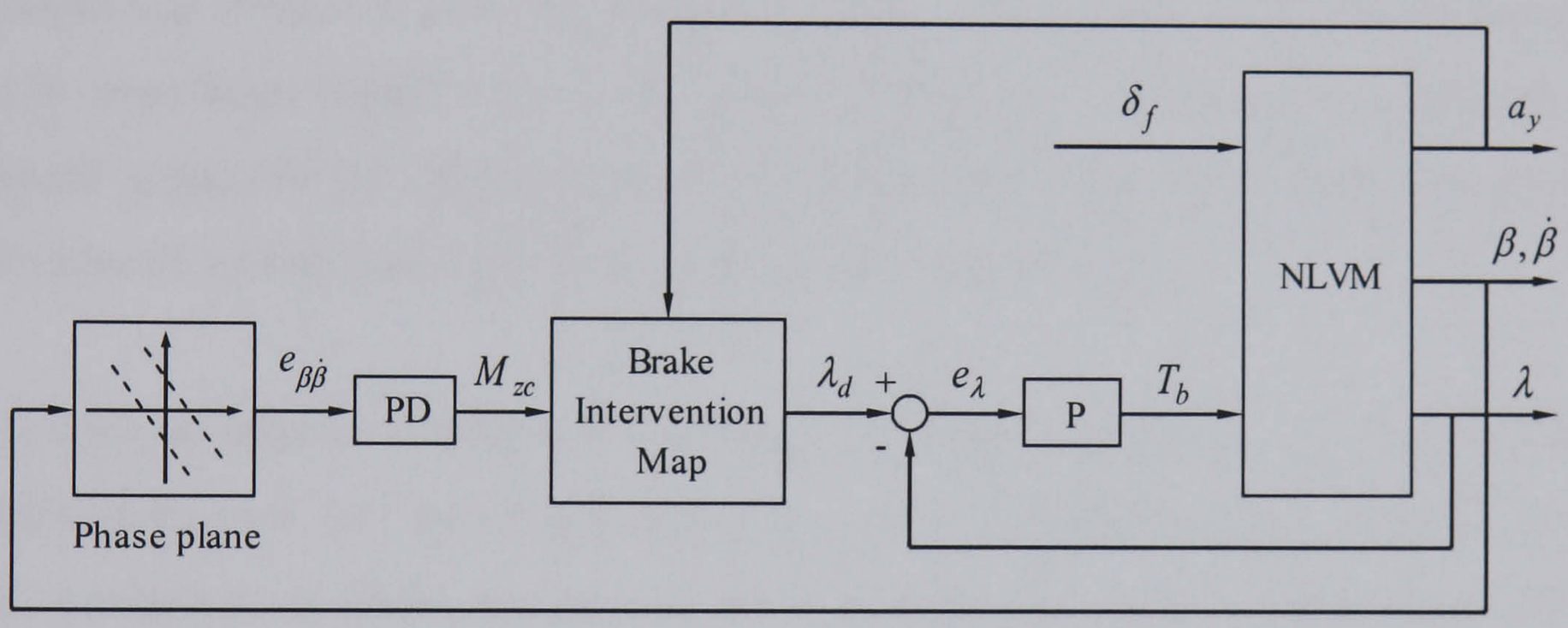

Figure 6.15 Block diagram of the brake based DSC subsystem

6.4.3 Driveline plus brake based dynamic stability subsystem

In the case of driveline based DSC, when vehicle stability is in question, torque should be transferred from the outer driving wheel to the inner driving wheel to generate the required contra-cornering yaw moment. However, during cornering, due to lateral load transfer, the vertical loads on the inner wheels are decreased. The effect of load transfer on the vertical wheel load becomes dominant with the increase in lateral acceleration, especially when the vehicle approaches the handling limit. Under such conditions, excessive torque transfer may make the inner wheel spin on slippery roads. If this happens at the front axle, the driver will lose control of the direction of the vehicle. If this takes place at the rear axle, vehicle instability will worsen.

Therefore, even though the driveline based DSC system can stabilise the vehicle to certain extent over the entire handling regime through actively controlling the left/right torque distribution, its ability to generate the required corrective yaw moment is limited by the inherent load transfer effect. In other words, the driveline based DSC system does have its own functional limitation and cannot completely replace the conventional brake based DSC system. It can however be used to complement its brake based counterpart and reduce the influence of brake intervention on the longitudinal vehicle dynamics.

Figure 6.16 shows the contra-cornering yaw moments generated by independently driving the front inner wheel and braking the front outer wheel, respectively. Here it is assumed that the vehicle negotiates a right hand turn on nominal road surfaces and the front inner wheel can be driven independently. The mechanism of yaw moment generation is similar to that described in Chapter 5 for active steering subsystems. As can be seen from Figure 6.16, on account of lateral load transfer, the maximum yaw moment generated by independently driving the front inner wheel is much less than that induced by independently braking the front outer wheel.

Therefore, in order to minimise the influence of brake intervention on the longitudinal vehicle dynamics and avoid wheelspin caused by excessive torque transfer, a new DSC subsystem in which the two actuation concepts for vehicle stability control are both employed and aimed to complement each other is proposed. In this system, the stability controller designed in the previous section remains unchanged and the only difference from the two single actuation concept based DSC subsystems is that the required corrective yaw moment is shared between torque transfer and single-wheel braking.

More specifically, if the corrective yaw moment demanded by the stability controller is relatively small, it will be entirely generated through torque transfer. If the required corrective yaw moment is large, a part of the yaw moment will be generated through torque transfer and the remainder will be produced by braking the appropriate wheel. This new DSC subsystem is illustrated as block diagram of Figure 6.17 where the schemes for transforming the required corrective yaw moment into torque transfer and slip ratio are the same as those in Figures 6.10 and 6.15, respectively.

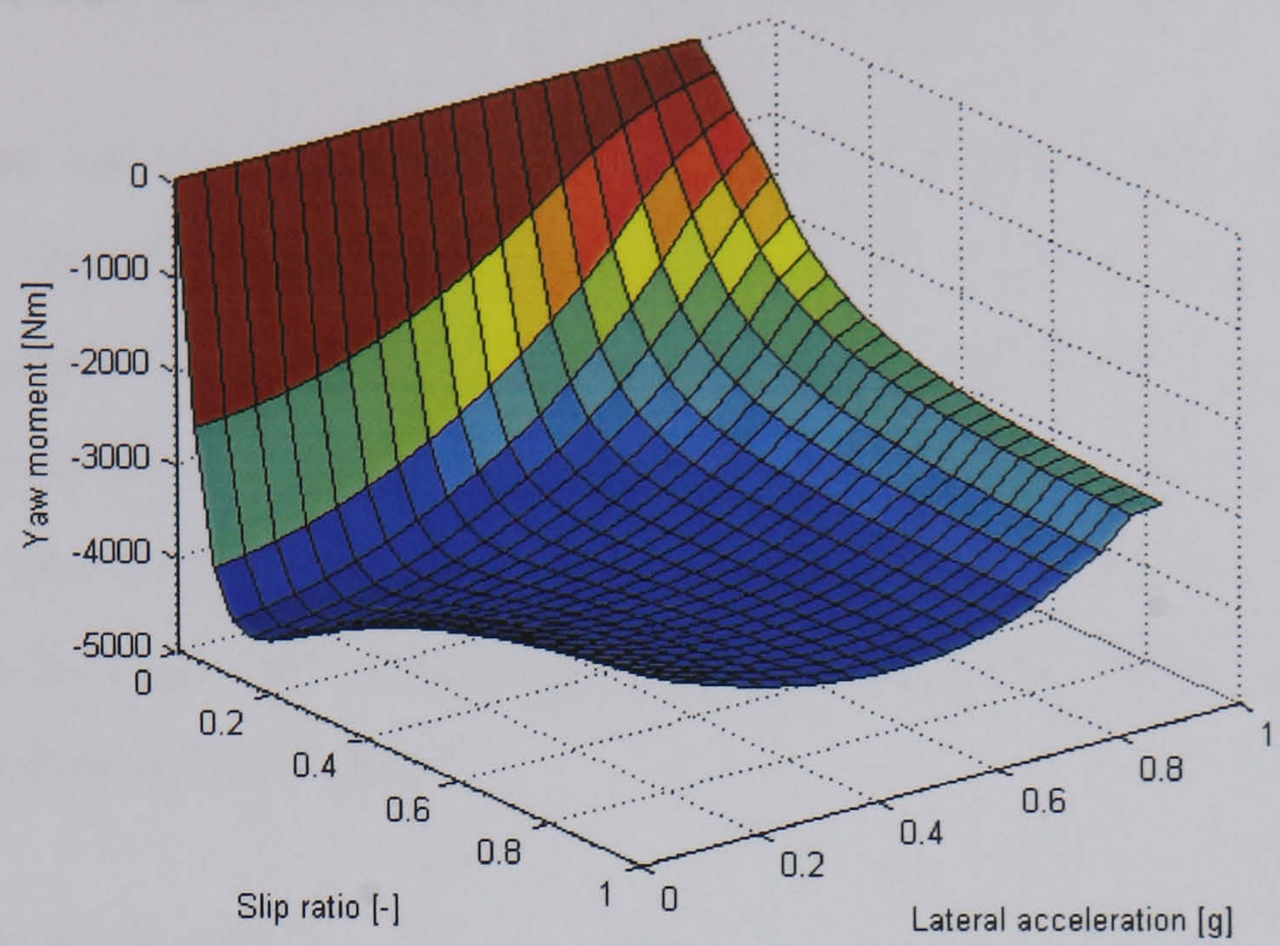

(a) Contra-cornering yaw moment generated by driving the front inner wheel

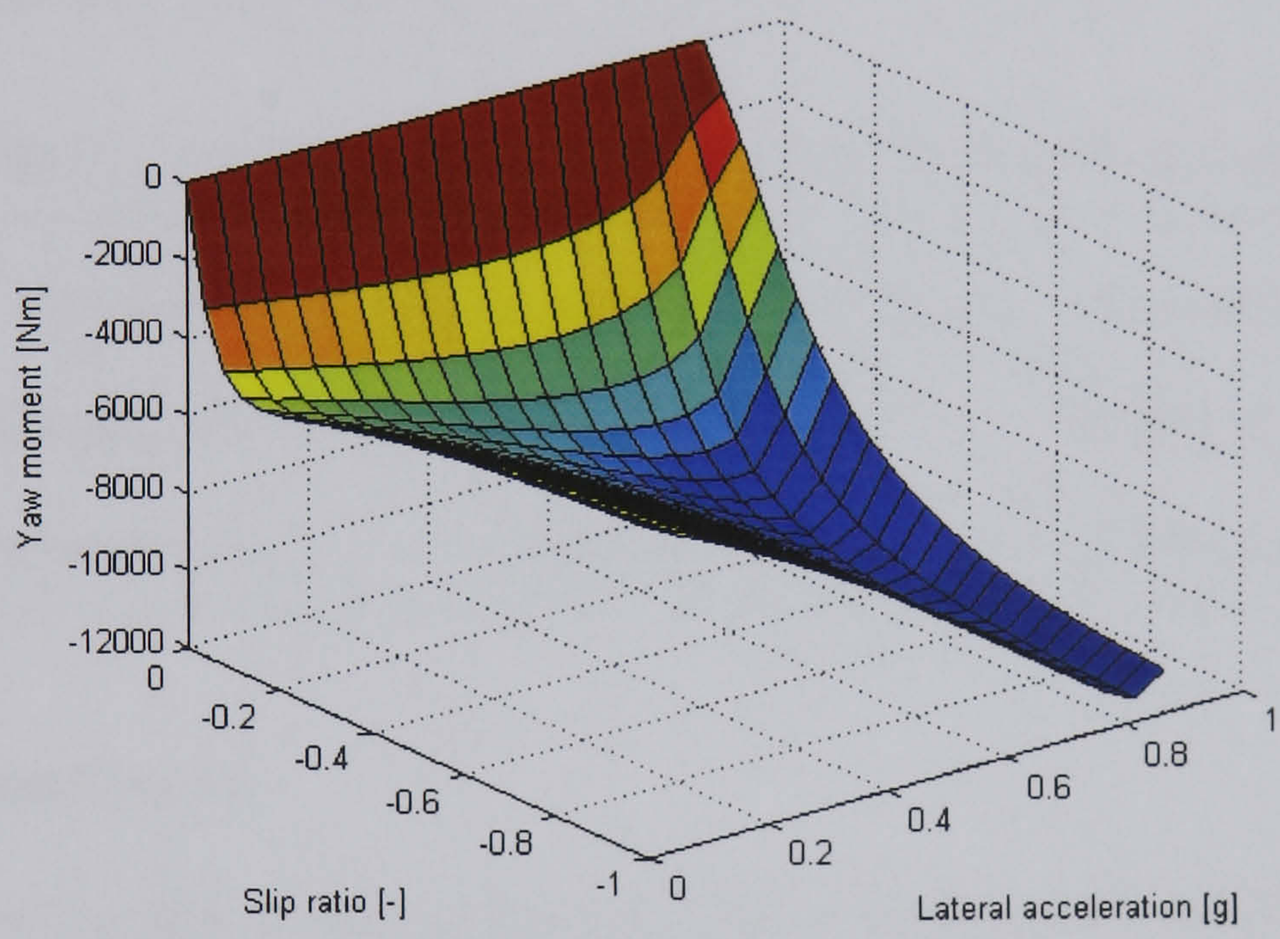

(b) Contra-cornering yaw moment generated by braking the front outer wheel

Figure 6.16 Contra-cornering yaw moments generated by independently driving or braking wheels on nominal road surfaces

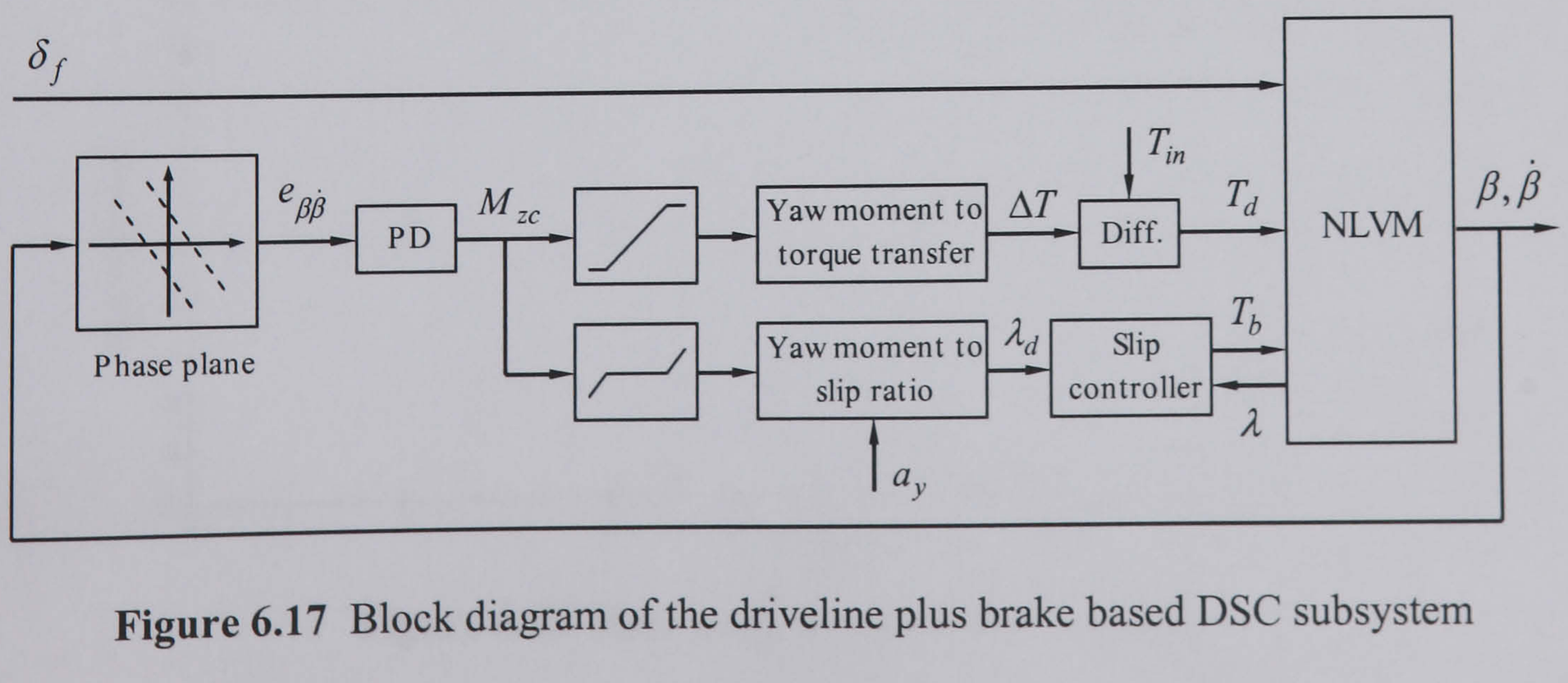

Figure 6.17 Block diagram of the driveline plus brake based DSC subsystem

6.5 Evaluation of the Dynamic Stability Subsystem Controller

The evaluation of the stand-alone dynamic stability subsystem controller will be performed on the NLVM using the following manoeuvres. The driveline and brake actuator saturation levels and slew rates are given in Table 6.1 (Crolla *et al.*, 2000) where the achievable braking effort is the torque that locks the wheel. In addition, in the driveline plus brake based DSC subsystem, in order to prevent the inner wheel from running at high slip ratios, the amount of allowed torque transfer is limited between -1000Nm and 1000Nm.

- Single sine steer input;
- Sine steer input with increasing amplitude;
- Braking on split- μ surfaces.

Table 6.1 Driveline and brake actuator saturation levels and rate limits

Actuator	Max value	Min value	Max rate	Min rate
Torque transfer differential	1500Nm	0	6000Nm/s	6000Nm/s
Brake (each wheel)	2500Nm	0	6000Nm/s	6000Nm/s

Single sine steer input

The steer input for this manoeuvre is the same as the one used in Chapter 4, as shown in Figure 6.18. The simulation results are shown in Figures 6.19 to 6.21. In the passive case, the vehicle cannot follow the steer input and spins. The vehicle with DSC can however successfully follow the steer input and remain stable.

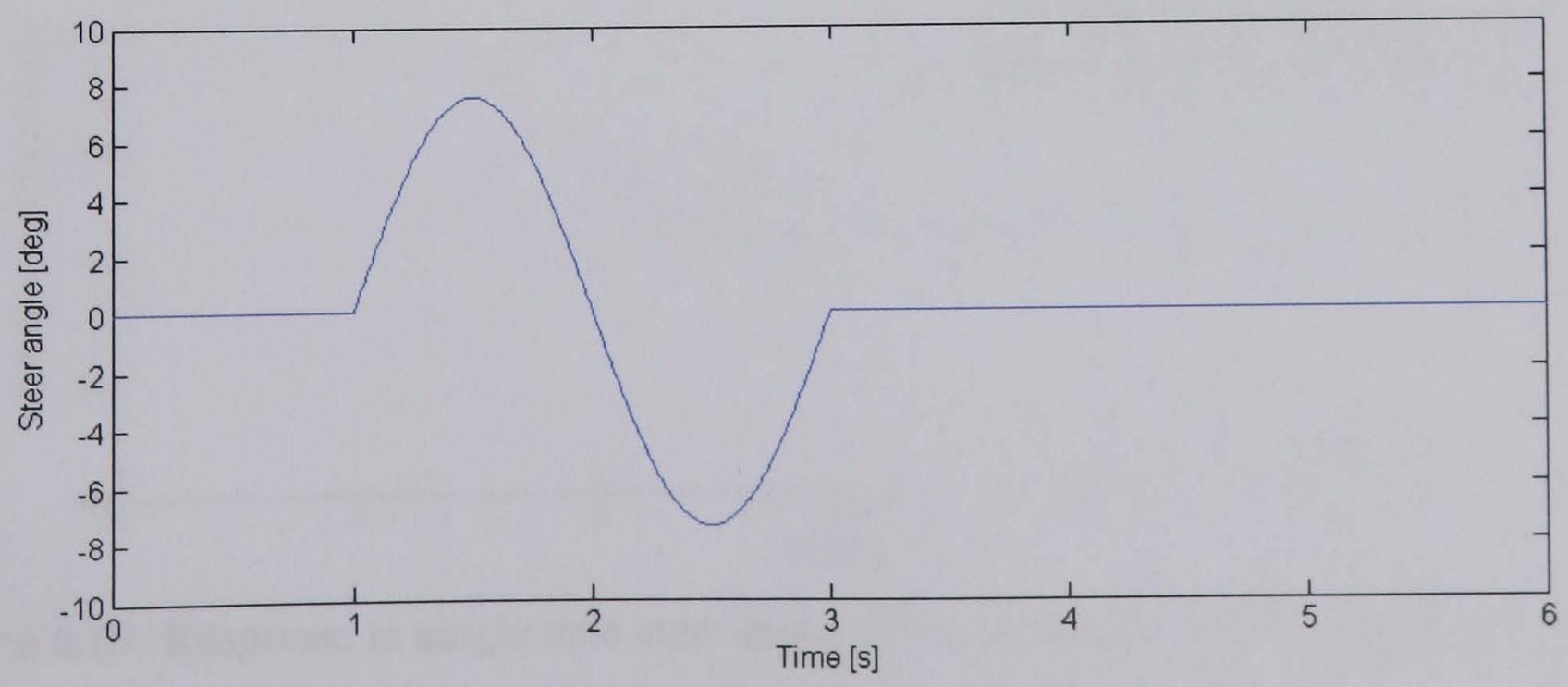

Figure 6.18 Steer angle for single sine steer input

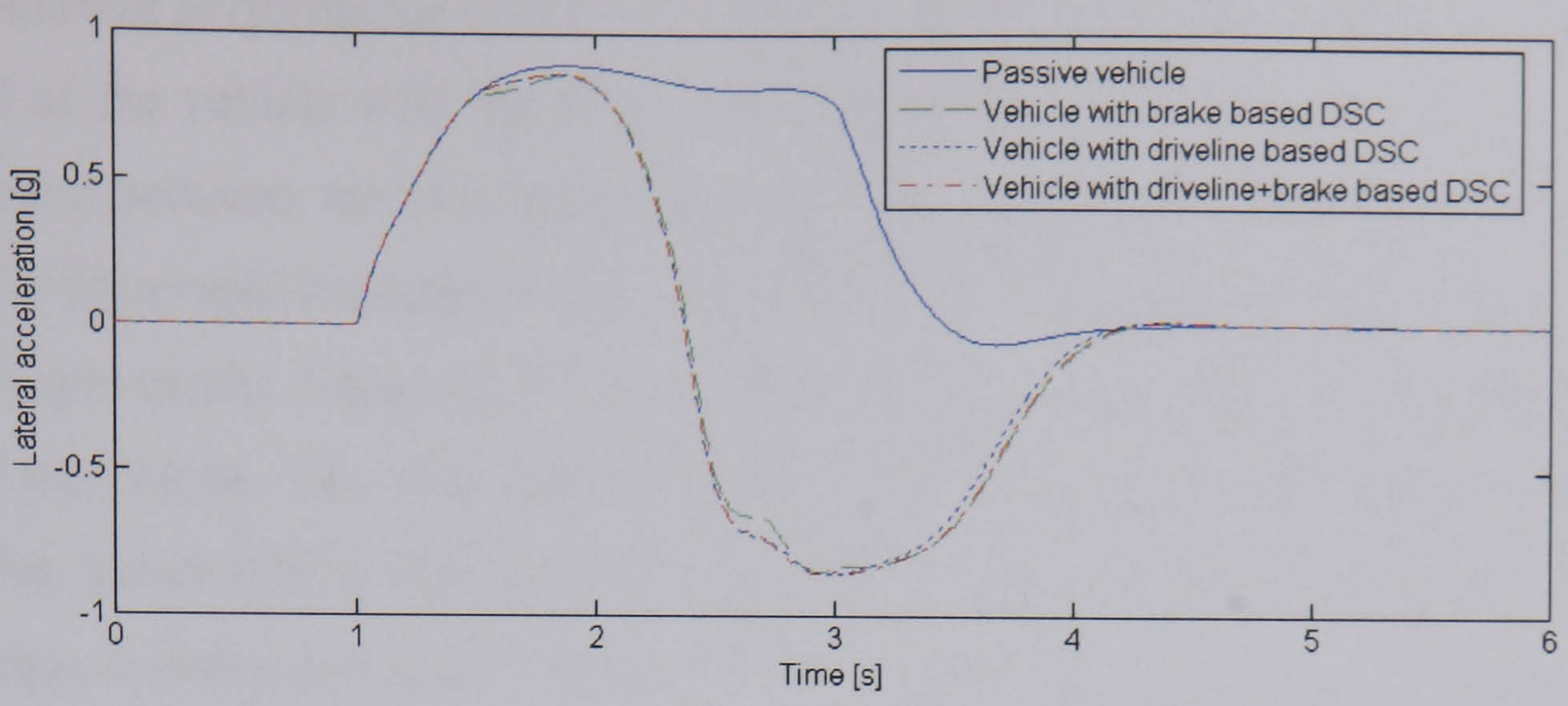

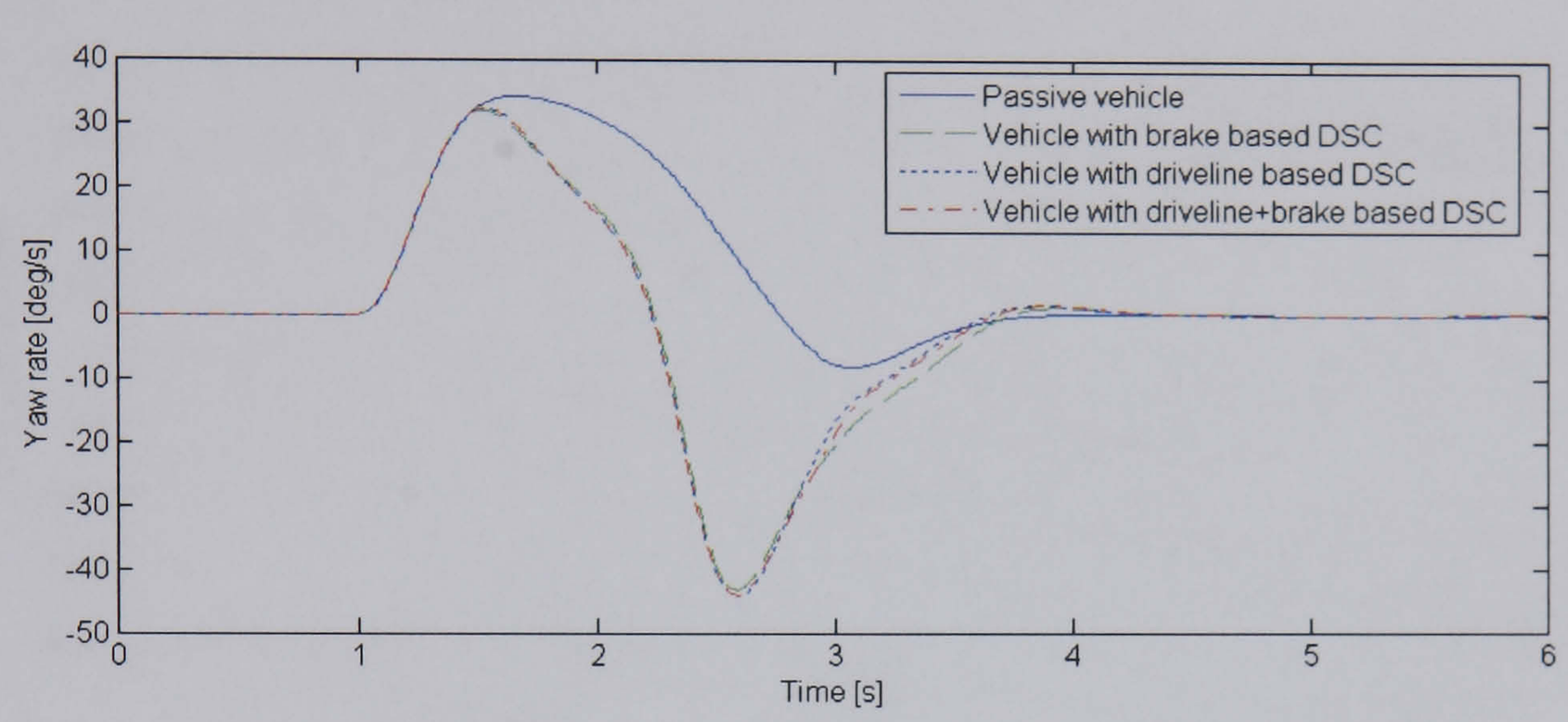

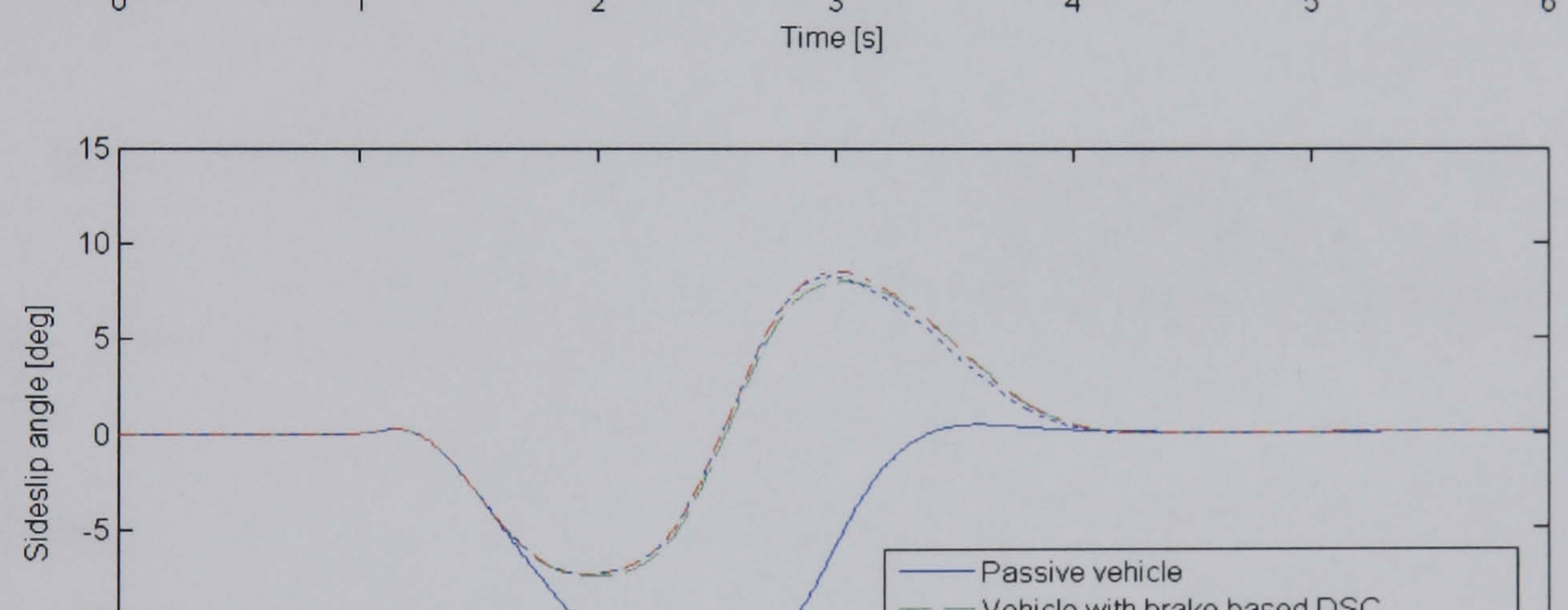

Figure 6.19 Response to single sine steer input of the NLVM with and without stand-alone stability controller at 100km/h

The handling performance of the vehicle with the driveline based DSC is comparable to that of the vehicle with the brake based one for this specific manoeuvre. The big difference between the two actuation concepts can be seen in the vehicle forward speed, with a rapid decrease in speed for the vehicle with the brake based DSC due to brake intervention. Figure 6.20 shows the required torque transfer, brake torques and wheel slip ratios. The slip ratio of the front inner wheel for the vehicle with the driveline based DSC is seen to slightly exceed the desired maximum value of 0.2 and the torque transfer is already close to the actuation limits.

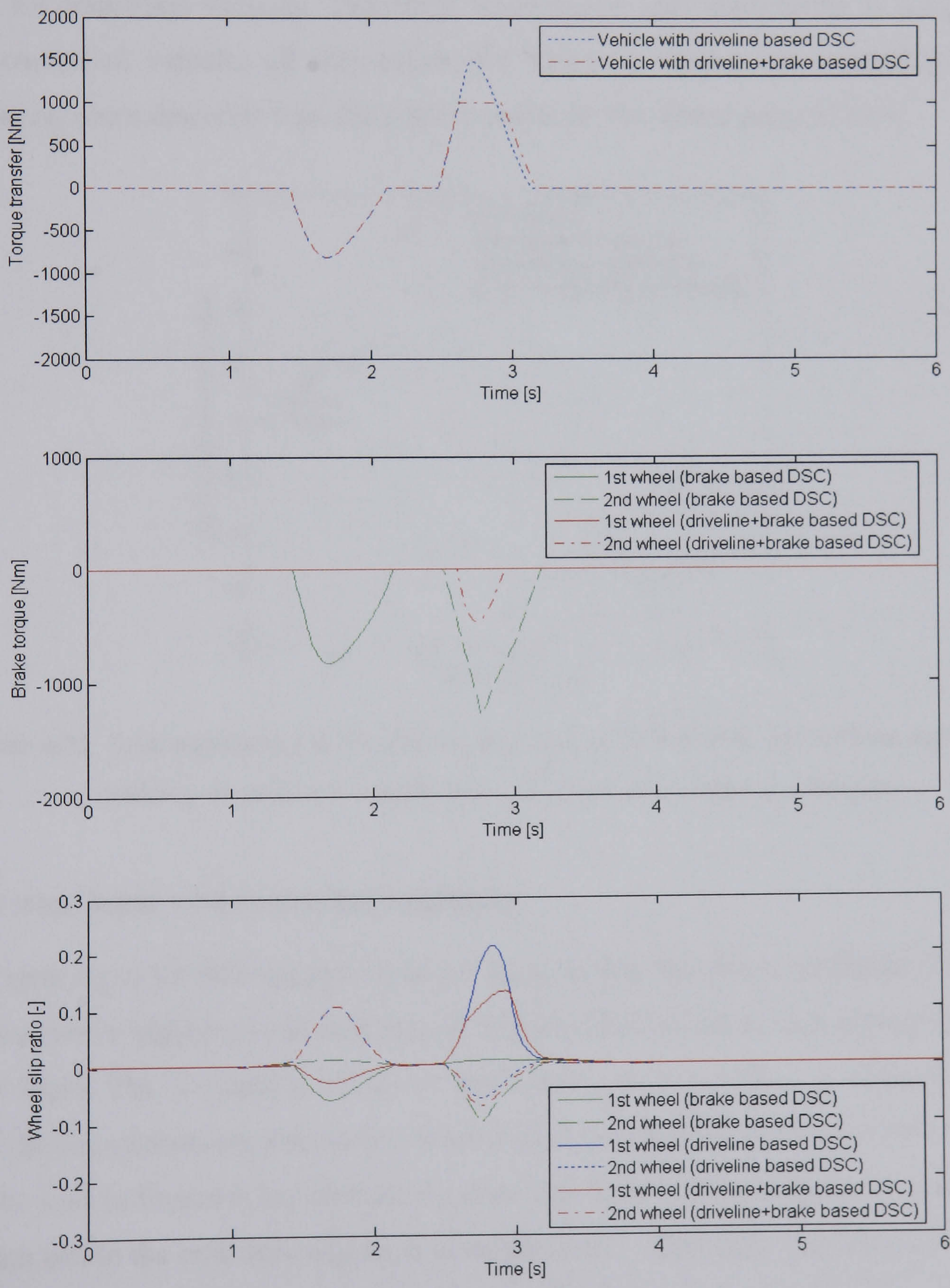

Figure 6.20 Required torque transfer, brake torques and wheel slip ratios for the NLVM with stand-alone stability controller in response to single sine steer input at 100km/h

For the brake based DSC, the wheel slip ratios however remain relatively small. In addition, the vehicle with the driveline plus brake based DSC also shows almost identical lateral dynamics to that with single actuation concept based DSC. Through sharing the required corrective yaw moment between torque transfer and one-wheel braking, the two actuation concepts are seen to complement each other and negative effects of individual actuation concepts discussed in the preceding section are reduced to a large extent. The phase portraits of the passive and controlled vehicles are shown in Figure 6.21. Compared to the passive vehicle, peak sideslip angle is reduced by 48% for controlled vehicles. Therefore, whereas the state trajectories of the passive and controlled vehicles all stay inside the reference region, the controlled case is obviously more desirable than the passive one from the driver point of view.

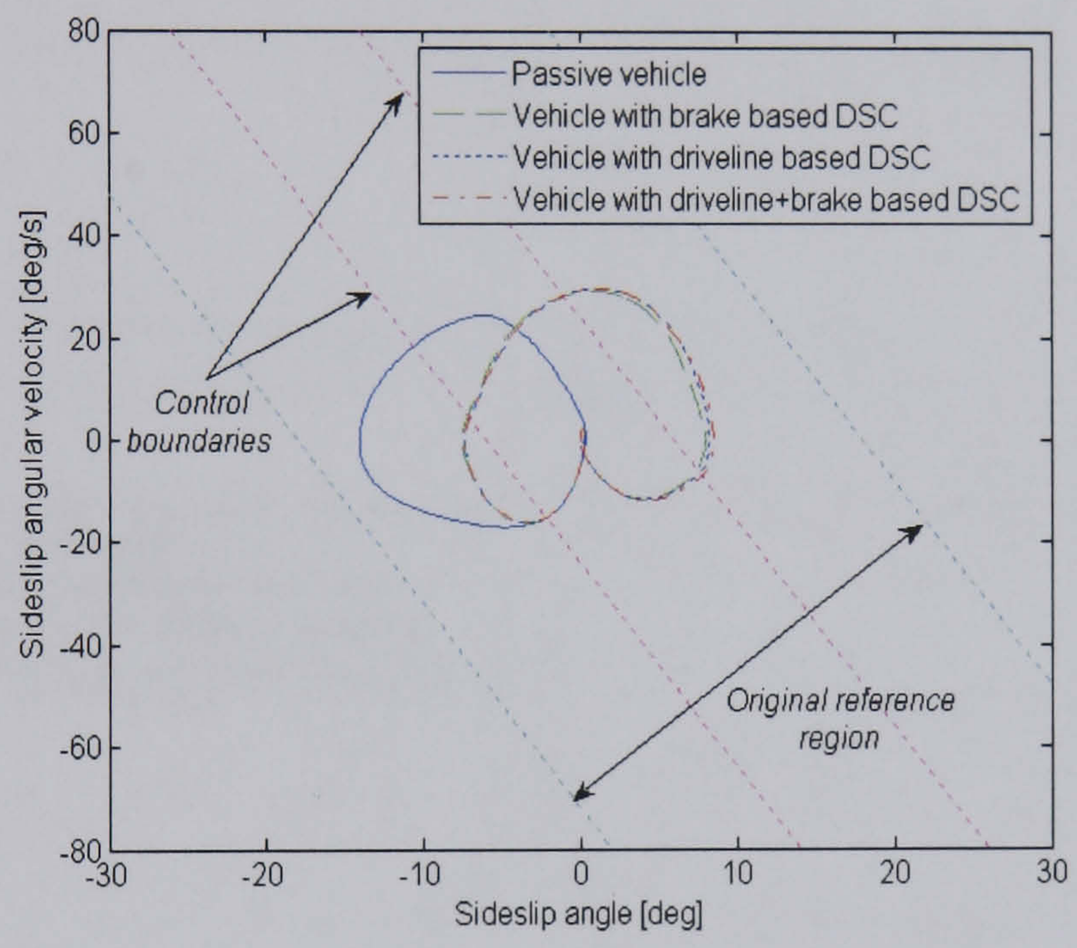

Figure 6.21 State trajectories in the phase plane for the NLVM with and without stand-alone stability controller in response to single sine steer input at 100km/h

Sine steer input with increasing amplitude

The steer input for this manoeuvre is the same as the one shown in Figure 5.17. This manoeuvre is highly critical in terms of vehicle stability due to high amplitude of the steer input. The simulation results of this manoeuvre are shown in Figures 6.22 to 6.24. In this manoeuvre, the passive vehicle fails to properly follow the steer input. As can be seen in Figure 6.24, whereas the state trajectories of the passive vehicle largely remain inside the reference region, it is subjectively undesirable due to high values of sideslip angle. The DSC controlled vehicle is however seen to successfully follow the steer input at all times and stay well away from the unstable regions.

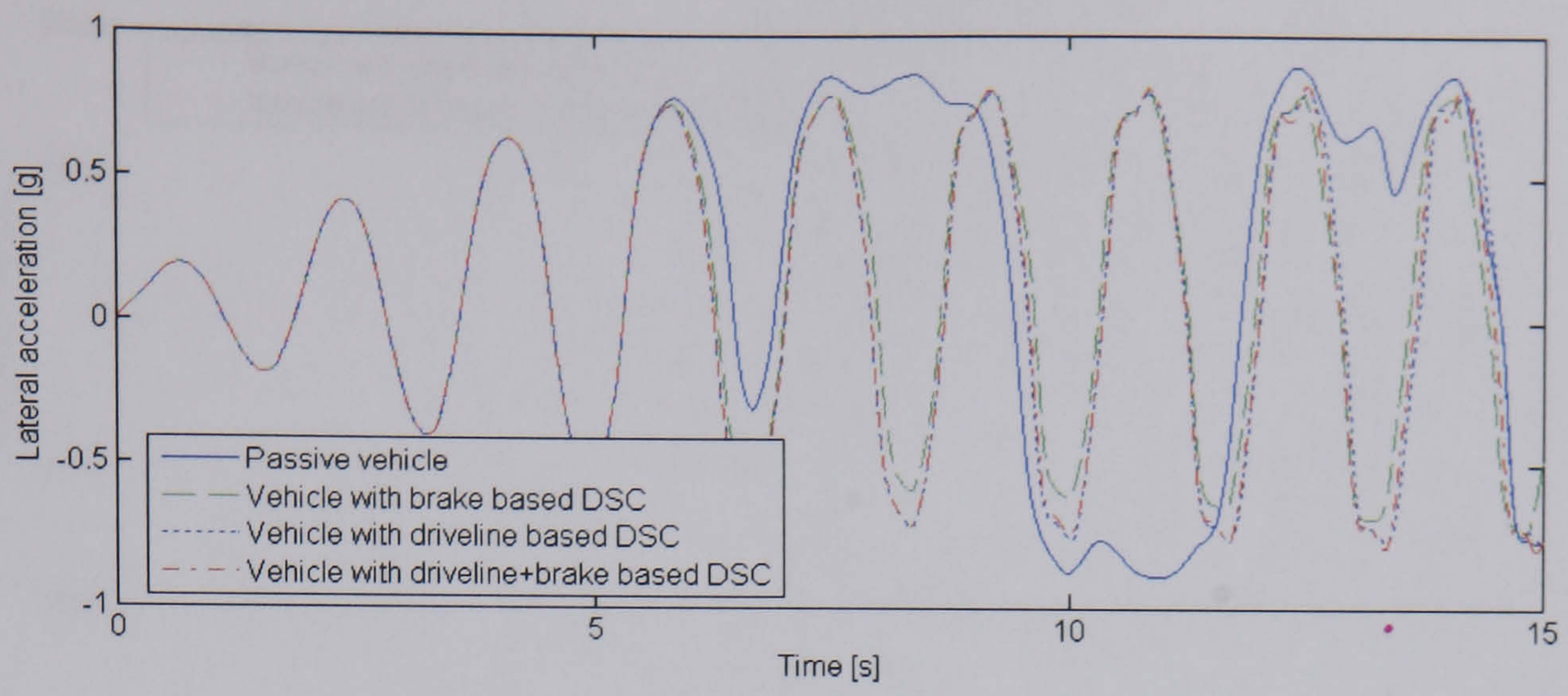

Figure 6.22 Response to sine steer input with increasing amplitude of the NLVM with and without stand-alone stability controller at 100km/h

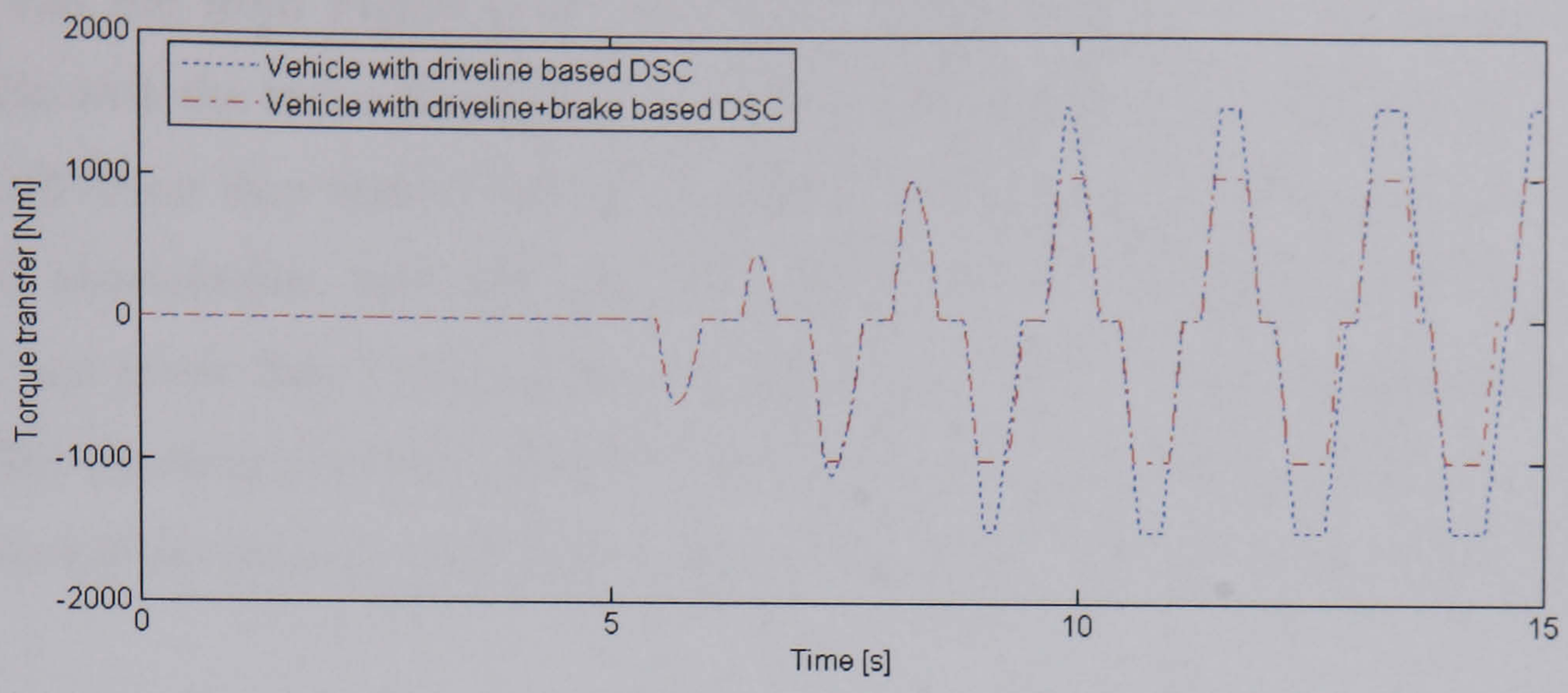

Figure 6.23 Required torque transfer, brake torques and wheel slip ratios for sine steer input with increasing amplitude for the NLVM with stand-alone stability controller at 100km/h

One can see from Figure 6.22, as a result of brake intervention, the speed of the vehicle with the brake based DSC decreases quite rapidly and the final value is about 20km/h lower than that of the vehicle with the driveline based DSC. Hence the peak lateral acceleration, yaw rate and sideslip angle of the vehicle with the brake based DSC are lower than those of the driveline based DSC controlled vehicle when the stability controller becomes active. Due to this reduction in vehicle forward speed, the required brake torques reach a maximum at a specific time and decrease thereafter.

In this specific manoeuvre, while the driveline based DSC can keep the state trajectories of the vehicle inside the reference region, the actuation limits of torque transfer are already reached and slip ratio of the front inner wheel is beyond 0.2, as shown in Figure 6.23. This is obviously undesirable since a tyre running under such conditions will experience a sharp decrease in the corresponding lateral tyre force (see Figure 3.12) and the steering response of the vehicle will be significantly reduced. Therefore, the control performance of the driveline based DSC is slightly poorer than that of its brake based counterpart, with slightly higher peak sideslip angle.

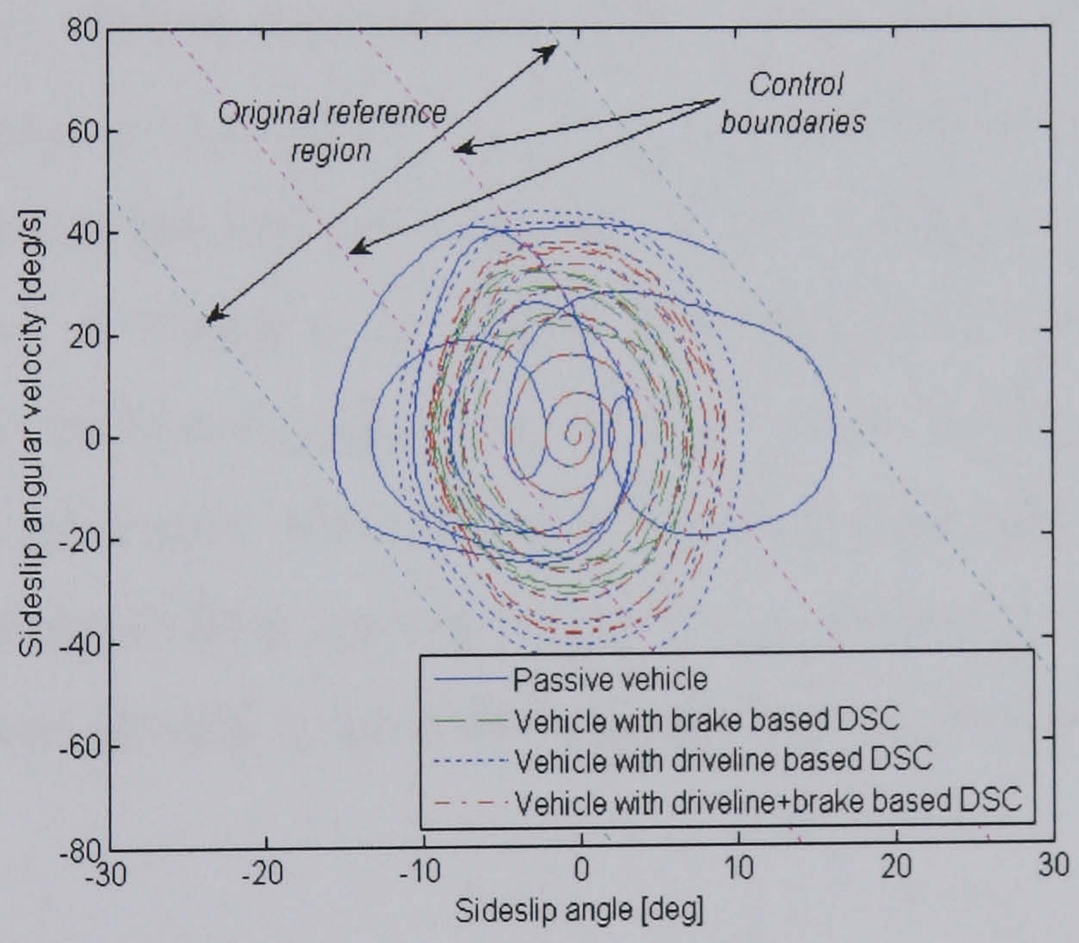

Figure 6.24 State trajectories in the phase plane for the NLVM with and without stand-alone stability controller in response to sine steer input with increasing amplitude at 100km/h

By contrast, the required brake torques demanded by the slip controller and levels of slip ratio for the driveline plus brake based DSC are less than those for the single actuation concept based DSC, while the performance of the driveline plus brake based DSC is still comparable to that of the brake based DSC. In other words, by exploiting

both actuation concepts for the same control task, vehicle stability is maintained and the interference with the longitudinal vehicle dynamics induced by brake intervention is reduced. Peak sideslip angle is reduced by 47% for brake based DSC, 32% for driveline based DSC and 42% for driveline plus brake based DSC, respectively.

Braking on split-μ surfaces

This manoeuvre is the same as the one used in Chapter 5. The simulation results of braking on a split-μ surface with and without the stand-alone stability controller are shown in Figures 6.25 and 6.26. Here the brake based and driveline based DSC are examined. The DSC plus ABS controlled vehicle is seen to respond to such a disturbance similarly to the vehicle with the stand-alone ABS controller. The stability controller is not activated until the vehicle state trajectories cross the control boundaries and enter the unstable regions (at around 0.8s).

In the case of brake based DSC, when the stability controller becomes active, a corrective yaw moment command is generated and consequently the front left (1^{st}) wheel on the low-μ surface is further braked to stabilise the vehicle. However, since the longitudinal force of this wheel has been saturated and the ABS controller has become active to adjust the relevant brake torque before the activation of the stability controller, as shown in Figure 6.25, additional braking action applied at this wheel does not produce extra braking force any more and thus the required corrective yaw moment cannot be generated. This effect can be clearly seen in the time response of the brake torque demanded by the slip controller, as shown in Figure 6.26. Whereas such a braking action already reaches the actuator saturation level, the vehicle is still out of control.

For the driveline based DSC, when the stability controller is activated, torque transfer from the front left (1^{st}) wheel to the front right (2^{nd}) wheel takes place. Hence the front left wheel on the low-μ surface will be further braked and the brake torque at the front right wheel will be reduced. Similar to the brake based DSC controlled case, additional brake torque applied at the front left wheel cannot generate extra braking force and then the required corrective yaw moment. In addition, the reduction in the brake torque applied at the front right wheel and consequently the braking force does

reduce the overall yaw moment on the vehicle, it is however not large enough to push the vehicle back to the path, resulting in a bit slower decrease in vehicle speed and more lateral deviation. Here actuation limits of the driveline based DSC are already reached as well. Therefore, in comparison to the active steering subsystem controllers described in Chapter 5, both brake based and driveline based DSC are not capable of stabilising the vehicle in this specific manoeuvre.

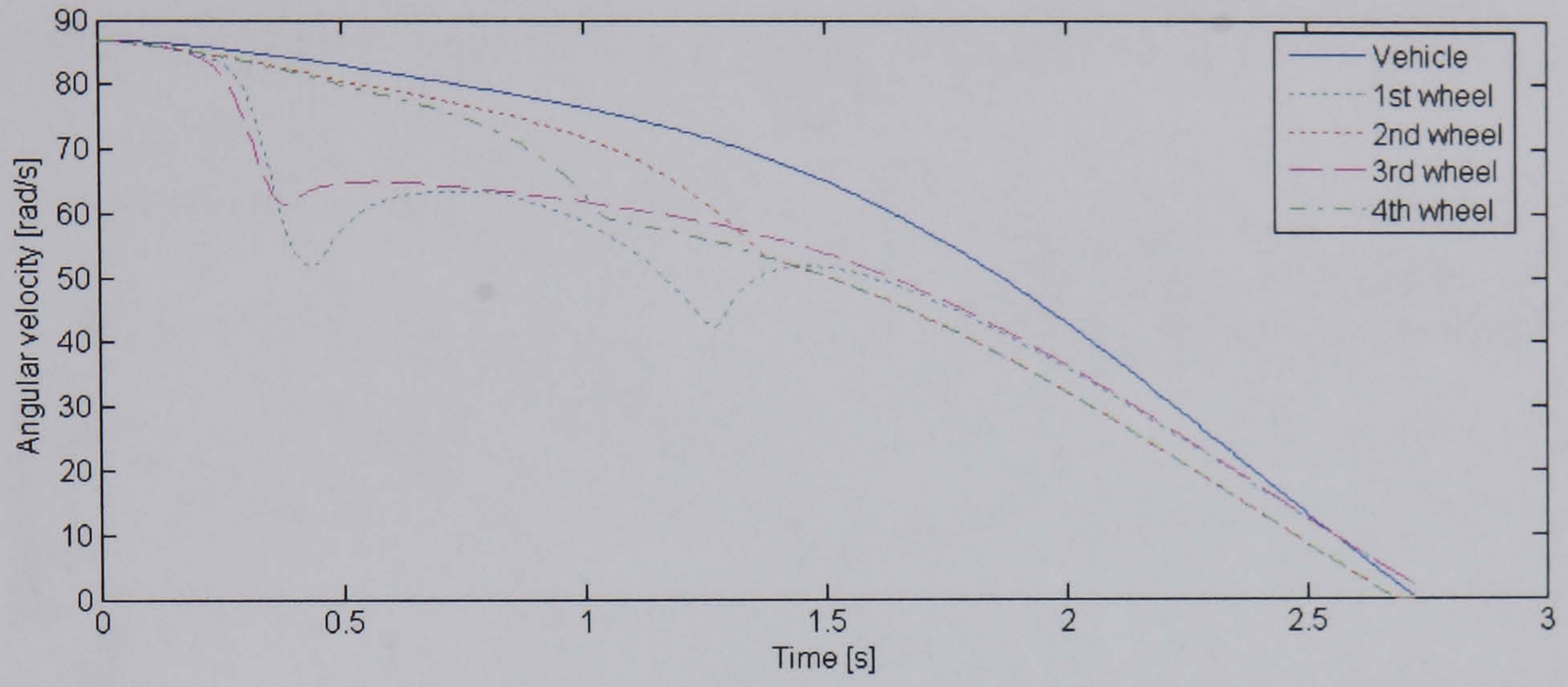

(a) Vehicle with ABS + brake based DSC

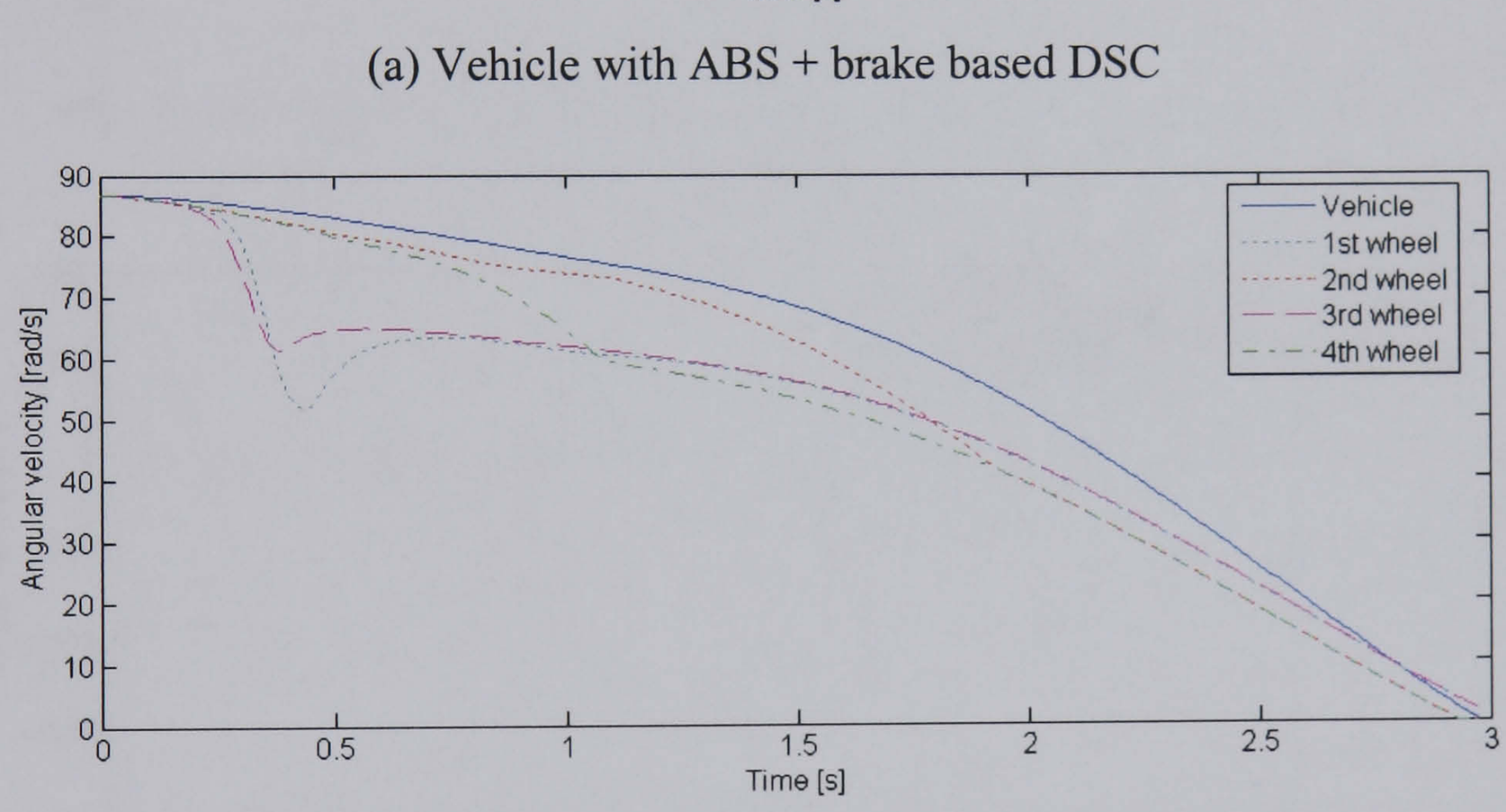

(b) Vehicle with ABS + driveline based DSC

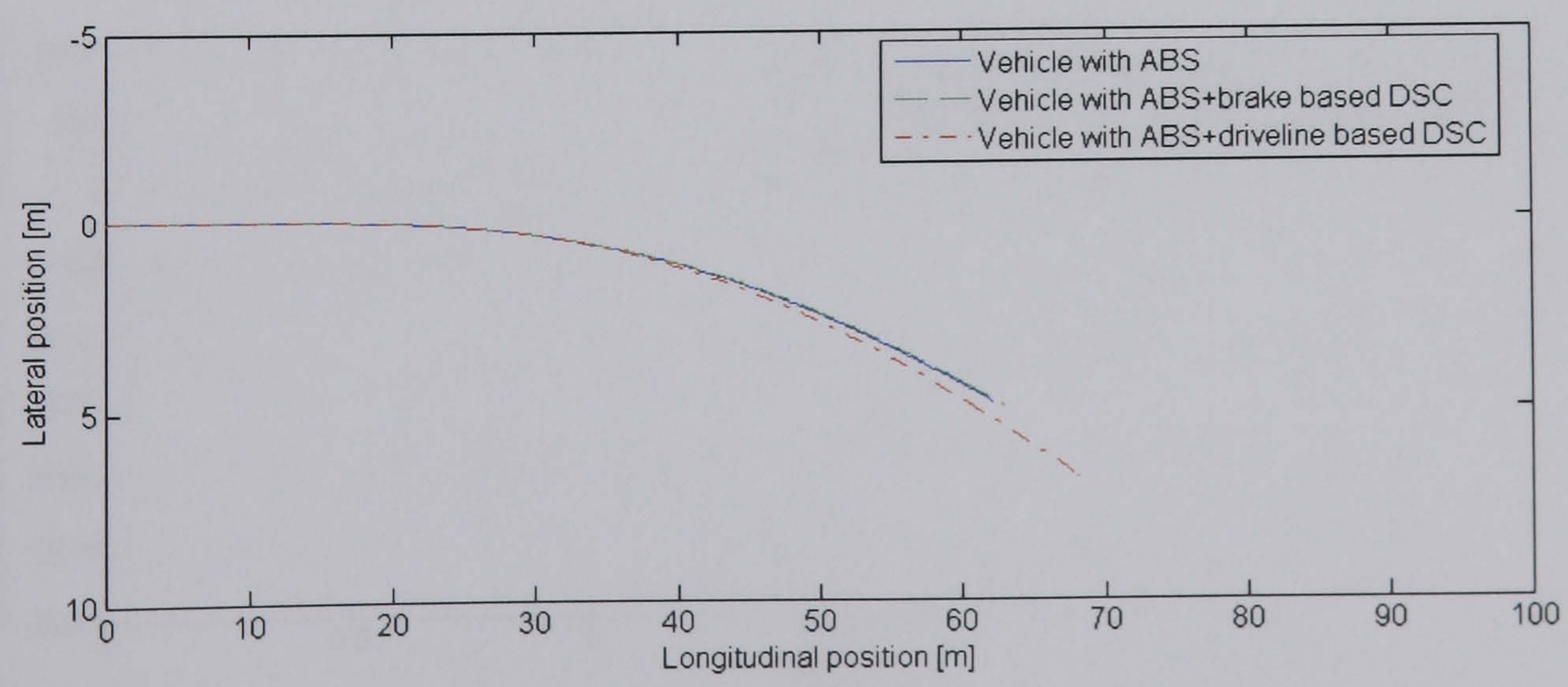

Figure 6.25 Velocities and vehicle path for the NLVM with stability controller and ABS controller during braking on a split-μ surface

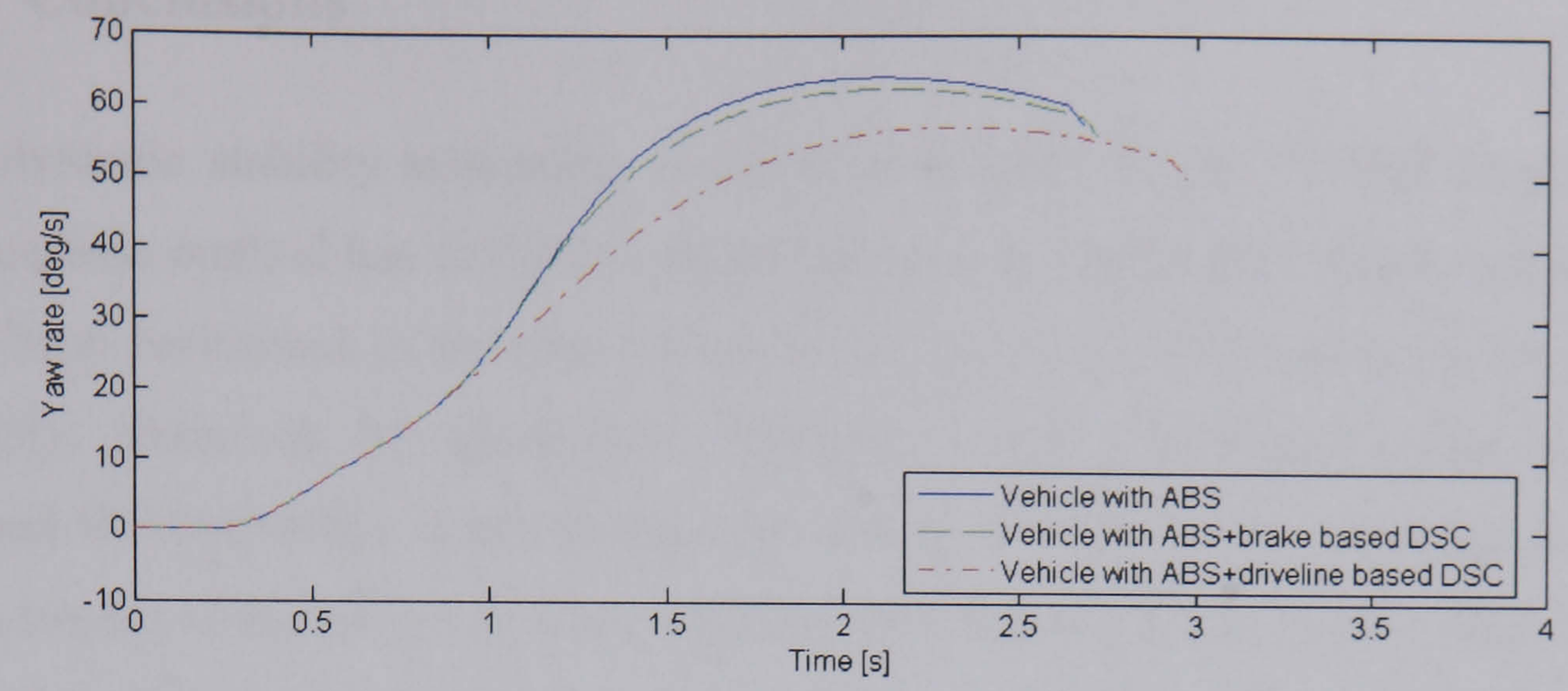

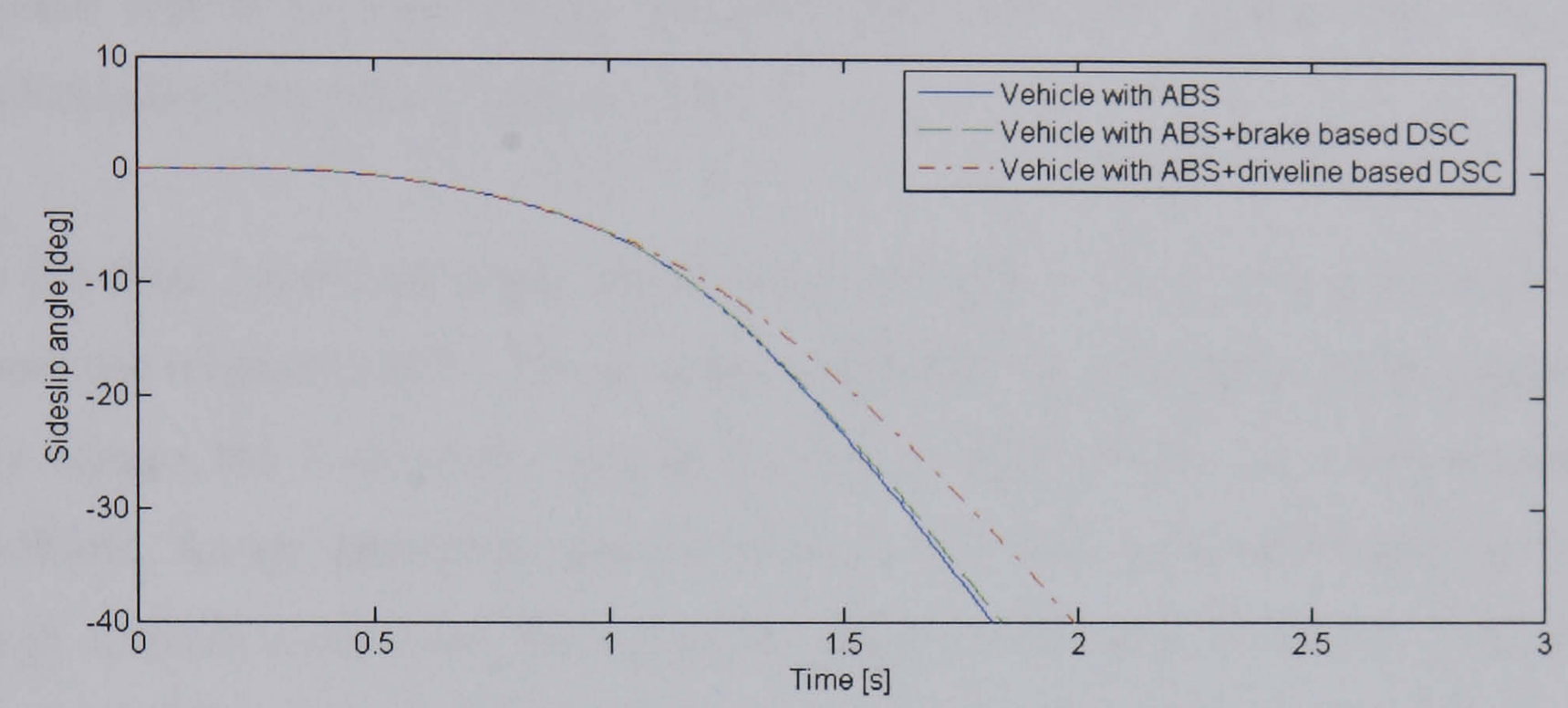

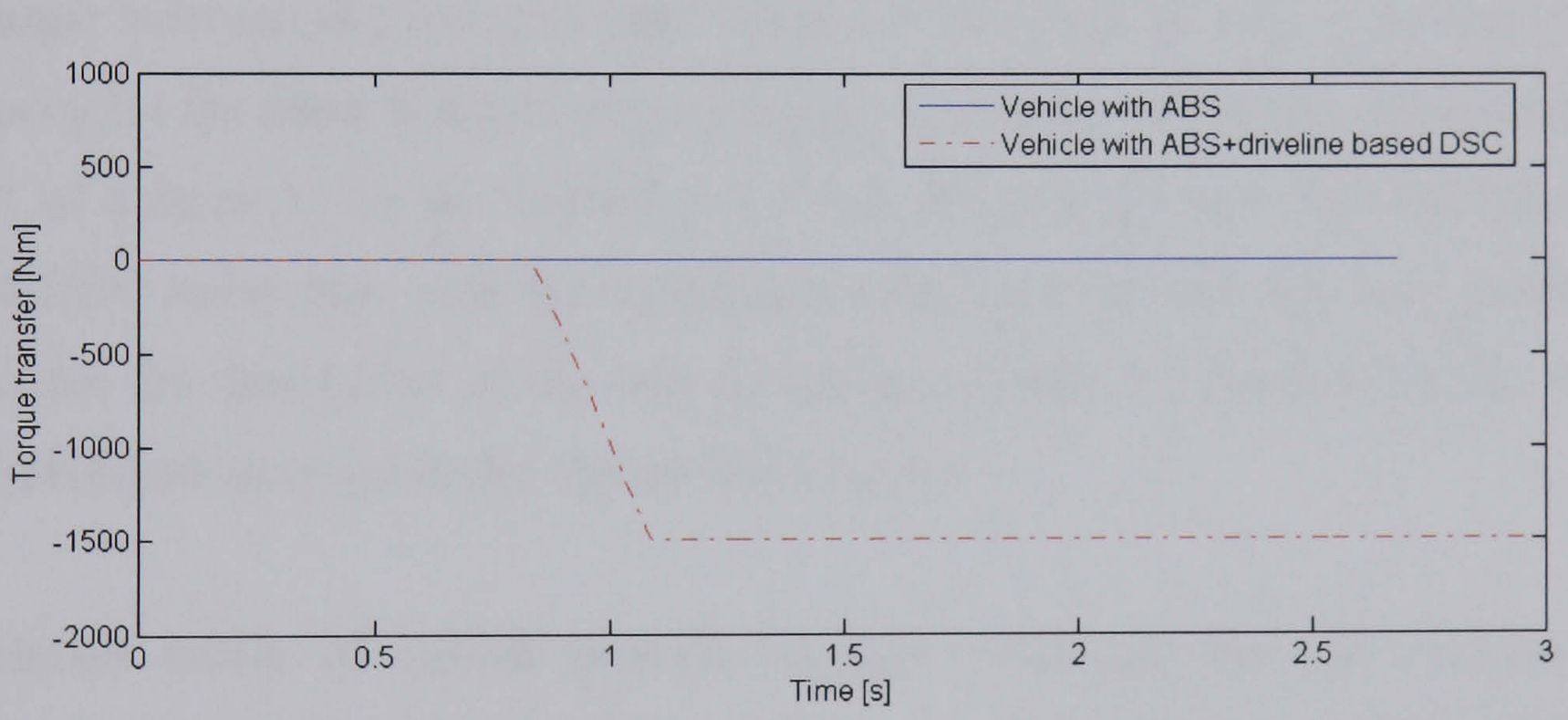

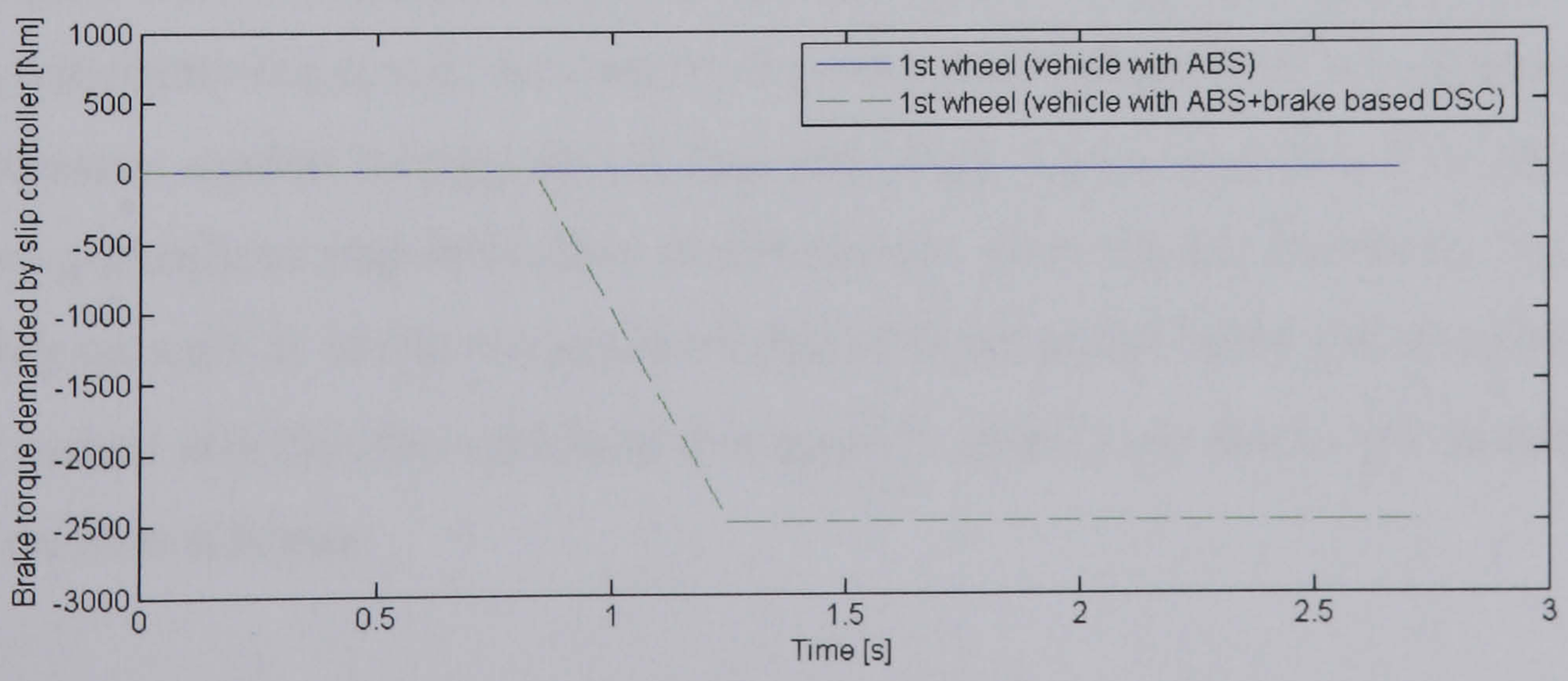

Figure 6.26 Response of the NLVM with and without stand-alone stability controller to braking on a split- μ surface

6.6 Conclusions

The dynamic stability subsystem controller has been designed in this chapter. The phase-plane method has first been introduced and the analysis of vehicle stability has then been performed in the phase plane of the vehicle sideslip angle and its angular velocity. Based on the phase-plane analysis, a reference stable region has been defined for stand-alone stability controller design. A simple PD control algorithm has been employed for the stand-alone stability controller to pull the vehicle back into the reference region as soon as the state trajectories of the vehicle cross the control boundaries and enter the unstable regions.

Both driveline based and brake based DSC subsystems have been examined in order to show the relative merits. The conventional brake based DSC is an important active safety feature, but it slows the vehicle down and compromises the traction potential of the vehicle. As an alternative, driveline based DSC can be used to stabilise vehicles through actively controlling the left/right torque distribution. However, the difference in torque between the left and right wheels of the driving axle is attributed to the tendency for the inner wheel to spin owing to the presence of excess driving force as a result of a decrease in the vertical tyre load. Therefore a new driveline plus brake based DSC subsystem with the unchanged stability controller has been proposed to overcome the drawbacks of the two actuation concepts by distributing the required corrective yaw moment to the appropriate actuator.

Simulation results of critical manoeuvres have confirmed the effectiveness of the developed DSC subsystems and these results also indicate that vehicle stability has been noticeably improved. As a result, the controlled vehicle does not experience any unnecessary motion during critical transient manoeuvres, and thus it is capable of showing excellent responsiveness to subsequent steer inputs. However, the test of braking on split-μ surfaces has shown that both the brake based and driveline based DSC cannot stabilise the vehicle in this specific manoeuvre due to the limitations of the actuation schemes.

Chapter 7

Design of Integrated Vehicle Dynamics Control System

Abstract: *An integrated vehicle dynamics control system is developed in this chapter. This control system is based on the two subsystems, AFS and driveline plus brake based DSC, designed independently in the preceding chapters. Combined control of the two subsystems is first examined to investigate the potential for overall performance improvement over the corresponding subsystems and to form the benchmark for further integration analysis. Subsequently a novel rule based integration scheme is proposed to coordinate the control actions of the two stand-alone controllers and the effectiveness of the integrated control system is verified through computer simulations. Conclusions are finally given at the end of the chapter.*

7.1 Introduction

Due to functional limitations of individual subsystems as analysed previously, different stand-alone vehicle dynamics control systems are optimised individually in specific handing regions and there is no single system which can be effective over the entire range of vehicle handling. The stand-alone active steering subsystem can improve vehicle steering response up to the handling limit but fails to maintain

vehicle stability at the handling limit. The stand-alone dynamic stability control subsystem can maintain vehicle stability under all driving conditions. However, the direct influence of the control action on the longitudinal vehicle dynamics limits its application to only highly critical driving situations.

Therefore, simultaneous presence of various stand-alone control systems in a vehicle is inevitable in order to keep the vehicle stable and under control at all times. However, due to the strong couplings of various aspects of vehicle dynamics and potential conflicts in control objectives, a certain amount of undesirable interactions between different stand-alone control systems arises when these systems are simply combined without coordination. Hence, in order to achieve an improved overall vehicle performance, vehicle dynamics control should be performed in an integrated rather than combined manner. A novel rule based integration scheme will be proposed in this chapter to eliminate performance trade-offs and to extend functionalities of individual subsystems.

In addition, as discussed in Chapter 5, whereas ARS is comparable to AFS in terms of improving vehicle steering response up to the handling limit, ARS is much less capable of generating contra-cornering yaw moment and consequently less effective to assist DSC than AFS in maintaining vehicle stability when the handling limit is approached as stability is the primary concern in this region. Therefore only AFS and the driveline plus brake based DSC will be further examined in this chapter.

7.2 Combined Control

7.2.1 Introduction

Before the final integration is investigated, combined control of the two stand-alone active subsystems designed in Chapters 5 and 6 will be examined. As defined in Chapter 1, in the combined control configuration, the two stand-alone controllers operate in parallel. The key features of such a configuration are therefore as follows:

- There is no communication between the two control loops;
- Each loop has its own reference model, controller and control input.

The block diagram of this configuration is shown in Figure 7.1. The analysis of combined control aims to investigate if such a configuration can provide overall performance improvement over the corresponding stand-alone subsystems or such two control loops can complement each other. The results of the simulations and analyses will form the benchmark for further integration analysis.

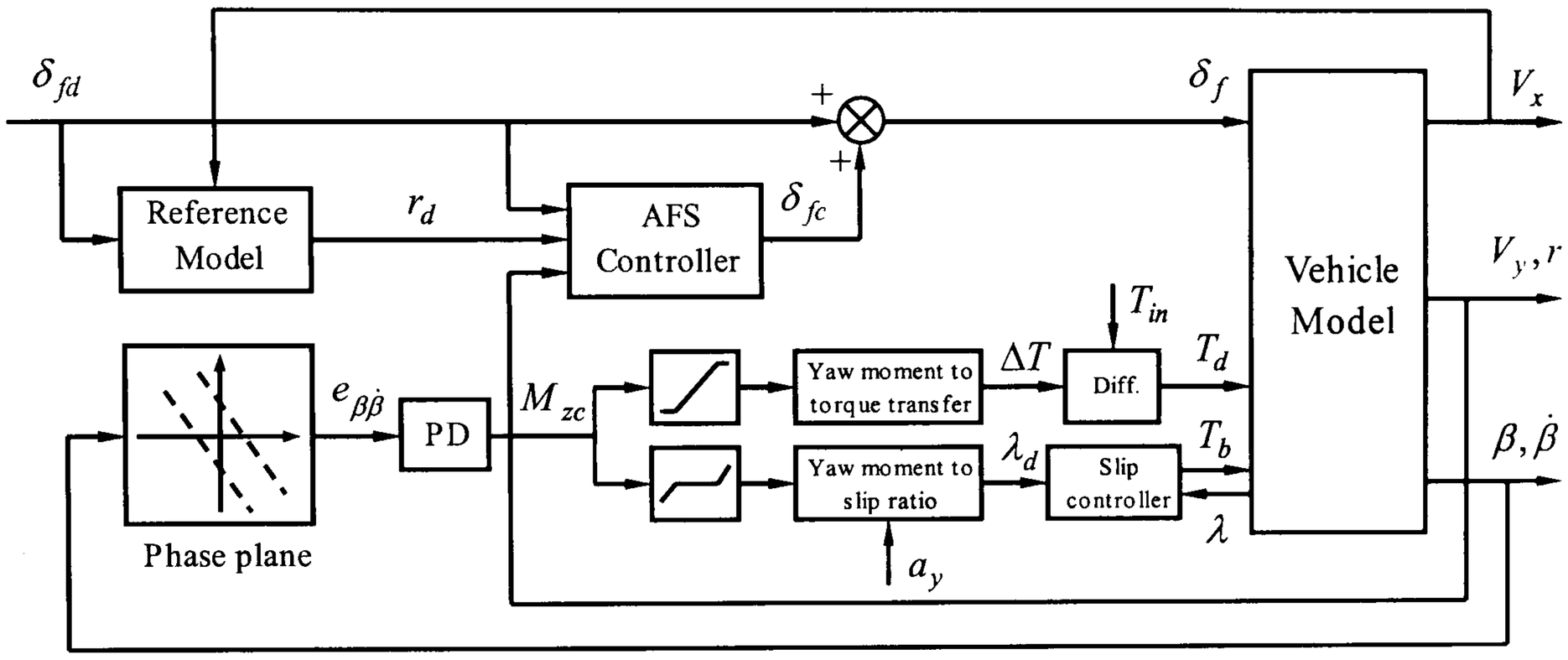

Figure 7.1 Block diagram of combined control of AFS and driveline plus brake based DSC

7.2.2 Evaluation of combined control

The following manoeuvres are employed to assess combined control. These manoeuvres are chosen so as to make the two stand-alone controllers active simultaneously during the tests. More specifically, the stand-alone steerability controller is always active and the stand-alone stability controller becomes activated only when vehicle stability is in question.

Single sine steer input

The steer input for this test is the same as that used in Chapters 5 and 6, as shown in Figure 7.2. The simulation results of this manoeuvre are shown in Figure 7.3.

The vehicle with the stand-alone AFS controller is seen not to be able to successfully follow the steer input, i.e. vehicle stability cannot be maintained by the stand-alone AFS controller at the handling limit. Both the stand-alone stability controller and corresponding combined control can however stabilise the vehicle during such a critical manoeuvre.

One can see the difference between stand-alone DSC and combined control. More specifically, the vehicle with combined control has a bit higher peak yaw rate and sideslip angle than that with stand-alone DSC. This effect is mainly caused by the additional control action from the AFS controller in combined control. This control action pulls the state trajectories of the vehicle further away from the control boundaries, as shown in the β-$\dot{\beta}$ phase plane, and consequently leads to more control effort from the stability controller, i.e. more torque transfer and brake intervention. The vehicle with combined control therefore finishes the manoeuvre with a slightly lower forward speed than the vehicle with stand-alone DSC. In addition, the tracking performance of combined control is not noticeably better than that of stand-alone DSC.

From this simulation one can see that the simultaneous optimisation of vehicle steerability and stability through combined control results in a conflict in control objectives at the limit of handling. Therefore, combined control does not achieve overall performance improvement over stand-alone DSC for this particular manoeuvre.

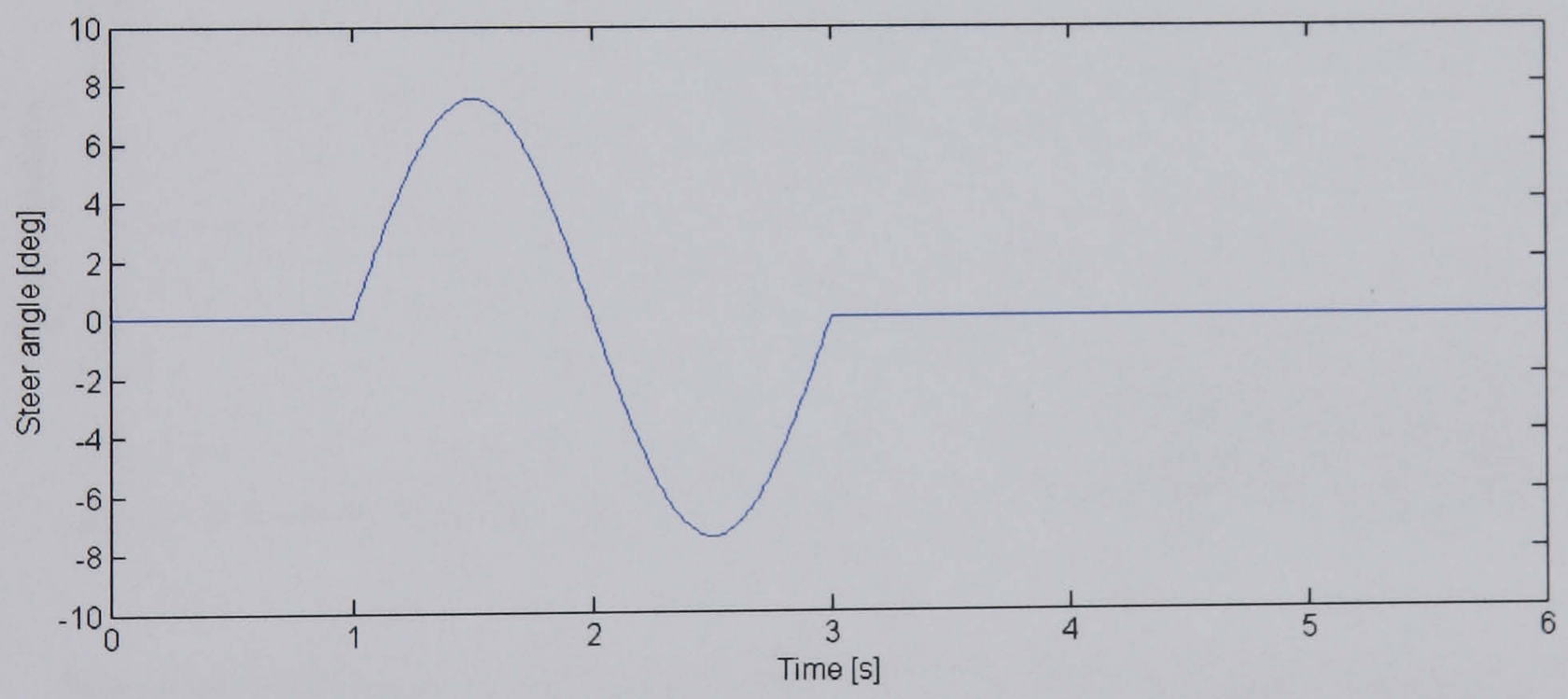

Figure 7.2 Steer angle for single sine steer input

Sine steer input with increasing amplitude

The steer input for this manoeuvre is also the same as that used in Chapters 5 and 6, as shown in Figure 7.4. Figure 7.5 shows the simulation results of this manoeuvre. In this specific manoeuvre, the stand-alone steerability controller cannot properly track the reference yaw rate any more at the handling limit and the vehicle becomes unstable.

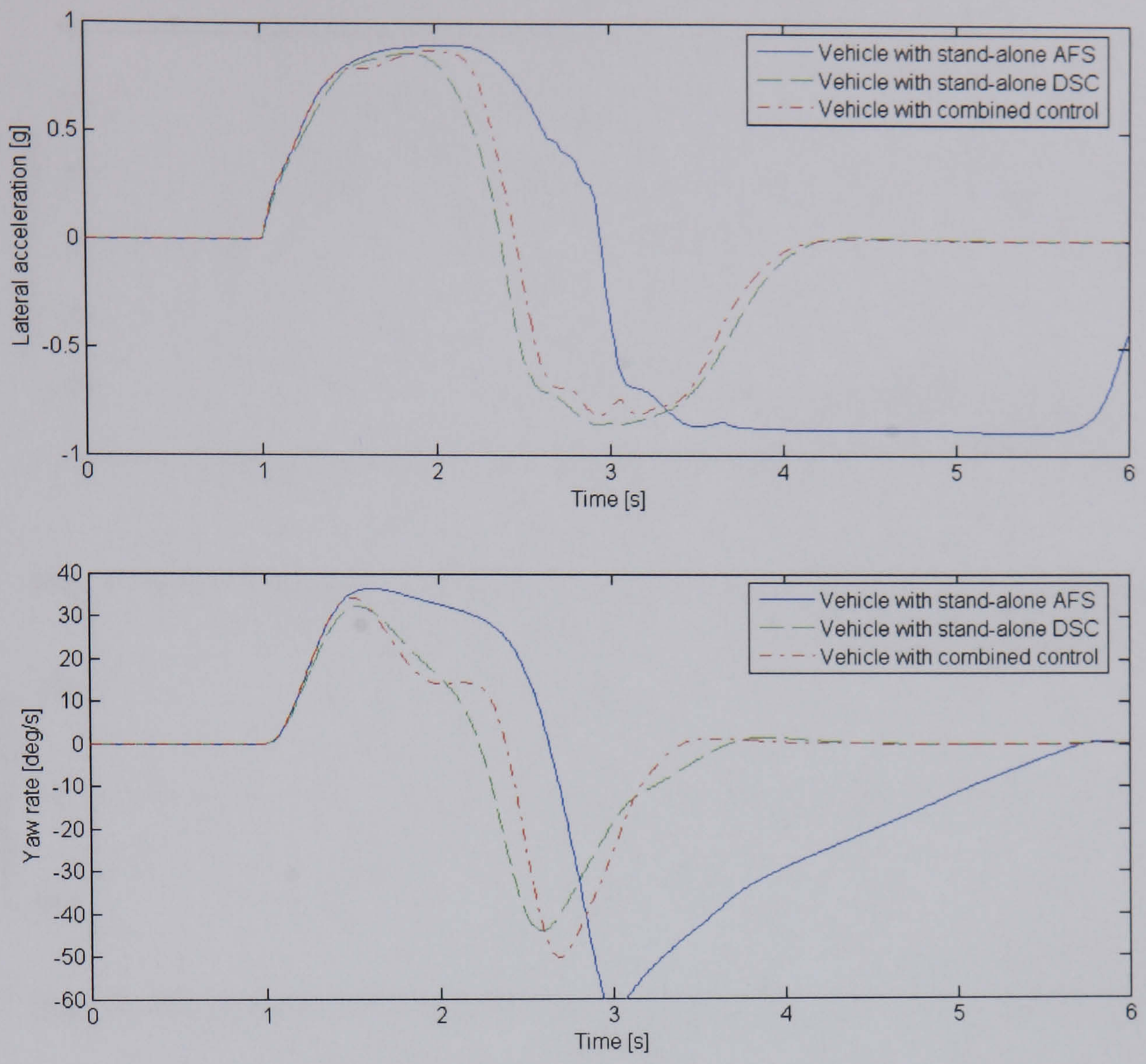

(a) Time response

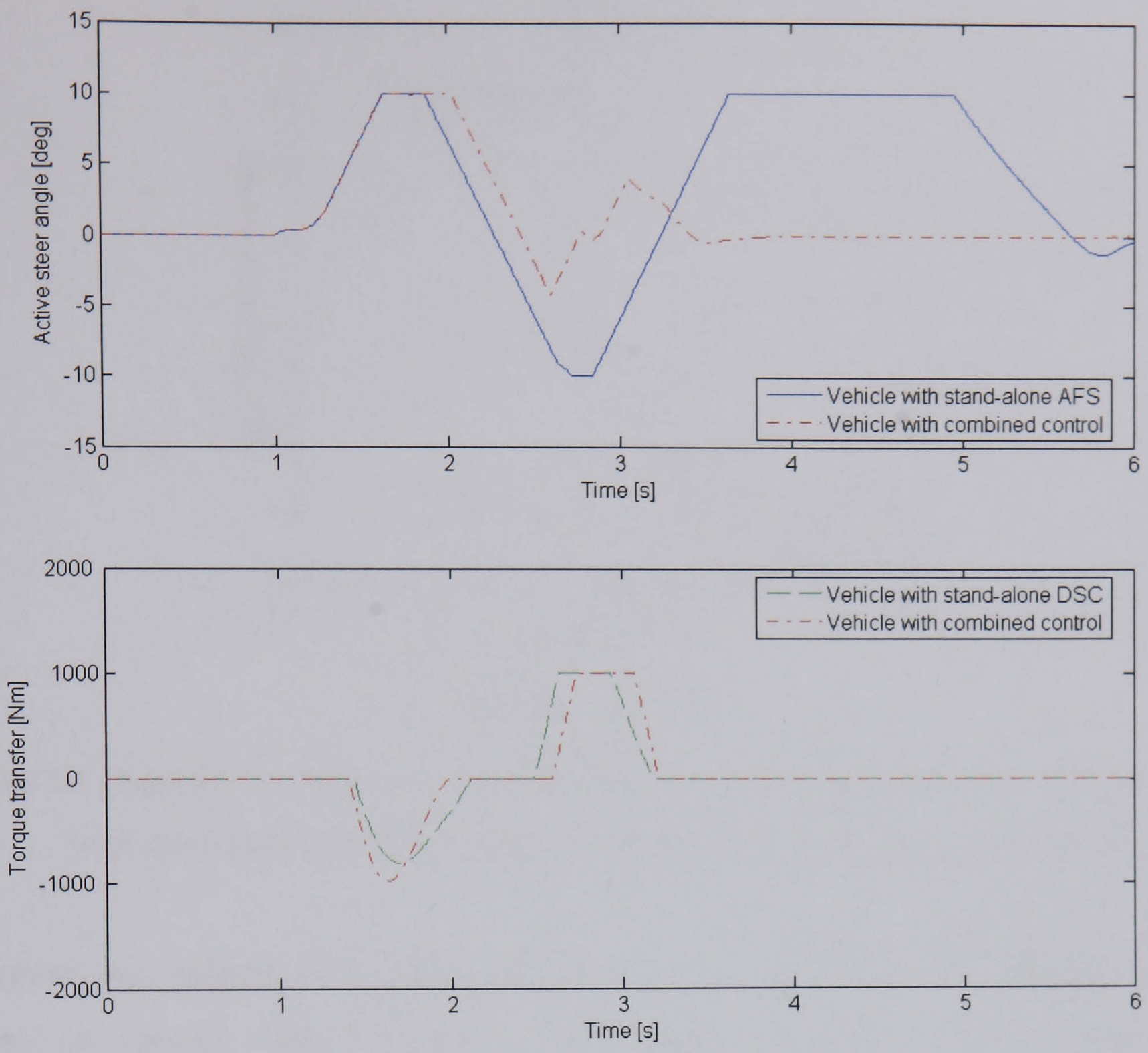

(b) Time response

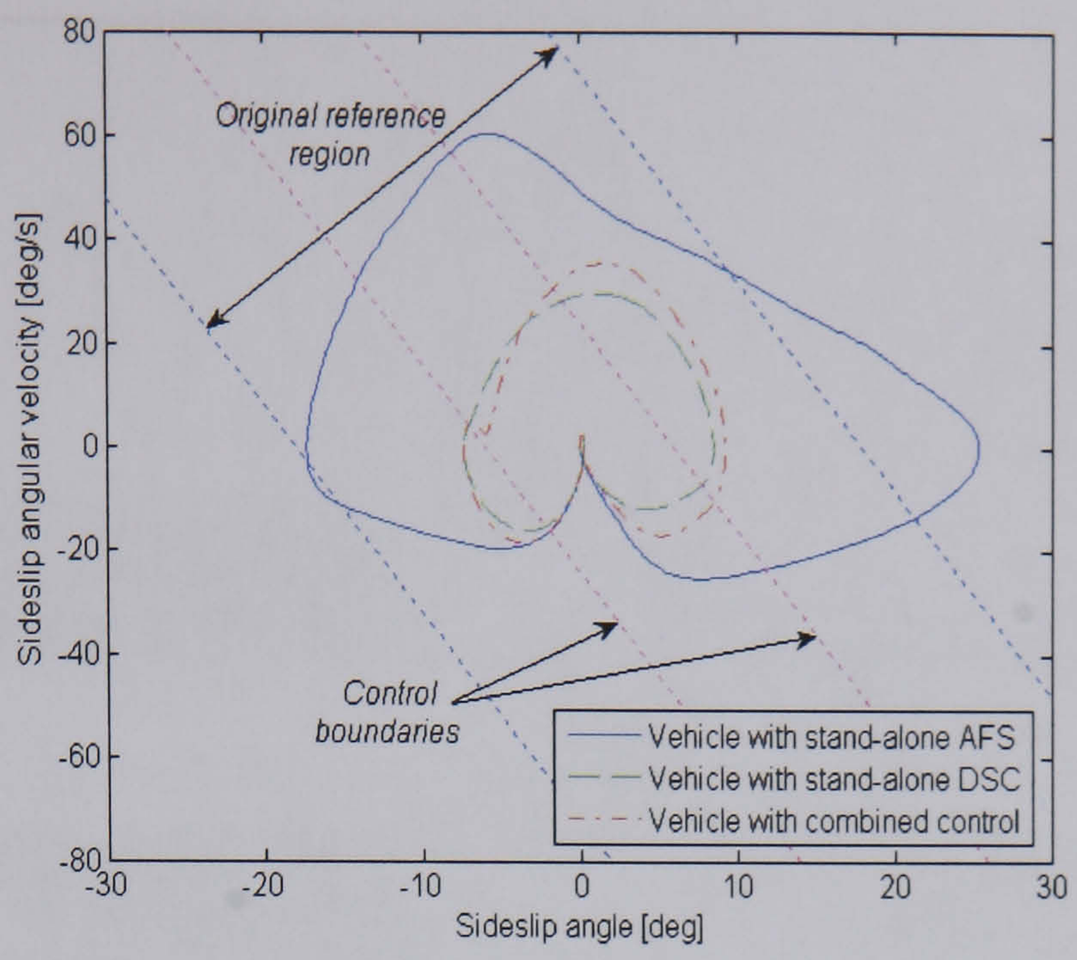

(c) Phase plane plot

Figure 7.3 Response to single sine steer input of the NLVM with stand-alone AFS controller, with stand-alone stability controller and with combined control at 100km/h

However the vehicle with either the stand-alone stability controller or combined control can remain stable at all times. The basic features observed in the above single sine steer input simulation can be seen here again. The vehicle with combined control requires more torque transfer and brake intervention than that with stand-alone DSC and consequently finishes the simulation with a lower forward speed. In addition, for both stand-alone DSC and combined control, due to the rapid reduction in the vehicle forward speed as a result of brake intervention, the required corrective yaw moment reaches a maximum at a specific time and then decreases thereafter although the amplitude of the steer input still increases linearly, so does the sideslip angle. This is particularly the case for the combined control.

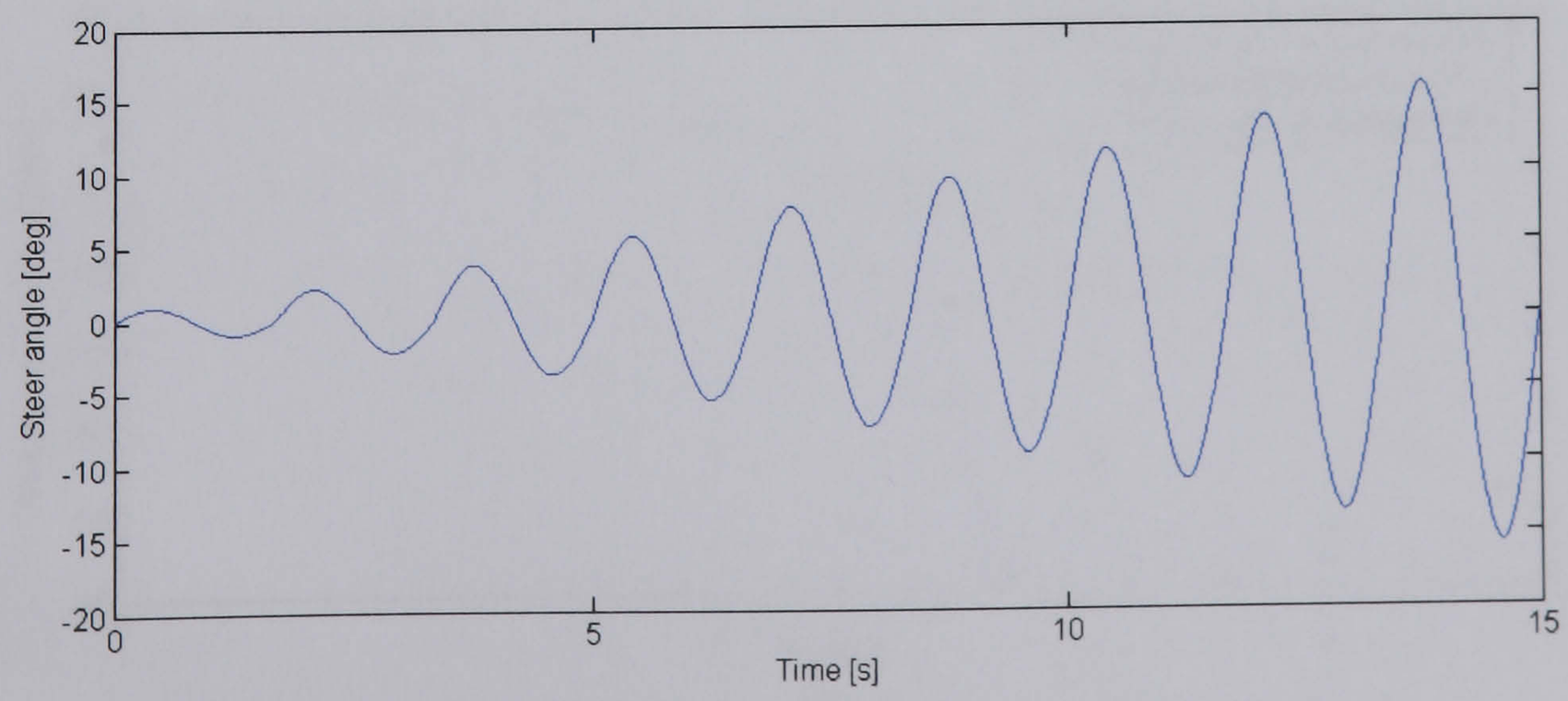

Figure 7.4 Steer angle for sine steer input with increasing amplitude

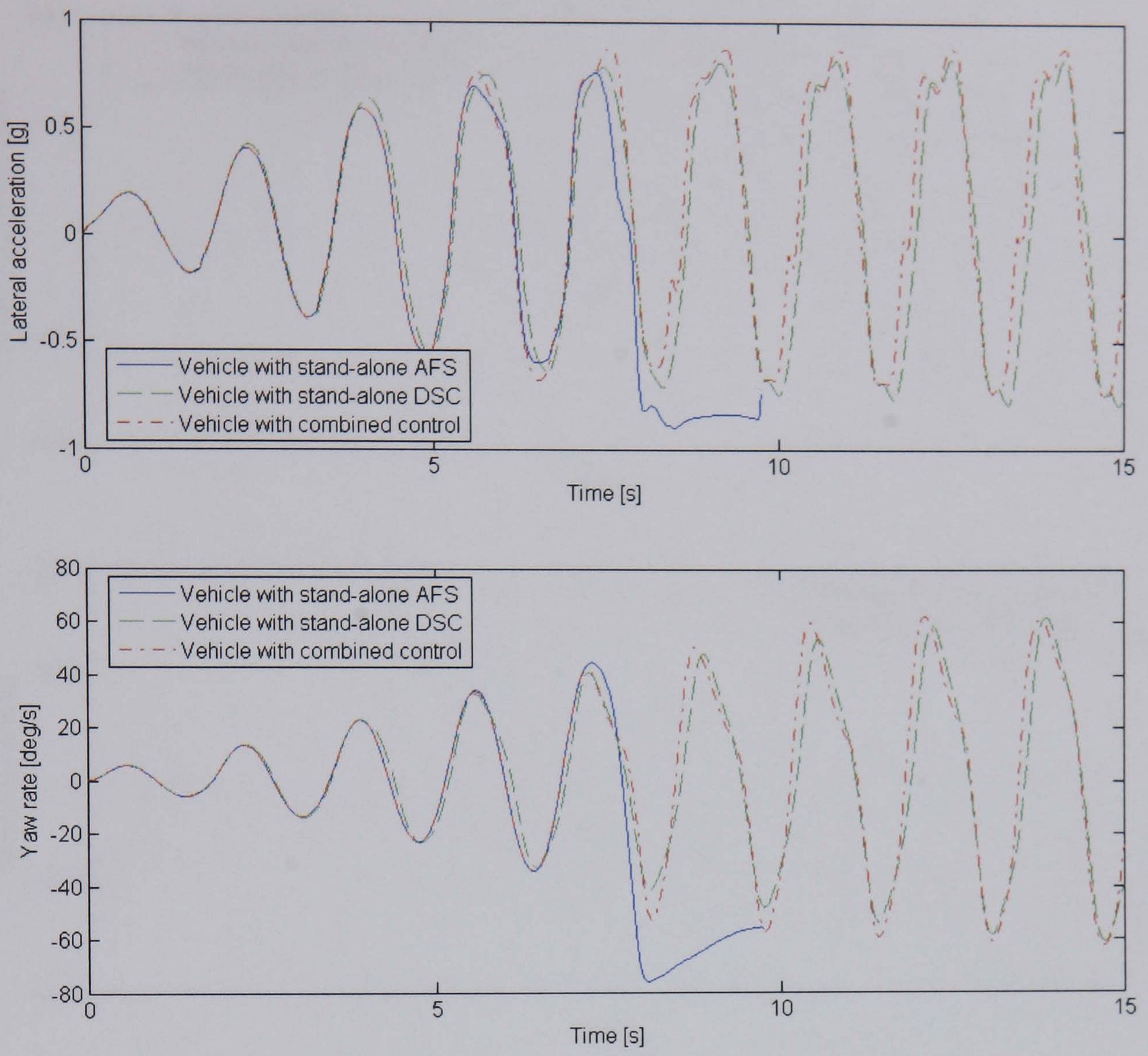

(a) Time response

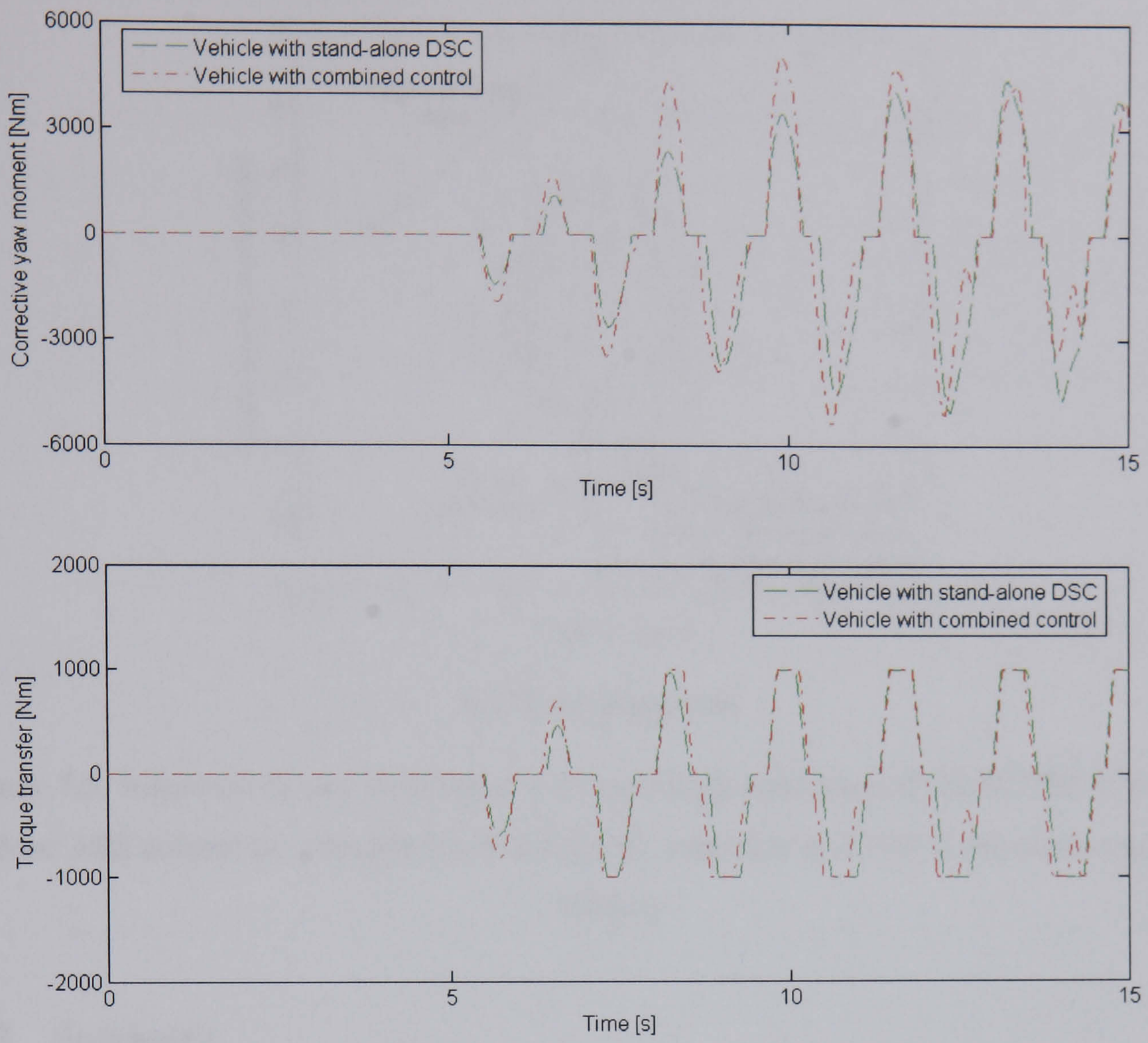

(b) Time response

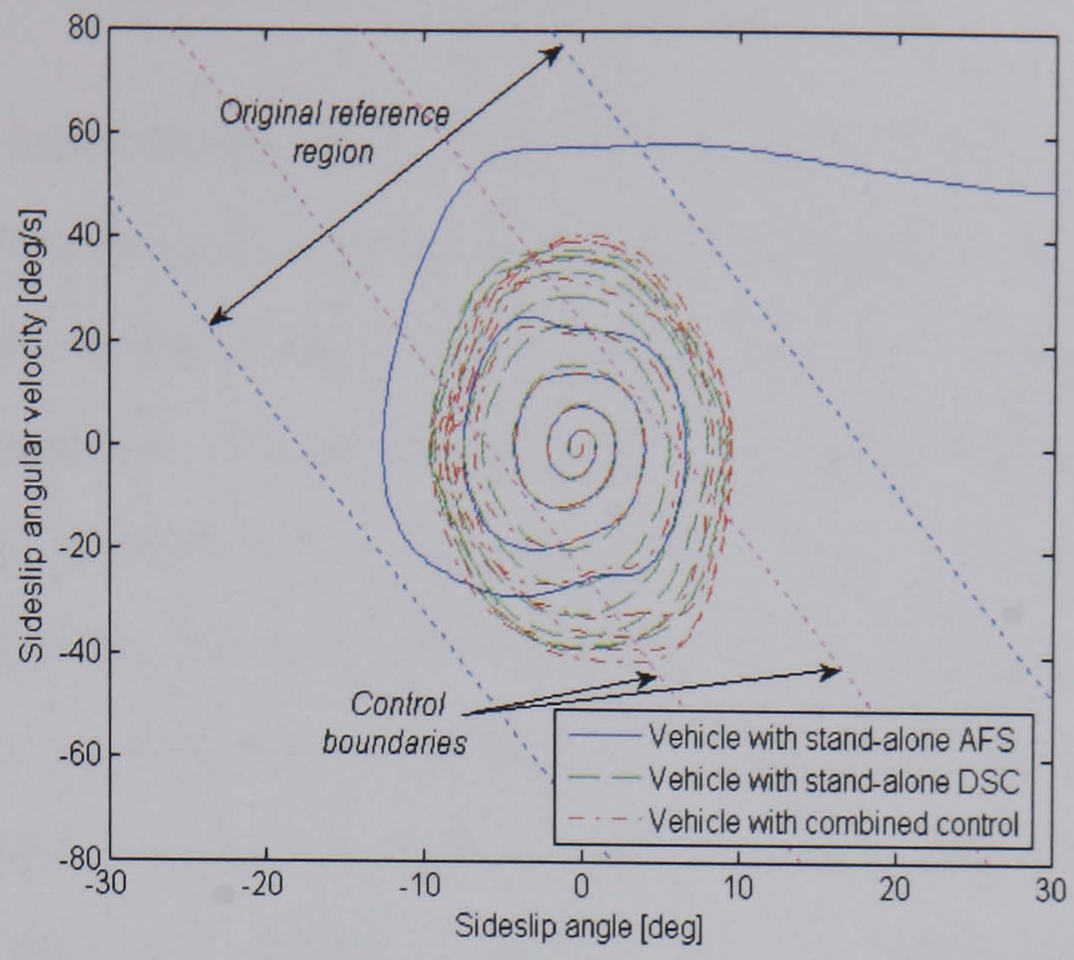

(c) Phase plane plot

Figure 7.5 Response to sine steer input with increasing amplitude of the NLVM with stand-alone AFS controller, with stand-alone stability controller and with combined control at 100km/h

7.2.3 Summary

This section has examined combined control of AFS and driveline plus brake based DSC and compared its performance with those of the corresponding stand-alone controllers.

This configuration does achieve both control objectives, steerability and stability through operating the two stand-alone subsystems in parallel. However, computer simulations have shown that the two stand-alone active subsystems cannot be optimised simultaneously through such a configuration. In other words, combined control cannot achieve the optimal individual control performance of both stand-alone subsystems. This is mainly due to the interferences between the two subsystems as a result of inharmonious control objectives.

Although the combined control configuration does not achieve an increase of the individual control objectives, it does provide a potential for improvement. This indeed raises the demand for integrated vehicle dynamics control which will be examined in the following section.

7.3 Integrated Vehicle Dynamics Control

Previous analyses have shown that on one hand different vehicle dynamics control systems do have their own functional limitations and none can be effective over the entire range of vehicle handling; on the other hand, due to undesirable interactions between different systems, operating these active systems in a combined fashion does not offer overall performance improvement over corresponding stand-alone subsystems. Therefore, some levels of integrated vehicle dynamics control need to be developed in order to achieve an improved vehicle handling performance. In this section an integrated vehicle dynamics control system will be designed using the bottom-up design approach introduced in Chapter 2 to exploit synergies and prevent interferences between different active subsystems.

7.3.1 Design objectives

As discussed previously, in order to improve vehicle steering response, the stand-alone steerability controller accelerates the yaw motion and consequently the sideslip motion of the vehicle. On the contrary, the stand-alone stability controller aims to bound the sideslip motion and thus the yaw motion of the vehicle to maintain vehicle stability during critical manoeuvres. Interferences between the two stand-alone controllers therefore do exist when the vehicle approaches the handling limit due to conflicts in control objectives.

Hence, in order to avoid undesirable interactions between the two stand-alone vehicle dynamics control subsystems and reduce performance trade-offs in vehicle handling, a novel rule based integration scheme is proposed to coordinate the control actions of the two stand-alone controllers. In light of the definition of control objective for the integrated vehicle dynamics control system in Chapter 4 (see Figure 4.13) and previous analyses of stand-alone active subsystems, the proposed integrated control system will be designed to achieve the following objectives:

- To improve vehicle steerability at low to mid-range lateral accelerations;
- To maintain vehicle stability close to and at the limit of handling;
- To minimize the influence of brake intervention on the longitudinal vehicle dynamics;

- To achieve seamless transition from one control task to the other.

7.3.2 Rule based integration scheme

The rule based integration scheme is directly related to the above objectives and will be described in more detail in this section.

This scheme needs to determine the activation sequences and active regions of the two stand-alone controllers in terms of the current vehicle operating point to avoid control objective conflicts. It is therefore necessary to measure the vehicle operating point. The operating point of the vehicle ranges from normal driving to limit handling. A quantitative measure of this is the lateral acceleration of the vehicle. However the relationship between the operating point and the lateral acceleration is a function of the road surface coefficient of friction. Since the road surface coefficient of friction is difficult to measure or estimate, it is inappropriate to use this metric in the integration scheme that is expected to perform under all road conditions. Therefore the β-$\dot{\beta}$ phase plane which has been shown to be robust to road surface friction variations in Chapter 6 will be used as a measure of the vehicle operating points.

Specifically, when the state trajectories of the vehicle remain inside the reference region defined in the β-$\dot{\beta}$ phase plane and stay far away from the control boundaries, the control priority is given to the steerability controller, i.e. the sole control task in this region is to improve steering response of the vehicle. When the vehicle state trajectories approach the control boundaries, the control task of improving vehicle steerability will gradually die away. As soon as the vehicle state trajectories cross the control boundaries and enter the unstable regions, the stability controller will become active and the steerability controller will be finally disabled, i.e. the control task transits from improving vehicle steerability to maintaining vehicle stability. The transition of control tasks is illustrated in Figure 7.6 where a fuzzy membership function is proposed to distinguish the current task, steerability or stability. The operating point is related to the control boundaries defined in Eq. (6.9) and the relative location of the current operating point to the control boundaries is measured by a straight line with the same slope as the control boundaries. Here the slope of the fuzzy membership function for the steerability task is roughly tuned to be

5. The switching strategy in Figure 7.6 aims to achieve a smooth transfer of control tasks, and consequently to avoid abrupt system responses which can be induced by sudden hard switching actions.

In addition, the integration scheme also needs to make the actuation decision, i.e. the required corrective yaw moment demanded by the stability controller will be distributed to the available actuators corresponding to the two active subsystems in order to delay the onset of brake intervention and consequently to reduce its influence on the longitudinal vehicle dynamics, i.e. active steering will be utilised to support DSC in maintaining vehicle stability when needed. In other words, the brake intervention will be performed only if the stabilising by active steering and torque transfer is not sufficient. Thus the driver can experience more driving pleasure.

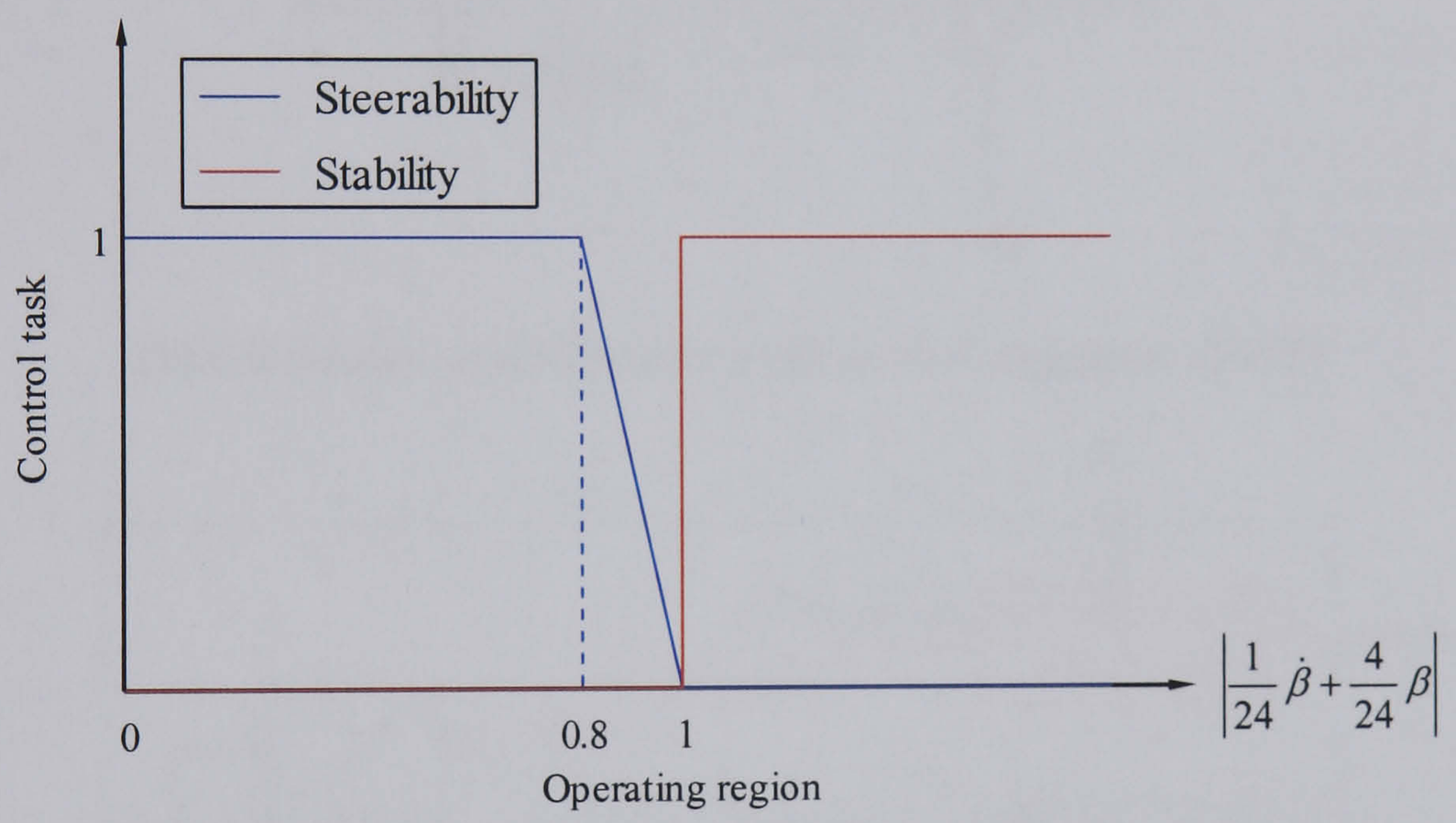

Figure 7.6 Transition of control tasks in the rule based integration scheme

Herein the required corrective yaw moment demanded by the stability controller can be transformed into an active steer angle input for AFS (see Figure 5.24) using similar method to the Brake Intervention Map of Figure 6.14 for the brake based DSC system. The distribution of the required corrective yaw moment to different actuation concepts are based on the analysis of control authority of different subsystems presented in Chapters 5 and 6. Figure 7.7 shows the complete structure of the proposed integrated control system. In the system block diagram, the desired yaw rate and the reference region are included in the corresponding controllers. Figure 7.8 illustratively describes the proposed integration scheme in the form of different regions in the β - $\dot{\beta}$ phase plane.

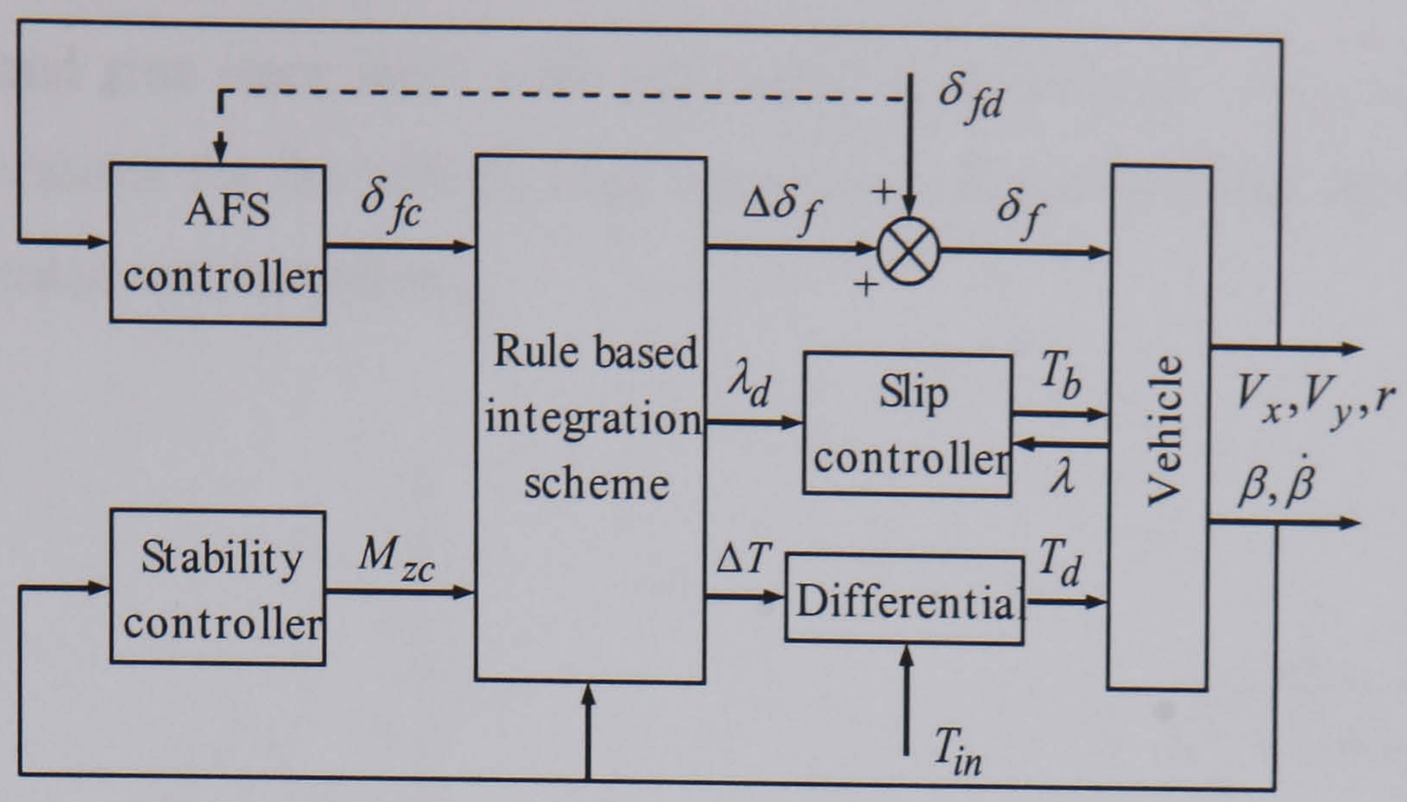

(a) Block diagram of the integrated vehicle dynamics control system

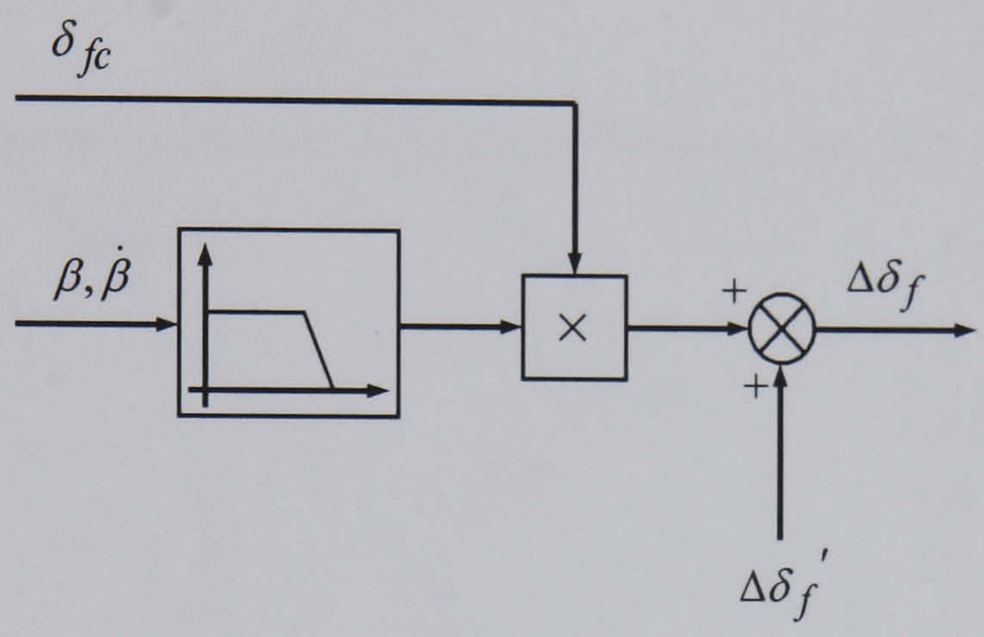

(b) Calculation of active steer angle in the integration scheme

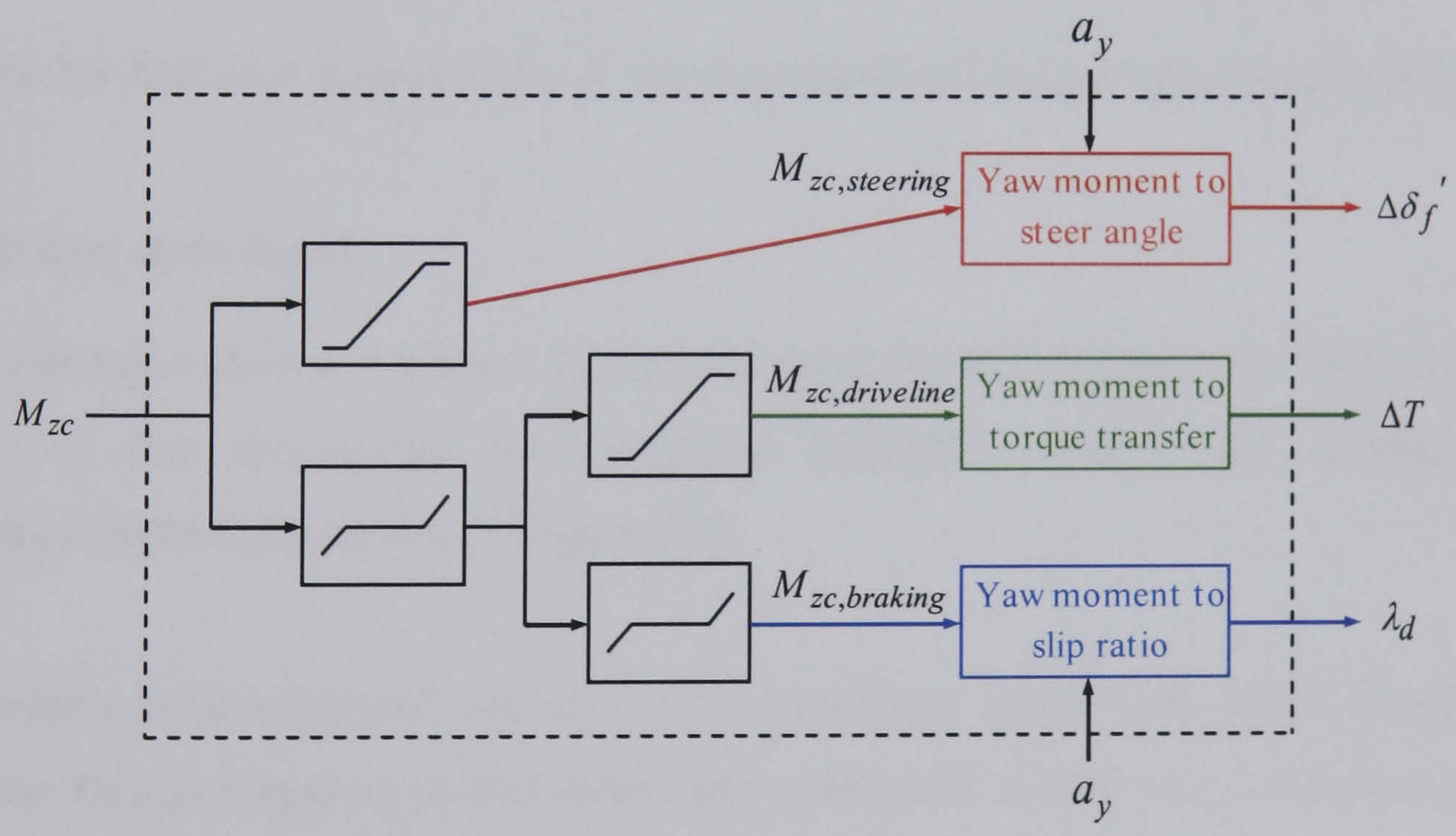

(c) Required corrective yaw moment distribution and interpretation

Figure 7.7 Schematics of the proposed integrated vehicle dynamics control system

7.3.3 Evaluation of the integrated vehicle dynamics control system

In order to assess the performance of the integrated vehicle dynamics control system designed above, computer simulations of the critical manoeuvres including single sine

steer input and sine steer input with increasing amplitude will be conducted on the NLVM and results for the vehicle with integrated control and with combined control will be presented and compared.

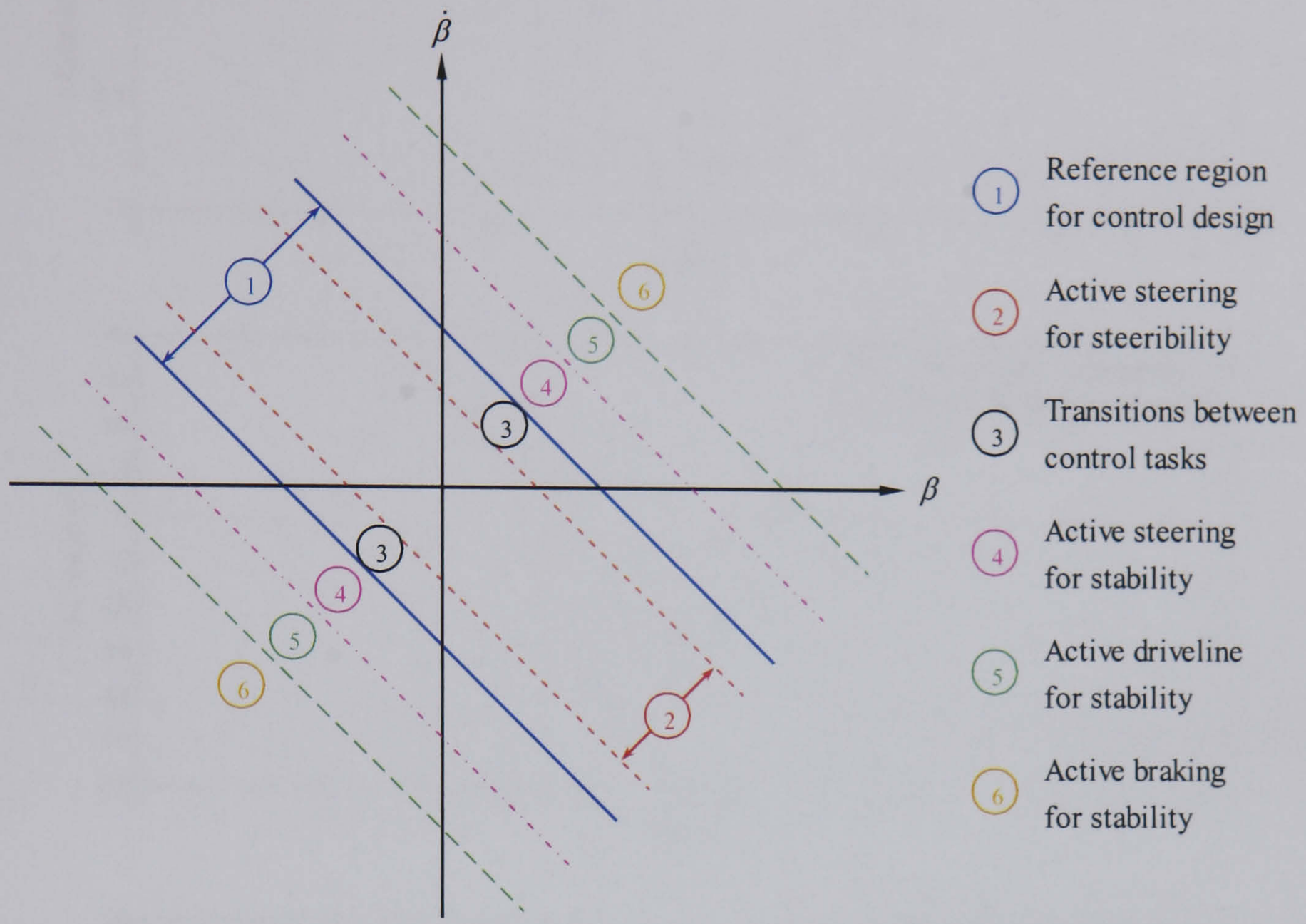

Figure 7.8 Different regions in the β - $\dot{\beta}$ phase plane for the rule based integration scheme

Single sine steer input

The steer input shown in Figure 7.2 is used again for this manoeuvre. The simulation results of this manoeuvre for integrated AFS/DSC control and corresponding combined control are shown in Figure 7.9.

The vehicle with integrated control is seen to achieve lower peak lateral acceleration and yaw rate in response to this steer input compared to that with combined control when the stability controller becomes active. The peak yaw rate reduces by 11% for integrated control in this specific manoeuvre. This is mainly due to the disablement of the steerability controller when the task of maintaining vehicle stability is dominant, as can be seen from the steerability control task response. When the vehicle approaches the handling limit or equivalently the vehicle state trajectories cross the control boundaries, the task of improving vehicle steerability will become zero and so will the acceleration of the yaw motion and sideslip motion induced by AFS.

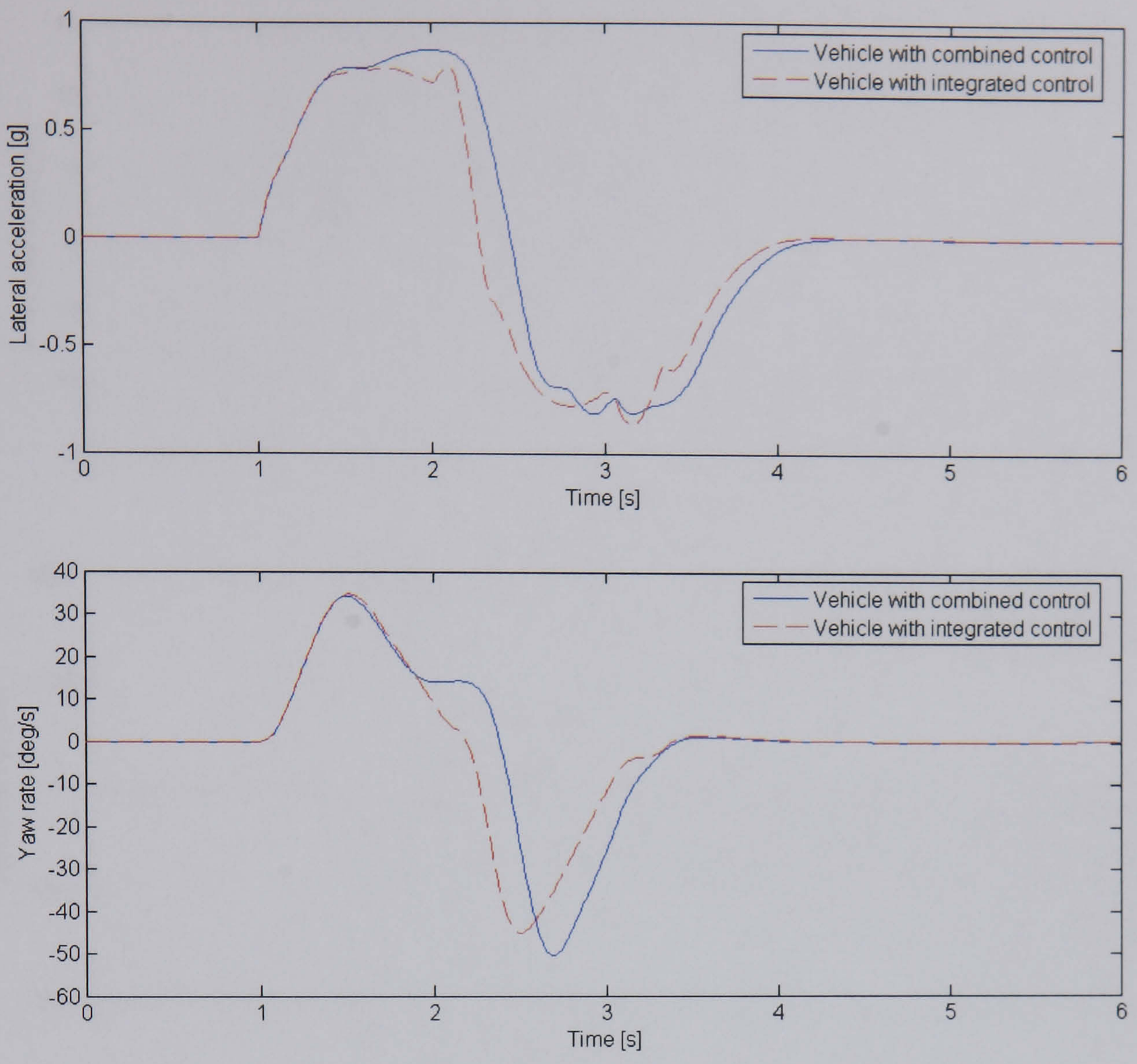

(a) Time response

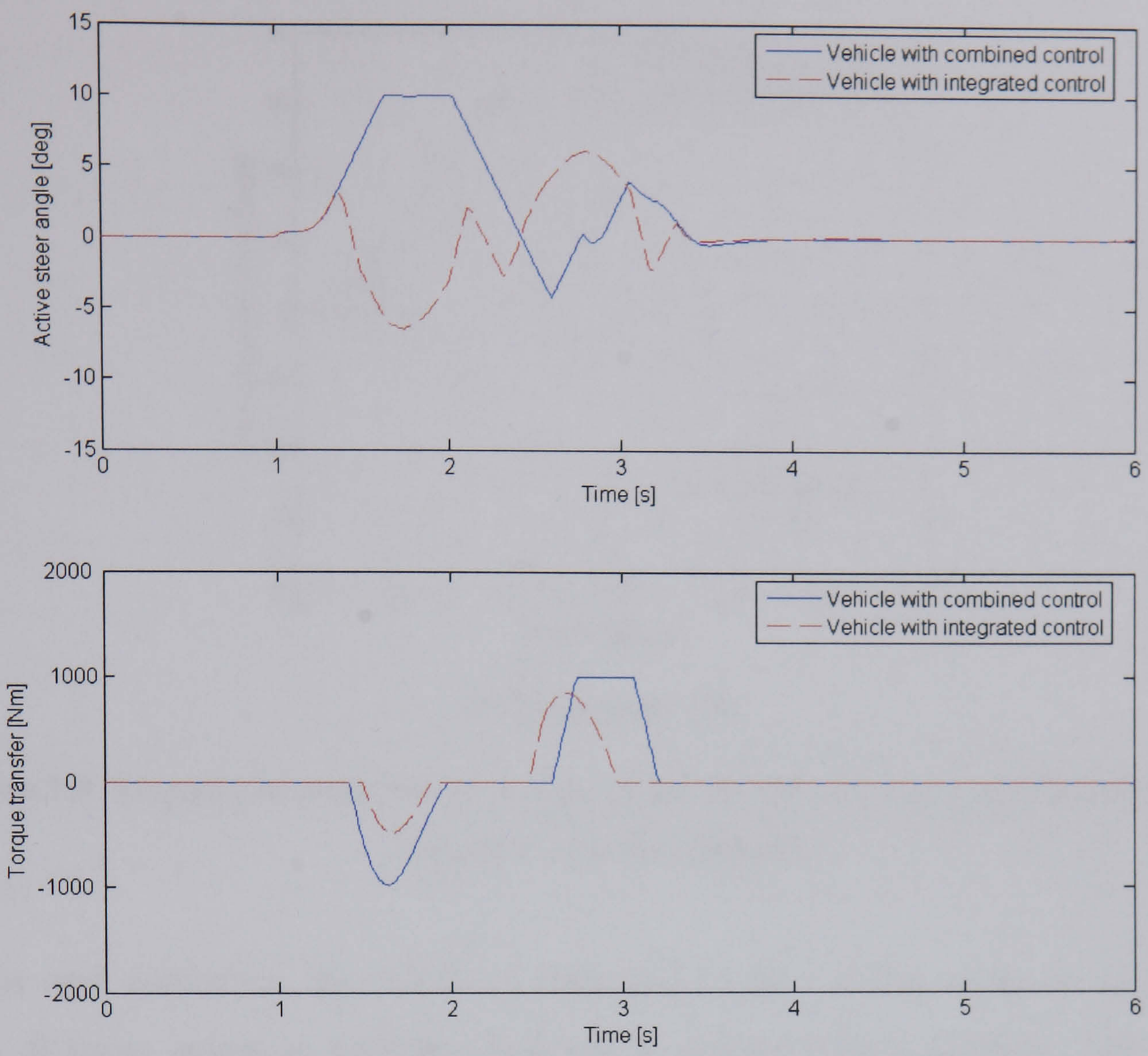

(b) Time response

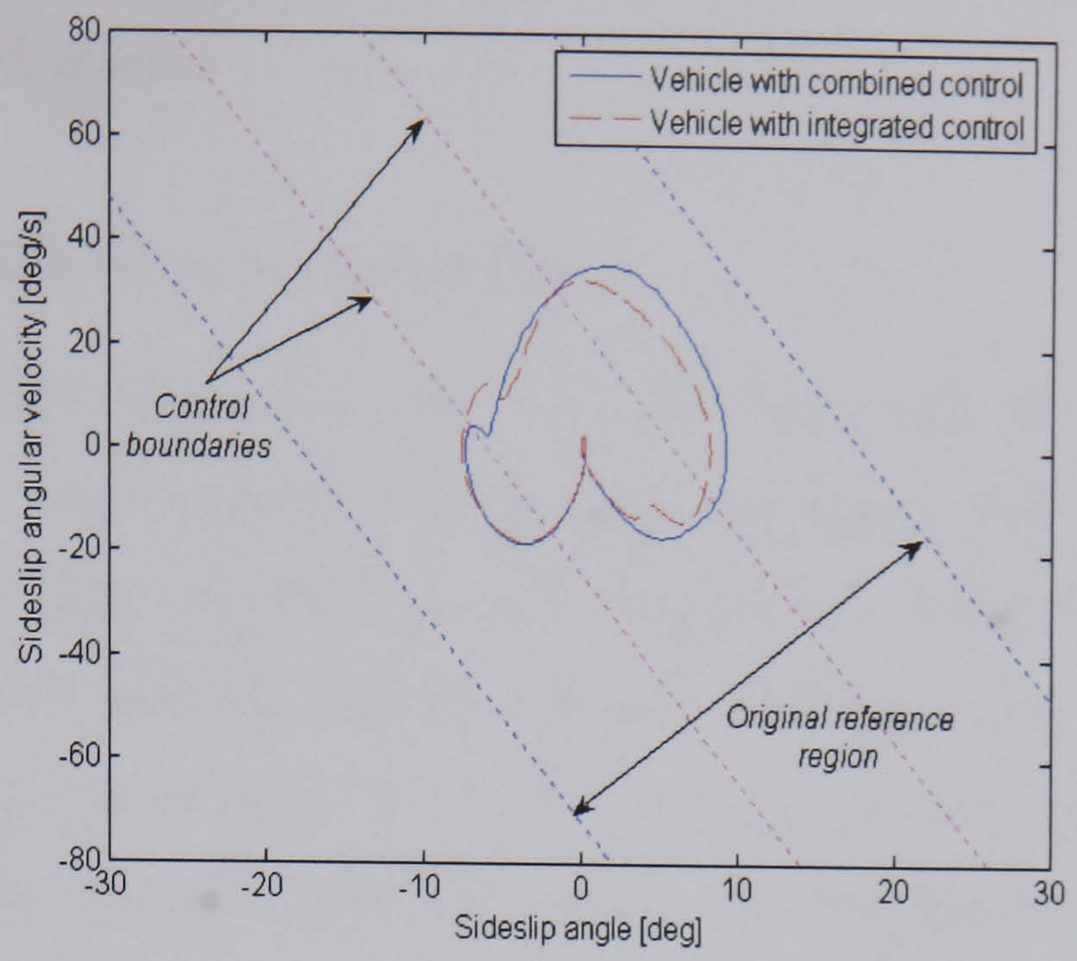

(c) Phase plane plot

Figure 7.9 Response to single sine steer input of the NLVM with combined control and with integrated control at 100km/h

Under such conditions, the vehicle is controlled by the stability controller on its own with different actuation concepts involved to ensure vehicle stability. That is, the conflicts in control objectives of the two stand-alone controllers are eliminated by the proposed integration scheme. Furthermore, when vehicle stability is in question, lateral acceleration and yaw rate will be further reduced by applying active countersteering to stabilise the vehicle, as can seen in the active steer angle response.

The sideslip behaviour of the controlled vehicle is presented in both time domain and phase plane. Similarly, the use of integrated control is seen to reduce the peak sideslip angle of the vehicle by 12%. Vehicle stability is therefore improved by the proposed integrated control system in comparison to corresponding combined control.

In addition, due to the support of steering function in maintaining vehicle stability, the amount of torque transfer is reduced and no brake intervention is required, i.e. in this specific manoeuvre, the task of maintaining vehicle stability can be completely performed by active steering and torque transfer. Hence the influence of brake intervention on the longitudinal vehicle dynamics is reduced, resulting in less reduction in the vehicle forward speed. Here the reduction in the vehicle forward speed is reduced by 44% for integrated control. This effect can be clearly seen from

the time responses of torque transfer, brake torques demanded by the slip controller and vehicle forward speed.

Sine steer input with increasing amplitude

The advantage of the integration scheme is also examined for the more aggressive manoeuvre of sine steer input with increasing amplitude. The steer input shown in Figure 7.4 is used again for this test. The simulation results of this manoeuvre are shown in Figure 7.10. Similar features found in the single sine steer input case can also be observed in this manoeuvre. The peak yaw rate and peak sideslip angle are found to reduce by 8% and 11% respectively for integrated control. Both torque transfer and brake intervention are successfully delayed and reduced. Most significantly, the final speed of the vehicle with integrated control is around 10km/h (20%) higher than that with combined control. This is enjoyable from the driver's perspective. Due to the high steer inputs and less reduction in the vehicle forward speed, the vehicle with integrated control finishes the simulation with slightly higher brake torques than that with combined control. This further confirms the analysis in Chapter 5, i.e. at the handling limit, when the driver steer inputs are large, the contra-cornering yaw moment generated by AFS is also relatively small.

7.3.4 Summary

A rule based integration scheme for integrated vehicle dynamics control has been developed in this section. This scheme aims to extend functionalities of individual subsystems and to minimise the undesirable interactions or functional overlaps between the two stand-alone subsystems AFS and DSC as so to avoid negative or detrimental effects on overall vehicle handling behaviour.

In comparison to combined control, the integration scheme proposed has been seen to offer extra improvements in overall vehicle handling characteristic. One effect observed includes a reduction in sideslip angle and consequently better vehicle stability. This, in turn, leads to delayed brake intervention and reduced influence on the longitudinal vehicle dynamics. In addition, the support of active steering intervention in maintaining vehicle stability also contributes to the delay of brake intervention and reduction in interference with the longitudinal vehicle dynamics.

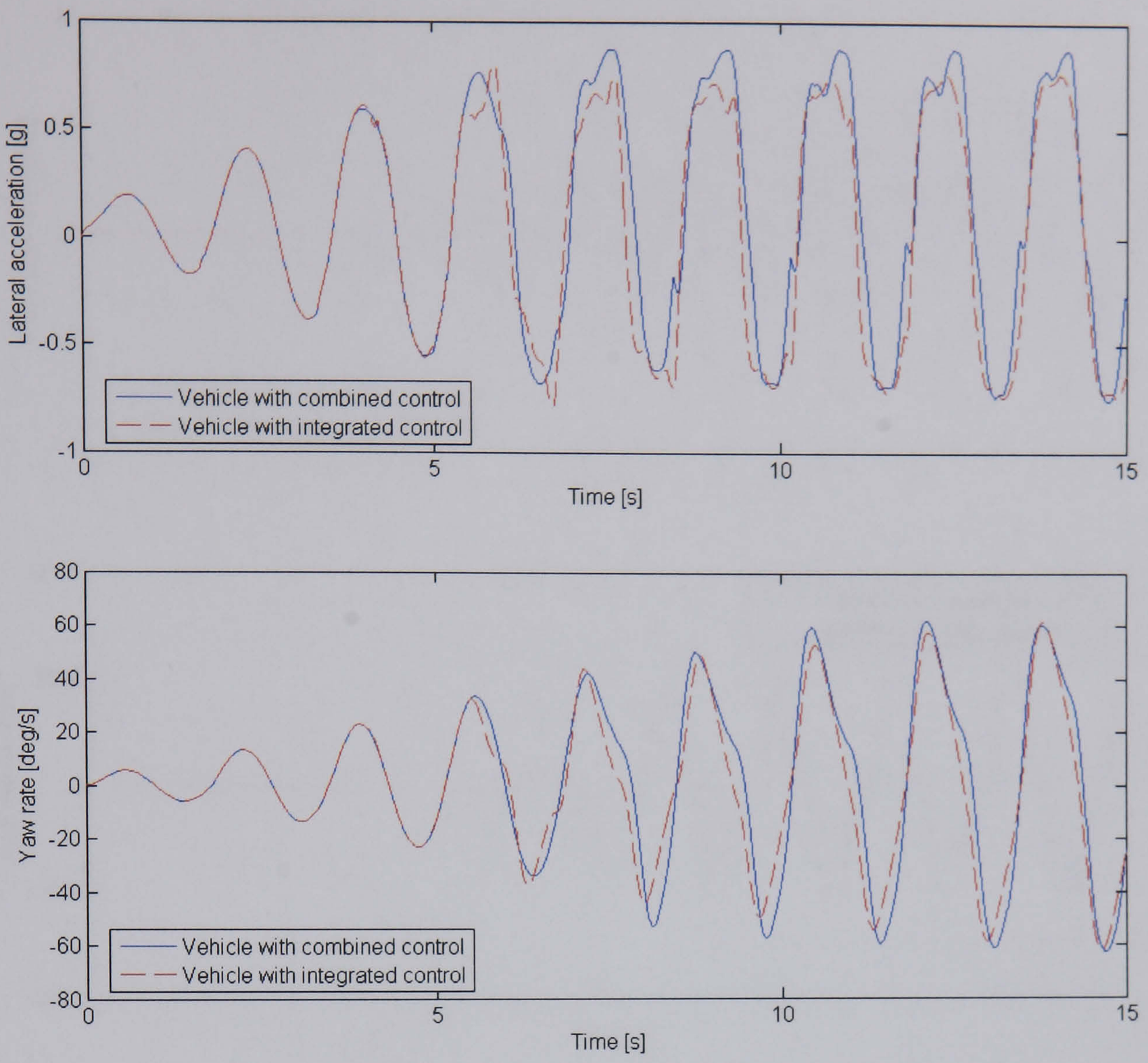

(a) Time response

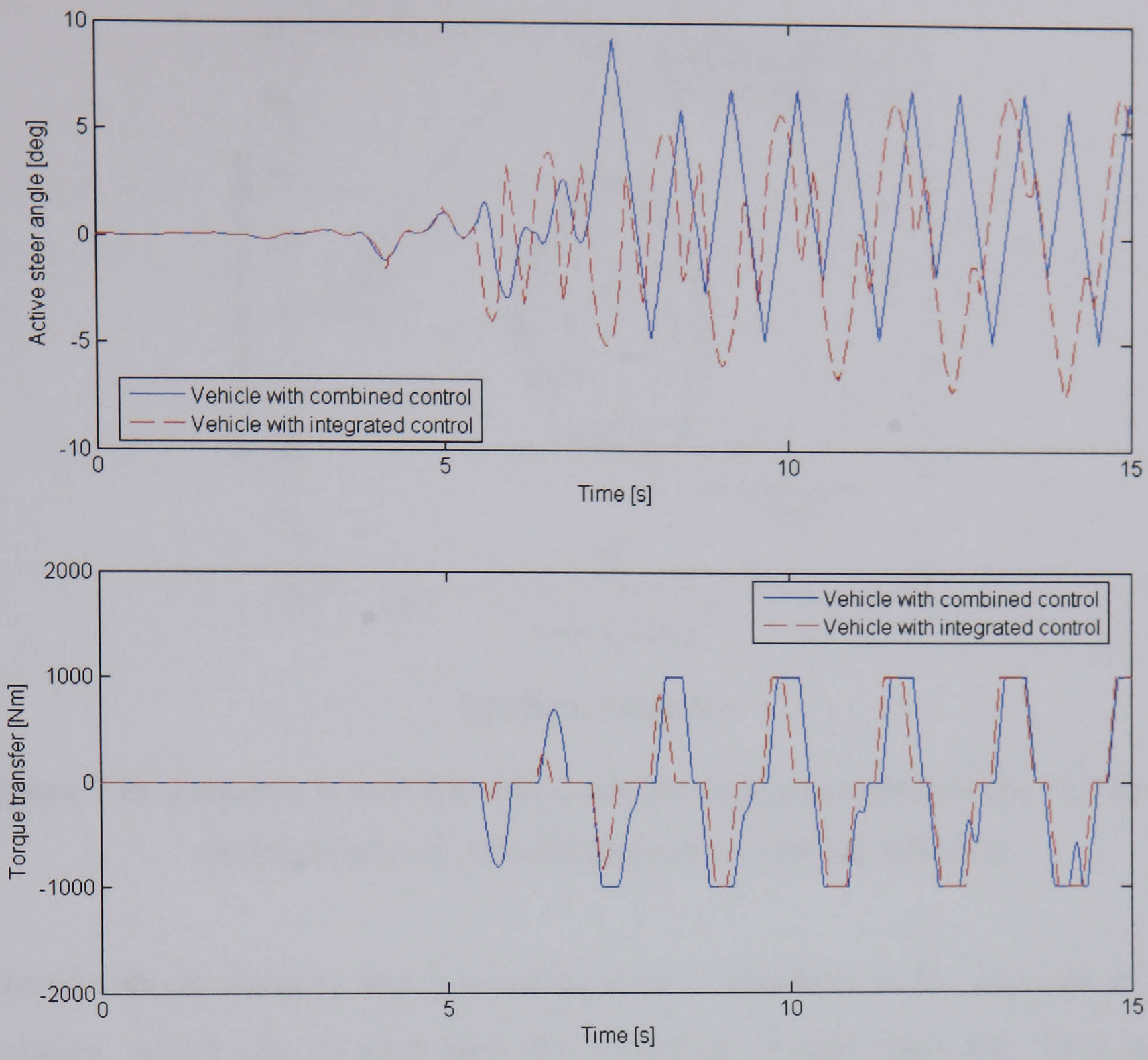

(b) Time response

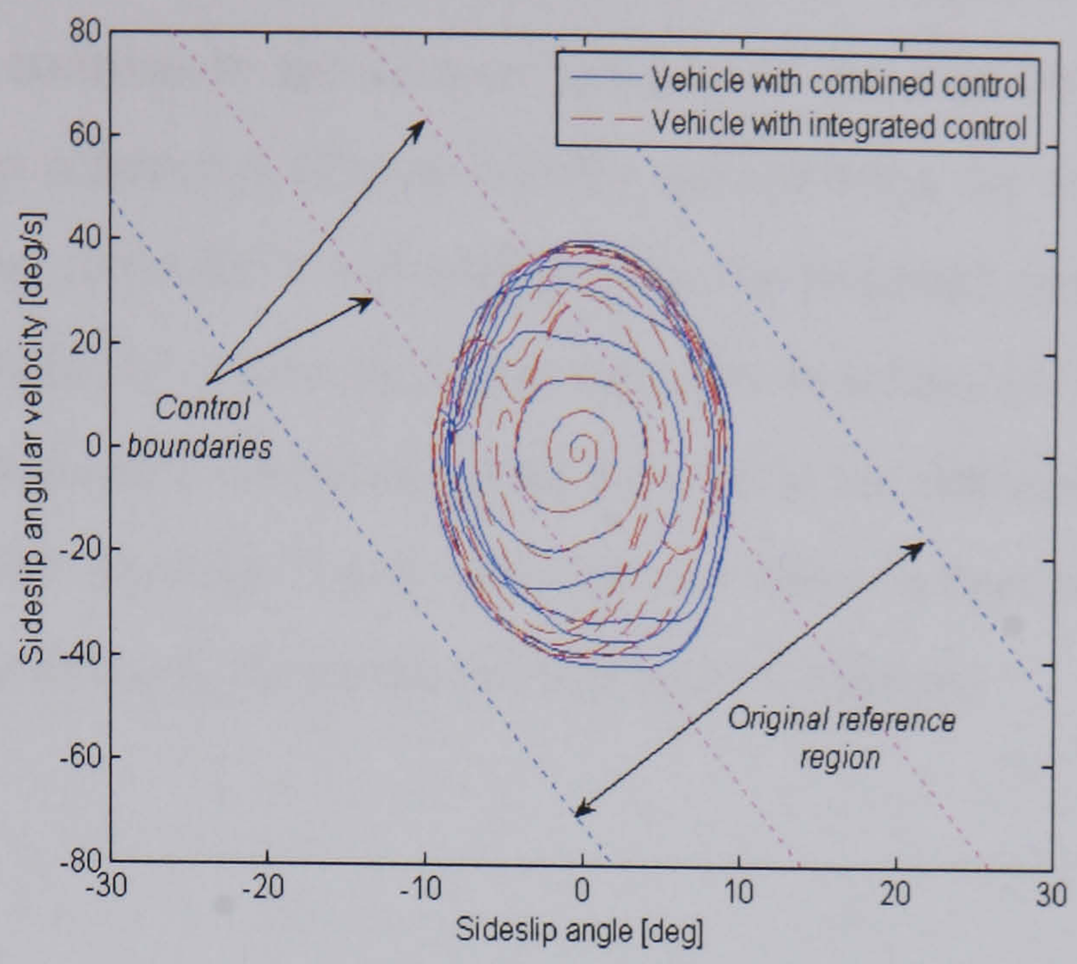

(c) Phase plane plot

Figure 7.10 Response to sine steer input with increasing amplitude of the NLVM with combined control and with integrated control at 100km/h

Improved vehicle stability at the handling limit is however at the expense of vehicle steerability, which can be seen from the reduction in peak yaw rate. This reduction could be viewed as subjectively undesirable. Therefore whilst the proposed integration scheme does provide a clear increase of the overall vehicle handling performance, it is not suggested that the scheme proposed here is optimal in all aspects of vehicle handling behaviour.

7.4 Conclusions

This chapter has presented the design of an integrated vehicle dynamics control system using the bottom-up design approach. A configuration of combined control of the two independently developed active subsystems, AFS and driveline plus brake based DSC, has been examined to form the benchmark for further integration analysis. Simulation results of combined control have shown that due to control objective conflicts between the two stand-alone controllers, such a configuration cannot achieve the overall performance improvement over the corresponding stand-alone active subsystems. This indicates a demand for integrated vehicle dynamics control.

Based on the analysis of combined control, a novel rule based integration scheme has been proposed to coordinate the control actions of the two stand-alone controllers. Such an integration scheme is responsible for determining the actuation sequences of the two stand-alone controllers and distributing the required corrective yaw moment demanded by the stability controller to the appropriate actuators. Computer simulation studies show that although the result obtained here is not optimal in terms of the yaw response, significant benefits have nevertheless been achieved in overall vehicle handling behaviour through the proposed integration scheme.

Chapter 8

Conclusions and Recommendations

Abstract: *In this chapter the results and achievements of this thesis are summarised. The conclusions are presented and recommendations for further research are proposed.*

8.1 Conclusions

Active control of vehicle dynamics has been shown to have the potential to lead to improved safety, performance and ease of use of vehicles. The increase in the number of stand-alone vehicle dynamics control systems in a vehicle can however result in increased system complexity, undesirable interactions and performance deterioration. Integrated vehicle dynamics control is a solution to this problem. It aims to achieve optimised overall vehicle performance by managing interactions between subsystems to avoid detrimental effects.

In order to investigate the current development of vehicle dynamics control for handling, a detailed review of literature relating to both stand-alone and integrated control systems for affecting vehicle handling has been performed and the conclusions have been drawn. In particular, consistent shortcomings in previous work were identified as:

- Inappropriate use of the necessary level of detail of linear and nonlinear vehicle models;
- Inappropriate range of realistic test conditions to assess the proposed controllers over a representative range of vehicle handling conditions;
- Weak definitions of the control objectives in relation to different vehicle handling regimes of interest;
- Lack of clarity of interactions between systems and approaches to system integration.

The review allowed a clear direction for this research to be defined and led to the aims and objectives outlined in Section 2.5. In order for these objectives to be met, the following work has been carried out and the relevant conclusions have been drawn.

To enable controller design and analysis of the lateral vehicle dynamics, the conventional 2DOF linear bicycle model and an 8DOF nonlinear handling model have been developed. The 8DOF model includes three planar motions of the vehicle, longitudinal, lateral and yaw plus body roll motion and the rotational dynamics of four wheels. The Pacejka Tyre Model has been utilised to model the nonlinear tyre characteristics under both pure and combined slip conditions. It has been concluded that the dominant nonlinear effects of the vehicle dynamics result from the highly nonlinear tyre properties since the tyres dominate in generating forces to determine the vehicle dynamics. The modelling complexity is in line with the scope of this work so as to avoid being overcomplicated for implementation convenience. Both models of an average passenger car have been implemented in Matlab/Simulink for the purpose of simulation.

Through studying both steady-state and transient handling characteristics of the passive vehicle, different aspects of the lateral vehicle dynamics and three distinct regions with respect to the level of lateral acceleration have been identified as a first step towards the definition of control objectives. Two distinct control objectives, steerability and stability which cover the whole range of vehicle handling have been defined. The corresponding control tasks can be assigned to any suitable active subsystems. The former objective is related to the steering response or handling

quality of a vehicle and corresponds to the low to mid lateral acceleration region of vehicle handling. The latter is characterised by the fact that the vehicle may spin or drift out in critical driving situations and corresponds to the high lateral acceleration manoeuvres. It has been shown that the task of improving vehicle steerability requires yaw rate control and maintaining vehicle stability needs to bound the sideslip motion of the vehicle. In addition, the relationship between the two control objectives established in this thesis over the entire range of vehicle handling has enabled a new control configuration to be proposed in which the control tasks, improving vehicle steerability and maintaining vehicle stability are scheduled as a function of vehicle operating points.

In order to optimise individual control tasks, the subsystem controllers have been designed independently. More specifically, the AFS and ARS controllers have been designed to perform the control task of improving vehicle steerability and the stability controller has been designed to fulfil sideslip motion bounding.

In the design of the active steering subsystem controllers, in order to achieve robustness with respect to system parameter variations (e.g. vehicle forward speed and road surface coefficient of friction) and external disturbances (e.g. split-μ braking), the SMC technique has been employed. To fully assess the performance of the stand-alone steerability controllers, a number of test manoeuvres which cover the complete range of lateral vehicle dynamics and the NLVM have been used. New results which clarify the relative performance properties of AFS and ARS have been presented. Of particular importance from a practical viewpoint is that these results have been generated over a range of different handling regimes of interest. It has been found that AFS and ARS are very effective in improving vehicle steering response up to the limit of handling but they fail to bound the sideslip motion of the vehicle at the handling limit due to the limitations of the control strategy. In addition, the proposed AFS and ARS controllers have been proven to be robust to parameter variations and external disturbances.

In order to choose the appropriate active steering subsystem for the final integration, a comparative study of AFS and ARS in terms of the ability to generate the required

corrective yaw moment has been performed. This study has shown that ARS is less capable of generating contra-cornering yaw moment than AFS when the handling limit is approached.

The dynamic stability subsystem controller which is based on the β - $\dot{\beta}$ phase-plane method for assessing vehicle stability has been designed and found to be capable of performing the task of maintaining vehicle stability at the operating points where the active steering subsystems cannot. Both driveline based and brake based DSC subsystems have been developed based on the same stability controller and have been evaluated on the NLVM through critical handling manoeuvres. New results which compare the relative merits of the driveline based and brake based DSC subsystems have been presented.

It has been found that the driveline based DSC subsystem is highly likely to cause the front inner wheel with excessive torque applied to spin due to lateral load transfer during cornering and thus result in loss of vehicle direction or worsen vehicle instability. In other words, the driveline based DSC subsystem cannot completely replace its brake based counterpart. In addition the inherent interference with the longitudinal vehicle dynamics of the brake intervention limits the application of the brake based DSC subsystem to extreme driving situations. Therefore, in order to complement each other, a new DSC subsystem based on a combination of torque transfer and single-wheel braking has been proposed. In the new subsystem the brake intervention has been favoured. Simulations using a reasonably realistic model of the left/right torque transfer differential have shown subtle, but significant improvements compared to the brake based DSC subsystem.

Combined control of the two aforementioned active subsystems, AFS and driveline plus brake based DSC has been examined and found to be unable to achieve overall vehicle performance improvement over the corresponding stand-alone controllers. This study has shown that conflicts in control objectives hinder the simultaneous optimisation of the two control tasks, improving vehicle steerability and maintaining vehicle stability.

In order to optimise overall vehicle performance over a broad range of handling regimes, a novel integrated control strategy for AFS and driveline plus brake based DSC has been proposed. In this new control configuration, the two control objectives, steerability and stability have both been taken into consideration and the use of the β-$\dot{\beta}$ phase plane has been extended from purely describing vehicle stability to quantitatively measuring vehicle operating points. Based on this measure of vehicle operating points, a rule based integration scheme has been developed to coordinate the control actions of the two stand-alone controllers.

The proposed integrated control system has been assessed on the NLVM by comparing it to corresponding combined control under critical driving conditions. Simulation results have shown that it offers significant improvements in overall vehicle handling behaviour, resulting in better vehicle stability and reduced influence on the longitudinal vehicle dynamics.

Specifically, with respect to the aims and objectives of this thesis, the following has been achieved:

- Through a thorough analysis of the lateral vehicle dynamics over the entire range of vehicle handling, an objective definition of the control task has been developed. This involved separating the overall handling requirements into two distinct aspects: steerability and stability. This new characterisation of the vehicle handling performance into distinct regimes was then used in the proposal of a novel integration scheme, involving a coordination of active steering and dynamic stability control.

- Two categories of active subsystems, including AFS, ARS, driveline based DSC and brake based DSC, have been developed. New simulation results, which have been generated over a range of different handling regimes of interest, have clarified the relative performance properties of the same category of active subsystem. These analyses have indeed led to the proposal of a new DSC subsystem based on a combined actuation concept and facilitated the choice of appropriate active subsystems for the final integration design.

- Based on the extended use of the β-$\dot{\beta}$ phase plane, a metric, that is used to measure the vehicle operating points, has been proposed. In the novel rule based integration scheme, this metric was used, through a fuzzy membership function, to arbitrate between the stand-alone steerability controller and the stand-alone stability controller. The benefits in overall vehicle handling performance available from the proposed integrated control system have been quantitatively assessed through critical test manoeuvres. In comparison to combined control, the integrated control system has been found to lead to a trade-off between stability and limit steerability, improved vehicle stability and reduced influence on the longitudinal vehicle dynamics.

8.2 Recommendations for Further Work

This thesis has proposed a novel approach to integrated vehicle dynamics control for handling. The objectives stated in Section 2.5 have been achieved. However, in the light of work undertaken in this thesis, some possible areas are considered to require further investigation in future research.

As a generic structure, the proposed approach to integration is not limited to the two active subsystems examined in this thesis. Active roll moment distribution control can also be added to the integrated control system as control authority of RMD increases with lateral acceleration. RMD may be a useful tool to be coordinated with AFS/ARS and DSC to influence the lateral vehicle dynamics at mid to high-range lateral accelerations. In addition, along with the time based test procedures used in this thesis, the analysis in the frequency domain may be carried out to assess the proposed controllers.

The vehicle dynamics controllers designed in this thesis serve as the secondary controller to assist the primary controller, driver in handling the vehicle. There is however one key aspect of the vehicle system not covered in this thesis, and this concerns the role of the driver and his/her interactions with the vehicle dynamics control systems. In everyday driving, the driver and the vehicle indeed form a closed-loop system and interact with external environment (e.g. other vehicles and highway

systems). Therefore, in order to fully assess the control performance, implementation of the controllers on an actual vehicle platform and subjective evaluation by an actual driver must be an eventual goal. In case of practical implementation, additional dynamics such as the steering system dynamics, the driveline dynamics and the actuator dynamics should be taken into account. In addition, the accurate estimation of the vehicle sideslip angle for dynamic stability control will be one of the most difficult technical subjects.

The global or fully centralised concept through the top-down design approach may be the final solution to integrated vehicle dynamics control. In such control architectures, all aspects of vehicle dynamics will be controlled as a whole and the interactions between subsystems will be taken into consideration in the design of the global or central vehicle dynamics controller. Such a controller is usually designed using multivariable control techniques and thus accurate measure or estimation of all vehicle states and time-consuming control computation may become the major practical constraints in control system design. Research in this field is currently ongoing whereas more work still needs to be done before they become commercially viable.

References

Abe, M. (1992) "Roll moment distribution control in active suspension for improvement of limit performance of vehicle handling," *SAE Paper*, 923068.

Abe, M., Ohkubo, N., and **Kano, Y.** (1996) "A direct yaw moment control for improving limit performance of vehicle handling – comparison and cooperation with 4WS -," *Vehicle System Dynamics Supplement*, Vol. 25, pp. 3-23.

Abe, M. (1999) "Vehicle dynamics and control for improving handling and active safety: from 4WS to DYC," *Proceedings of the I Mech E Part K: Journal of Multi-body Dynamics*, Vol. 213, No. 2, pp. 87-101.

Abe, M., Kano, Y., Shibahata, Y. and **Furukawa, Y.** (1999) "Improvement of vehicle handling safety with vehicle side-slip control by direct yaw moment," *Vehicle System Dynamics Supplement*, Vol. 33, pp. 665-679.

Abe, M., Kano, Y., Suzuki, K., Shibahata, Y. and **Furukawa, Y.** (2001) "Side-slip control to stabilize vehicle lateral motion by direct yaw moment," *JSAE Review*, Vol. 22, No. 4, pp. 413-419.

Ackermann, J. (1990) "Robust car steering by yaw rate control," *Proc. of IEEE Conf. Decision Contr.*, pp. 2033-2034.

Ackermann, J. and **Sienel, W.** (1993) "Robust yaw damping of cars with front and rear wheel steering," *IEEE Trans. on Control Systems Technology*, Vol. 1, No. 1, pp. 15-20.

Ackermann, J. (1994) "Yaw rate and lateral acceleration feedback for four-wheel steering," *Proc. of the 2nd Int. Symposium on Advanced Vehicle Control, AVEC '94*, pp. 165-170.

Ackermann, J., Bünte, T., Sienel, W., Jeebe, H. and **Naab, K.** (1996) "Driving safety by robust steering control," *Proc. of the 3rd Int. Symposium on Advanced Vehicle Control, AVEC'96*, pp. 377-394.

Ackermann, J. (1997) "Robust Control Prevents Car Skidding," *IEEE Control Systems Magazine*, Vol. 17, No. 3, pp. 23-31.

Ackermann, J. and **Bünte, T.** (1997) "Yaw disturbance attenuation by robust decoupling of car steering," *Control Eng. Practice*, Vol. 5, No. 8, pp. 1131-1136.

Aga, M., Kusunoki, H., Saitoh, R. and **Ito, M.** (1990) "Design of 2-degree-of-freedom control system for active front-and-rear-wheel steering," *SAE Paper*, 901746.

Alberti, V. and **Babbel, E.** (1996) "Improved driving stability by active braking of the individual wheels," *Proc. of the 3rd Int. Symposium on Advanced Vehicle Control, AVEC'96*, pp. 717-732.

Alleyne, A. and **Hedrick, J.K.** (1995) "Nonlinear adaptive control of active suspensions," *IEEE Trans. on Control Systems Technology*, Vol. 3, No. 1, pp. 94-101.

Buckholtz, K. (2002) "Use of fuzzy logic in wheel slip assignment - Part I: yaw rate control," *SAE Paper*, 2002-01-1221.

Buckholtz, K. (2002) "Use of fuzzy logic in wheel slip assignment - Part II: yaw rate control with sideslip angle limitation," *SAE Paper*, 2002-01-1220.

Buckholtz, K. (2002) "Reference input wheel slip tracking using sliding mode control," *SAE Paper*, 2002-01-0301.

Clover, C.L. and **Bernard, J.E.** (1998) "Longitudinal tyre dynamics," *Vehicle System Dynamics*, Vol. 29, No. 3, pp. 231-259.

Coelingh, E., Chaumette, P. and **Andersson, M.,** (2002) "Open-interface definitions for automotive systems application to a brake by wire system," *SAE Paper*, 2002-01-0267.

Crolla, D.A. (1992) *An introduction to vehicle dynamics*, School of Mechanical Engineering, University of Leeds, UK.

Crolla, D.A., Brown, M.D., Manning, W.J. and **Selby, M.A.** (2000) *IVMC: Intelligent vehicle motion control*, Progress report, School of Mechanical Engineering, University of Leeds.

Demerly, J.D. and **Youcef-Toumi, K.** (2000) "Non-linear analysis of vehicle dynamics (NAVDyn): a reduced order model for vehicle handling analysis," *SAE Paper*, 2000-01-1621.

Dixon, J.C. (1996) *Tire, Suspension and Handling*, Second Edition, Society of Automotive Engineers, Warrendale.

Doniselli, C., Mastinu, G., and **Cal, R.** (1993) "Traction control for front-wheel-drive vehicles," *Proceedings of 13th IAVSD Symposium*, pp. 87-104.

Esmailzadeh, E., Vossoughi, G.R. and **Goodarzi, A.** (2001) "Dynamic modelling and analysis of a four motorised wheels electric vehicle," *Vehicle System Dynamics*, Vol. 35, No. 3, pp. 163-194.

Esmailzadeh, E., Goodarzi, A. and **Vossoughi, G.R.** (2002) "Directional stability and control of four-wheel independent drive electric vehicles," *Proc. Instn. Mech. Engrs. Part K: J Multi-body Dynamics*, Vol. 216, No. 4, pp. 303-313.

Everett, N., Brown, M. and **Crolla, D.** (2000) "Investigation of the integration of a roll control system and a traction force distribution system for an off-road vehicle," *Proc. of the 5th Int. Symposium on Advanced Vehicle Control, AVEC 2000.*

Fujika, T. and **Yanase, N.** (1994) "Torque split control for electric vehicle with 4-wheel direct-drive motors," *Proc. of the 2nd Int. Symposium on Advanced Vehicle Control, AVEC '94*, pp. 122-127.

Fujita, K., Ohashi, K. and **Fukatani, K.** (1998) "Development of active rear steer system applying H_∞-μ synthesis," *SAE Paper*, 981115.

Fukui, K., Miki, K., Hayashi, Y., and **Hasegawa, J.** (1988) "Analysis of driver and a four wheel steering vehicle system using a driving simulator," *SAE Paper*, 880641.

Furukawa, Y., Yuhara, N. and **Takeda, H.** (1989) "A review of four-wheel steering studies from the viewpoint of vehicle dynamics and control," *Vehicle System Dynamics*, Vol. 18, pp. 151-186.

Furukawa, Y. and **Abe, M.** (1996) "On-board-tyre-model reference control for cooperation of 4WS and direct yaw moment control for improving active safety of vehicle handling," *Proc. of the 3rd Int. Symposium on Advanced Vehicle Control, AVEC'96*, pp. 507-526.

Furukawa, Y. and **Abe, M.** (1997) "Advanced chassis control systems for vehicle handling and active safety," *Vehicle System Dynamics*, Vol. 28, pp. 59-86.

Gianone, L., Palkovics, L. and **Bokor, J.** (1995) "Design of an active 4WS system with physical uncertainties," *Control Engineering Practice*, Vol. 3, No. 8, pp. 1075-1083.

Gillespie, Thomas D. (1992) *Fundamentals of vehicle dynamics*, Society of Automotive Engineers, Warrendale.

Gordon, T., Howell, M. and **Brandao, F.** (2003) "Integrated control methodologies for road vehicles," *Vehicle System Dynamics*, Vol. 40, Nos. 1-3, pp. 157-190.

Güvenc, B.A., Bünte, T., Odenthal, D. and **Güvenc, L.** (2001) "Robust two degree of freedom vehicle steering controller design," *Proc. of the American Control Conference*, pp. 13-18.

Hac, A. and **Bodie, M.O.**, (2002) "Improvements in vehicle handling through integrated control of chassis systems," *Int. J. of Vehicle Design*, Vol. 29, Nos. 1/2, pp. 23-50.

Hancock, M.J. and **Williams, R.A.** (2003) "The use of active differentials in vehicle dynamics control," *Proc. of 16th Int. Conf. on Systems Engineering, ICSE'2003*, pp. 231-236.

Hattori, Y., Koibuchi, K. and **Yokoyama, T.** (2002) "Force and moment control with nonlinear optimum distribution for vehicle dynamics," *Proc. of the 6th Int. Symposium on Advanced Vehicle Control, AVEC'02*, pp. 595-600.

Higuchi, M., Kusaka, K., Shibusawa, K., Hirata, H. and **Tsukagoshi, M.** (1996) "Handling analysis and prediction during cornering," *Proc. of the 3rd Int. Symposium on Advanced Vehicle Control, AVEC '96*, pp. 1027-1036.

Hirano, Y., Sato, Y., Ono, E. and **Takanami, K.** (1992) "Integrated control system of 4WS and 4WD by H_∞ control," *Proc. of the 1st Int. Symposium on Advanced Vehicle Control, AVEC '92*, pp. 419-423.

Hirano, Y., Ono, E., Harada, H. and **Takanami, K.** (1993) "Development of an integrated system of 4WS and 4WD by H_∞ control," *SAE Paper*, 930267.

Hirano, Y. (1994) "Non-linear robust control for an integrated system of 4WS and 4WD," *Proc. of the 2nd Int. Symposium on Advanced Vehicle Control, AVEC '94*, pp. 147-152.

Hirano, Y. and **Fukatani, K.** (1996) "Development of robust active rear steering control," *Proc. of the 3rd Int. Symposium on Advanced Vehicle Control, AVEC'96*, pp. 359-375.

Horiuchi, S., Yuhara, N. and **Takei, A.** (1996) "Two degree of freedom/ H_∞ controller synthesis for active four wheel steering vehicles," *Vehicle System Dynamics Supplement*, Vol. 25, pp. 275-292.

Horiuchi, S., Okada, K. and **Nohtomi, S.** (1998) "Integrated control of four wheel steering and wheel torques using nonlinear predictive controller," *Proc. of the 4th Int. Symposium on Advanced Vehicle Control, AVEC'98*, pp. 111-116.

Horiuchi, S., Okada, K. and **Nohtomi, S.** (1999) "Improvement of vehicle handling by nonlinear integrated control of four wheel steering and four wheel torque," *JSAE Review*, Vol. 20, No. 4, pp. 459-464.

Huchtkoetter, H. and **Klein, H.** (1996) "The effect of various limited slip differentials in front wheel drive vehicles on handling and traction," *SAE Paper*, 960717.

Huh, K. and **Kim, J.** (2001) "Active steering control based on the estimated tire forces," *J. of Dynamic Systems, Measurement and Control*, Vol. 123, No. 3. pp. 505-511.

Ikushima, Y. and **Sawase, K.** (1995) "A study on the effects of the active yaw moment control," *SAE Paper*, 950303.

Inagaki, S., Kshiro, I. and **Yamamoto, M.** (1994) "Analysis on vehicle stability in critical cornering using phase-plane method," *Proc. of the 2nd Int. Symposium on Advanced Vehicle Control, AVEC'94*, pp. 287-292.

Itkis, Y. (1976) *Control systems of variable structure*, Wiley, New York.

Jackson, A.E. (2003) *Intelligent mobility control of a hybrid electric off-road vehicle with individual wheel control*, PhD Dissertation, University of Leeds, UK.

Kazemi, R., Hamedi, B. and **Javadi, B.** (2000) "A new sliding mode controller for four-wheel anti-lock braking system (ABS)," *SAE Papers*, 2000-01-1639.

Kim, C. and **Ro, P.I.** (1998) "A sliding mode controller for vehicle active suspension systems with non-linearities," *Proc. Instn. Mech. Engrs., Part D: Journal of Automobile Engineering*, Vol. 212, No. 2, pp. 79-92.

Kleine, S. and **Van Niekerk, J.** (1998) "Modelling and control of a steer-by-wire vehicle," *Vehicle System Dynamics Supplement,* Vol. 28, pp. 114-142.

Koibuchi, K., Yamamoto, M., Fukada, Y. and **Inagaki, S.** (1996) "Vehicle stability control in limit cornering by active brake," *SAE Papers*, 960487.

Konik, D., Bartz, R., Bärnthol, F., Bruns, H., and **Wimmer, M.** (2000) "Dynamic drive - the new active roll stabilization system from the BMW Group - system description and functional improvements," *Proc. of the 5th Int. Symposium on Advanced Vehicle Control, AVEC 2000.*

Kuriki, N. and **Shibahata, Y.** (1998) "Development of active torque transfer system," *FISITA 1998 World Automotive Congress*, F98T065.

Kwak, B. and **Park, Y.** (2000) "Robust vehicle stability controller by multiple sliding mode control," *Proc. of the 5th Int. Symposium on Advanced Vehicle Control, AVEC 2000.*

Lakehal-ayat, M. and **Diop, S.** (2002) "A combined suspension and brake control for a cornering vehicle," *Proc. of the 6th Int. Symposium on Advanced Vehicle Control, AVEC'02.*

Lin, Y. (1992) "Improving vehicle handling performance by a closed-loop 4WS driving controller," *SAE Paper*, 921604.

Lukowshi, S.A., Chu, M.L., Tener, D.R. and **Claar, P.W.** (1990) "Open-loop, fixed-control simulation of a vehicle undergoing steering and acceleration maneuvers," *SAE Paper*, 901658.

Mammar, S. and **Baghdassarian, V.B.** (2000) "Two-degree-of-freedom formulation of vehicle handling improvement by active steering," *Proc. of the American Control Conference,* pp. 105-109.

Mammar, S. and **Koenig, D.** (2002) "Vehicle handling improvement by active steering," *Vehicle System Dynamics,* Vol. 38, No. 3, pp. 211-242.

Manning, W., Crolla, D. A., Brown, M. and **Selby, M.** (2000) "Co-ordination of chassis control systems for vehicle motion control," *Proc. of the 5th Int. Symposium on Advanced Vehicle Control, AVEC 2000*, pp. 313-319.

Manning, W., Crolla, D.A., Brown, M. and **Selby, M.** (2002) "IVMC: Intelligent Vehicle Motion Control," *SAE Paper*, 2002-01-0821.

Matsuno, K. et al. (2000) "Development of a new all-wheel drive control system," *Seoul 2000 World Automotive Congress*, FISITA 2000, F2000G347.

Matsuo, Y., Okada, A., Kasuga, S. and **Sekido, S.** (1993) "Intelligent four-wheel-drive system," *SAE Paper*, 930670.

Motoyama, S., Uki, H., Isoda, K., and **Yuasa, H.** (1993) "Effect of traction force distribution control on vehicle dynamics," *Vehicle System Dynamics*, Vol. 22, pp. 455-464.

Nagai, M. (1989) "Active four-wheel-steering system by model following control," *Proc. of the 11th IAVSD Symposium,* pp. 428-439.

Nagai, M., Hirano, Y. and **Yamanaka, S.** (1997) "Integrated control of active rear wheel steering and direct yaw moment control," *Vehicle System Dynamics*, Vol. 27, pp. 357-370.

Nagai, M., Shino, M. and Gao, F. (2002) "Study on integrated control of active front steer angle and direct yaw moment," *JSAE Review*, Vol. 23, No. 3, pp. 309-315.

Naito G., Yaguchi, E., Matuda, T., and **Inokuchi, I.** (1990) "New electronically controlled torque split 4WD system for improving cornering performance," *SAE Paper*, 900556.

Naito, G., Ozaki, K. and **Yaguchi, E.** (1992) "Improving vehicle dynamics by torque split control system," *Proc. of the 1st Int. Symposium on Advanced Vehicle Control, AVEC '92*, pp. 458-463.

Nalecz, A.G. and **Bindemann, A.C.** (1989) "Handling properties of four wheel steering vehicles," *SAE Paper*, 890080.

Okcuoglu, M. (1995) "A descriptive analysis of gerodisc type limited slip differential and AWD couplings," *SAE Paper*, 952642.

Ono, E., Iwama, N., Hirano, Y., Takanami, K. and **Hayashi, Y.** (1994) "Vehicle integrated control for steering and traction systems by μ-synthesis," *Automatica*, Vol. 30, No. 11, pp. 1639-1647.

Ono, E., Hosoe, S., Tuan, H.D. and **Doi, S.** (1996) "Robust stabilization of vehicle dynamics by active front wheel steering control," *Proc. of the 35th Conf. on Decision and Control*, pp. 1777-1782.

Ono, E., Hosoe, S., Doi, S., Asano, K. and **Hayashi, Y.** (1998) "Theoretical approach for improving the vehicle robust stabilization and maneuverability by active front wheel steering control," *Vehicle System Dynamics Supplement,* Vol. 28, pp. 748-753.

Pacejka, H. B. and **Bakker, E.** (1991) "The Magic Formula tyre model," *Proc. of the 1st Tyre Colloquium*, Delft, Netherlands.

Pacejka, H. B. and **Besselink, I. J. M.** (1997) "Magic Formula tyre model with transient properties," *Vehicle System Dynamics Supplement*, Vol. 27, pp. 234-249.

Pacejka, H.B. (2002) *Tyres and vehicle dynamics*, Butterworth-Heinemann, Oxford.

Park, J. and **Ahn, W.** (1999) "H_∞ yaw moment control with brakes for improving driving performance and stability," *Proc. of the IEEE/ASME International Conference on Advanced Intelligent Mechatronics*, pp. 747-752.

Park, K., Heo, S. and **Baek, I.** (2001) "Controller design for improving lateral vehicle dynamic stability," *JSAE Review*, Vol. 22, No. 4, pp. 481-486.

Ro, P.I. and **Kim, H.** (1996) "Four wheel steering system for vehicle handling improvement: a robust model reference control using the sliding mode," *Proc. Instn. Mech. Engrs., Part D: Journal of Automobile Engineering*, Vol. 210, No. 5, pp. 335-346.

Sakai, S., Sado, H. and **Hori, Y.** (1999) "Motion control in an electric vehicle with four independently driven in-wheel motors," *IEEE/ASME Transactions on Mechatronics*, Vol. 4, No. 1, pp. 9-16.

Sano, S., Furukawa, Y., and **Shiraishi, S.** (1986) "Four wheel steering system with rear wheel steer angle controlled as a function of steering wheel angle," *SAE Paper,* 860625.

Sano, S., Furukawa, Y., Nihei, T., Abe, M. and **Shiraishi, S.** (1988) "Handling characteristics of steer angle dependent four wheel steering system," *SAE Paper,* 885034.

Sastry, S. (1999) *Nonlinear systems: analysis, stability and control*, Springer, New York.

Sato, H., Hirota, A., Yanagisawa, H., and **Fukushima, T.** (1983) "Dynamic characteristics of a whole wheel steering vehicle with yaw velocity feedback rear wheel steering," *Proc. of IMechE,* C124/83.

Sato, H., Kawai, H. and **Isikawa, M.** (1991) "Development of four wheel steering system using yaw rate feedback control," *SAE Paper*, 911922.

Sawase, K. and **Sano, Y.** (1999) "Application of active yaw control to vehicle dynamics by utilising driving/braking force," *JSAE Review*, Vol. 20, No. 2, pp. 289-295.

Selby, M., Manning, W.J., Brown, M.D. and **Crolla, D.A.** (2001) "A coordination approach for DYC and active front steering," *SAE Paper*, 2001-01-1275.

Selby, M., Manning, W.J., Brown, M.D. and **Crolla, D.A.** (2001) "A comparison of the relative benefits of active front steering and active rear steering when coordinated with direct yaw moment control," *Proc. of 2001 ASME Int. Mechanical Engineering Congress and Exposition,* pp. 1-6.

Selby, M. (2003) *Intelligent vehicle motion control*, PhD Dissertation, University of Leeds, UK.

Senger, K.H. and **Schwartz, W.** (1987) "The influence of a four wheel steering system on the stability behaviour of a vehicle-driver system," *Vehicle System Dynamics Supplements*, Vol. 17, pp. 388-402.

Sharp, R. and **Crolla, D.A.** (1988) "Controlled rear steering for cars--a review," *Proc. of IMechE,* C437/88.

Shibahata, Y., Irie, N., Iton, H. and **Nakamura, K.** (1986) "The development of an experimental four-wheel-steering vehicle," *SAE Paper,* 860623.

Shibahata, Y., Shimada, K. and **Tomari, T.** (1992) "The improvement of vehicle maneuverability by direct yaw moment control," *Proc. of the 1st Int. Symposium on Advanced Vehicle Control, AVEC'92*, pp. 452-457.

Shimada, K. and **Shibahata, Y.** (1994) "Comparison of three active chassis control methods for stability yaw moments," *SAE Paper*, 940870.

Shino, M., Miyamoto, N., Wang, Y. and **Nagai, M.** (2000) "Traction control of electric vehicles considering vehicle stability," *Proc. of American Control Conference*, pp. 311-316.

Shino, M., Paksincharoensak, P, and **Nagai, M.** (2002) "Vehicle handling and stability control by integrated control of direct yaw moment and active steering," *Proc. of the 6th Int. Symposium on Advanced Vehicle Control, AVEC'02.*

Sienel, W. (1997) "Estimation of the tire cornering stiffness and its application to active car steering," *Proc. of the 36th Conference on Decision & Control,* pp. 4744-4749.

Slotine, J.J. (1984) "Sliding controller design for nonlinear system," *Int. J. of Control*, Vol. 40, No. 2, pp. 421-434.

Slotine, J.J. and **Li, W.** (1991) *Applied nonlinear control*, Prentice-Hall.

Smakman, H.T. (2000) "Functional integration of active suspension with slip control for improved lateral vehicle dynamics," *Proc. of the 5th Int. Symposium on Advanced Vehicle Control, AVEC 2000.*

Smakman, H.T. (2000) *Functional integration of slip control with active suspension for improved lateral vehicle dynamics*, PhD Dissertation, Delft University of Technology, the Netherlands.

Szosland, A. (2000) "Fuzzy logic approach to four-wheel steering of motor vehicle," *Int. J. of Vehicle Design*, Vol. 24, No. 4, pp. 350-359.

Tagawa, Y., Ogata, H., Morita, K., Nagai, M. and **Mori, H.** (1996) "Robust active steering system taking account of nonlinear dynamics," *Vehicle System Dynamics Supplement*, Vol. 25, pp. 668-681.

Takiguchi, T., Yasuda, N., Furutani, S., Kanazawa, H. and **Inoue, H.** (1986) "Improvement of vehicle dynamics by vehicle-speed-sensing four-wheel-steering system," *SAE Paper,* 860624.

Tanizaki, S. and **Yamanaka, T.** (1998) "The effect of active rear steer system," *Proc. of the 4th Int. Symposium on Advanced Vehicle Control, AVEC'98,* pp. 87-92.

Uematsu, K. and **Gerdes, J.C.** (2002) "A comparison of several sliding surfaces for stability control," *Proc. of the 6th Int. Symposium on Advanced Vehicle Control, AVEC'02.*

Utkin, V., Guldner, J. and Shi. J. (1999) *Sliding model control in electromechanical systems*, Taylor & Francis.

Wakamatsu, K., Akuta, Y., Ikegaya, M., and **Asanuma, N.** (1996) "Adaptive yaw rate feedback 4WS with friction coefficient estimator between tire and road surface," *Proc. of the 3rd Int. Symposium on Advanced Vehicle Control, AVEC'96,* pp. 333-343.

Wang, L. and **Ackermann, J.** (1998) "Robust stabilizing PID controllers for car steering systems," *Proc. of the American Control Conference,* pp. 41-42.

Wang, Y. and **Nagai, M.** (1992) "Intelligent vehicle motion control by adaptive front steering system," *Proc. of the 1st Int. Symposium on Advanced Vehicle Control, AVEC'92*, pp. 390-395.

Wang, Y and **Nagai, M.** (1996) "Integrated control of four-wheel-steer and yaw moment to improve dynamic stability margin," *Proc. of the IEEE Conference on Decision and Control*, pp. 1783-1784.

Weir, D.H. and **DiMarco, R.J.** (1978) "Correlation and evaluation of driver/vehicle directional handling data," *SAE Paper*, 780010.

Whitehead, J.C. (1988) "Four wheel steering: maneuverability and high speed stabilization," *SAE Paper*, 880642.

Whitehead, J.C. (1990) "Rear wheel steering dynamics compared to front steering," *Journal of Dynamic Systems, Measurement and Control*, Vol. 112, pp. 88-93.

Williams, D.E. and **Haddad, W.M.** (1995) "Nonlinear control of roll moment distribution to influence vehicle yaw characteristics," *IEEE Trans. on Control Systems Technology*, Vol. 3, No. 1, pp. 110-116.

Wong, J.Y. (2001) *Theory of ground vehicles*, 3rd ed., John Wiley & Sons, New York.

Xia, X. and **Law, E.H.** (1992) "Nonlinear analysis of closed loop driver/automobile performance with four wheel steering control," *SAE Paper*, 920055.

Yamamoto, M., Harada, H and **Matsuo, Y.** (1989) "A study on active controlled chassis system for vehicle dynamics," *Proc. of 11th IAVSD Symposium*, pp. 603-615.

Yamamoto, M. (1991) "Active control strategy for improved handling and stability," *SAE Paper*, 911902.

Yasui, Y., Tozu, K., Hattori, N. and **Sugisawa, M.** (1996) "Improvement of vehicle directional stability for transient steering maneuvers using active brake control," *SAE Papers*, 960485.

Yi, K., Chung, T., Kim, J. and **Yi, S.** (2003) "An investigation into differential braking strategies for vehicle stability control," *Proc. Instn. Mech. Engrs. Part D: J. Automobile Engineering*, Vol. 217, No. 12, pp. 1081-1093.

Yoshioka, T., Adachi, T., Butsuen, T., Okazaki, H. and **Mochizuki, H.** (1998) "Application of sliding-mode control to control vehicle stability," *Proc. of the 4th Int. Symposium on Advanced Vehicle Control, AVEC'98*, pp. 455-460.

Yoshioka, T., Adachi, T., Butsuen, T., Okazaki, H. and **Mochizuki, H.** (1999) "Application of sliding-mode theory to direct yaw moment control," *JSAE Review*, Vol. 20, No. 4, pp. 523-529.

Yu, S.H. and **Moskwa, J.J.** (1994) "A global approach to vehicle control: coordination of four wheel steering and wheel torque," *Journal of Dynamic Systems, Measurement and Control*, Vol. 116, No. 4, pp. 659-667.

Zanten, A.T. Van., Erhardt, R. and **Pfaff, G.** (1995) "VDC, the vehicle dynamics control system of Bosch," *SAE Paper*, 950759.

Zanten, A.T. Van., Erhardt, R., Landesfeind, K. and **Pfaff, G.** (1998) "VDC systems development and perspective," *SAE Paper*, 980235.

Zanten, A.T. Van. (2000) "Bosch ESP systems: 5 years of experience," *SAE Paper*, 2000-01-1633.

Appendix A

Equations of Motion of the NLVM

The Newtonian approach is adequate to derive the equations of motion for a simple model but for more complex models such as the nonlinear vehicle handling model employed in this thesis a Lagrangian approach is more appropriate. In Lagrange's method the total kinetic and potential energies must be expressed in terms of the primary variables describing the system. These are then substituted into a set of partial differential equations called *Lagrange's equations*. The partial derivatives are then evaluated to give the equations of motion (Crolla, 1992). The general Lagrange's equations may be written as:

$$\frac{d}{dt}\left(\frac{\partial T}{\partial \dot{q}_i}\right)-\frac{\partial T}{\partial q_i}+\frac{\partial V}{\partial q_i}+\frac{\partial D}{\partial \dot{q}_i}=Q_i,\ i=1 \text{ to } n \qquad \text{(A.1)}$$

where

n the number of degrees of freedom of the system;

q_i the generalised coordinates describing the system;

Q_i the generalised forces (i.e. forces or moments) applied to the system;

T the total kinetic energy;

V the total potential energy;

D the total dissipated energy.

This form of Lagrange's equation may be applied directly to systems where integration of the real velocities $\dot{q}_i$ with respect to time yields corresponding coordinates q_i. In the case of the vehicle dynamics model developed in this thesis, proper coordinates are longitudinal and lateral displacements of the vehicle CG, X and Y, the yaw angle ψ of the moving vehicle x axis with respect to the inertial X axis, and the body roll angle ϕ about the roll axis. However, as V_x, V_y and r which are of interest are velocities in the moving vehicle axes system, the modified Lagrangian equations in which the above three velocities and the remaining real

coordinate ϕ are used as the generalised motion variables will be employed to generate the equations of motion. With reference to Figure 3.3, the two sets of velocities in the two coordinate systems, i.e. the vehicle fixed and earth fixed, have the following relationships:

$$\begin{Bmatrix} V_x \\ V_y \\ r \\ p \end{Bmatrix} = \begin{bmatrix} \cos\psi & \sin\psi & 0 & 0 \\ -\sin\psi & \cos\psi & 0 & 0 \\ 0 & 0 & 1 & 0 \\ 0 & 0 & 0 & 1 \end{bmatrix} \begin{Bmatrix} \dot{X} \\ \dot{Y} \\ \dot{\psi} \\ \dot{\phi} \end{Bmatrix} \tag{A.2}$$

where $p = \dot{\phi}$ is the roll velocity of the sprung mass.

The modified Lagrangian equations for V_x, V_y, r and ϕ take on the special forms (Lukowski *et al.*, 1990; Pacejka, 2002):

$$\frac{d}{dt}\left(\frac{\partial T}{\partial V_x}\right) - r\frac{\partial T}{\partial V_y} = Q_1,\ q_1 = V_x \tag{A.3a}$$

$$\frac{d}{dt}\left(\frac{\partial T}{\partial V_y}\right) + r\frac{\partial T}{\partial V_x} = Q_2,\ q_2 = V_y \tag{A.3b}$$

$$\frac{d}{dt}\left(\frac{\partial T}{\partial r}\right) - V_y\frac{\partial T}{\partial V_x} + V_x\frac{\partial T}{\partial V_y} = Q_3,\ q_3 = r \tag{A.3c}$$

$$\frac{d}{dt}\left(\frac{\partial T}{\partial \dot{\phi}}\right) - \frac{\partial T}{\partial \phi} + \frac{\partial V}{\partial \phi} + \frac{\partial D}{\partial \dot{\phi}} = Q_4,\ q_4 = \phi \tag{A.3d}$$

Kinetic energy

Both transitional and angular velocities contribute to the kinetic energy. The total kinetic energy of the vehicle T can be expressed in terms of the four velocities V_x, V_y, r and p and split into three terms: T_s, T_f and T_r, corresponding to the sprung mass and the front and rear axles, respectively. With the assumption of small roll angles, the three terms can be expressed as:

$$T_s = \frac{1}{2}m_s[(V_x - hr\phi)^2 + (V_y + h\dot{\phi})^2] + \frac{1}{2}(I_{xxs}\dot{\phi}^2 - 2I_{xz}r\dot{\phi} + I_{zzs}r^2) \tag{A.4}$$

$$T_f = \frac{1}{2} m_{uf} (V_{xf}^2 + V_{yf}^2) + \frac{1}{2} I_{zzf} r^2 \tag{A.5}$$

$$T_r = \frac{1}{2} m_{ur} (V_{xr}^2 + V_{yr}^2) + \frac{1}{2} I_{zzr} r^2 \tag{A.6}$$

where

$$V_{xf} = V_{xr} = V_x$$

$$V_{yf} = V_y + l_f r \,,\; V_{yr} = V_y - l_r r$$

Potential and dissipative energy

The total potential energy V is built up in the suspension and through the reduction in height of the sprung mass CG as it rolls. Here, the suspension is assumed to be linear and thereby can be approximated by a constant torsional stiffness coefficient $K_{\phi f} + K_{\phi r}$ and a constant torsional damping coefficient $C_{\phi f} + C_{\phi r}$. The corresponding potential and dissipative energies are given as:

$$V_\phi = \frac{1}{2} (K_{\phi f} + K_{\phi r}) \phi^2 \tag{A.7}$$

$$V_g = -m_s g h (1 - \cos\phi) \tag{A.8}$$

$$D = \frac{1}{2} (C_{\phi f} + C_{\phi r}) \dot{\phi}^2 \tag{A.9}$$

If the suspension forces are nonlinear, the potential and dissipated energy terms in Eqs. (A.7) and (A.9) must be included in the generalised forces acting on the body. In fact, with reference to Eq. (A.1), any potential and dissipated energy may be differentiated with respect to q_i and $\dot{q}_i$, respectively, and the resulting terms may be included with Q_i on the right hand side of the Lagrange equation. Thus, the terms V and D in Eq. (A.1) may be moved from the left hand side of the Lagrange equation and included instead with Q_i as $-\partial V / \partial \phi$ and $-\partial D / \partial \dot{\phi}$, respectively. Eq. (A.3d) may therefore be rearranged as:

$$\frac{d}{dt}\left(\frac{\partial T}{\partial \dot{\phi}}\right) - \frac{\partial T}{\partial \phi} = Q_4 \tag{A.10}$$

where

$$Q_4 = m_s gh\sin\phi - (K_{\phi f} + K_{\phi r})\phi - (C_{\phi f} + C_{\phi r})\dot{\phi}$$

Generalised forces

Referring to Eqs. (A.3) and (A.10), there are four generalised forces, corresponding to the generalised coordinates V_x, V_y, r and ϕ. The generalised forces Q_i are derived from the virtual work:

$$\delta W = \sum_{i=1}^{4} Q_i \delta q_i \tag{A.11}$$

where δq_i is a small displacement in the generalised coordinate q_i, with $\delta q_j = 0$ when $i \neq j$. Here, q_i refers to the quasi coordinates x and y (X and Y cannot be found by directly integrating V_x and V_y), and the real coordinates ψ and ϕ. For the vehicle model considered here the virtual work can be described as a function of δx, δy, $\delta\psi$ and $\delta\phi$:

$$\delta W = Q_1\delta x + Q_2\delta y + Q_3\delta\psi + Q_4\delta\phi \tag{A.12}$$

with

$$\begin{aligned}
Q_1 &= \sum F_x = F_{x1} + F_{x2} + F_{x3} + F_{x4} - F_r \\
Q_2 &= \sum F_y = F_{y1} + F_{y2} + F_{y3} + F_{y4} \\
Q_3 &= \sum M_z = l_f(F_{y1} + F_{y2}) - l_r(F_{y3} + F_{y4}) + \frac{t_f}{2}(F_{x1} - F_{x2}) + \frac{t_r}{2}(F_{x3} - F_{x4}) \\
Q_4 &= \sum M_x = m_s gh\sin\phi - (K_{\phi f} + K_{\phi r})\phi - (C_{\phi f} + C_{\phi r})\dot{\phi}
\end{aligned} \tag{A.13}$$

Substituting Eqs. (A.4) to (A.6) into Eq. (A.3) and with small angle assumption for roll angle ϕ, the equations of motion for the vehicle model with respect to four motion variables V_x, V_y, r and ϕ are expressed as:

$$\begin{aligned}
&m(\dot{V}_x - V_y r) + (m_{ur}l_r - m_{uf}l_f)r^2 - 2m_s hr\dot{\phi} - m_s h\dot{r}\phi = \sum F_x \\
&m(\dot{V}_y + V_x r) + (m_{uf}l_f - m_{ur}l_r)\dot{r} + m_s h\ddot{\phi} - m_s hr^2\phi = \sum F_y \\
&I_{zz}\dot{r} + (m_{uf}l_f - m_{ur}l_r)V_x r + (m_{uf}l_f - m_{ur}l_r)\dot{V}_y - I_{xz}\ddot{\phi} = \sum M_z \\
&I_{xx}\ddot{\phi} - m_s h^2 r^2\phi + m_s h(\dot{V}_y + V_x r) - I_{xz}\dot{r} = \sum M_x
\end{aligned} \tag{A.14}$$

with

$$m = m_s + m_{uf} + m_{ur}$$

$$I_{xx} = I_{xxs} + m_s h^2$$

$$I_{zz} = I_{zzs} + m_s l_{cg}^2 + I_{zzf} + m_{uf} l_f^2 + I_{zzr} + m_{ur} l_r^2 \tag{A.15}$$

$$I_{zzf} = m_{uf}\left(\frac{t_f}{2}\right)^2$$

$$I_{zzr} = m_{ur}\left(\frac{t_r}{2}\right)^2$$

Eq. (A.14) may be rearranged as:

$$\dot{V}_x = \frac{\sum F_x + (m_{uf} l_f - m_{ur} l_r) r^2 + 2 m_s h r \dot{\phi} + m_s h \dot{r} \phi}{m} + V_y r$$

$$\dot{V}_y = \frac{\sum F_y - (m_{uf} l_f - m_{ur} l_r)\dot{r} - m_s h \ddot{\phi} + m_s h r^2 \phi}{m} - V_x r \tag{A.16}$$

$$\dot{r} = \frac{\sum M_z - (m_{uf} l_f - m_{ur} l_r)(\dot{V}_y + V_x r) + I_{xz}\ddot{\phi}}{I_{zz}}$$

$$\ddot{\phi} = \frac{\sum M_x - m_s h(\dot{V}_y + V_x r) + m_s h^2 r^2 \phi + I_{xz}\dot{r}}{I_{xx}}$$

Since the yaw and roll rates are known to be small compared to the vehicle speed and $m_{uf} l_f - m_{ur} l_r$ is also a small value, the product of these terms in Eq. (A.16) may be left out for simplicity. Therefore, the above equations of motion can be simplified as:

$$\dot{V}_x = \frac{\sum F_x + m_s h \dot{r} \phi}{m} + V_y r$$

$$\dot{V}_y = \frac{\sum F_y - m_s h \ddot{\phi}}{m} - V_x r \tag{A.17}$$

$$\dot{r} = \frac{\sum M_z + I_{xz}\ddot{\phi}}{I_{zz}}$$

$$\ddot{\phi} = \frac{\sum M_x - m_s h(\dot{V}_y + V_x r) + I_{xz}\dot{r}}{I_{xx}}$$

Appendix B

Wheel Kinematics

With reference to Figures B.1 and B.2, the speed components V_{xi} and V_{yi} of the wheel centres along the vehicle fixed axes can be expressed as:

$$V_{x1} = V_x + \frac{t_f}{2} r,\ V_{y1} = V_y + l_f r \tag{B.1}$$

$$V_{x2} = V_x - \frac{t_f}{2} r,\ V_{y2} = V_y + l_f r \tag{B.2}$$

$$V_{x3} = V_x + \frac{t_r}{2} r,\ V_{y3} = V_y - l_r r \tag{B.3}$$

$$V_{x4} = V_x - \frac{t_r}{2} r,\ V_{y4} = V_y - l_r r \tag{B.4}$$

For the 2DOF linear bicycle model, since $V_x >> \frac{t_{f,r}}{2} r$, the approximation $V_{xi} = V_x$ is valid. The lateral speed component V_{yi} takes the forms:

$$V_{yf} = V_y + l_f r \tag{B.5}$$

$$V_{yr} = V_y - l_r r \tag{B.6}$$

at the front and rear axles, respectively, resulting in Eqs. (3.7), (3.8) and (3.15). Hence the speed component of the wheel centre in the direction of wheel heading is given as:

$$V_{xwi} = \begin{bmatrix} \cos\delta_i & \sin\delta_i \end{bmatrix} \begin{Bmatrix} V_{xi} \\ V_{yi} \end{Bmatrix},\ (i = 1,\ldots,4) \tag{B.7}$$

The above speed component will be used to estimate the individual longitudinal slip ratio defined in Eq. (3.49).

In addition, with reference to Figure B.2, for 4WS vehicles, the tyre slip angle α_i can be computed based on the vehicle states:

$$\alpha_1 = \tan^{-1}\left(\frac{V_y + l_f r}{V_x + t_f r/2}\right) - \delta_1 \tag{B.8}$$

$$\alpha_2 = \tan^{-1}\left(\frac{V_y + l_f r}{V_x - t_f r/2}\right) - \delta_2 \tag{B.9}$$

$$\alpha_3 = \tan^{-1}\left(\frac{V_y - l_r r}{V_x + t_r r/2}\right) - \delta_3 \tag{B.10}$$

$$\alpha_4 = \tan^{-1}\left(\frac{V_y - l_r r}{V_x - t_r r/2}\right) - \delta_4 \tag{B.11}$$

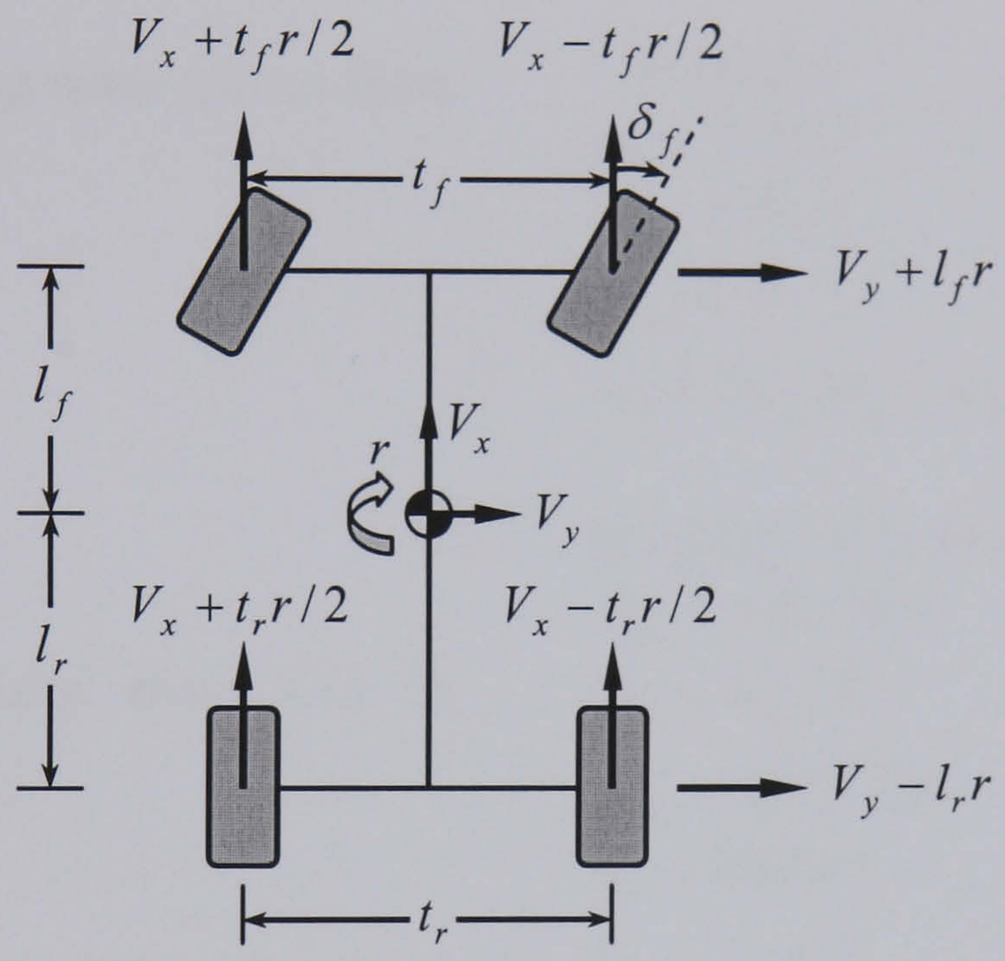

Figure B.1 Definition of wheel centre speed components

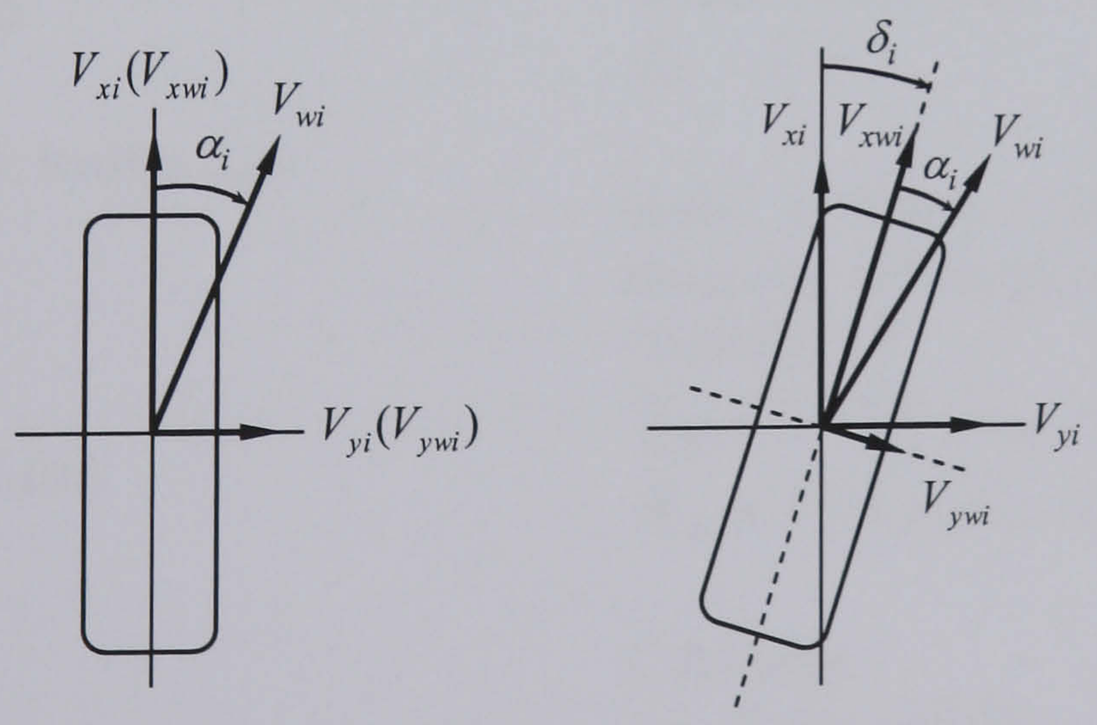

Figure B.2 Definition of tyre slip angle for unsteered and steered wheels

Appendix C

Vehicle and Pacejka Tyre Model Parameters

Vehicle parameters

Here are the vehicle parameters used in the NLVM to represent an average passenger car (Demerly and Youcef-Toumi, 2000).

Distance from sprung mass CG to front and rear axles (m)

$l_{fs} = 1.015$

$l_{rs} = 1.675$

Wheelbase (m)

$l = l_{fs} + l_{rs} = 2.69$

Distance from sprung mass CG to vehicle CG (m)

$l_{cg} = 0.02$

Distance from vehicle CG to front and rear axles (m)

$l_f = l_{fs} + l_{cg} = 1.035$

$l_r = l_{rs} - l_{cg} = 1.655$

Front and rear track widths (m)

$t_f = 1.540$

$t_r = 1.530$

Height of mass CG (m)

$h_{cgs} = 0.568$

$h_{cg} = 0.542$

$h_{uf} = 0.313$

$h_{ur} = 0.313$

Distance from sprung mass CG to roll axis (m)

$h = 0.445$

Height of front and rear roll centres (m)

$h_f = 0.130$

$h_r = 0.110$

Mass (kg)

$m = 1704.7$

$m_{uf} = 98.1$

$m_{ur} = 79.7$

$m_s = m - m_{uf} - m_{ur} = 1527.0$

Moments of inertia (kgm^2)

$I_{xxs} = 440.911$

$I_{xx} = 744.0$

$I_{zzs} = 2619.280$

$I_{zz} = 3048.1$

$I_{xz} = 21.09$

$I_w = 0.99$

Wheel radius (m)

$R_w = 0.313$

Roll stiffness (Nm/rad) and roll damping (Nm/rad/s) of front and rear suspensions

$K_{\phi f} = 47298$, $C_{\phi f} = 2823$

$K_{\phi r} = 37311$, $C_{\phi r} = 2653$

Constants

$g = 9.81$; (m/s^2)

$n_s = 20$; (-)

$f_r = 0.015$; (-)

$RL_x = 0.091$; (m)

Pacejka Tyre Model parameters

The 205/60R15 data of the Pacejka Tyre Model (PTM) used in this thesis is listed below (Pacejka, 2002).

$R_0 = 0.313\text{m}$, $F_{z0} = 4000\text{N}$

----------Longitudinal Force

$p_{Cx1} = 1.685$

$p_{Dx1} = 1.210$

$p_{Dx2} = -0.037$

$p_{Ex1} = 0.344$

$p_{Ex2} = 0.095$

$p_{Ex3} = -0.020$

$p_{Ex4} = 0.0$

$p_{Kx1} = 21.51$

$p_{Kx2} = -0.163$

$p_{Kx3} = 0.245$

$p_{Hx1} = -0.002$

$p_{Hx2} = 0.002$

$p_{Vx1} = 0.0$

$p_{Vx2} = 0.0$

$r_{Bx1} = 12.35$

$r_{Bx2} = -10.77$

$r_{Cx1} = 1.092$

$r_{Hx1} = 0.007$

----------Overturing Moment

$q_{sx1} = 0.0$

$q_{sx2} = 0.0$

$q_{sx3} = 0.0$

----------Lateral Force

$p_{Cy1} = 1.193$

$p_{Dy1} = -0.990$

$p_{Dy2} = 0.145$

$p_{Dy3} = -11.23$

$p_{Ey1} = -1.003$

$p_{Ey2} = -0.537$

$p_{Ey3} = -0.083$

$p_{Ey4} = -4.787$

$p_{Ky1} = -14.95$

$p_{Ky2} = 2.130$

$p_{Ky3} = -0.028$

$p_{Hy1} = 0.003$

$p_{Hy2} = -0.001$

$p_{Hy3} = 0.075$

$p_{Vy1} = 0.045$

$p_{Vy2} = -0.024$

$p_{Vy3} = -0.532$

$p_{Vy4} = 0.039$

$r_{By1} = 6.461$

$r_{By2} = 4.196$

$r_{By3} = -0.015$

$r_{Cy1} = 1.081$

$r_{Hy1} = 0.009$

$r_{Vy1} = 0.053$

$r_{Vy2} = -0.073$

$r_{Vy3} = 0.517$

$r_{Vy4} = 35.44$

$r_{Vy5} = 1.9$

$r_{Vy6} = -10.71$

----------Rolling Resistance Moment

$q_{sy1} = 0.01$

$q_{sy2} = 0.0$

----------Self-aligning Moment

$q_{Bz1} = 8.964$

$q_{Bz2} = -1.106$

$q_{Bz3} = -0.842$

$q_{Bz4} = -0.227$

$q_{Bz5} = 0.0$

$q_{Bz9} = 18.47$

$q_{Bz10} = 0.0$

$q_{Cz1} = 1.180$

$q_{Dz1} = 0.100$

$$q_{Dz2} = -0.001$$
$$q_{Dz3} = 0.007$$
$$q_{Dz4} = 13.05$$
$$q_{Dz6} = -0.008$$
$$q_{Dz7} = 0.0$$
$$q_{Dz8} = -0.296$$
$$q_{Dz9} = -0.009$$
$$q_{Ez1} = -1.609$$
$$q_{Ez2} = -0.359$$
$$q_{Ez3} = 0.0$$
$$q_{Ez4} = 0.174$$
$$q_{Ez5} = -0.896$$
$$q_{Hz1} = 0.007$$
$$q_{Hz2} = -0.002$$
$$q_{Hz3} = 0.147$$
$$q_{Hz4} = 0.004$$
$$s_{sz1} = 0.043$$
$$s_{sz2} = 0.001$$
$$s_{sz3} = 0.731$$
$$s_{sz4} = -0.238$$

Appendix D

The 2DOF Nonlinear Vehicle Model

Description of the model

In Chapter 4 the 2DOF nonlinear vehicle model (2NVM) was introduced to allow the influence of lateral acceleration on the lateral vehicle dynamics to be analysed. The detailed description of this model will be presented in this appendix.

The basic assumptions in Chapter 3 for vehicle modelling still apply to this model. As the name implies, of the three degrees of freedom in the horizontal plane, only the lateral motion and yaw motion will be examined. Hence the longitudinal vehicle dynamics is neglected and the vehicle forward speed is assumed to be constant. In addition, the quasi-static lateral load transfer effect is also taken into account and the lateral tyre forces are calculated separately for four corners of the vehicle. With the small angle assumptions, the equations of motion of this model are quite similar to those of the 2DOF linear bicycle model, Eqs. (3.3) and (3.4) and take the form:

$$m(\dot{V}_y + V_x r) = F_{yw1} + F_{yw2} + F_{yw3} + F_{yw4} \tag{D.1}$$

$$I_{zz}\dot{r} = l_f(F_{yw1} + F_{yw2}) - l_r(F_{yw3} + F_{yw4}) \tag{D.2}$$

where the lateral tyre forces F_{ywi} $(i = 1,...,4)$ are calculated by using the pure lateral slip "Pacejka Tyre Model" which was introduced in Chapter 3. In addition the lateral tyre force lags are also included in this model and given by:

$$\tau_{yli}\dot{F}_{ywi} + F_{ywi} = F_{ywssi} \tag{D.3}$$

$$\tau_{yli} = \frac{RL_{yi}}{V_x} = \frac{R_{wi}}{V_x}, \quad (i = 1,...,4) \tag{D.4}$$

The lateral acceleration and sideslip angle at the vehicle CG can then be expressed as:

$$a_y = \frac{\sum_{i=1}^{4} F_{ywi}}{m} \tag{D.5}$$

$$\beta = \tan^{-1}\left(\frac{V_y}{V_x}\right) \tag{D.6}$$

The slip angles at four tyres are the same as those defined in Eqs. (B.8) to (B.11). In addition, the vertical tyre loads F_{zi} $(i = 1,...,4)$ are derived according to Eqs. (3.45) to (3.48):

$$F_{z1} = \frac{mgl_r}{2l} + \frac{ma_y h_{cg} l_r}{t_f l} \tag{D.7}$$

$$F_{z2} = \frac{mgl_r}{2l} - \frac{ma_y h_{cg} l_r}{t_f l} \tag{D.8}$$

$$F_{z3} = \frac{mgl_f}{2l} + \frac{ma_y h_{cg} l_f}{t_r l} \tag{D.9}$$

$$F_{z4} = \frac{mgl_f}{2l} - \frac{ma_y h_{cg} l_f}{t_r l} \tag{D.10}$$

Model linearisation

For analysis purposes, the 2NVM will be linearised around certain operating points. A general nonlinear system can be described by the following state-space model:

$$\dot{x}(t) = f(x(t), u(t)) \tag{D.11}$$

$$y(t) = g(x(t), u(t)) \tag{D.12}$$

where $x(t)$ is the state variable vector, $u(t)$ is the input vector and $y(t)$ is the output vector.

Assume that $\{x_0(t), u_0(t), y_0(t); t \in \Re\}$ is a steady-state operating point that satisfies Eqs. (D.11) and (D.12). The variations of $x(t)$, $u(t)$ and $y(t)$ around this point:

$$\Delta x(t) = x(t) - x_0(t) \tag{D.13}$$

$$\Delta u(t) = u(t) - u_0(t) \tag{D.14}$$

$$\Delta y(t) = y(t) - y_0(t) \tag{D.15}$$

are assumed to be small enough. Then the first-order Taylor series can be used to approximate the above model around this point. This approach leads to:

$$\dot{x}(t) \approx f(x_0(t),u_0(t)) + \left(\frac{\partial f}{\partial x}\right)_{\substack{x=x_0 \\ u=u_0}} (x(t)-x_0(t)) + \left(\frac{\partial f}{\partial u}\right)_{\substack{x=x_0 \\ u=u_0}} (u(t)-u_0(t)) \quad \text{(D.16)}$$

$$y(t) \approx g(x_0(t),u_0(t)) + \left(\frac{\partial g}{\partial x}\right)_{\substack{x=x_0 \\ u=u_0}} (x(t)-x_0(t)) + \left(\frac{\partial g}{\partial u}\right)_{\substack{x=x_0 \\ u=u_0}} (u(t)-u_0(t)) \quad \text{(D.17)}$$

The above equations can be written in the form of increment:

$$\Delta\dot{x}(t) = \left(\frac{\partial f}{\partial x}\right)_{\substack{x=x_0 \\ u=u_0}} \Delta x(t) + \left(\frac{\partial f}{\partial u}\right)_{\substack{x=x_0 \\ u=u_0}} \Delta u(t) \quad \text{(D.18)}$$

$$\Delta y(t) = \left(\frac{\partial g}{\partial x}\right)_{\substack{x=x_0 \\ u=u_0}} \Delta x(t) + \left(\frac{\partial g}{\partial u}\right)_{\substack{x=x_0 \\ u=u_0}} \Delta u(t) \quad \text{(D.19)}$$

Thus one can have the following state-space linear model around the steady-state operating point $\{x_0(t),u_0(t),y_0(t);t\in\Re\}$:

$$\Delta\dot{x}(t) = \mathbf{A}\Delta x(t) + \mathbf{B}\Delta u(t) \quad \text{(D.20)}$$

$$\Delta y(t) = \mathbf{C}\Delta x(t) + \mathbf{D}\Delta u(t) \quad \text{(D.21)}$$

where

$$\mathbf{A} = \left(\frac{\partial f}{\partial x}\right)_{\substack{x=x_0 \\ u=u_0}}, \quad \mathbf{B} = \left(\frac{\partial f}{\partial u}\right)_{\substack{x=x_0 \\ u=u_0}}$$

$$\mathbf{C} = \left(\frac{\partial g}{\partial x}\right)_{\substack{x=x_0 \\ u=u_0}}, \quad \mathbf{D} = \left(\frac{\partial g}{\partial u}\right)_{\substack{x=x_0 \\ u=u_0}}$$

are matrices with appropriate dimensions.

The linearised 2NVM will then have the form of Eqs. (D.20) and (D.21) with:

$$\Delta x(t) = \begin{bmatrix} \Delta V_y \\ \Delta r \\ \Delta F_{ywss1} \\ \Delta F_{ywss2} \\ \Delta F_{ywss3} \\ \Delta F_{ywss4} \end{bmatrix}$$

$$\Delta u(t) = \begin{bmatrix} \Delta\delta_f \\ \Delta\delta_r \end{bmatrix} \quad \text{(D.22)}$$

$$\Delta y(t) = \begin{bmatrix} \Delta a_y \\ \Delta r \\ \Delta \beta \end{bmatrix}$$

In this model, due to the additional tyre dynamics, each tyre produces one additional state. In this thesis, the model linearisation around a certain operating point is performed by using the ***Linmod*** command in Matlab/Simulink.

Appendix E

Analysis of Yaw Moments

In order to negotiate a turn, a yaw moment needs to be developed on a vehicle. The primary yaw moment is determined by the balance of tyre forces between front and rear axles. In addition, external disturbances such as side wind gust or braking/accelerating on split-μ surfaces may also result in yaw moments on the vehicle. The characteristic of the yaw moment on the vehicle during critical cornering situations is crucial to vehicle stability. Active control can be used to generate the required corrective yaw moment through affecting and optimising the tyre forces acting on the vehicle. This appendix will present the method that is utilised in this thesis to analyse the achievable yaw moments on the vehicle brought about by active steering, driveline and braking control. The tyre model that is used for the analysis is the full Pacejka Tyre Model described in Chapter 3.

For the purpose of analysis, the roll dynamics of the NLVM is neglected. This implies that the load transfer from the inner wheels to the outer wheels during cornering occurs instantaneously. The initial state of the vehicle is the steady-state cornering at a specific level of lateral acceleration. During this manoeuvre, the vehicle dynamics control systems are not activated. This establishes the steady-state operating point for the vehicle and tyres. From this initial condition active control will be applied to the vehicle and the control action will result in a change in the tyre forces. In this analysis, the lateral load transfer at front and rear axles is assumed to remain unchanged after active control is applied.

In the case of active steering, the corrective steer angle induced by AFS or the rear wheel steer angle exerted by ARS results in changes in the tyre slip angles, and consequently changes in the tyre forces at the corresponding axle. For actively braking or driving an individual wheel, the braking or driving action leads to longitudinal slip, and thus changes in longitudinal and lateral forces at the corresponding wheel. In addition, the braking or driving action also results in

longitudinal acceleration and a longitudinal load transfer which in turn influences the vertical tyre loads and all tyre forces. This effect is dealt with in an iterative manner: the longitudinal acceleration is first calculated according to the applied braking or driving force at each operating point; then the corresponding longitudinal load transfer and the resulting tyre forces are calculated. In the course of braking or driving individual wheels, the slip angles of all tyres are assumed to be constant.

The resulting yaw moment on the vehicle after the application of active control can therefore be calculated according to the resulting tyre forces:

$$M_{zc} = l_f(F_{y1} + F_{y2}) - l_r(F_{y3} + F_{y4}) + \frac{t_f}{2}(F_{x1} - F_{x2}) + \frac{t_r}{2}(F_{x3} - F_{x4}) \qquad \text{(E.1)}$$

Appendix F

Validation of the NLVM

In order to prove that the developed vehicle model accurately simulate the behaviour of the actual vehicle, it is necessary to compare simulation data with data obtained from field tests. However, since this research does not focus on one specific vehicle or class, it is quite difficult to get full vehicle test data. The vehicle parameters used in the NLVM come from the NAVDyn (Demerly and Youcef-Toumi, 2000) and therefore the NLVM has been validated by comparing the model response with the NAVDyn and actual vehicle responses presented in the above paper. In addition, since the tyre model and data used in the NLVM are different from those employed in the NAVDyn, this appendix just aims to show the similarity between the two models. The following three test manoeuvres are used for comparison purposes.

- Slowly increasing steer;
- Constant speed J-Turn;
- Straight line braking.

Demerly and Youcef-Toumi (2000) compared the NAVDyn with both actual vehicle and CarSim (a computer simulation package for vehicle dynamics analysis) and it was found that the NAVDyn did very well at predicting actual vehicle response.

Slowly increasing steer

This test is used to evaluate the model's ability to predict the steady-state gain of the vehicle in response to driver steer inputs from low levels of lateral acceleration up to the handling limit. In this test, the vehicle speed is held constant and the steering wheel angle is slowly increased. The test is carried out at two speeds of 40km/h and 80km/h, respectively. Figure F.1 shows the lateral acceleration gain comparison. As can be seen, the NLVM model shows highly similar response to the actual vehicle and the NAVDyn up to the handling limit for both speeds. In addition, for both models and the actual vehicle, the lateral acceleration gain is seen to increase with speed.

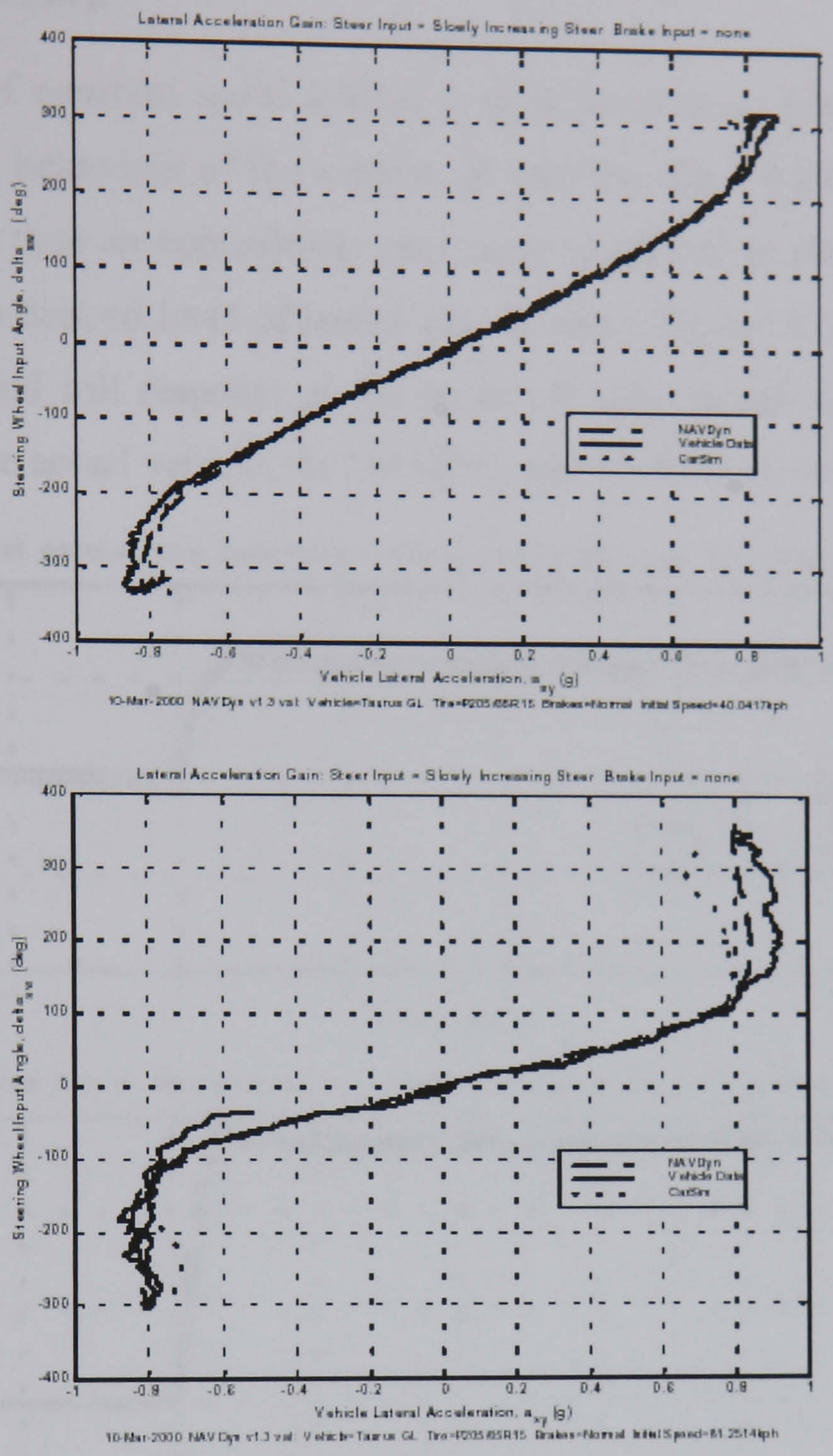

(a) Lateral acceleration gain of the actual vehicle and NAVDyn at 40km/h (upper) and 80km/h (lower)

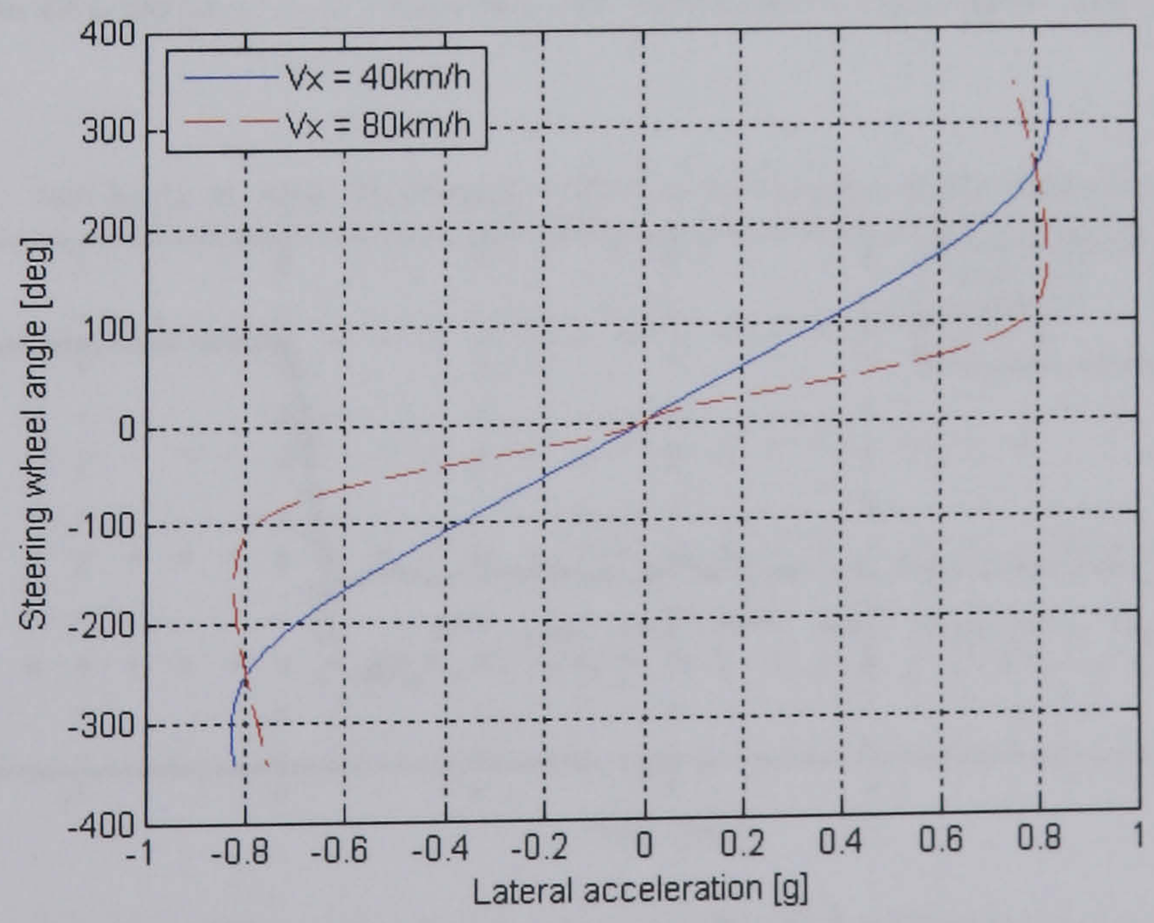

(b) Lateral acceleration gain of the NLVM at 40km/h and 80km/h

Figure F.1 Comparison of actual vehicle and NAVDyn with NLVM for slowly increasing steer

Constant speed J-Turn

The manoeuvre of constant speed J-Turn is used to evaluate both steady-state and transient handling behaviour of the vehicle. In this test, the vehicle forward speed is kept constant and then an approximate step input is applied at the steering wheel in order to achieve a desired level of lateral acceleration. Figures F.2 and F.3 show the lateral response and roll response at the speed of 40km/h and 142degrees steering wheel angle for the actual vehicle, the NAVDyn and the NLVM, respectively.

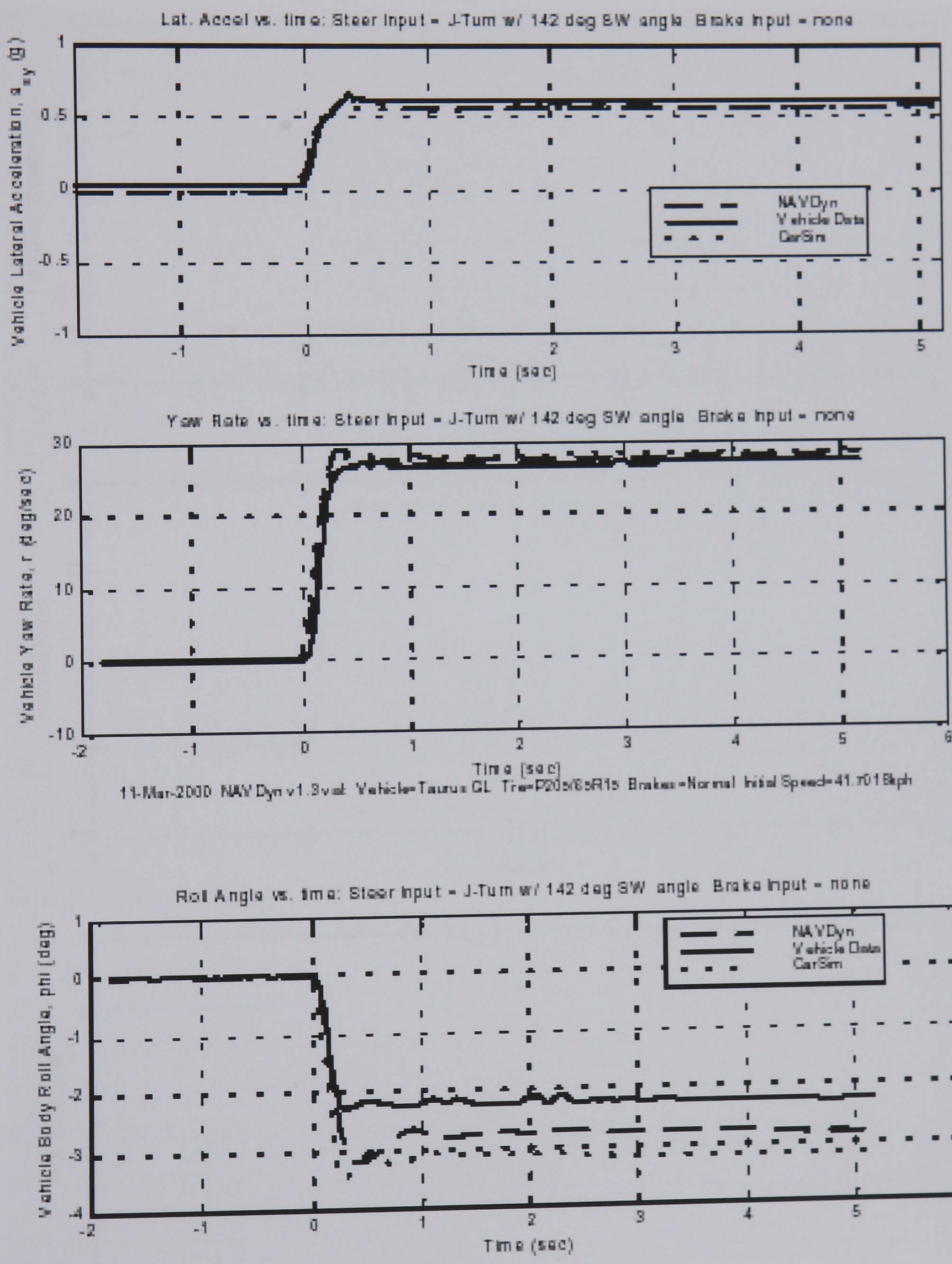

Figure F.2 Responses of the actual vehicle and the NAVDyn to constant speed J-Turn at 40km/h and 142deg steering wheel angle

Figures F.4 and F.5 show the same responses at 80km/h and -49degrees steering wheel angle for the actual vehicle, the NAVDyn and the NLVM, respectively. As can be seen, both simulation results show a very high similarity between the actual vehicle and the NLVM. The lateral dynamics of the vehicle are represented quite well with the NLVM and the inclusion of roll angle shows that some aspect of the suspension system is accurately modelled. The slight difference in steady-state gain and transient response of the two models is mainly due to the different tyre models employed.

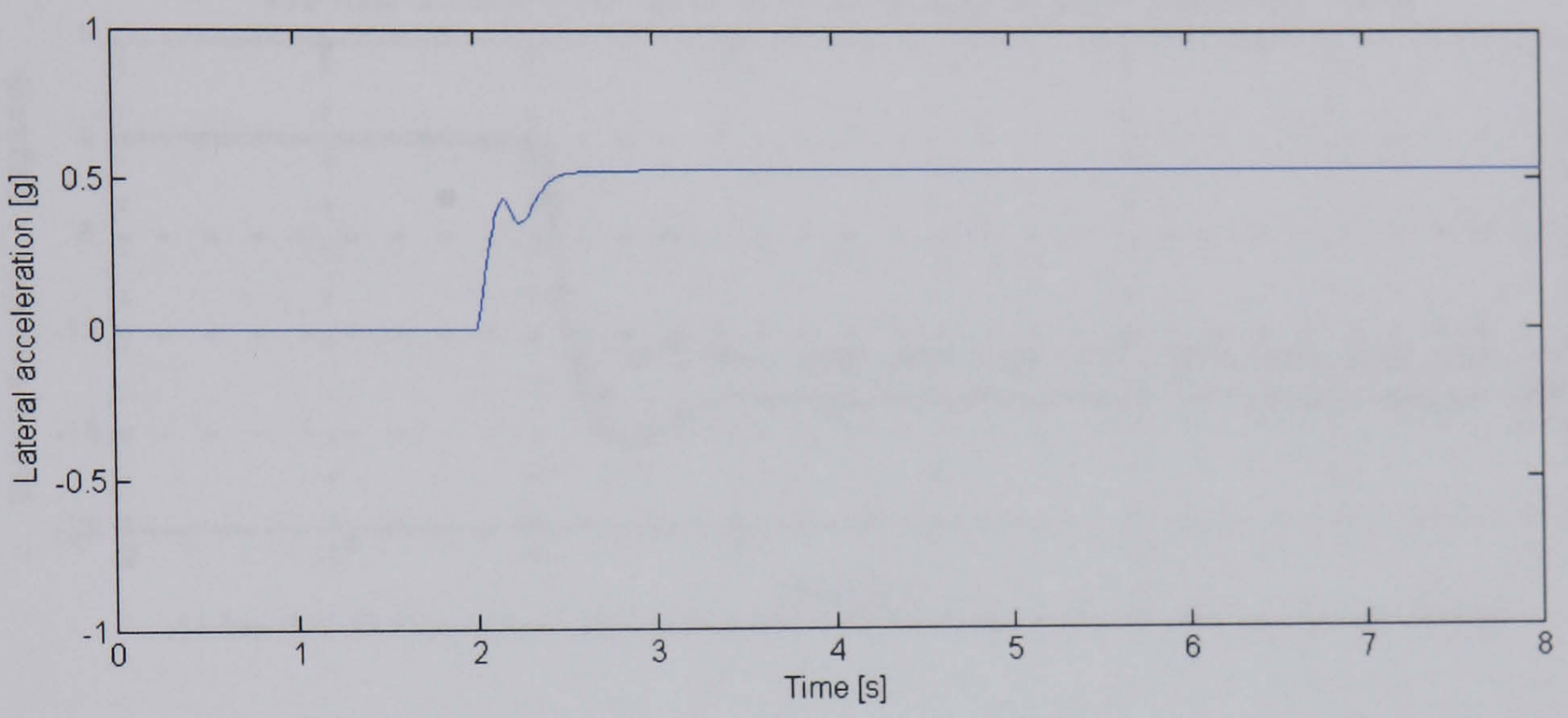

Figure F.3 Response of the NLVM to constant speed J-Turn at 40km/h and 142deg steering wheel angle

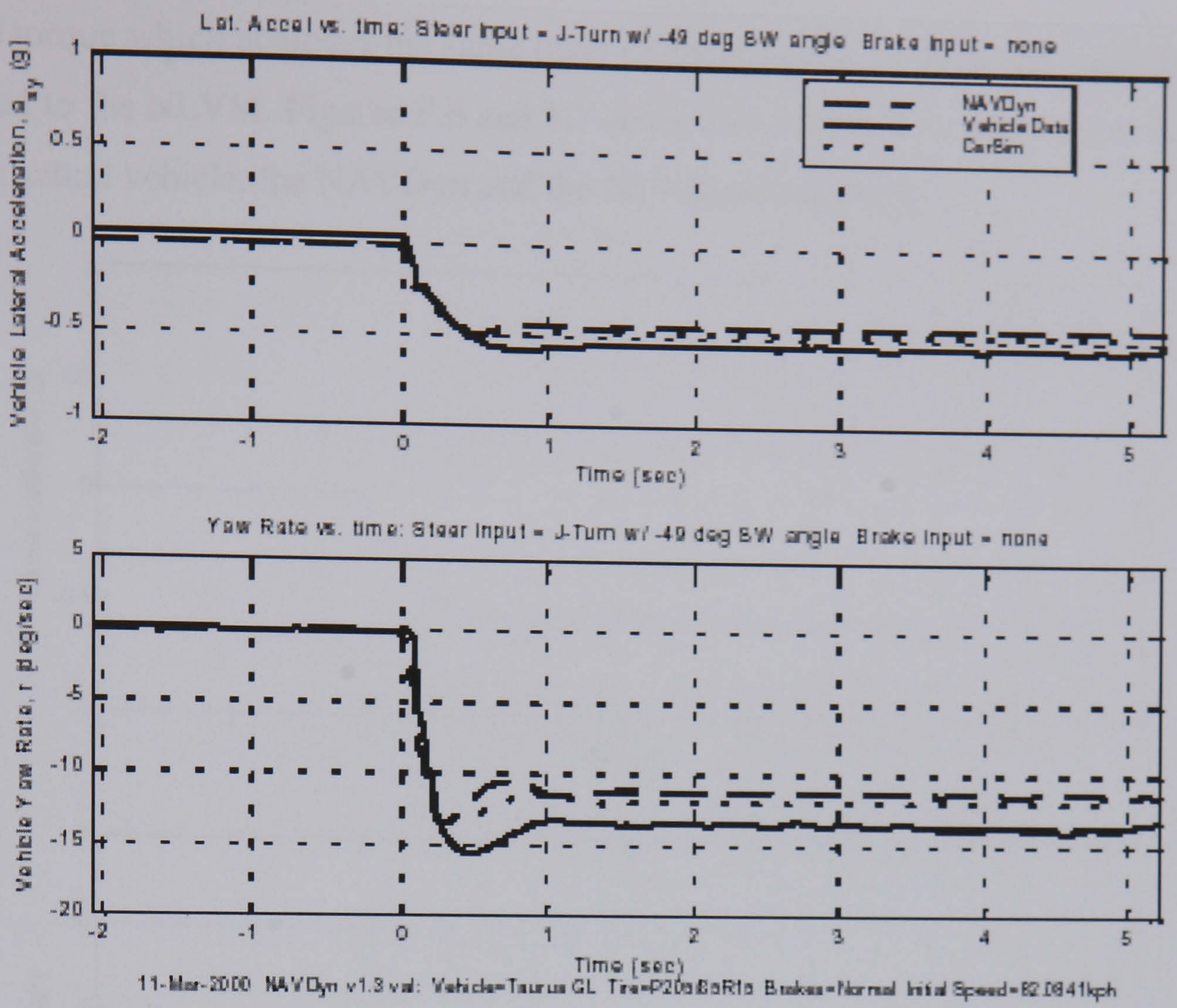

Figure F.4 Responses of the actual vehicle and the NAVDyn to constant speed J-Turn at 80km/h and -49deg steering wheel angle

Straight line braking

The final manoeuvre used for validation is straight line braking. For this manoeuvre, the vehicle is driven straight ahead at a speed of 80km/h and then an approximate step input in brake torque is applied to achieve a desired level of deceleration. It should be noted that the brake system is included in the NAVDyn and therefore the brake input to the NAVDyn is the brake pedal force. The brake system dynamics are neglected in the NLVM and brake torques are thus applied directly to the wheels. In this test, a

brake torque which achieves the same level of deceleration as the brake pedal force is applied to the NLVM. Figures F.6 and F.7 show the responses to straight line braking of the actual vehicle, the NAVDyn and the NLVM, respectively.

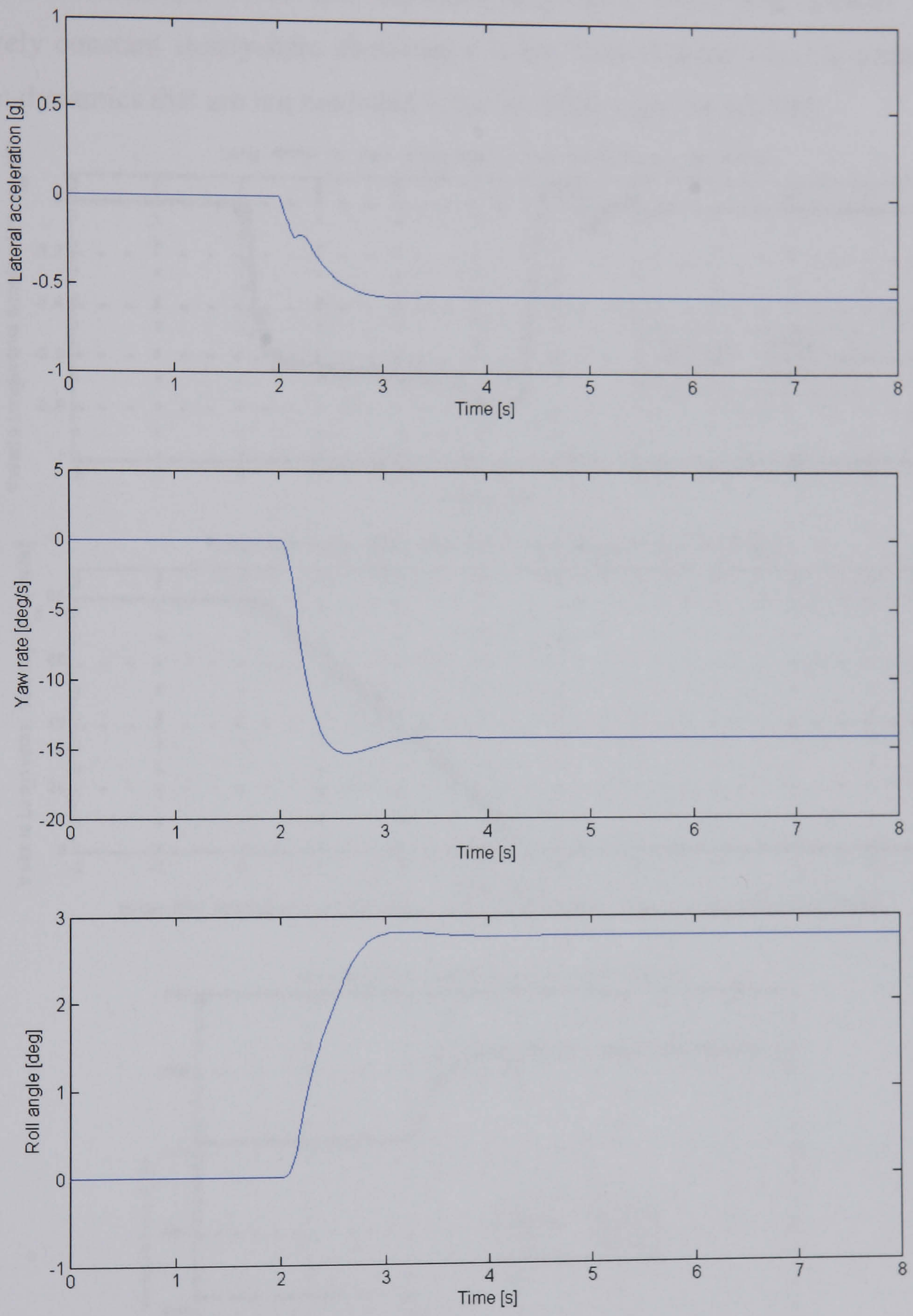

Figure F.5 Response of the NLVM to constant speed J-Turn at 80km/h and -49deg steering wheel angle

The longitudinal acceleration, vehicle forward speed and vertical tyre load are shown as a function of time. Once again the NLVM is seen to show quite similar response to the actual vehicle and the NAVDyn. However, there are two clear differences. First,

the actual vehicle and the NAVDyn have a slightly slow time response compared to the NLVM. This is due to the fact that the NAVDyn includes lags in the brake system and the NLVM does not. The second difference to note is that the actual vehicle shows a deceleration level that increases with time while both models predict relatively constant steady-state deceleration level. This is mainly due to some brake system dynamics that are not modelled in the NAVDyn and the NLVM.

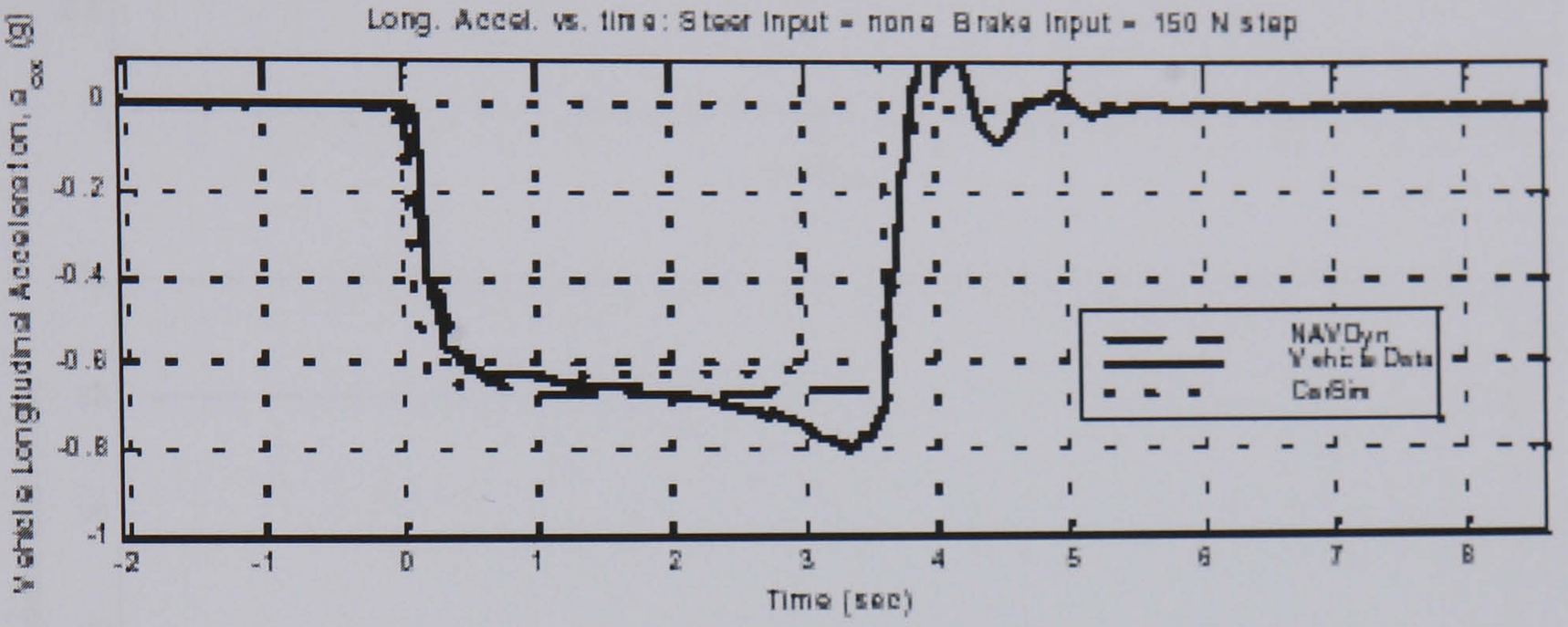

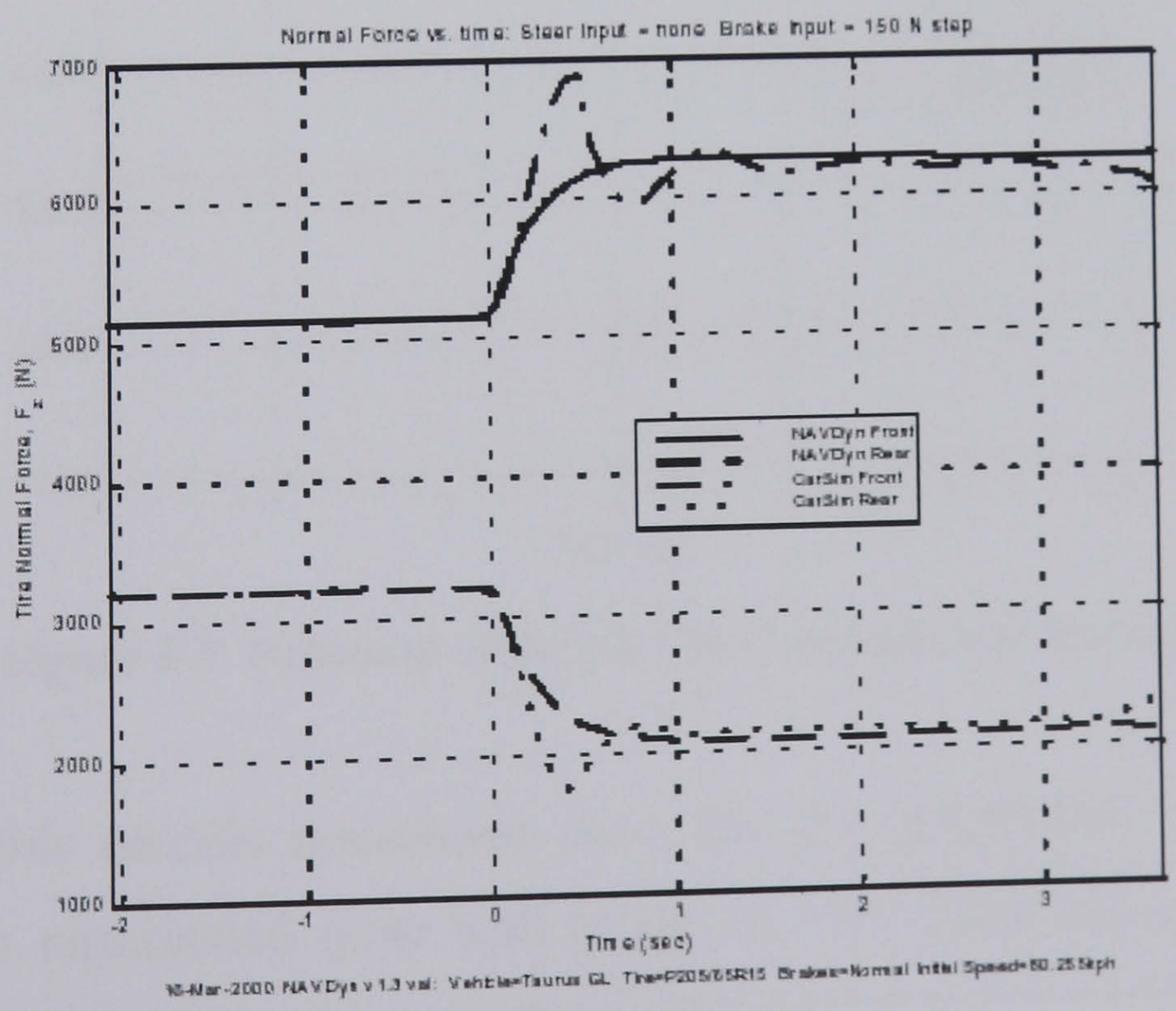

Figure F.6 Responses of the actual vehicle and the NAVDyn to straight line braking

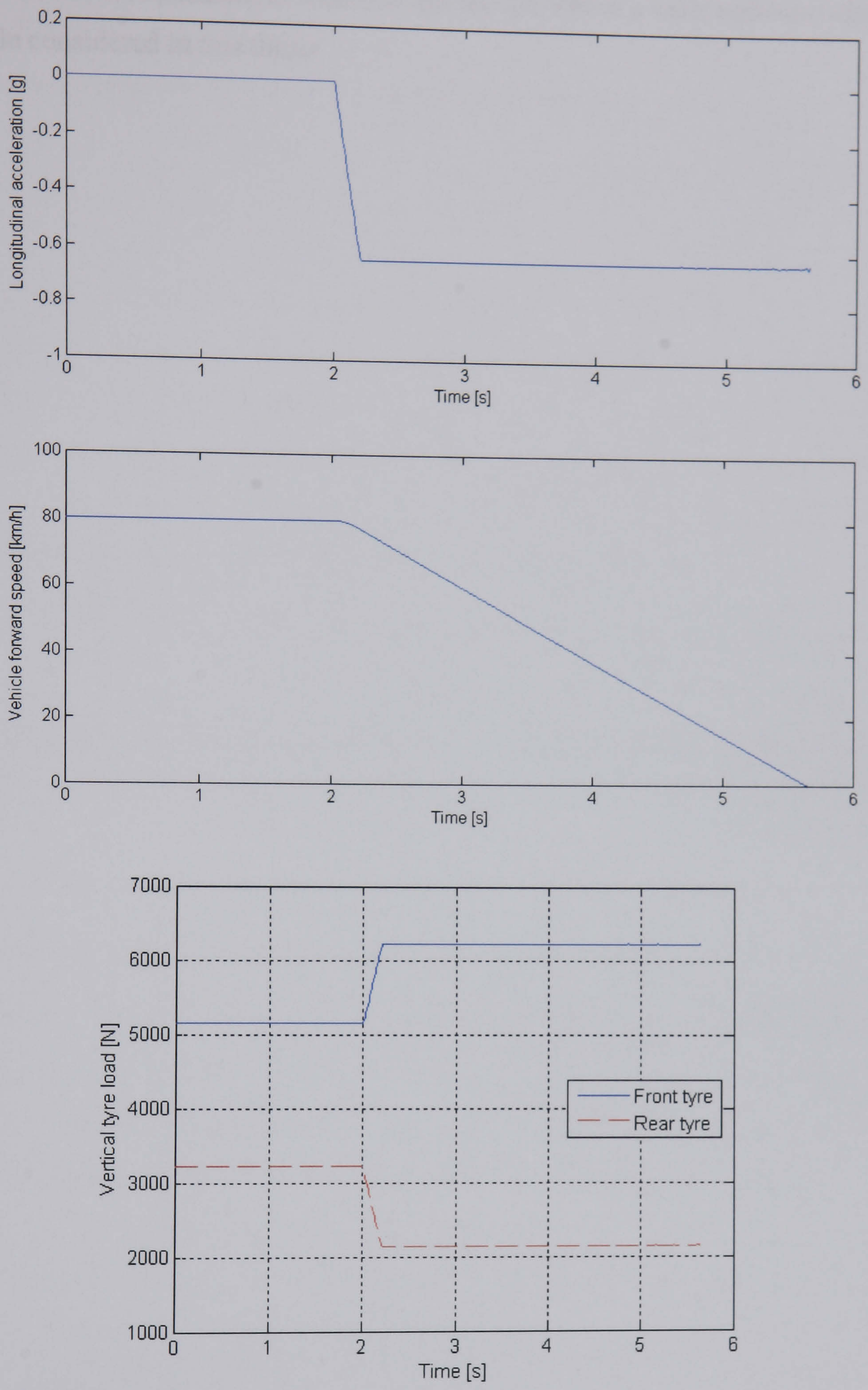

Figure F.7 Response of the NLVM to straight line braking

The results of this specific manoeuvre show that the longitudinal dynamics of the vehicle are also represented quite well in the NLVM. From the above simulation results a very high similarity between the actual vehicle and the NLVM can be seen

and therefore it is possible to conclude that the NLVM is a valid representation of the vehicle considered in this thesis.

Appendix G

Phase-plane Method

The phase-plane method is a graphical method for finding the transient response of second-order systems to initial conditions or simple constant inputs and particularly powerful for the stability analysis. The basic idea of the method is a) to generate motion trajectories corresponding to various initial conditions in the state space of a second-order dynamic system and b) to examine the qualitative features of the trajectories. A major class of second-order systems can be described by the following differential equation:

$$\ddot{x} + f(x, \dot{x}) = 0 \tag{G.1}$$

In state space form, this dynamic system can be represented as:

$$\begin{aligned} \dot{x}_1 &= x_2 \\ \dot{x}_2 &= -f(x_1, x_2) \end{aligned} \tag{G.2}$$

where $x_1 = x$ and $x_2 = \dot{x}$ are the states of the system, and f is a nonlinear function of the states. Geometrically, the state space of the system (G.2) is a plane having x_1 and x_2 as coordinates which is called the *phase plane*. A state trajectory in the phase plane is denoted as a phase plane *trajectory*. A family of phase plane trajectories corresponding to various initial conditions is called a *phase portrait* of the system (Slotine and Li, 1991). The power of the phase-plane method lies in the fact that once the phase portrait of a system is obtained, the nature of the system response such as stability and other motion patterns is directly displayed on the phase plane. Traditionally, the phase-plane method is developed for the dynamics of (G.1). Actually, one may consider more general form of second-order systems described by the following two first-order equations:

$$\begin{aligned} \dot{x}_1 &= f_1(x_1, x_2) \\ \dot{x}_2 &= f_2(x_1, x_2) \end{aligned} \tag{G.3}$$

where f_1 and f_2 are nonlinear functions of the states x_1 and x_2. It causes no difficulty to extend the phase-plane method to more general dynamics of the form (G.3) since these dynamics can be easily transformed into a scalar second-order differential equation of (G.1).

Being the special case of nonlinear systems, linear systems can also be analysed through the phase-plane method. Linear systems usually have only one singular point, which is an equilibrium point in the phase plane, and only one type of behaviour around such a point. The nature of the singular point depends on the eigenvalues of the system matrix and the trajectories either start or end at the singular point or even encircle it. The stability characteristics of linear systems are uniquely determined by the nature of their singular points. In addition, other information concerning system dynamic properties such as oscillations and damping of the system can be examined in such a manner as well. Phase portraits of linear systems corresponding to different cases of the eigenvalues are shown in Figure G.1.

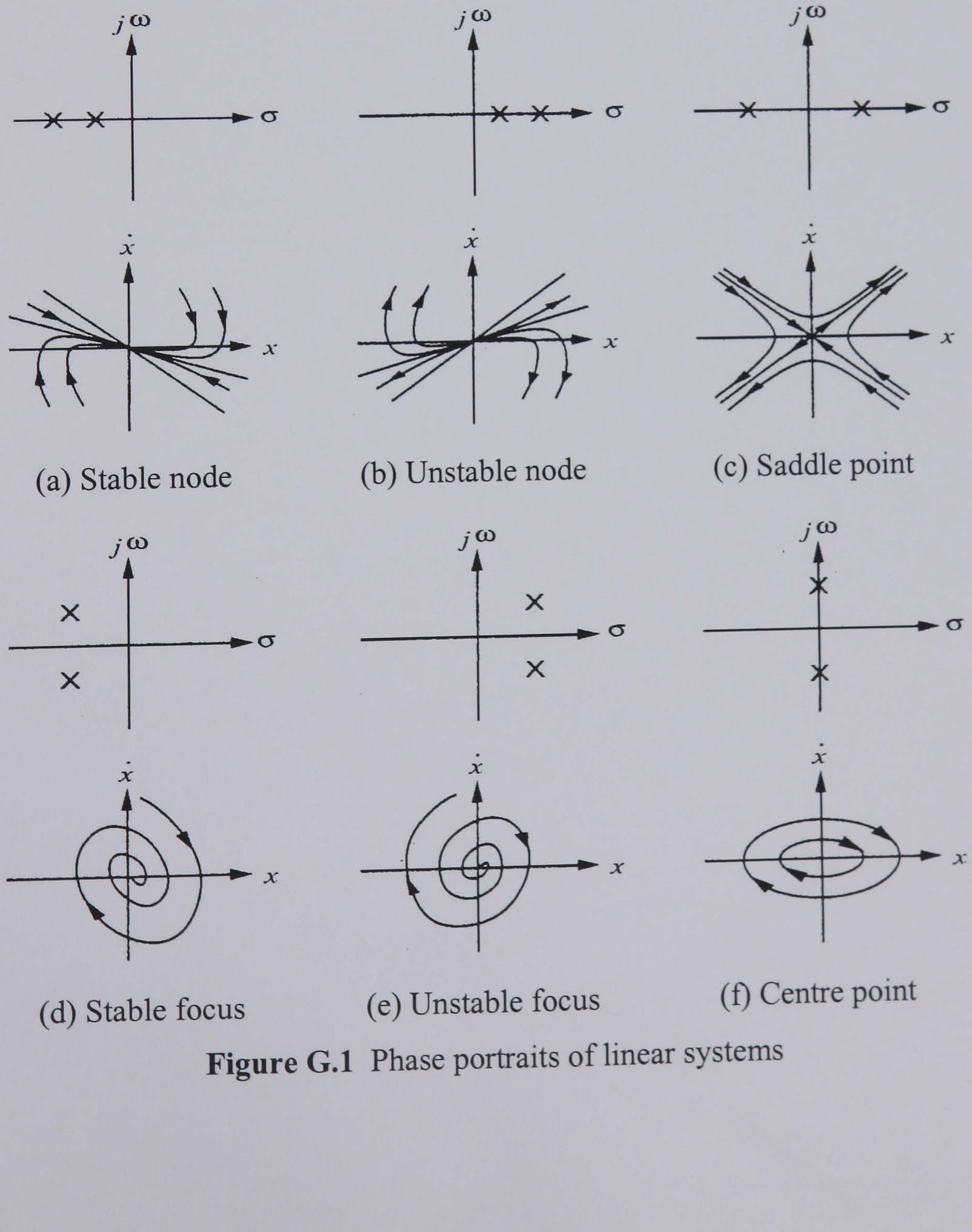

(a) Stable node (b) Unstable node (c) Saddle point

(d) Stable focus (e) Unstable focus (f) Centre point

Figure G.1 Phase portraits of linear systems

In contrast to linear systems, on one hand, nonlinear systems often have more than one isolated singular point and the motion patterns of the systems in the vicinity of the different singular points have different natures. On the other hand, phase plane analysis of nonlinear systems should be related to that of linear systems as the local behaviour of a nonlinear system around each equilibrium point can be approximated by the behaviour of a linear system. Stability analysis and control design can then be carried out based on the phase portrait of the system of interest.

Appendix H

Description of the Torque Transfer Differential

The key drawback of conventional differentials is that they can only transfer torque to the slower spinning wheel. For vehicle stability control applications, it is desirable to have control over the direction as well as magnitude of the torque transfer. The torque transfer differential developed by Sawase and Sano (1999) can achieve this target. This appendix will detail the operating principles of such a differential.

With reference to Figure 6.9, this mechanism places a set of two friction clutches on the right-hand shaft of the conventional differential gearing. In addition, it also features a three-gang gearing system connected to the differential case, with the right clutch slip-linked to the faster end and the left clutch slip-linked to the slower end. The direction and magnitude of torque transfer between the left and right driveshafts can thus be controlled by the two clutches, Cl and Cr. If torque transfer to the left-hand wheel is desired, the left-hand clutch Cl will be engaged and if torque transfer to the right-hand wheel is desired, the right-hand clutch Cr will be engaged.

However, like the LSD, this torque transfer differential still relies on a sufficient speed difference between two clutch plates in order to produce the desired amount of torque transfer. The additional gearing system between the differential case and the clutch plates is designed to guarantee such a speed difference. For a bevel gear type differential, the left- and right-hand wheel speeds ω_l and ω_r have the following relationship with the differential case speed ω_c:

$$\omega_l + \omega_r = 2\omega_c \tag{H.1}$$

When the vehicle travels straight ahead, the left- and right-hand wheels and the differential case turn at the same speed, i.e. $\omega_l = \omega_r = \omega_c$. Through the three-gang gearing system, the speeds of the left- and right-hand inner clutch plates can also be expressed in terms of the differential case speed as follows:

$$\omega_{cl} = \frac{Z_1 Z_6}{Z_3 Z_4} \omega_c \tag{H.2}$$

$$\omega_{cr} = \frac{Z_1 Z_5}{Z_2 Z_4} \omega_c \tag{H.3}$$

where the gear teeth numbers are set to be $Z_1 = Z_2 = Z_3 = 42$, $Z_4 = 32$, $Z_5 = 36$ and $Z_6 = 28$ (Sawase and Sano, 1999). Substituting the gear teeth numbers into Eqs. (H.2) and (H.3) yields:

$$\omega_{cl} = 0.875\omega_c \tag{H.4}$$

$$\omega_{cr} = 1.125\omega_c \tag{H.5}$$

Therefore the right-hand clutch is speeded up relative to the differential case and the left-hand clutch is slowed down. If the right-hand clutch is engaged, the right-hand wheel speed can be expressed as:

$$\omega_r = \omega_{cr} = 1.125\omega_c \tag{H.6}$$

and the left-hand wheel speed must satisfy:

$$\omega_l = 2\omega_c - \omega_r = 0.875\omega_c \tag{H.7}$$

i.e. the right-hand wheel will be speeded up by 12.5% while the left-hand wheel will be slowed down by 12.5%. The maximum wheel speed difference that can be generated by these gear ratios is thus 25%. As long as the wheel speed difference falls within this range, it is possible to control the direction of torque transfer by selectively engaging the two clutches.

The relationship between the input torque T_{in}, the torque transfer at the clutches T_{cr}, T_{cl} and wheel torques T_r, T_l during clutch engagement can be derived through analysis of torque balances across the differential gearing and the three-gang gearing, respectively. During engagement of the right-hand clutch Cr, the torque transfer at this clutch T_{cr} will induce a reaction torque T_x on the differential case, the torque balance of the three-gang gearing can thus be expressed as:

$$\frac{Z_4}{Z_1} T_x - \frac{Z_5}{Z_2} T_{cr} = 0 \tag{H.8}$$

The torque balance of the differential gearing can be expressed as:

$$T_{in} - T_x - T_l - T_r + T_{cr} = 0 \tag{H.9}$$

$$T_l = T_r - T_{cr} \tag{H.10}$$

Rearranging Eqs. (H.8) to (H.10) gives:

$$T_l = \frac{T_{in}}{2} - \frac{Z_1 Z_5}{2 Z_2 Z_4} T_{cr} \tag{H.11}$$

$$T_r = \frac{T_{in}}{2} + \left(1 - \frac{Z_1 Z_5}{2 Z_2 Z_4}\right) T_{cr} \tag{H.12}$$

The torque difference between the left- and right-hand wheels is simply the torque transfer at the clutch, i.e.

$$T_l - T_r = -T_{cr} \tag{H.13}$$

With a hydraulic actuation system, clutch torque capacities in excess of 1000Nm are feasible (Hancock and Williams, 2003). The actual torque difference that can be achieved at any given time is the torque that is required to lock the clutch pack. This may well be less than the clutch torque capacity when, for example, the vehicle is on a low-μ surface.

Similarly, the left-hand wheel torque, the right-hand wheel torque and the lateral torque difference during engagement of the left-hand clutch Cl can be expressed as:

$$T_l = \frac{T_{in}}{2} + \frac{Z_1 Z_6}{2 Z_3 Z_4} T_{cl} \tag{H.14}$$

$$T_r = \frac{T_{in}}{2} - \left(1 - \frac{Z_1 Z_6}{2 Z_3 Z_4}\right) T_{cl} \tag{H.15}$$

$$T_l - T_r = T_{cl} \tag{H.16}$$

Combining Eqs. (H.11) and (H.12) with Eqs. (H.14) and (H.15) gives the full expression of wheel torques:

$$T_l = \frac{T_{in}}{2} - \frac{Z_1 Z_5}{2 Z_2 Z_4} T_{cr} + \frac{Z_1 Z_6}{2 Z_3 Z_4} T_{cl} \tag{H.17}$$

$$T_r = \frac{T_{in}}{2} + \left(1 - \frac{Z_1 Z_5}{2 Z_2 Z_4}\right) T_{cr} - \left(1 - \frac{Z_1 Z_6}{2 Z_3 Z_4}\right) T_{cl} \qquad \text{(H.18)}$$

These equations show that the lateral torque difference can be controlled regardless of the input torque from the engine.